# TUDelft

Delft University of Technology

## On the ecology and applications of glucose and xylose fermentations

Rombouts, Jules

**DOI**

**Publication date**

2020

**Document Version**

Final published version

**Citation (APA)**

**Important note**

To cite this publication, please use the final published version (if applicable).
Please check the document version above.

# On the ecology and applications of glucose and xylose fermentations

Julius Laurens ROMBOUTS

**On the ecology and applications of glucose and xylose fermentations**

**Proefschrift**

ter verkrijging van de graad van doctor
aan de Technische Universiteit Delft,
op gezag van de Rector Magnificus prof.dr.ir. T.H.J.J. van der Hagen,
voorzitter van het College voor Promoties,
in het openbaar te verdedigen op
vrijdag 7 februari 2020 om 10:00 uur

Door

Julius Laurens ROMBOUTS

Ingenieur in de Levenswetenschappen,
Technische Universiteit Delft, Nederland
geboren te Rotterdam, Nederland

Dit proefschrift is goedgekeurd door de
promotor:    Prof. dr. dr. h.c. ir. M.C.M. van Loosdrecht
copromotor:   Dr. ir. R. Kleerebezem, Dr. ir. D.G. Weissbrodt


Samenstelling promotiecommissie

Rector Magnificus                           voorzitter
Prof. dr. dr. h.c. ir. M.C.M. van Loosdrecht    Technische Universiteit Delft
Dr.ir. R. Kleerebezem                        Technische Universiteit Delft
Dr.ir. D.G. Weissbrodt                       Technische Universiteit Delft


Onafhankelijke leden
Prof.dr. P. Daran-Lapujade               Technische Universiteit Delft
Prof.dr.ir. A.J.M. Stams                   Wageningen University & Research
Prof.dr.ir. R. van Kranenburg           Wageningen University & Research
Dr. I.D. Ofiteru                             Newcastle University
Prof. Dr. U. Hanefeld                       Technische Universiteit Delft, reservelid

An electronic version of this dissertation is available at

http://repository.tudelft.nl/

"I observed certain animalcules, within whole bodies I saw so quick a motion, as to exceed belief"


Antonie van Leeuwenhoek
17th century microbiologist and cloth merchant

Delft, the Netherlands

Disclaimer

All material is original and was primarily written by Julius Laurens Rombouts.

# Samenvatting

Microbiële fermetnaties zijn een essentieel proces in natuurlijke en menselijk gebouwde ecosystemen. Microbiële fermentaties spelen een cruciale rol in het verzorgen en verteren van ons voedsel en ze zijn bruikbaar in het ontwerpen van bio-processen die biogas, biobrandstof en vele andere functionele moleculen kunnen produceren (**Hoofdstuk 1**). Daarnaast kan het bestuderen van de competitie en samenwerking in microbiële fermentatieve ecosystemen bijdragen aan het oplossen van de vraag hoe microbiële diversiteit gevormd wordt. Glucose is een molecuul dat centraal staat aan de meeste vormen van leven, daarom werd glucose gekozen als model substraat om fermentatieve ophopingsculturen mee uit te voeren. Xylose is een belangrijke monomeer in vele typen hemicellulose en is daarom gekozen als tweede model substraat. Glucose en xylose kunnen gefermenteerd worden naar vluchtige vetzuren, alcoholen of melkzuur. De biomassa specifieke opname end productiesnelheid waarbij microbiële fermentaties verlopen zijn hoog vergeleken met andere biologische anaerobe koolstof conversies. Dit snelheidsverschil is nuttig wanneer men fermentaties bestudeerd door middel van ophopingsculturen.

Dergelijke fermentatieve ophopingsculturen kunnen gebruikt worden om mengcultuur fermentatie technologieën te ontwikkelen. Mengcultuur fermentatie technologieën bieden een alternatieve mogelijkheden om grondstoffen en afvalstromen met koolhydraten te verwerken (**Hoofdstuk 1**). Biogas productie is een relatief grote industrie, maar blijft economisch inferieur aan aardgas. De markt voor (bio-)waterstof productie is relatief groot, want de waterstof economie was in 2017 130 miljard USD waard. Werkende grootschalige bio-waterstof productie en opslag door middel van biologische systemen moet zich nog bewijzen. Lactaat en ethanol kunnen beiden geproduceerd worden met mengcultuur fermentatie, waarbij ethanol productie een uitdagende business case blijft vanwege krappe winstmarges. Middellange keten vetzuren zijn ook een potentieel product. Deze moleculen hebben in potentie veel toepassingen, met waarschijnlijk een hogere toegevoegde waarde dan biogas of biobrandstof en dus beloven ze een gezonde *business case* te bieden. Vluchtige vetzuren geproduceerd met behulp van een mengcultuur fermentatie kunnen gebruikt worden voor het produceren van polyhydroxyalkanoaten, wat een gezonde industriële haalbaarheid beloofd.

Wanneer men alleen de competitie van substraten in oogpunt neemt, dan zal het limiteren van een enkel substraat in een microbieel ecosysteem in verwachting leiden tot één dominant micro-organisme. De resultaten van **Hoofdstuk 2** bevestigen deze hypothese, tot de mate dat >85% van het geobserveerde celoppervlak behoort aan één enkel microbiële soort, voor drie van de vier ophopingculturen. Een populatie van *Enterobacter cloacae* en *Citrobacter freundii* domineerde de glucose en xylose gelimiteerde sequentiele batch culturen respectievelijk. Continue glucose limitatie toonde de dominantie van *Clostridium intestinale*. De xylose gelimiteerde ophopingscultuur resulteerde in een populatie waarbij een populaties van *Citrobacter freundii*, een *Lachnospiraceae* en *Muricomes* co-existeerden. **Hoofdstuk 3** heeft als doel om een antwoord te vinden hoe duale substraat limitatie een fermentatieve microbiële gemeenschap beïnvloed. Duale xylose en glucose limitatie resulteerde in een generalistische populatie van *Clostridium intestinale* in continu voeding, en een generalistische populatie van *Citrobacter freundii* in sequentiële batch verrijking. Geen klaarblijkelijke katabole koolstof repressie was waarneembaar wanneer een batch cyclus werd geanalyseerd, of wanneer er een batch experiment werd uitgevoerd in de continu duaal gelimiteerde ophopingscultuur. Deze respons is van belang wanneer men een grootschalig fermentatief bio-proces ontwerpt, want in de industrie worden veelal micro-organismen gebruikt die een katabole koolstof repressie vertonen in mengsels van glucose en xylose.

De kinetische, stoichiometrische en bioenergetische analyse van ophopingsculturen in continu gelimiteerde of sequentieel batch milieus laten zien dat sequentiële batch milieus selecteren voor snelheid, terwijl continu gelimiteerde systemen selecteren voor efficiëntie (**Hoofdstuk 2**). Snelheid word hier gesteld als de biomassa specifieke substraat opname snelheid ($q_s^{max}$).

Efficiëntie word gesteld als de opbrengst van biomassa per ATP geoogst in het katabolisme ($Y_{x,ATP}$). Deze bevindingen passen in de r- en K-selectie theorie. Daarnaast is het bevonden dat butyraat productie gekoppeld is aan een lagere opname snelheid dan gecombineerde acetaat en ethanol productie. Potentieel kan er meer energie worden geoogst in butyraat productie vergeleken met acetaat en ethanol productie, door middel van elektron bifurcatie.

Meer microbiële diversiteit (*i.e.* meer dan één soort) werd gevonden dan er van tevoren was verwacht vanuit een puur competitief oogpunt in alle zes ophopingsculturen uitgevoerd in **Hoofdstuk 2 en 3**. Daarom is er in **Hoofdstuk 5** gekozen voor een complementaire aanpak van *metabolomics*, *metagenomics* en isolatie studies, die het genereren van een op bewijs gebaseerde hypothese mogelijk maakte hoe de *Enterobacteriaceae* en *Clostridiales* populaties in de continu gelimiteerde xylose ophopingscultuur interacteerden. The metagenoom analyse resulteerde in drie dominante *bins*, één voor *Citrobacter freundii*, één voor "*Ca.* Galacturonibacter soehngenii" en één voor een *Ruminococcus* soort. De interactie tussen *Citrobacter freundii* en "*Ca.* Galacturonibacter soehngenii" wordt gesteld om voor een deel te bestaan uit het delen van biotine, pyridoxine en alanine van *Citrobacter freundii* met "*Ca.* Galacturonibacter soehngenii". Een differentiële ophopingscultuur-studie liet zien dat inderdaad de fractie van "*Ca.* Galacturonibacter soehngenii" steeg en de fractie *Enterobacteriaceae* daalde, wanneer aan het inkomende medium deze drie metabolieten werden toegevoegd. Dus, het is waarschijnlijk dat commensalisme en competitie beiden verantwoordelijk zijn voor het vormen van microbiële diversiteit in deze cultuur.

**Hoofdstuk 4** had als doel om de ecologie van melkzuurbacteriën te bestuderen. Bacteriën kunnen melkzuur produceren vanuit glucose, wat een ander metabolisme is dan het produceren van acetaat en butyraat vanuit glucose. Sequentiële batch reactoren zijn gebruikt om te verrijken, waarbij een mineraal en complex medium werden vergeleken. De media waren identiek, behalve dat er aan het complexe medium 9 B-vitaminen en een peptide mengsel waren toegevoegd. Glucose werd gefermenteerd naar een mengsel van melkzuur en ethanol wanneer er verrijkt werd in een complex medium, ofwel een heterofermentatie. Met het minerale medium werd glucose gefermenteerd naar een mengsel van acetaat, butyraat en waterstof, met kleinere hoeveelheden melkzuur en ethanol. Een populatie van *Lactobacillus*, *Lactococcus* en *Megasphaera* werd verrijkt met complex medium. Met mineraal medium domineerde een populatie van *Ethanoligenens*, met een kleine fractie *Clostridium*. Melkzuur producerende bacteriën worden gesteld de fermentatie over te nemen door een hogere biomassa specifieke substraat opname snelheid ($q_s^{max}$ was 94% hoger), welke leidt naar een hogere groeisnelheid. De verhoging van groeisnelheid wordt gesteld te worden veroorzaakt door middel van *resource allocation*, waarbij melkzuurbacteriën hun enzym niveaus hebben geoptimaliseerd in het anabolisme en katabolisme. Hierdoor behalen ze een hogere groeisnelheid dan mineraal-minnende fermenterende micro-organismen, zoals *Ethanoligenens*.

**Hoofdstuk 6** heeft als doel om verder onderzoek te sturen, wat ligt in het bestuderen van het effect van verschillende parameters op fermentatieve ecosystemen. Deze parameters zijn de concentraties van: gasvormige stoffen (I), pH-neutraliserende kationen (II), en nutriënten zoals B-vitaminen (III). Daarnaast wordt het bestuderen van zeer lage pH milieus (pH<3.5) als onderzoek kans gezien (IV). Als laatste wordt het analyseren van de compositie van "echte" fermenteerbare stromen en hun effect op het product spectrum van de fermentatie van belang geacht (V). Kinetiek en bio-energetica worden hier bediscussieerd aan den hand van enzymatische Michaelis-Menten kinetiek en van het concept *resource allocation*. Op deze manier, kunnen pogingen in het mogelijk sturen van product formatie in fermentatieve ecosystemen *a priori* voorspeld worden. Toekomstige experimenten worden aangemoedigd uitgevoerd te worden op vier niveaus. Bruikbare experimenten om enkele concepten in deze dissertatie te toetsen zijn hier beschreven. Als laatste zal toekomstig werk moeten uitwijzen of commensalisme en/of mutualisme beiden relevante coöperatieve mechanismen zijn in open microbiële gemeenschappen.

# Summary

Microbial fermentations are a key process in naturally and man-made ecosystems. Microbial fermentations play a key role in creating and digesting our food and they are useful in designing bioprocesses that can produce biogas, biofuels, bioplastics, and many other functional molecules (**Chapter 1**). Furthermore, studying the competition and cooperation in microbial fermentative ecosystems can help to solve the question how microbial diversity is shaped. Glucose is a molecule central to most forms of life, therefore glucose was chosen as a model substrate to perform fermentative enrichment studies. Xylose is an important monomer in many types of hemicellulose and was therefore chosen as second model substrate. Glucose and xylose can be fermented to volatile fatty acids, alcohols or lactic acid. The biomass specific uptake and production rates at which microbial fermentations are performed are high compared to other biological anaerobic carbon conversions. This rate difference is useful when studying fermentation using an enrichment culture approach.

Such fermentative enrichment cultures can be used to develop mixed culture fermentation technologies, which offer alternative technological possibilities for processing feedstocks and residual streams containing carbohydrates (**Chapter 1**). Biogas production is a relatively well-established industry, but remains to be economically outcompeted by natural gas. The market for (bio)hydrogen production is relatively big, as the hydrogen economy stood for 130 billion USD in 2017. Actual large-scale hydrogen production and capture using biological systems has yet to prove itself. Lactate and ethanol can both be produced using mixed culture fermentation, where ethanol production remains to be a challenging business case due to small profit margins. Medium chain fatty acids are also a potential product. These molecules are expected to have many applications, with a likely higher value than biogas or biofuel, thus promising a healthy business case. Producing polyhydroxyalkanoates from volatile fatty acids produced by mixed culture fermentation promises a healthy industrial feasibility.

When assuming solely competition on substrates to occur, limiting a single substrate in a microbial ecosystem is expected to result in one dominant species. The results of **Chapter 2** confirm this hypothesis, to the extent of >85% of the observed cell surface belonging to a single species for three out of the four enrichment cultures. A population of *Enterobacter cloacae* and *Citrobacter freundii* dominated the glucose and xylose limited sequencing batch cultures respectively. Continuous glucose limitation showed the dominance of *Clostridium intestinale*. A xylose limited continuous enrichment culture resulted in the coexistence of *Citrobacter freundii*, and a *Lachnospiraceae* and *Muricomes* population. **Chapter 3** aims to answer the question how dual substrate limitation influences a fermentative microbial community. Dual xylose and glucose limitation led to a generalist population of *Clostridium intestinale* in continuous feeding, and a generalist population of *Citrobacter freundii* in sequencing batch culturing. No apparent carbon catabolite repression was observed when analysing a batch cycle or when performing a batch experiment in the continuous dual limited enrichment culture. This response is of value when designing large scale fermentative bioprocesses, as in industry, typically microorganisms are used which show carbon catabolite repression in mixtures of glucose and xylose.

The kinetic, stoichiometric and bioenergetic analysis of enrichment cultures in continuously limited or sequencing batch environments showed that sequencing batch enrichments select for rate, while continuous limited enrichments select for efficiency (**Chapter 2**). Rate is considered as the biomass-specific substrate uptake rate ($q_s^{max}$) and efficiency is considered as yield of

biomass on ATP harvested in catabolism ($Y_{x,ATP}$). These findings fit within the r- and K-selection theory. Furthermore, it was found that butyrate production is linked to a lower uptake rate than combined acetate and ethanol production. Potentially, more energy is harvested in butyrate production than in combined acetate and ethanol production, through electron bifurcation.

More microbial diversity (*i.e.* more than one species) was observed than what was expected from a competitive point of view in all six enrichments performed in **Chapter 2 and 3**. Therefore, in **Chapter 5** a complementary approach of metabolomics, metagenomics and isolation studies where performed to generate an evidence based hypothesis on how the *Enterobacteriaceae* and *Clostridiales* populations in the continuous xylose limited enrichment culture interacted. The metagenomic evaluation resulted in three dominant bins, one for *Citrobacter freundii*, one for "*Ca.* Galacturonibacter soehngenii" and one for a *Ruminococcus* sp. The interaction between *Citrobacter freundii* and "*Ca.* Galacturonibacter soehngenii" is proposed to be a sharing of biotin, pyridoxine and alanine by *Citrobacter freundii* with "*Ca.* Galacturonibacter soehngenii". A differential enrichment study showed that indeed the fraction of "*Ca.* Galacturonibacter soehngenii" increased and *Enterobacteriaceae* decreased, when these three metabolites were directly supplemented to the enrichment culture. Thus, commensalism and competition were likely to driving microbial diversity in this culture.

**Chapter 4** aimed to study the ecology of lactic acid bacteria. Bacteria can produce lactic acid from glucose, which is a different metabolism than producing acetate and butyrate. Sequencing batch reactors were used to enrich, comparing a mineral and complex medium. The media were identical, except for the addition of peptides and 9 B vitamins in the complex medium. Glucose was fermented to a mixture of lactic acid and ethanol when using the complex medium, thereby a heterofermentation. Using the mineral medium, glucose was fermented to a mixture of acetate, butyrate and hydrogen, with smaller amounts of lactic acid and ethanol. A population of *Lactobacillus, Lactococcus* and *Megasphaera* was enriched on complex medium. On mineral medium, a population of *Ethanoligenens* dominated the enrichment with a small fraction of *Clostridium*. Lactic acid producing bacteria are hypothesised to have taken over the fermentation, due to a 94% increase in biomass-specific substrate uptake rate, leading to a higher growth rate. The increase in growth rate is argued to be caused due to resource allocation, whereby lactic acid bacteria optimise their enzyme levels in anabolism and catabolism, attaining a higher growth rate than mineral-type fermenters such as *Ethanoligenens*.

**Chapter 6** aims to direct further research, which lies in studying the effect of different parameters on fermentative ecosystems. These parameters are concentrations of: gaseous compounds (I), cations used to neutralise (II), nutrients, such as B vitamins (III). Also, very low pH environments (pH<3.5) are considered an opportunity (IV). Finally, analysing the composition of "real" fermentable streams and their effect on the arising product spectra is of interest (V). Kinetics and bioenergetics are discussed using enzymatic Michaelis-Menten kinetics and the concept of resource allocation. In this way, efforts can be directed into the ability to predict product formation *a priori* in fermentative ecosystems. Future experimentation is guided to take place on four distinct levels, and useful experiments to verify concepts in this thesis are outlined. Finally, commensalism and/or mutualism might both be relevant in open microbial ecosystems which remains to be settled by future work.

# Table of contents

# List of abbreviations

| | |
|---|---|
| ABC | ATP-binding cassette |
| Adh | Alcohol dehydrogenase |
| ADP | Adenosine diphosphate |
| ATP | Adenosine trisphosphate |
| B.V. | Besloten vennootschap (private limited company) |
| BLASTn | Basic Local Alignment Search Tool (for nucleotides) |
| cAMP | Cyclic adenosine monophosphate |
| CCR | Carbon catabolite repression |
| CoA | Coenzyme A |
| COD | Chemical oxygen demand |
| CSTR | Continuous-flow stirred tank reactor |
| DAPI | 4',6-diamidino-2-phenylindole |
| DGGE | Denaturing gradient gel electrophoresis |
| DNA | Deoxyribonucleic acids |
| ESI | Electrospray ionisation |
| ETC | Electron transport chain |
| Fd | Ferredoxin |
| FISH | Fluorescent *in situ* hybridisation |
| GC | Gas chromatography |
| HPLC | High performance liquid chromatography |
| HRT | Hydraulic retention time |
| KEGG | Kyoto Encyclopedia of Genes and Genomes |
| LamB | Lambda receptor protein B |
| Ldh | Lactate dehydrogenase |
| MCF | Mixed culture fermentation |
| MCFA | Medium chain fatty acids |
| Mgl | Methyl-galactoside transport system, an ATP-binding protein |
| MS | Mass spectrometer |
| NADH | Nicotinamide adenine dinucleotide |
| NCBI | National Center for Biotechnology Information |
| OmpC | Outer membrane protein C |
| OTU | Operational taxonomic unit |
| PCR | Polymerase chain reaction |
| PEP | Phosphoenolpyruvic acid |
| Pfo | pyruvate:ferredoxin-2-oxidoreductase |
| PHA | Polyhydroxyalkanoates |
| PKP | Phosphoketolase pathway |
| PLA | Polylactic acid |
| PPP | Pentose phosphate pathway |
| PTS | Phosphotransferase system |
| QUIPS | Quantimet interactive programming system |
| RbsB | Ribose ABC transport system |
| RNA | Ribonucleic acids |
| RP | Reversed phase |
| rRNA | ribosomal RNA |

| | |
|---|---|
| SBR | Sequencing batch reactor |
| SLP | Substrate level phosphorylation |
| smf | Sodium motive force |
| SRT | Solids retention time |
| TOF | Time of flight |
| TSS | Total suspended solids |
| USD | US Dollars |
| VFA | volatile fatty acid |
| VSS | volatile suspended solids |
| WWTP | Wastewater treatment plant |

# List of symbols

| Kinetics | |
|---|---|
| $\mu$ | Biomass specific growth rate |
| $\mu^{max}$ | Maximum biomass specific growth rate |
| $Y_{x,s}$ | Biomass yield on substrate |
| $q_s$ | Biomass specific substrate uptake rate |
| $q_s^{max}$ | Maximum biomass specific substrate uptake rate |
| $m_s$ | Maintenance coefficient |
| $C_s$ | Residual substrate concentration |
| $K_s$ | Affinity constant for substrate (Monod kinetics) |
| **Thermodynamics** | |
| Cmol | Carbon mole |
| $\Delta G$ | Gibbs energy change of a reaction |
| $\Delta G^0$ | Standard Gibbs energy change of a reaction (p = 1 atm, T = 298.15 K and 1M of reactants) |
| $\Delta G^{0\prime}$ | Biochemical standard Gibbs energy change of a reaction (as $\Delta G^0$, except pH = 7) |
| T | Temperature |
| p | Pressure |
| **Bioenergetics** | |
| $Y_{ATP,s}$ | Yield of ATP produced per substrate consumed |
| $Y_{x,ATP}$ | Yield of biomass produced on ATP harvested in catabolism |
| **Enzyme kinetics – Michaelis-Menten** | |
| $r_e$ | Enzymatic rate |
| $k_{cat}$ | Turnover number of an enzymatic reaction |
| $c_e$ | Enzyme concentration |
| S | Substrate concentration of substrate used in enzymatic reaction |
| K | Michaelis-Menten constant of an enzymatic reaction |
| **Other** | |
| $\sigma$ | Standard deviation |
| $k_L a$ | mass transfer coefficient from gas to liquid |

# Chapter 1 - An introduction to the ecology and applications of xylose and glucose fermentations

*This chapter was written and revised by*

*J.L. Rombouts & R. Kleerebezem*

## 1.1 The ecology of carbohydrate fermenting systems

Microbial fermentations are a key process in many natural and man-made systems. They are used to conserve food, to produce chemicals and fuels, and in nature they play a role in the degradation of organic matter. It is a process not exclusive to the microbial world, as the acidification of human muscle tissue during intensive exercise is also fermentation. Environmentally relevant microorganisms can ferment glucose into a number of products (Figure 1.1). Both bacteria and eukaryotes are capable of carbohydrate fermentation and can be found virtually everywhere in nature.

In essence, fermentation is the conversion of an organic substrate to one or more products without the use of external electron acceptors (such as oxygen). During fermentation, three key enzymes are responsible for the direction into which the carbon is sent (Figure 1.1). The Kyoto Encyclopaedia of Genes and Genomes (KEGG) database [1] contained 5245 bacterial genomes (accessed August 2018), of which approximately 10% contain either of the three genes. Though bacterial genomes obtained from isolated species likely do not represent the microbial genomic potential present in environments [2], it is likely that fermentation is a common trait amongst bacteria. The fact that there might be a trillion ($10^9$) microbial species on earth [3], and only 100-1000 ($10^3$-$10^4$) total relevant fermentative pathways poses a challenging question, why is there such an enormous amount of microbial diversity? Why are there in the order of $10^4$ competitive species per fermentation pathway? Studying the competition and cooperation in microbial fermentative ecosystems can help to solve this question.
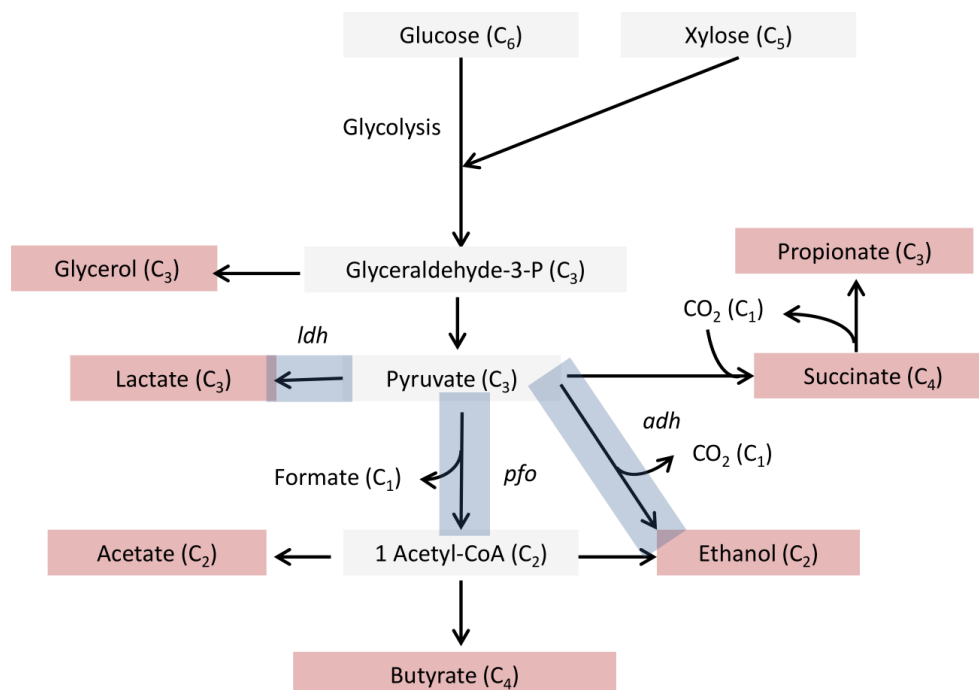


*Figure 1.1: Key catabolic pathways in microbial fermentation. Glucose is fermented to pyruvate, a central metabolite in fermentation. Xylose is assumed to enter glycolysis through the pentose phosphate pathway (PPP). Pyruvate can be converted directly to lactate using lactate dehydrogenase (ldh), or to acetaldehyde and then to ethanol and CO2 using alcohol dehydrogenase (adh) or to acetyl-CoA using pyruvate:ferredoxin 2-oxidoreductase (pfo). Based on* [4]*.*

Glucose is a molecule central to most forms of life: it is assimilated by organisms in many natural polymers, such as cellulose, starch and glycogen. These polymers serve as storage of fermentable substrate or as structural polymers. Sugar polymers can be depolymerised (or digested) back to their monomers to serve as a substrate to drive catabolism (energy generating redox reaction)

and with that anabolism (production of functional biomass). Fermentation is an intermediate step in the anaerobic digestion process [5]. In anaerobic digestion, complex organic carbon is converted through hydrolysis to the corresponding monomers such as glucose. Glucose can be subsequently fermented to volatile fatty acids (VFAs) lactic acid, or alcohols, after which the fermentation products are fermented to acetate, $CO_2$, $H_2$ and formate (acetogenesis). These compounds can then be used by archaea to form methane and $CO_2$ (methanogenesis) [4].

## 1.2 The concept of an ecological niche

Microorganisms compete and cooperate in a multitude of environments. Essentially, a specific environment is an ecological niche. An environment is in principle determined by its physical and chemical state, *e.g.* concentration of protons (pH), temperature, pressure, presence of salts (ionic strength) and molecular composition. Interestingly, fermentative microorganisms are found in many different environments: low pH (acidophiles), high pH (alkaliphiles), a temperature of 20-41°C (mesophiles) and 42-122°C (thermophiles). All microorganisms require three rudimentary elements: nitrogen, phosphorous and sulphur, to biosynthesise their biomass. Microorganisms can grow in two distinct environments: without organic nutrients, with only minerals (prototrophic) and high organic nutrients (eutrophic). Organic nutrients are organic molecules such as amino acids and B vitamins. Auxotrophic microorganisms depend on one or more organic nutrients, for which they have an auxotrophy and are therefore found in more eutrophic environments. Trace elements also define an environment, as these elements are used by microorganisms in their metabolism. Trace elements are used as cofactor in enzymes (Table 1.1), as solute to create an energetic gradient (*e.g.* a sodium motive force, smf) or as components of structural molecules (cell membranes, extracellular polymeric substances or intracellular structures).

***Table 1.1***: *A selection of elements and trace elements used in this thesis to create a certain ecological niche. The trace element solution used in this thesis is replicated from Temudo* [6] *and given in Appendix I. Examples of important functions in fermentation are given in between brackets.*

| Element | Salt form used | Function in fermentative microbial systems |
|---|---|---|
| Nitrogen (N) | $NH_4^+$ | Used to form proteins, ribonucleic acids (RNA) and deoxyribonucleic acids (DNA) |
| Sulphur (S) | $SO_4^{2-}$ | Used to form proteins (cysteine and methionine) |
| Phosphor (P) | $PO_4^{3-}$ | Used to form adenosine tri phosphate (ATP), RNA and DNA |
| **Trace elements** | | |
| Sodium (Na) | $Na^+$ | Solute used to create an energetic gradient (smf) |
| Potassium (K) | $K^+$ | Solute used to create an energetic gradient |
| Calcium (Ca) | $Ca^{2+}$ | Cofactor in metabolic enzymes (*ldh*) |
| Magnesium (Mg) | $Mg^{2+}$ | Cofactor in metabolic enzymes (glycolysis) |
| Iron (Fe) | $Fe^{2+}$ | Cofactor in metabolic enzymes (*pfo* and dehydrogeneases) |
| Nickel (Ni) | $Ni^{2+}$ | Cofactor in metabolic enzymes (dehydrogenases) |
| Manganese (Mn) | $Mn^{2+}$ | Cofactor in metabolic enzymes (*ldh*) |
| Cobalt (Co) | $Co^{2+}$ | Cofactor in metabolic enzymes |
| Copper (Cu) | $Cu^{2+}$ | Cofactor in metabolic enzymes |

## 1.3 Metabolic interactions in microbial ecosystems

Members of microbial communities present in mixed culture ecosystems, usually referred to as strains, are competing for substrates (and space) while they can simultaneously cooperate. Großkopf and Soyer have outlined six different mechanisms by which members of microbial

communities can interact, divided in two participating microbial strains [7]. In the context of this thesis four will be introduced (Figure 1.2). Competition for substrates (1) is negative for both parties (-/-). Commensalism (2) is an example where one strain is producing an essential growth substrate for another strain, which can occur without the benefit for the supplying party (+/0). Syntrophy (3) is an example were both parties benefit (+/+). The product of one party (A) is inhibiting this party and the other party (B) converts this inhibiting product to a new product. Thereby, the overall metabolism is enabled. Syntrophy is traditionally explained through the example of methanogenic degradation of specific VFAs where hydrogenotrophic methanogens scavenge hydrogen produced during anaerobic oxidation of a VFA. Herewith the methanogens maintain the hydrogen partial pressure below the thermodynamic limit for hydrogen production [8].

Mutualism (4) is not listed in the publication of Großkopf and Soyer and is the example where both parties share a product which the other party can use in its metabolism without either of the exchanged products being inhibiting. This is also a positive relationship for both parties (+/+). Insight in interactions between microbial species can help to explain and understand why microbial communities display a relatively high degree of microbial diversity and "functional redundancy", which is the sharing of the same metabolic properties by multiple species or strains in a community.
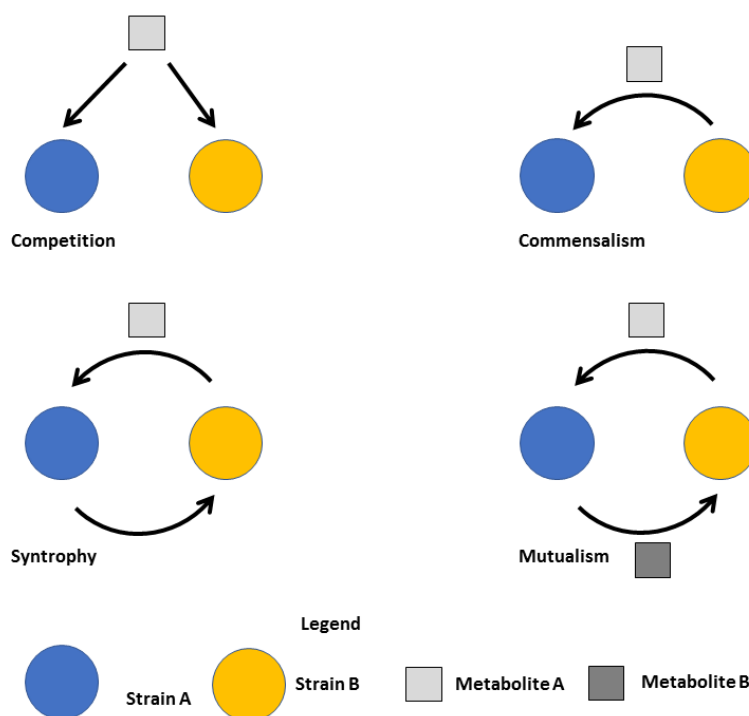


*Figure 1.2: Four microbial interactions considered relevant for this thesis. Based on the six interactions proposed by Großkopf and Soyer [7]. Non-metabolite arrow in syntrophy is the thermodynamic and kinetic enabling of the metabolism of both organisms to perform a reaction.*

## 1.4 Quantification of microbial growth using a bioreactor set-up

Microorganisms competing for space and resources in a given niche need to multiple themselves, which is microbial growth. Microbial growth can be quantified by using the Hebert-Pirt equation for substrate uptake [9]:

$$\mu = Y_{xs} \cdot q_s + m_s \tag{1.1}$$

Here, the biomass specific growth rate ($\mu$) is related to the biomass yield on substrate ($Y_{x,s}$), the biomass specific substrate uptake rate ($q_s$) and the maintenance coefficient ($m_s$). Microorganisms can grow in a batch environment where nutrients are not limiting, where they attain their maximum growth rate, $\mu^{max}$. In a substrate limited environment, where one or more nutrients are limiting, microorganisms grow at $\mu$. Often, these two environments can be recreated in a reproducible fashion as a sequencing batch reactor (SBR), to simulate batch conditions and a continuous-flow stirred tank reactor (CSTR), to simulate substrate limited conditions.

In waste water engineering, the hydraulic retention time (HRT) is used commonly to express the volume exchange in a vessel. In a stirred tank environment, microorganisms grow in suspension, and the suspended biomass is exchanged with volume outflow. The solids retention time (SRT) and the HRT are therefore equal. Using such bioreactor set-ups enable the possibility to directly control microbial growth, which to control $\mu$.

## 2 Taxonomy of fermentative ecosystems: fermentative microbiomes and their function the human gut and food and energy production

Ecosystems are inhabited by multiple microbial species. Mixed cultures are consortia of microbial species, also termed microbial communities or microbiomes. Manmade pure culture systems represent the only situation in which a single microbial species is fully dominant (with very low amounts of other bacteria, typically $10^6$ times lower). Mixed culture fermentation (MCF) is a concept of fermentation performed by a microbial community. Many traditional foods and beverages use mixed culture fermentation as conservation method [10], such as *pulque* and *kefir*. Lactate production decreases the pH to 4 or lower, making the environment unfavourable for other bacterial or fungal growth. Famous products containing lactate are for example sauerkraut, sourdough bread, yoghurt and *kimchi*. Lactate production is enabled through the enzyme lactate dehydrogenase (*ldh*, see Figure 1.1). The class of *Bacillus* contains often encountered genera associated with lactic acid producing microbiomes, such as *Lactobacillus*, *Lactococcus*, *Streptococcus*, *Leuconostoc* and *Bacillus*. The *Bacillus* class is part of the *Firmicutes* phylum (Figure 1.3).

Ethanol can also be used as preservation method. The eukaryote *Saccharomocyes cerevisiae* or baker's yeast is commonly used to convert sugars into ethanol and $CO_2$ [4]. In the bacterial domain, *Zymomonas mobilis* is a well characterised *Proteobacteria* (Figure 1.3) that can also selectively produce ethanol and $CO_2$ from sugars [4]. Historically, beer production was used to decontaminate drinking water and to add calories. Beer was made more suitable for human consumption through the combined pathogen inhibiting activity of ethanol, a lower pH and growth inhibiting compounds added through hop. Pathogens tend to grow more rapidly in alcohol free beer [11]. Acidification and ethanol formation are therefore two preservation methods used in food technology, which are enabled through the activity of fermentative microorganisms.

Moving from food technology to other niches of fermentation, the human gut microbiome and the anaerobic digestor microbiome are two other intensively studied environments where fermentation plays an essential role. A relatively large microbial diversity is encountered in these eutrophic environments compared to low nutrient or oligotrophic environments, such as desert soils or salty lakes. This difference in microbial diversity is illustrated by the study of Castro *et al.*, who analysed the microbial diversity of methanogenic populations in eutrophic and oligotrophic sites in the Florida Everglades [12]. Important phyla present in the human gut microbiome are *Firmicutes* and *Bacteriodetes* [13], while in the digester microbiome *Actinobacteria*, *Chloroflexi* and *Proteobacteria* are also important [14][15]. Polymer degradation limits the fermentation rate in these systems, as there is little mixing and the sugars are present in slowly degradable polymers, like pectin or cellulose. The genus of *Clostridium* (part of the phylum of *Firmicutes*) is characterised as an important cellulose degrading taxa [16] and is found to be dominant in

anaerobic digesters [17]. It can be argued that fermentation is a quite widespread trait throughout the bacterial tree of life (Figure 1.3), while specific phyla and genera are observed in specific niches.
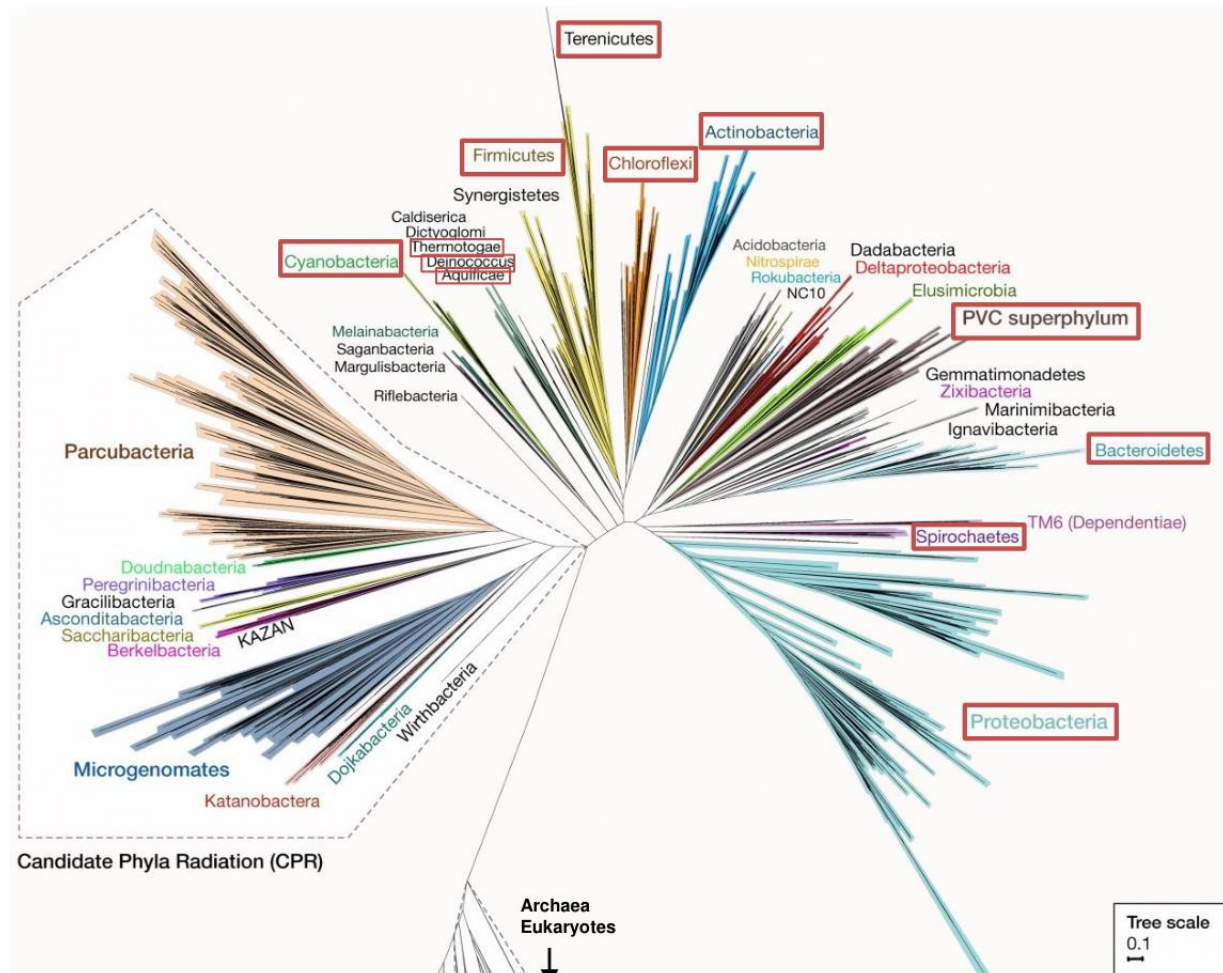


*Figure 1.3: Phylogenetic tree of bacteria, adapted from Castelle et al. [18]. Archaeal and eukaryotic phyla are left out of this image. The highlighted phyla contain one or more isolated microorganisms of which the L-ldh gene is identified in a genome submitted to the NCBI database. 1055 genomes contained L-ldh out of 205,659 published genomes (accessed August 2019).*

## 3.1 The force driving fermentative microbial ecosystems: carbohydrate fermentation

Glucose and xylose are chosen in this thesis as model substrates for carbohydrate fermentation. Glucose is an abundant monomer in industrially relevant fermentable feedstocks such as food waste. In 2010, it has been estimated that 89 million tonnes of food waste was generated in the European Union alone [19], which is about 180 kilogrammes per capita annually. Glucose contains 24 electrons compared to $CO_2$ and is energetically very similar to other six carbon and twenty-four electron sugars, such as galactose, mannose and fructose (Figure 1.4). Galacturonic acid is industrially relevant as it is found in pectin, an abundant agro-industrial polymer. This monomer contains six carbon and twenty electrons, thus it is more oxidised than glucose.
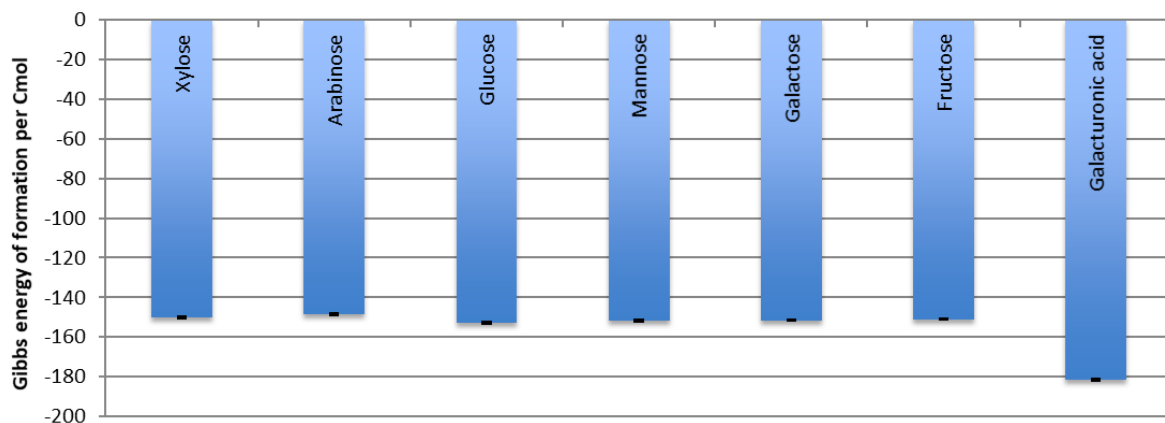
***Figure 1.4:*** *Gibbs energy of formation per carbon mole (Cmol) at 298.15 K (25°C). A lower energy state means that less energy can be gained by the conversion of this substrate. Galacturonic acid is displayed to highlight the minor difference between the other six carbohydrates. Thermodynamic properties are obtained from Goldberg and Tewari* [20]

Xylose is an important monomer in many types of hemicellulose, which is a mixed polymer consisting of mainly glucose, xylose and arabinose (also a five-carbon sugar). Hemicellulose is estimated to be the second most abundant polymer in nature, after cellulose [21]. Xylose and arabinose contain twenty electrons resulting in the same oxidation state per unit of carbon compared to glucose. Xylose is energetically similar to other six carbon and twenty-four electron containing sugars, such glucose (Figure 1.4), but has more potential energy than galacturonic acid.

## 3.2 Biochemistry and ATP harvesting in fermentative ecosystems

Microbial growth (anabolism) needs to be fuelled by an energy producing reaction, the catabolism, and combined these two reactions form the metabolism of a microorganism [22]. Therefore, microorganisms utilise energy harvesting systems and store the energy in the form of ATP to use for energy consuming reactions (Figure 1.5). In fermentation, the electrons present in the substrate are directed into products, thus performing a conversion which yields energy. This energy is known as the Gibbs energy change of a chemical reaction ($\Delta G$) and can be expressed at standard conditions as $\Delta G^0$ (1 atm, 298.15 K and 1M of reactants). Electrons flow from the substrate into products and are used to form biomass. To obey the law of mass conservation, electrons have to be balanced. Electrons can be carried by electron carriers, such as nicotinamide adenine dinucleotide (NADH) and ferredoxin (Fd). These intracellular energy and electron carriers have to be balanced as they are costly to produce and only fulfil a transferring role, and are termed conserved moieties [23].
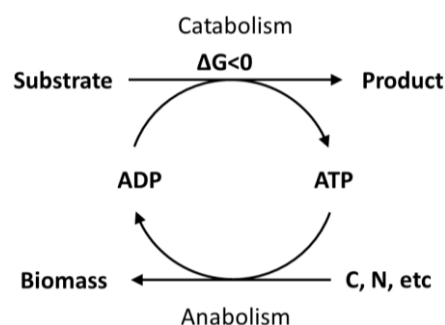


***Figure 1.5****: Microbial metabolism represented as a coupled network of anabolism and catabolism as proposed by Kleerebezem and van Loosdrecht* [22]*. Catabolism yields net energy ($\Delta G$ is negative) to drive the anabolism. Carbon (C) and nitrogen (N), and other elements, are used for anabolism. ADP is adenosine diphosphate.*

## 3.3 Energy conserving mechanisms used in microbial ecosystems

Two different mechanisms can be used by microorganisms to generate energy in catabolism (Figure 1.6). Substrate level phosphorylation (SLP) is a process that directly converts the energy available in a reaction, using a high energy yielding enzymatic reaction to create one ATP (or an energetic equivalent). ATP is estimated to represent 60 kJ mol$^{-1}$ in typical intracellular conditions [4]. Alternatively, an electron transport chain (ETC) can be used to use energy present in a low energy yielding reaction to translocate a positively charged molecule or cations, *e.g.* a proton, over a membrane to create an energetically charged gradient over this membrane. An ATPase can use this gradient to harvest energy as ATP. Depending on the number of cations used by the ATPase, a certain amount of energy is required to translocate the cation. If four protons are used to produce one ATP and 1 ATP equals 60 kJ mol$^{-1}$, then the electrochemical potential needed is at least 15 kJ mol$^{-1}$.
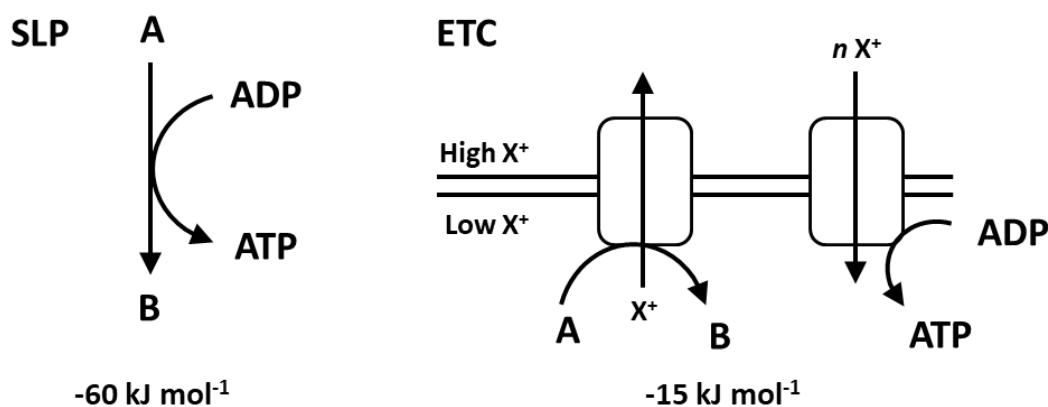


***Figure 1.6***: *Substrate level phosphorylation versus electron transport chain energy harvesting. Substrate A is used to produce product B in an enzymatic reaction directly producing one ATP. Cation X$^+$ is used by a translocation complex of enzymes (electron transport chain) to create an electrochemical potential, after which X$^+$ is translocated back over the membrane with a certain stoichiometry n, which is four in this example.*

Anaerobic microorganisms have developed a third mechanism to conserve energy: electron bifurcation. In essence, this system uses the energy available in low energy yielding enzymatic reactions (typically less than 15 kJ mol$^{-1}$) to transfer electrons from electron carriers that have a low potential to electron carriers that have a higher potential. These higher potential carriers can transfer their electrons back to low potential carriers to drive an ETC. Alternatively, electrons can be redirected to produce ATP by directing more carbon to substrate level phosphorylation type reactions. In an example of fermentation, electrons coming from glycolysis through NADH, are transferred to ferredoxin to produce hydrogen which enables the production of more acetate besides butyrate, generating 10% extra ATP through SLP, as discussed by Buckel and Thauer [24].

## 4 Microbial thermodynamics and kinetics in fermentative ecosystems

The growth rate of a microorganism determines its ability to outgrow or outcompete other microorganisms. Glucose can be fermented through several pathways (Figure 1.1), of which five relevant ones are listed in Table 1.2. Lactic acid production yields 2 ATP per substrate converted, while propionate and coupled acetate production yields 3 ATP. Acetate and butyrate production can yield an extra ATP through SLP by coupling the Coenzyme A (CoA) transfer to ATP production. Energy conservation in propionate production is possible using the methylmalonyl pathway which partly conserves the energy in the fumarate reduction to succinate [4], directly coupling this step to the creation of a sodium motive force (smf). More energy can be conserved also in butyrate production, as the step from crotonyl-CoA to butyryl-CoA is proposed to generate energy

using a sodium motive force [25] or using electron bifurcation to produce extra ATP by producing more acetate and hydrogen [24].

**Table 1.2**: *Typical experimental $\mu^{max}$ value for different types of catabolic reactions at pH = 7 and 30℃ unless reported otherwise. The catabolic stoichiometries used to estimate $\Delta G^{0'}$ can be found in* **Appendix II**. *Experimental $\mu^{max}$-values are obtained from studies using a mineral or very low nutrient medium as most media used in this thesis are mineral media. The $\mu^{max}$-values are corrected for temperature to 30°C using the Arrhenius equation, if the used temperature was not 30°C.*

| No. | Catabolism | $\mu^{max}$ $(h^{-1})$ | Organism | $\Delta G^{0'}$ (kJ $mol_S^{-1}$) | ATP SLP ($mol_{ATP}$ $mol_S^{-1}$) | Ref. |
|---|---|---|---|---|---|---|
| | Fermentative pathways from glucose | | | | | |
| 1 | Glucose to ethanol and $CO_2$ | 0.40 | *Zymomonas mobilis* | -235 | 2 | [26] |
| 2 | Glucose to lactate | 0.30 | *Lactococcus lactis* | -197 | 2 | [27] |
| 3 | Glucose to butyrate and hydrogen and $CO_2$* | 0.12[2] | *Clostridium tyrobutyricum* | -264 | 3 | [28] |
| 4 | Glucose to propionate, acetate, hydrogen and $CO_2$ | 0.22[2] | *Propionibacter avidum* | -288 | 3 | [29] |
| 5 | Glucose to ethanol, acetate, formate, hydrogen and $CO_2$ | 0.21 | *Citrobacter* sp. CMC-1 | -226 | 3 | [30] |
| | Secondary fermentative pathways | | | | | |
| 6 | Lactate to propionate, acetate and $CO_2$* | 0.40[1] | *Clostridium homopropionicum* | -55.2 | 0.33 | [31] |
| 7 | Lactate and acetate to butyrate, hydrogen and $CO_2$* | 0.18[3] | *Eubacterium hallii* | -45.7 | 0.5 | [32] |
| 8 | Ethanol to propionate, acetate and $CO_2$* | 0.12[1] | *Pelobacter propionicus* | -36.0 | 0.33 | [31] |
| | Other relevant catabolic pathways | | | | | |
| 9 | Lactate and sulphate to acetate, $CO_2$ and $H_2S$* | 0.070[2] | *Desulfovibrio vulgaris* | -85.6 | 1 | [33] |
| 10 | $H_2$ and $CO_2$ to methane* | 0.060 | *Methanolacinia paynteri* | -131 | 0 | [34] |
| 11 | $H_2$ and $CO_2$ to acetate | 0.056 | *Acetobacterium woodii* | -94.9 | 0.5 | [35] |
| 12 | Ethanol and acetate to butyrate* | 0.036 | *Clostridium kluyveri* | 2.44 | 0.4 | [36] |

*catabolic reactions (potentially) harvesting ATP using an ETC
[1]including a vitamin solution and measured at 28°C
[2]measured at 37°C
[3]measured at pH 6.5 and 37°C

When looking at glucose consuming catabolic reactions, low energy yielding reactions, such as lactic acid production ($\Delta G^{0'}$=-197 kJ $mol_S^{-1}$) and solely ethanol production ($\Delta G^{0'}$=-235 kJ $mol_S^{-1}$) are accompanied by higher growth rates (Table 1.2). A reason for this apparent rate vs. energy trade off is discussed further in **Chapter 4 and 6**. Fermentative products such as lactate and ethanol can be used as a substrate by propionate producing bacteria, with lactate utilising bacteria being relatively fast compared to ethanol consuming propionate producers (Table 1.2). Lactate consumption will be discussed in **Chapter 4**. In a fermentative ecosystem, other relevant catabolic pathways can occur such as sulphate reduction and methanogenesis, which are relatively slow

processes (6-8 times lower $\mu$-values) compared to fermentative processes (Table 1.2). Hydrogen and $CO_2$ can also be used to form acetate, which is termed homoacetogenesis [4]. Ethanol can also be used in a process called chain elongation, to elongate acetate to butyrate. Ethanol-based chain elongation is argued to rely solely on SLP in the well characterised model organism *Clostridium kluyveri* [37], though Wang *et al.* have shown the activity of electron bifurcation in *C. kluyveri* [38]. Concluding, fermentative microorganisms exhibit relatively high growth rates compared to sulphate reducing, methanogenic or chain elongating microorganisms. This kinetic knowledge was used to design the experiments presented in this thesis, as growth rates can be controlled using bioreactor-based enrichment culturing.

## 5.1 Mixed culture fermentation in an industrial context

The concept of mixed culture fermentation can be placed in an industrial setting where its purpose is to provide consumers with biobased products. MCF-based processes are able to use a wide variety of biobased resources, such as food waste, agricultural residues and waste water containing fermentable carbohydrates (Figure 1.7). By directing product formation to a certain desired product spectrum novel bioprocesses can be designed. This concept is fundamentally different from pure culture based industrial production processes, where *a priori* a certain microbial strain is chosen. This strain is often genetically modified to perform the desired conversion. Mixed culture-based processes can use diluted streams, which are expensive to sterilise, and mixed cultures are more resilient to shifts in environmental conditions and bacteriophage infections. Pure cultures on the other hand offer higher yields and microbial strains can be designed to produce thermodynamic and kinetic unfavourable products.
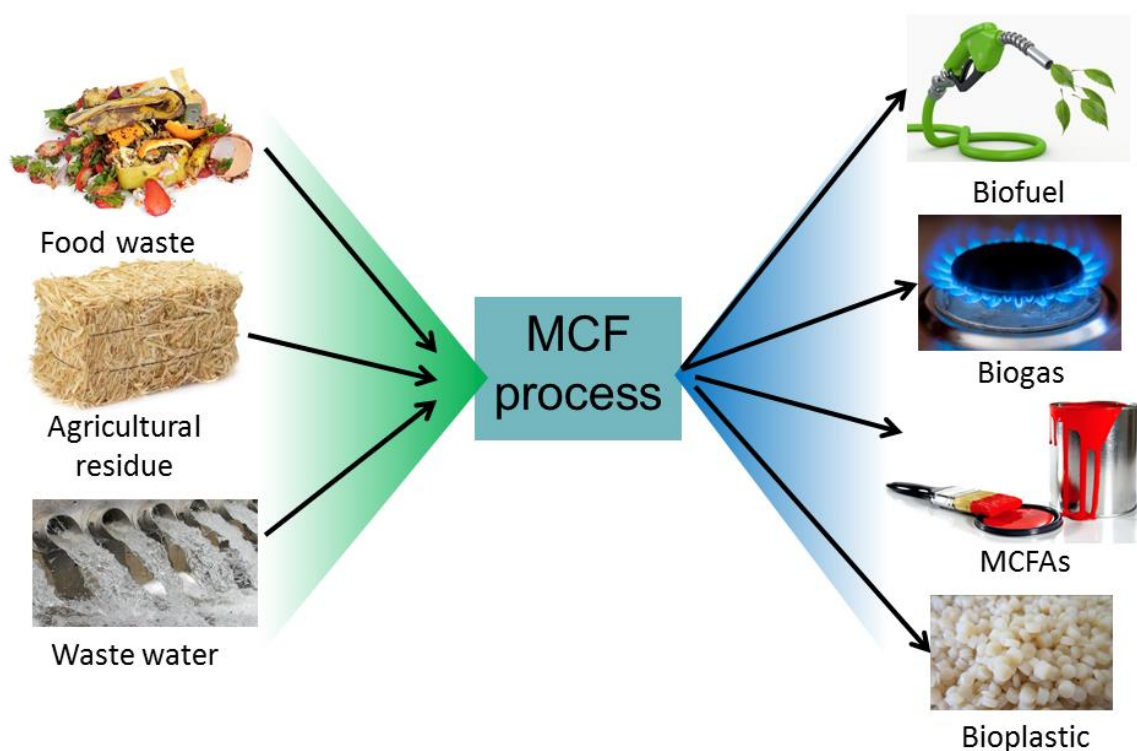


*Figure 1.7*: *Suitable streams that can be used in MCF-based process can be converted to biofuels such as bioethanol, biogas (methane), medium chain fatty acids (MCFAs, such as valerate, $C_5$) and bioplastics (such as PHA and PLA).*

Biofuels, bioplastics, biogas and medium chain fatty acids (MCFAs) are relevant products that can be produced in integrated MCF bioprocesses (Figure 1.7). Examples of biofuels are methanol, ethanol and butanol. Bioplastics can be polyhydroxyalkanoates (PHA) and polylactic acid (PLA). Non-purified biogas is a mixture of methane and $CO_2$ and contains ammonia and hydrogen

sulphide ($H_2S$). MCFAs are fatty acids from five to fourteen carbon lengths. The industrial opportunities for MCF processes are quite extensive, as will be introduced in the following seven sections.

## 5.2 Ecology based design of industrial fermentative bioprocesses

Five and six carbon sugars can be fermented to the VFAs acetate, propionate and butyrate (Figure 1.8). The conversion of lignocellulosic biomass using a VFA based process has been termed the "carboxylate platform" by Holtzapple and Granda [39] and these VFAs can be directly recovered as products or used to produce MCFAs, PHA or methane. Under low pH conditions (pH<6.25), hydrogen is co-produced when producing VFAs. A substantial amount of research has been contributed to hydrogen production through fermentation, usually termed dark fermentation an reviewed by Mishra *et al.* [40]. Ethanol and $CO_2$ can be sole end products of fermentation, though very little experimental effort is taken using mixed cultures for this production platform. Lactic acid production has received recently a new interest from research, mainly focussing on either direct lactate recovery [41] or chain elongation proceeding through the "lactate" route [42].
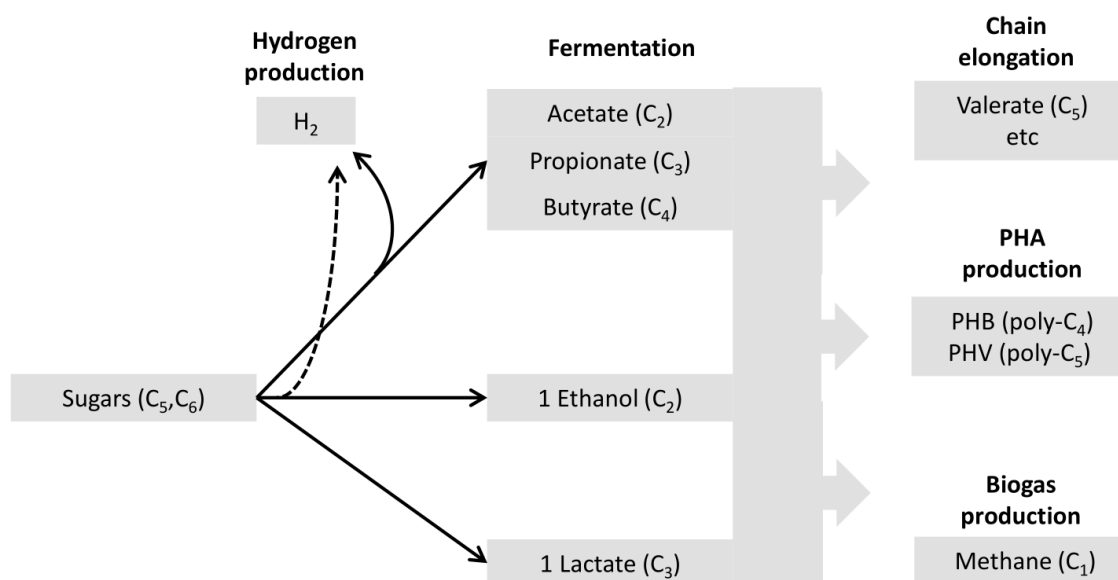
**Figure 1.8**: *Sugars present in feedstocks or waste streams can be directed to hydrogen through the production of VFAs or ethanol using mixed culture fermentation. Ethanol can also solely be produced, as for lactate. Three second step processes are listed which utilise fermentation products, chain elongation (i), PHA production (ii) and biogas production (iii).*

## 5.3 Biogas production and market

Biogas production is the most studied and most employed technology that uses a MCF approach. The execution of biogas production and recovery is simple and effective when compared to the production of soluble organic compounds such as ethanol, lactate and VFAs. Product separation occurs *in situ* in one single reactor. Biogas production can help to close carbon loops on an industrial site. Waste or residual streams containing organic carbon, also expressed as chemical oxygen demand (COD), can be converted to biogas. COD refers to the oxygen needed to oxidise these compounds to $CO_2$ in an aerobic process. The value of MCF studies is limited for enabling biogas production, as the technological bottlenecks are (i) poor hydrolysis of residues and needs for pre-treatment [43], (ii) ammonia inhibition when co-digesting manure [44] and (iii) VFA accumulation during methanogenesis, specifically propionate accumulation [45].

A single bioreactor and limited purification are used to obtain a usable biogas product. Methane production can be performed from a large variety of feedstocks, ranging from agricultural crops to waste water treatment sludge residues [45]. Feedstocks can be liquid or solid, even landfills with filled municipal waste can be converted into biogas production sites [8]. Biogas production generates a residual liquid fraction, which can be treated as waste water and a residual solid fraction, which can be utilised as fertiliser in agriculture. Biogas can be upgraded to have a similar heating value as that of natural gas. It has been estimated in 2013 that in the Netherlands a typical natural gas grade biogas price was around 0.50-0.55 €/m$^3$, while the price of natural gas was 0.25 €/m$^3$ [46]. Biogas production offers a simple and valuable way to close material loops but remains to be economically outcompeted by natural gas.

## 5.4 Hydrogen production and market

Hydrogen is currently mostly produced using steam reforming of natural gas, using mainly methane as feedstock [47]. The global hydrogen market is estimated to have a value of 130 billion USD in 2017 and is prospected to grow to 200 billion USD by 2025 [48], fuelled by an increasing use of hydrogen in industrial processes and "the introduction of green technologies", amongst other developments [48]. The hydrogen economy is thus more than 1000 times bigger than the PHA or chain elongation-based economies (<100 million USD per year). Hydrogen can be used as fuel, to produce electricity and to serve as a chemical building block. Hydrogen production is one of the most studied examples of mixed culture fermentation in an industrial context, with 10-20 publications on Scopus from 2008 onwards [49]. It has been postulated in 2004, to be a promising route to valorise waste streams [50], though currently chain elongation and PHA production (combined with MCF) can be argued to show a better economic competitiveness.

Hydrogen production using MCF, also termed biohydrogen production, relies on the emission and capturing of hydrogen from a fermentative ecosystem. Hydrogen is released during the production of VFAs and potentially during ethanol production (Figure 1.8). In anaerobic systems, hydrogen is in equilibrium with formate and depending on the pH the electrons released during fermentation are released as hydrogen or formate [51]. Hydrogen yields using mixed cultures that ferment glucose (or equivalent substrates) have yielded a maximum of 3.84 mol hydrogen per mol glucose-equivalent [49]. Further hydrogen production from VFAs can be achieved using photo-fermentation, a process that uses light to direct the electrons in VFAs to hydrogen [49], *e.g.* using purple non-sulphur bacteria. A coupling to biogas production is assumed to yield the most economic feasible process [49]. Summarising, the use of MCF to produce hydrogen in an economically feasible is yet to be proven possible using targeted pilot scale experiments and techno-economic evaluations.

## 5.5 Lactate production and its market

Lactate and ethanol are similar fermentative products as both contain 12 electrons and can thus be produced without redox equivalents from glucose or xylose. These products yield a 10-30% lower energetic yield compared to propionate and butyrate formation when produced from glucose (Table 1.2). Lactate is formed directly from pyruvate and has the lowest energetic yield per glucose of all the considered catabolic pathways (Table 1.2). Lactate production is commonly performed by pure cultures of lactic acid bacteria in industry, such as *Bacillus* and *Lactobacillus* species [52]. Lactate can be purified from a fermentation broth which involves considerably more downstream processing than biogas or bioethanol production. Lactate can be sold as end product, with applications in food and cosmetic, as well as in various industrial processes. Lactate can also be polymerised to poly lactic acid (PLA), a bioplastic which can be designed to be biodegradable under thermophilic conditions [53]. PLA offers the possibility to replace polyethylene, polypropylene and polystyrene and is sold at bulk prices of 3-4 USD per kg. The lactic acid market was valued at 2.2 billion USD in 2017 and is projected to grow to 8.8 billion USD in 2025, fuelled mainly by the demand in cosmetics and pharmaceuticals [54].

## 5.6 Ethanol production and its market

*Saccharomyces* pure cultures are used often in industry for ethanol production processes, such as beer and wine making or bioethanol production [4]. Stoichiometrically, ethanol formation can also be coupled to acetate production, which yields 1 mol of formate or hydrogen per mol of ethanol (Appendix II), as is observed for *Enterobacteriaceae* species such as *Escherichia coli* [4] or *Citrobacter* species (Table 1.2). This fermentation stoichiometry is further discussed in **Chapter 2 and 3**. The global ethanol market was estimated to be 108 billion litres in 2017 and was worth 39 billion USD [55]. The average ethanol price in the USA was 0.36 USD per litre or 0.28 USD per kg in 2017 [55]. This is low compared to lactic acid, which is sold on average at 1.7 USD per kg on average in 2018 [54]. Prices have decreased from 2011 onwards leading to a more unprofitable market situation [55]. Bioethanol is produced globally using a (semi-)pure culture approach, offering the advantage of relatively high yields (>90% on carbon basis) and high titres (>100 g L$^{-1}$ of ethanol).

Ethanol can be directly produced as sole fermentation product using fermentative mixed cultures. Enrichment cultures with mixtures of starch and glucose have been observed to produce mixtures of lactic acid and ethanol, with little acetate production [56]. Bioethanol production facilities operated in Brazil are often operated in an "open" fashion, allowing mixtures of yeast strains to dominate these fermentations [57]. The combination of high inoculum amounts of starter cultures (i), acidic treatment with sulphuric acid when recycling the cells (ii) and incidental usage on antibiotics (iii) is likely to lead to the selection of mainly yeast cells performing ethanol production using sucrose obtained from sugar cane. The bioethanol case proves to be a challenging business case and relies on government policies in the form of obligatory blending with fossil fuels and subsidies.

## 5.7 MCFA production through chain elongation and its market

MCFAs are currently produced by hydrolysing larger length fatty acids from plant-based resources. The European oleochemical industry currently produces MCFAs from imported resources such as coconut, palm and kernel oils, with a focus on the production of $C_{10}$ to $C_{14}$ fatty acids. The market for shorter chain MFCAs ($C_5$ to $C_8$) is currently very small (<100 million USD per year), but promises to grow fast with possibilities of using these compounds as growth promotor for livestock and as chemical building block. MCFAs can be produced through chain elongation using mixed cultures. This bioprocess has underwent a renewed interest to function as an industrial alternative to biogas production [42]. Directing carbohydrates into lactic acid can be coupled to chain elongation (Figure 1.8), as lactic acid is a substrate for this bioprocess [58]. Ethanol can also be used as substrate for chain elongation [59]. Currently an ethanol consuming MCFA producing process is commercialised by Chaincraft B.V., through the running of a demonstration plant producing kilotonnes of MCFA product annually in Amsterdam, the Netherlands [60]. Thus, MCFA production shows a potentially healthy business case.

## 5.8 PHA production and its market

The production of PHA is mainly dominated by the production of poly-3-hydroxybutyrate (PHB) by using pure cultures that utilise sugars or propionic acid [61], such as the company Yield10 Bioscience (formerly Metabolix). Poly-3-hydroxyvalerate (PHV) or higher carbon chain fatty acids are also produced in a limited amount. The market for PHA is small compared to PLA production, as it is predicted to reach a market value of 120 million USD in 2025 [62], though it is predicted to grow fast (>15% compound annual growth rate, CAGR). Prices currently range from 2-3 USD per kg and PHA offers to be an excellent substitute solely or in blends for polyethylene, polypropylene, polystyrene and polyethylene terephthalate (PET). Its biodegradability can be tuned also and it typically is more biodegradable than PLA [63].

PHA production using mixed cultures relies on the aerobic enrichment of bacteria that store PHA using VFAs [64]. High yield (>50% w:w) PHB accumulation has been shown using enrichment cultures fed with acetate [65], butyrate [66], while high yield PHV accumulation has been shown with propionate [67]. Enrichment culturing showed that lactate can be used to produce selectively PHB [68]. Ethanol was shown to be used to produce PHB using a pure culture of *Paracoccus denitrificans* [69], though Tamis *et al.* have demonstrated that that ethanol presence in the feed stream to the PHA production stage is unfavourable for PHA production [70]. In the same pilot study, coupled MCF and PHA accumulation was shown to yield 70% w:w inside the PHA storing cells [70]. Summarising, PHA production using VFAs promises a healthy industrial feasibility.

## 6 Developing ecology-based bioprocesses by using enrichment cultures

The aim of this thesis is to explore, understand and apply the ecology of fermentative ecosystems. Therefore, in **Chapter 2** the effect of continuous feeding as opposed to sequential batch feeding was tested for both xylose and glucose. CSTR set ups were used to study continuous feeding as opposed to pulse feeding using SBR set ups. These enrichments are evaluated on their thermodynamic, kinetic, bioenergetic performances in parallel analysing the microbial community structures. These results are used to formulate a general concept how fermentative pathways compete in these environments.



*Figure 1.9: Typical bioreactor enrichment set-ups used in this thesis. Here, the bioreactors ran in parallel to study xylose and glucose fermentations in SBR mode are shown, ran in September/October 2017.*

Temudo [6] has attempted to understand the impact of mixtures of xylose and glucose on continuous-fed fermentative enrichment cultures, discussing that when adding a second fermentable substrate generalist populations will be favoured over specialist populations. **Chapter 2 and 3** further explore this hypothesis using a complementary approach of microscopy-based and DNA-based techniques. **Chapter 2 and 3** together comprise a 6-enrichment dataset, where single substrates can be compared to mixed substrates. An aim was to validate the specialist and generalist concept in both continuous and sequential batch culturing. Carbon catabolite repression is a mechanism observed for multiple microbial species [71]. **Chapter 3** aims to evaluate this concept using enrichment cultures with mixtures of xylose and glucose.

The ecological niche of lactic acid bacteria is evaluated in **Chapter 4**. Using an SBR enrichment culture approach the niche of glucose fermentation in mineral medium or complex medium is evaluated. A complex medium was designed to promote the growth of lactic acid bacteria, containing peptides and 9 B vitamins**. Chapter 4** aims to evaluate the metabolisms and community structures that are enriched for, using a similar approach as Chapter 2 and 3. If carbohydrates can be directed specifically to lactate using a MCF process, lower value resources can be used compared to the currently widely used sucrose and starch resources. Ultimately, this can enable a cheaper and more sustainable lactic acid production platform

The origin of symbiotic microbial relationships is being discussed in **Chapter 5**, using a combined approach of metagenomics, metabolomics and culturing both mixed and pure populations. Hypothetically, the competition for a single limiting substrate should lead to the dominance of a single microbial species. Cooperative mechanisms (Figure 1.2) can increase the microbial diversity of a single substrate limited enrichment. **Chapter 5** aims to provide experimental proof for such cooperative mechanisms using an enrichment culture environment.

**Chapter 6** presents a set of conclusions drawn in this thesis. Furthermore, in **Chapter 6** several valuable research opportunities are proposed using enrichment cultures. These experiments can be useful to understand different relevant ecologies in fermentative processes. The kinetic and bioenergetic trade-off concept proposed in **Chapter 2** is put into an enzymatic context. **Chapter 4** is outlined in the context of the hypothesis of resource allocation and enzymatic substrate limitation. Future research is further directed in a multi-level approach, as presented in **Chapter 5,** to understand and evaluate microbial selection in fermentative ecosystems.

# Chapter 2 - Diversity and metabolism of xylose and glucose fermenting microbial communities in sequencing batch or continuous culturing
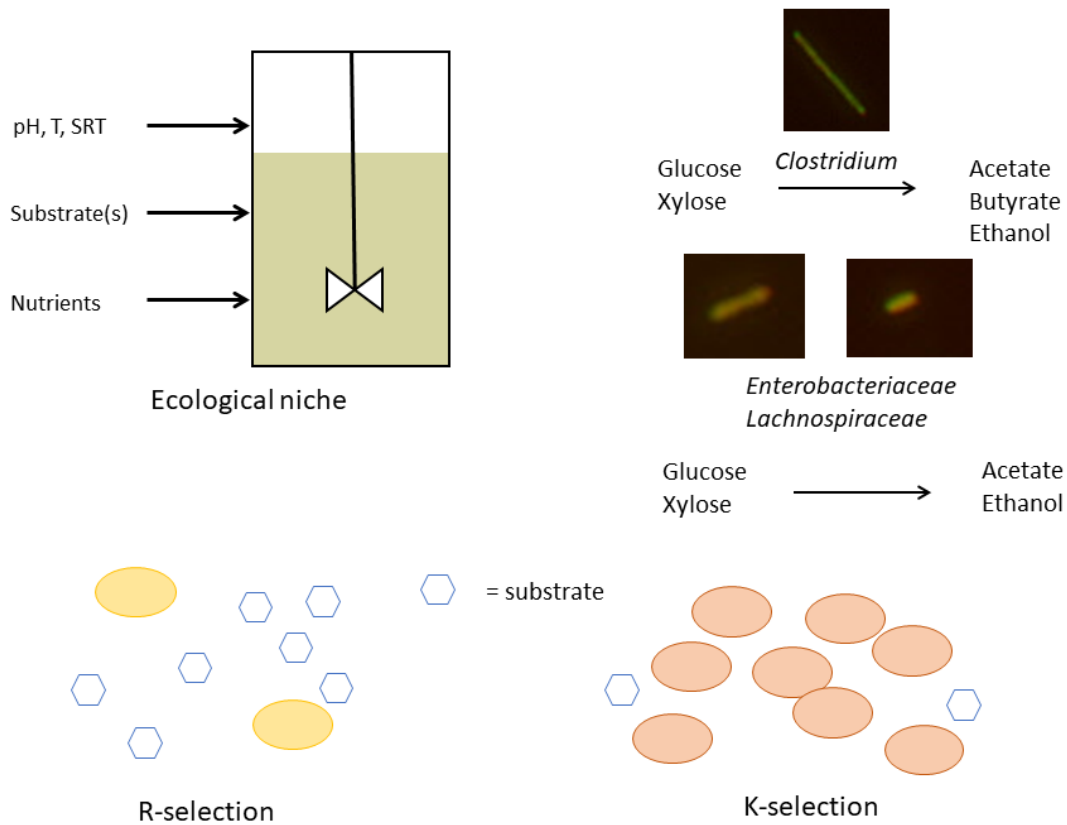
## Abstract

A mechanistic understanding of microbial community establishment and product formation in open fermentative systems can aid the development of bioprocesses utilising organic waste. Kinetically, a single rate-limiting substrate is expected to result in one dominant species. Four enrichment cultures were operated to ferment either xylose or glucose in a sequencing batch reactor (SBR) or a continuous-flow stirred tank reactor (CSTR) mode. The combination of 16S rRNA gene-based analysis and fluorescence *in situ* hybridization revealed no complete dominance of one species in the community. The glucose-fed and xylose-fed SBR enrichments were dominated >80% by one species. *Enterobacteriaceae* dominated the SBRs enrichments, with *Citrobacter freundii* dominant for xylose *and Enterobacter cloacae* for glucose. *Clostridium*, *Enterobacteriaceae* and *Lachnospiraceae* affiliates dominated the CSTRs enrichments. Independent of substrate, SBR communities displayed 2-3 times higher biomass specific rate of substrate uptake ($q_s^{max}$) and 50% lower biomass yield on ATP, to CSTR communities. Butyrate production was linked to dominance of *Clostridium* and low $q_s^{max}$ (1.06 $Cmol_s$ $Cmol_x^{-1}$ $h^{-1}$), while acetate and ethanol production was linked to dominance of *Enterobacteriaceae* and *Lachnospiraceae* and high $q_s^{max}$ (1.72 $Cmol_s$ $Cmol_x^{-1}$ $h^{-1}$ and higher). Overall, more diversity than expected through competition was observed, indicating mutualistic mechanisms might shape microbial diversity.

**Keywords**: Mixed culture fermentation – Bioreactor operation – Microbial diversity – r/K selection – Product spectrum – Kinetics

## Introduction

The global aim of most societies to develop more circular economies [72] urges for a better use of organic waste as a resource. Until now, anaerobic digestion is the most common technology used to valorise this waste in the form of biogas. Several novel bio-based options that provide extra value to resource recovery are arising such as the production of polyhydroxyalkanoates [73], alginate-like exopolymers [74], or medium chain length fatty acids [42]. The first step in these production routes consists of the conversion of polymeric carbohydrates into volatile fatty acids (VFAs) in a mixed-culture fermentative process [75]. The alignment of VFA production to subsequent processing requires the identification of factors that drive product formation in microbial communities as function of process conditions. First attempts to describe steady-state patterns of mixed culture fermentation as function of an environmental parameter have provided incomplete insights in the product formation pathways established [76, 77]. Observed product spectra at neutral pH could not be simulated properly using these models oriented to ATP production maximisation, indicating incomplete model assumptions. To aid model-based developments there is a need for experimental studies giving a more comprehensive insight into fermentation of specific carbohydrates into VFAs.

Xylose and glucose are the most abundant monomers found in lignocellulosic biomass [78]. Fermentation of glucose or xylose can lead to different products, such as lactic acid, ethanol, hydrogen, and VFAs (Figure 2.1). Xylose can be fermented through the pentose phosphate pathway (PPP) or the phosphoketolase pathway (PKP), resulting in a different stoichiometry. Using the PKP, 40% of the carbon is directly converted to acetate, while the remaining carbon enters into glycolysis. In PPP, all carbon is converted to intermediates for glycolysis, thereby bringing all carbon to pyruvate first (Figure 2.1). In the first part of glycolysis, one glucose is converted to pyruvate producing four electrons that can be transferred to NADH. If one acetate is produced, a net amount of one NADH is produced. These electrons cannot be transferred from NADH to hydrogen, as NADH does not possess sufficient energy to drive this reaction (-320 mV and -414 mV for NADH and hydrogen respectively, [24]). Hydrogen is produced through ferredoxin (-400 mV), which is produced when oxidising pyruvate to Acetyl-CoA (Figure 2.1). The NADH surplus is oxidised by other fermentative pathways, e.g. ethanol production, thereby stoichiometrically coupling acetate and ethanol formation. Recently, electron bifurcation has been proposed as a metabolic strategy in *Clostridium pasteurianum* [24] used to conserve energy in fermentation by directly coupling acetate and butyrate formation [79]. This mechanism has been successfully incorporated in balancing of NADH of product spectra over a range of pH values [80].

Microbial enrichment cultures offer a powerful way of studying the establishment of a specific microbial niche [81], depending on the ecological conditions applied, such as pH, temperature, redox couple supplied, nutrients among others. Glucose fermentation has been relatively widely studied, including impacts of pH [51, 82], temperature [83], solids retention time (SRT) [84], redox potential [85], inoculum type [86], or hydrogen partial pressure [87]. Xylose is much less studied but its fermentation has been compared to glucose fermentation previously [88].
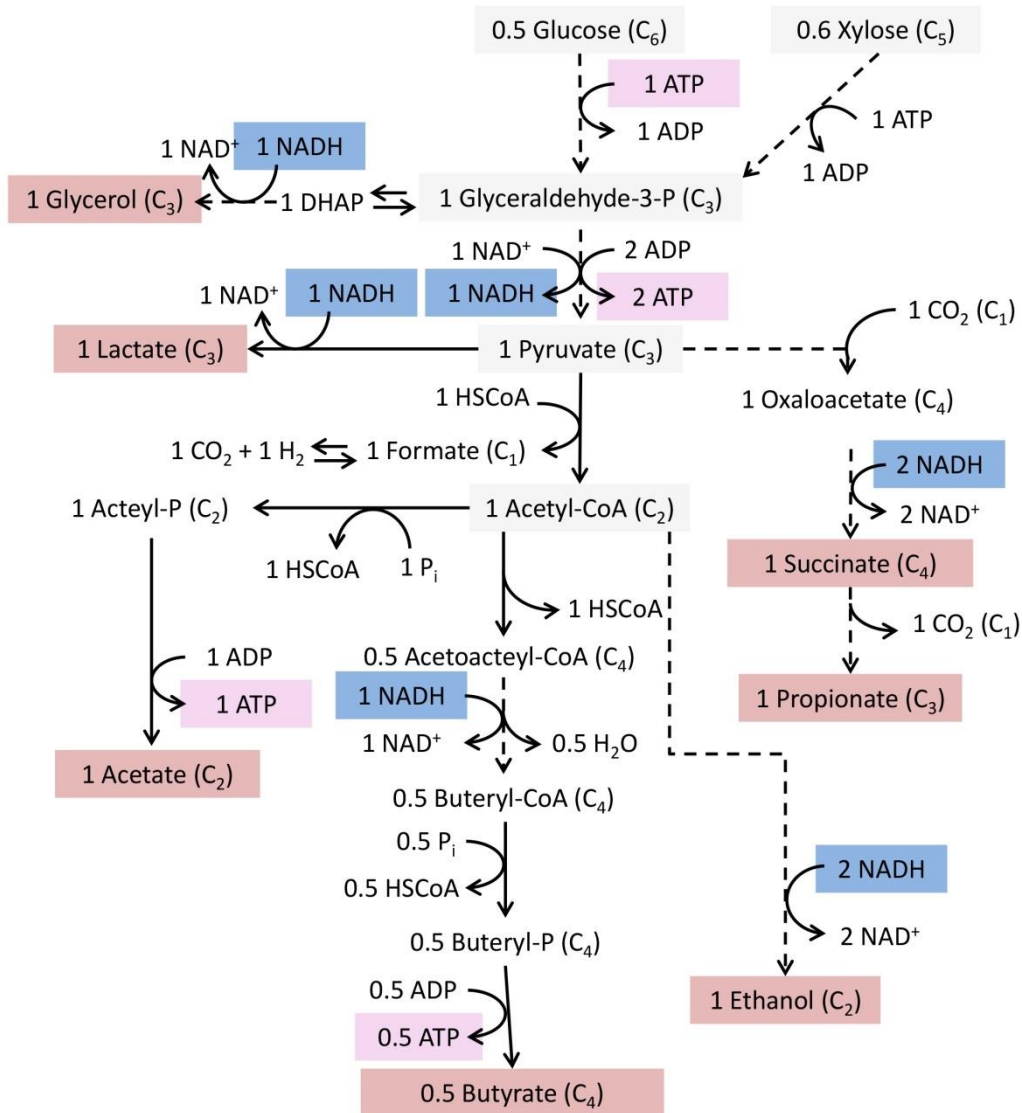
***Figure 2.1****: Intracellular metabolic network for xylose and glucose fermentations. Dashed lines indicate lumped reactions, straight lines indicate single reactions. Xylose comes into the glycolysis through the synthesis of 2 fructose-6-phosphate and 1 glyceraldehyde-3-phosphate, through the PPP. The Emden-Meyerhof-Parnass pathway is used as this is the common type of glycolysis encountered in energy limited anaerobes* [92]*. Figure is made on the basis of Madigan and Martinko* [4]*.*

Most studies have been conducted in continuous-flow stirred tank reactors (CSTR), under which regime one substrate is continuously limiting (*i.e.*, operation at low residual concentration). In CSTR systems, affinity dictates the selection: organisms establishing the lowest residual substrate concentration ($C_s$) will dominate the enrichment [89]. Affinity is governed by both the maximum biomass specific growth rate ($\mu^{max}$) and the affinity constant for substrate ($K_s$), as described by the Monod equation [90]:

$$\mu = \mu^{max} \cdot \frac{C_s}{C_s + K_s} \qquad\qquad (2.1)$$

Organisms competing for a substrate in a CSTR environment can, besides optimising their $\mu^{max}$, optimise their $K_s$ value to actively take up the substrate and dominate the microbial community.

In a sequencing batch reactor (SBR) operation, substrate is supplied in a pulse, leading to a high concentration in the environment of the microorganisms during most of the time that substrate is taken up. Organisms with the highest $\mu^{max}$ will eventually dominate when substrate uptake is directly coupled to growth. The batch selective environment is traditionally used in microbiology to enrich and isolate organisms, using the shake-flask approach in combination with dilution series. Consequently, fast-growing microorganisms are overrepresented in databases of pure cultures [91].

As introduced, microbial growth can be quantified by using the Hebert-Pirt equation for substrate uptake [9]:

$$\mu = Y_{xs} \cdot q_s + m_s \qquad\qquad\qquad (2.2)$$

For both CSTR and SBR environments, $\mu^{max}$ is a selective force, which is a function of the biomass specific rate of substrate uptake ($q_s^{max}$), the biomass yield on substrate ($Y_{x,s}$) and the maintenance rate on substrate ($m_s$) [9].

From a kinetic point of view, the microorganism with the highest competitive advantage in the environment will eventually outcompete the other microorganisms, which is either the highest $\mu^{max}$ (in SBR) or highest "affinity" (in CSTR) on glucose or xylose. Ultimately, we aim to investigate the hypothesis if limiting a single substrate in an enrichment culture leads to the enrichment of a single microbial species. From a competition point of view, one limiting substrate will select for the most competitive microorganism. Given enough generations or SRTs, this microorganism will eventually dominate the enrichment culture.

Next to microbial competition on substrate, the different pathways for product formation are competing within microorganisms. Anabolism needs chemical energy in the form of ATP to synthesize biomass. Under similar anabolic efficiency, the catabolic pathway that yields more ATP per substrate ($Y_{ATP,s}$) leads to the highest $Y_{x,s}$. Harvested ATP can also be used for active substrate transport. Hereby, microorganisms lower their $K_s$ and thereby create a lower $C_s$ to sustain their selection in a CSTR environment. Fermentative microorganisms are known to choose between a high flux pathway (optimizing $q_s^{max}$) or a high yield pathway (optimising $Y_{ATP,s}$), which is best described by lactate versus acetate and ethanol formation in *Lactobacillus casei* [93]. Under CSTR cultivation, at high dilution rates lactate is formed and at low dilution rates acetate, ethanol and formate are formed. Lactate formation yields 2 ATP from 1 glucose, while acetate and ethanol yield 3 ATP from 1 glucose. Thus lactate production is linked to high $q_s^{max}$, while acetate and ethanol production is linked to high $Y_{ATP,s}$. Thus, a microorganism will preferentially involve a metabolic pathway that maximizes $Y_{ATP,s}$ and/or $q_s^{max}$ in a SBR environment and $Y_{ATP,s}$, $q_s^{max}$ and/or $K_s$ in a CSTR environment.

Here, we investigated whether SBR or CSTR environments fermenting either xylose or glucose enrich for an equal microbial community composition and result in equivalent metabolism and kinetics. Three environmental settings were applied to enrich for fermentative microorganisms: (1) a mineral medium with only glucose or xylose as carbon source for fermentation; (2) a combination of temperature, pH, and SRT to select mainly for primary fermentative microorganisms; and (3) suspended cell cultures. The experimental set up was replicated from Temudo *et al.* [88] for a direct comparison of results. The catabolic products, $q_s^{max}$, and $Y_{x,s}$ were measured for each enrichment in steady state in order to verify if a certain stoichiometry was linked to a certain metabolic strategy. In parallel, we analysed the microbial community compositions to test the microbial diversity hypothesis for enrichment on single substrates, and to link community structures to fermentative products and metabolic strategies.

## Materials and methods

### Enrichment

All enrichments were performed in 3-L jacketed bioreactors (Applikon, the Netherlands) with working volumes of 2 L. pH was maintained at 8.0 ± 0.1 using NaOH at 4 mol $L^{-1}$ and HCl at 1 mol $L^{-1}$. Temperature was maintained at 30°C ± 0.1 using a E300 thermostat (Lauda, Germany). The cultures were stirred constantly at 300 rpm. Anaerobic conditions were maintained by sparging the reactor with a flow of 576 mmol $N_2$ $h^{-1}$ and off-gas was cooled to 5°C using a gas condenser. For the SBRs, a hydraulic retention time (HRT) of 8 h was maintained by removing 1 L of culture per cycle under a cycle time set to 4 h. For CSTRs, the HRT was directly linked to the dilution rate applied, which was aimed at 0.125 $h^{-1}$.

The synthetic cultivation medium was identical to the one used by Temudo [6] using 4 g of either xylose or glucose as carbon source per litre (see **Appendix I**). The carbon source and the ammonium, phosphate and trace elements were fed separately from 12.5× concentrated stock solutions and diluted using $N_2$-sparged demineralized water. Connected to the base pump was a pump supplying 3% (v:v) antifoam C (Sigma Aldrich, Germany), which ensured a flow of 3-5 mL $h^{-1}$ or 14-17 mL $cycle^{-1}$. The glucose and xylose solutions were sterilized at 110°C for 20 min.

The inoculum was obtained from cow rumen through a butcher in Est, the Netherlands, and on the same day, transported to lab at room temperature and filtered on 200 μm and aliquoted in 50-mL portions, and frozen at -20°C using 10% glycerol. The seed biomass was then thawed on ice before adding 10 mL to the reactor to start each enrichment culture. When a full first batch was performed the CSTRs were set to continuous mode and the SBRs were set in cycle mode, gradually moving from 24-h to 12-h and 6-h in 3 days to the final desired 4-h cycles to maintain a HRT of 8 h. Steady state was assumed if during a period of at least 5 days no variation in the product concentrations was measured.

### Analytical methods

Samples from the reactors were immediately filtered on 0.45 μm polyvinylidine fluoride membranes (Millipore, USA) and stored at -20°C until analysis. VFAs (formate to valerate), lactate, succinate, ethanol, glucose and xylose were analysed using high performance liquid chromatograph (HPLC) equipped with an Aminex HPX-87H column (BioRad, USA) maintained at 60 °C and coupled to ultraviolet (UV) and refraction index (RI) detectors (Waters, USA), using phosphoric acid at 0.01 mol $L^{-1}$ as eluent. For high butyrate concentrations above 1 mmol $L^{-1}$, samples were analysed using gas chromatography (GC), since butyrate overlapped with ethanol on the RI detector of the HPLC. GC was performed using a Chrompack 9001 (Agilent, USA) equipped with an injector maintained at 180°C, a fused-silica capillary column of 15 m × 0.53 mm HP-INNOWax (Agilent, USA) equilibrated at 80°C for alcohols with helium as carrier gas, and a flame ionization detector set at 200°C. Glycerol was detected using an enzymatic assay relying on glycerokinase, pyruvate kinase and L-lactate dehydrogenase, measuring NADH depletion at 340 nm (Megazyme, Ireland).

The off-gases were monitored on-line for $H_2$ and $CO_2$ by a connection to a NGA 2000 MLT 1 Multicomponent analyser (Rosemount, USA). Data acquisition (base, $H_2$, $CO_2$) was made using a BBI systems MFCS/win 2.1 (Sartorius, Germany).

Biomass concentration was measured using a standard method which relies on centrifugation to separate the cells from the medium [94]. This analysis was coupled to absorbance measurement at 660 nm to establish a correlation. Absorbance values were used to calculate the biomass concentration during the batch experiments.

## Cycle analysis

To characterise one cycle in SBR mode, one full cycle was sampled and product and biomass concentrations were measured in parallel to $H_2$ and $CO_2$ in the off-gas. In the CSTRs, one litre of volume was removed and one litre of medium was added to finally obtain a concentration of 4 g $L^{-1}$ of either xylose or glucose together with a stoichiometric amount of other nutrients. Sampling and off-gas analysis were carried out as in the SBRs.

## Microbial community analysis

Genomic DNA was extracted using the Ultra Clean Soil DNA extraction kit (MOBIO laboratories, USA) following manufacturer's instructions, with the exception of heating the samples for 5 minutes at 65°C prior to bead beating. High molecular weight DNA was obtained (>10 kb) with a concentration of 10 ng $\mu L^{-1}$ or higher. Extracted DNA was stored at -20°C until further use.

Analysis of 16S rRNA gene-based amplicon sequencing was conducted to get an overview of the predominant populations in the enrichments in time. The extracted DNA was sent for amplification and sequencing at a commercial company (Novogene, China). Amplification was achieved using the universal primer set 341f / 806r targeting the V3-V4 region of the 16S rRNA gene (Table 2.S1). All polymerase chain reactions (PCR) were carried out in 30 µL reactions with 15 µL of Phusion® High_fidelity PCR Master Mix (New England Biolabs, USA), 0.2 µmol $L^{-1}$ of forward and reverse primers and 10 ng template DNA. Thermal cycling started with an initial denaturation at 98°C for 10 s, annealing at 50°C for 30 s and elongation at 72°C for 60 s and ending with 72°C for 5 min. These pools of amplicon sequences were then sequenced using an IlluminaHiSeq2500 platform. The sequencing datasets were cleaned and trimmed according to Jia *et al.* [95] and processed with Qiime [96] using UCLUST with a 97% stringency to yield operational taxonomic units (OTUs). OTUs were taxonomically classified using the RDP classifier [97] with 0.85 confidence interval against the Greengenes database release of August 2013 [98]. Double check of OTUs identity factors was then obtained by alignment against the NCBI RefSeq database using the basic alignment search tool for nucleotides (BLASTn) [99].

Cloning-sequencing was conducted to obtain species level information. The near-complete 16S rRNA gene was amplified using the primers GM3f and GM4r (Table 2.S1). The PCR products were purified using QIAquick PCR purification kit (QIAGEN, Germany), ligated, and transformed into competent *Escherichia coli* cells using the TOPO TA Cloning Kit (Invitrogen, USA). Transformed cells were plated on Luria-Bertani medium plates containing 50 µg kanamycin $mL^{-1}$. After overnight incubation at 37°C, clones were randomly selected for amplification of the 16S insert into the PCR4-TOPO vector using the M13f and M13r primers (Table 2.S1). Depending on the diversity of the sample, 8 to 55 clones were sequenced using Sanger sequencing (Baseclear, the Netherlands). The first and last 100 bp were removed using CodonCode aligner, as sequence quality was insufficient in these regions. Qiime processing was performed on the sequences as described above using a similarity criterium >99% which is defined to be the minimum similarity between species [100]. BLASTn was used to retrieve the identity of each species, and BLAST results with the same species but a different strain were grouped together for phylogenetic resolution at species level. The closest relates strain was then used to retrieve genomic information. Sequences obtained are deposited under the BioProject accession number PRJNA505600 (raw merged amplicon reads) and MK185473 – MK185614 (1450 bp 16S genes) in the NCBI database.

Cell fixation and fluorescence *in situ* hybridisation (FISH) were carried out as described by Johnson *et al.* [65] using the probes listed in Table 2.S2, except that hybridization was carried out overnight. Additionally, DAPI staining was used to stain all microbial cells by incubating the multi-wells microscopy slides of fixed cells with 10 µL of a solution of 10 mg DAPI $mL^{-1}$ per well for 15 min. The samples were analysed using an epifluorescence microscope (Axioplan 2, Zeiss,

Germany). Digital images were acquired using a Zeiss MRM camera together with Zeiss imaging software (AxioVision version 4.7, Zeiss, Germany). The 1000x magnified images were improved by setting the 1x sharpening. Three images were taken at 400x and exported as TIFF and used for quantification of the cell surface using the QUIPS feature in Leica QWin V3 (Leica, Germany).

**Modelling of the cycle analysis**

To obtain the $q_s^{max}$ and $\mu^{max}$ for the CSTRs from the cycle analysis, a model was constructed. Herbert-Pirt equation for substrate uptake was simplified by neglecting maintenance, as maintenance is not measured and is assumed to be a small contribution compared to $q_s^{max}$:

$$\mu = Y_{xs} \cdot q_s \qquad\qquad (2.3)$$

Monod kinetics were used to describe the growth rate as a function of the substrate concentration at a value of 0.1 mmol $L^{-1}$ of either xylose or glucose. The model estimated $C_s$ and $C_x$ by varying the biomass and substrate concentration at the start of the cycle analysis ($C_{x,0}$, $C_{s,0}$) and $Y_{xs}$ and $q_s^{max}$ values giving the best fit, and a boundary value of $\mu$ is zero was applied when $C_s$ was zero. The modelled values were then optimised to the measured data with a minimisation of the sum-squared error, using the non-linear solver in Microsoft Excel (2010).

**Analysis of on-line data collected from the bioreactors**

For SBRs, the $\mu^{max}$ was calculated per cycle using the recorded base dosage values. Microbial growth was directly correlated to the base consumption due to acid production in fermentation (Figure 2.S3). A script was developed in Matlab (version 2014, USA), further explained in the supplementary information (SI) section.

**COD and carbon balances**

During steady state carbon and chemical oxygen demand (COD) balances were set up using the elemental matrix given in Table 2.S4. COD and carbon balances were set up by multiplying the values in the Table 2.S4 with the in- and outgoing rates in the reactor, while the NADH, ATP and Gibbs energy balances were set up by multiplying the values in table 2.S4 with the yield on glucose. Data reconciliation was used to obtain closed balances for H, C, O, N and charge using the method described by van der Heijden *et al.* [101]. These balances were used to calculate the Gibbs energy of dissipation.

Carbon and COD balances were set up for the cycle analyses by subtracting the amount of carbon or COD in the compounds measured at a time in the cycle from the measured available carbon or COD at the start of the cycle.

# Results

**Xylose and glucose fermentation product spectra are similar in SBRs and different in CSTRs**

Four different enrichment reactors were operated and analysed for their main products in liquid and gas phase after steady-state was established; this was obtained after 20 SRTs for all enrichments. The glucose SBR exhibited the largest shift in product spectrum during the adaptation, as initially acetate and propionate were the dominant products which changed to acetate and ethanol as dominant products after 18 SRTs. The product spectra in the xylose and glucose SBR enrichments was very similar, dominated by a catabolic reaction producing ethanol and acetate (Figure 2.2A), coupled with hydrogen and formate production (Figure 2.1). Regarding the by-products formed, the xylose SBR enrichment produced more succinate, while the glucose SBR enrichment produced more propionate and lactate.
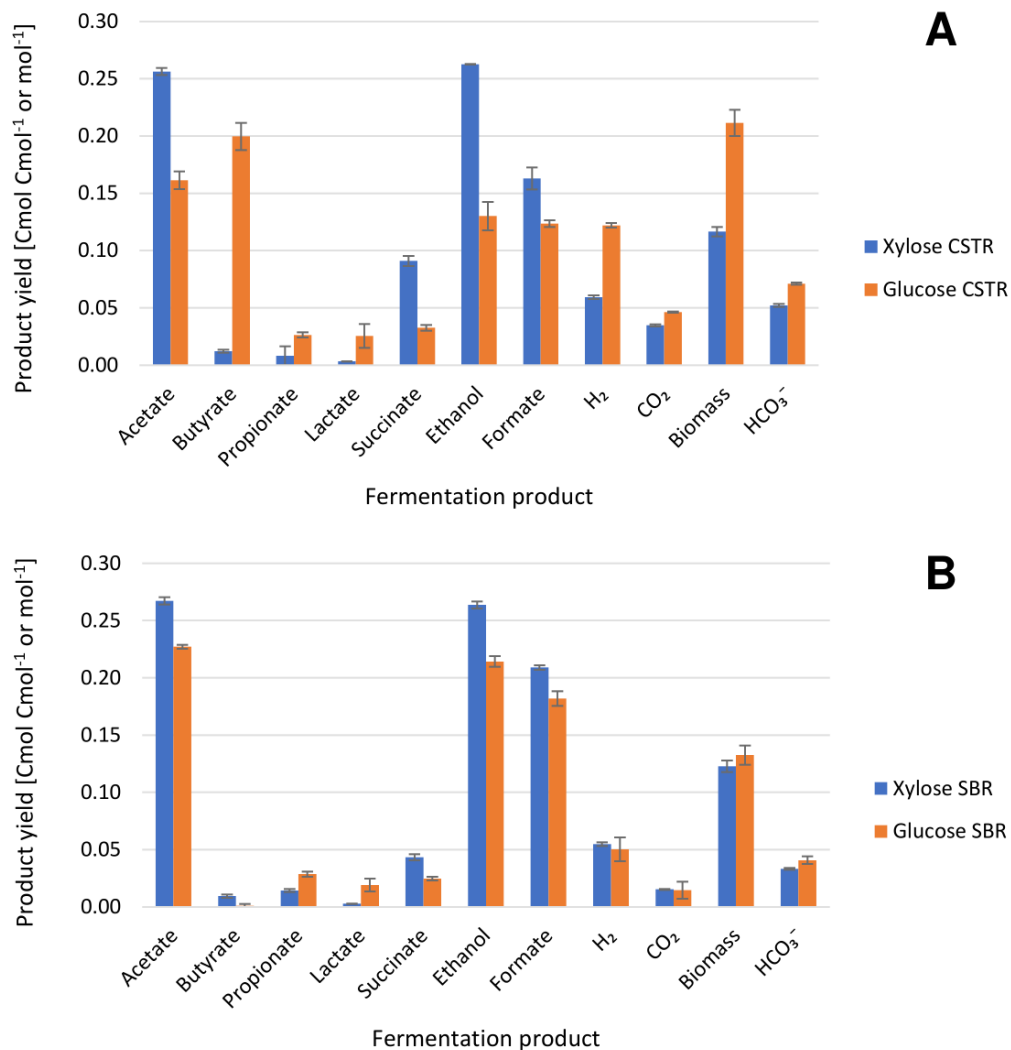
**Figure 2.2**: *Product spectra of mixed culture fermentations of SBRs (A) and CSTRs (B) determined in steady state (n=3). $H_2$ is plotted as mol per Cmol substrate. $HCO_3^{-1}$ is estimated using a $k_La$ value of 5.34 $h^{-1}$.*

The xylose CSTR enrichment also had a product spectrum dominated by acetate and ethanol (Figure 2.2B), coupled to the production of hydrogen and formate. In the glucose CSTR, butyrate was a dominant product, followed by acetate and ethanol (Figure 2.2B). Both these catabolic pathways were coupled with hydrogen and formate production. Regarding the by-products, similar to the SBRs, the glucose CSTR enrichment produced more propionate and lactate, while

the xylose CSTR enrichment produced more succinate, with a significant yield of succinate production in this enrichment of 0.09 Cmol $Cmol_S^{-1}$ succinate formed. Summing up, the glucose SBR and the xylose SBR and CSTR enrichment displayed similar product spectra dominated by acetate and ethanol, while the glucose CSTR showed a mixed product spectrum of butyrate, acetate and ethanol. Glycerol was not detected in a significant amount in any of the enrichments, to a maximum amount 0.002 Cmol per $Cmol_S^{-1}$. Glycerol was detected up to 0.1 Cmol $Cmol_S^{-1}$ by Temudo *et al.* [88].

## Carbon and COD balances were nearly closed in all enrichments

For all enrichments the carbon and chemical oxygen demand (COD, *i.e.*, electron) balances could be closed from the measured products at 95% and 105%, respectively (Table 2.S3). Only in the glucose SBR enrichment a significant amount of 10% of carbon and COD could not be recovered in the outflows of the reactor. A characteristic peak at a retention time of 19.1 min was present on the HPLC UV channel for the glucose SBR which could not be identified but was confirmed to be neither 1,3-propanediol nor malate, fumarate, 2,3-butanediol, acetoin or hydroxyvalerate.

## No storage response or sequential fermentation during cycle analysis

For all four enrichments a pulse experiment was performed, in which the substrate and products were measured in time and used to set up a carbon and COD balance over the cycle. A typical storage response would show COD "disappearing" during the initial fermentation phase until the substrate is depleted, while it reappears after substrate depletion as formed products. No such response was observed in both the CSTR and SBR enrichments (Figure 2.S2) and no sequential conversion of intermediate fermentation products was detected in the cycle analysis in SBRs (Figure 2.S3).

## Fast kinetics for SBR enrichments and high biomass yield for CSTR enrichment

At steady state, the yield of biomass formation on substrate was determined in all four enrichments (Table 2.1). There was no significant difference in biomass yield between the glucose CSTR enrichment reported here and by Temudo *et al.* [88]. The xylose CSTR enrichment displayed a 43% lower biomass yield than the glucose CSTR, and a 25% lower value compared to the xylose CSTR enrichment reported by Temudo *et al.* [88]. The glucose SBR, the xylose SBR and the xylose CSTR enrichment showed similar biomass yield values.

*Table 2.1*: $Y_{x,s}$ calculated on the basis of TSS/VSS measurements at steady state (n=3). For the SBRs, $\mu^{max}$ was obtained from on-line fermentation data (Figure 2.S6). For the CSTRs, $q_s^{max}$ was obtained from a substrate pulse experiment and subsequent fitting the substrate concentration data, with $R^2$ values of 0.97 and 0.92 for xylose and glucose respectively. The SBR $\sigma_{qsmax}$ is calculated using error propagation and the covariance of the $\mu^{max}$ and $Y_{x,s}$ values. The CSTR $\sigma_{qsmax}$ is calculated using error propagation and the covariance of the $C_s$ and $C_x$ measurement, while $\sigma_{\mu max}$ is calculated using error propagation and the covariance of $q_s^{max}$ and $Y_{x,s}$.

| Enrichment | $Y_{x,s}$ (Cmol$_x$ Cmol$_s^{-1}$) | $q_s^{max}$ (Cmol$_s$ Cmol$_x^{-1}$ h$^{-1}$) | $\mu^{max}$ (h$^{-1}$) | Reference |
|---|---|---|---|---|
| Xylose SBR | 0.12 ± 0.01 | 2.28 ± 0.10 | 0.28 ± 0.01 | This study |
| Glucose SBR | 0.13 ± 0.01 | 3.41 ± 0.24 | 0.45 ± 0.01 | This study |
| Xylose CSTR | 0.12 ± 0.01 | 1.72 ± 0.02 | 0.22 ± 0.01 | This study |
| | 0.16 ± 0.01 | 1.01 | 0.16 | Temudo *et al.* [88] |
| Glucose CSTR | 0.21 ± 0.01 | 1.06 ± 0.02 | 0.22 ± 0.01 | This study |
| | 0.21 ± 0.01 | NA | NA | Temudo *et al.* [88] |

Through analysis of the on-line fermentation data the $\mu^{max}$-value for each fermentation cycle could be determined for the SBR enrichments (see SI, figure 2.S5 and 2.S6). A cycle analysis in the CSTR enrichment cultures was used to estimate $q_s^{max}$. The actual $q_s$-value in the xylose CSTR enrichment was 1.06 $Cmol_S$ $Cmol_X^{-1}$ $h^{-1}$, which was 38% lower than the measured $q_s^{max}$. The actual $q_s$-value in the glucose CSTR enrichment was 0.55 $Cmol_S$ $Cmol_X^{-1}$ $h^{-1}$ which was 48% lower than the maximal rate of glucose uptake. The xylose CSTR enrichment exhibited a 62% higher $q_s^{max}$-value than the glucose CSTR enrichment. The $q_s^{max}$ value found for the xylose SBR enrichment was statistically significantly lower (33%) than for the glucose SBR enrichment (Table 2.1, p = 0.002).

**Microbial community analyses highlighted higher diversity with xylose**

Amplicon sequencing of the V3-V4 region of the 16S rRNA gene was used to obtain a relative snapshot of the dynamics of the community over time. Then, FISH analysis with three different probes targeting the 16S rRNA of populations of the genus *Clostridium* and of the families of *Enterobacteriaceae* or *Lachnospiraceae* was used to analyse the microbial communities in the enrichments. Lastly, clone libraries were created of the full 16S gene to obtain species-level information of the communities. Microbial diversity was evaluated by the abundance and number of families or genera present.

The xylose SBR enrichment was dominated by *Enterobacteriaceae* (Figure 2.3, Table 2.2, Figure 2.S7) and a side population of *Lachnospiraceae* and *Clostridium* (Table 2.2). The 16S amplicon sequencing revealed that the *Enterobacteriaceae* were dominated by *Citrobacter* species (Figure 2.3), which was confirmed to be *Citrobacter freundii* using the clone library (Figure 2.4).

The glucose SBR enrichment was dominated by *Enterobacteriaceae* (Figure 2.3, Table 2.2, Figure 2.S7) with a side population of *Lachnospiraceae*. The 16S amplicon sequencing shows that the *Enterobacteriaceae* were dominated by *Enterobacter* species (Figure 2.3), which is confirmed to be *Enterobacter cloacae* by the clone library (Figure 2.4). Two other species also were confirmed using the clone library, *Raoultella ornithinolytica* and *Citrobacter freundii*. Thus, both SBR enrichments were dominated by a single *Enterobacteriaceae* species, with side-populations of *Lachnospiraceae* in both SBRs, and *Clostridium* in the xylose SBR enrichment.

The glucose CSTR enrichment was dominated by *Clostridium* species (Figure 2.3, Table 2.2, figure 2.S7) with a side population of *Enterobacteriaceae* (Table 2.2). The 16S amplicon sequencing gave two main OTUs, an *Enterobacter* sp. and *Clostridium* sp. (Figure 2.3), which were confirmed to be *Clostridium intestinale* and *Raoultella ornithinolytica*.

The xylose CSTR enrichment was dominated by *Lachnospiraceae* and *Enterobacteriaceae* species (Figure 2.3, Table 2.2, Figure 2.S7). The 16S amplicon sequencing was dominated by a *Citrobacter* sp., while two OTUs from the *Lachnospiraceae* are present. The clone library revealed that the *Citrobacter* OTU corresponded to *Citrobacter freundii*, while only one of the *Lachnospiraceae* OTUs was confirmed up to family level, as it only shows 96% sequence similarity with the closest cultivated relative *Lachnotalea glycerini* (Table 2.S6).

Summing up, it can be argued that the glucose SBR and CSTR enrichment showed a similar level of diversity, with a dominant species and a small side-population. The xylose SBR enrichment was more diverse than the glucose enrichments, as the side population contains both *Clostridium* and *Lachnospiraceae* species. In the xylose CSTR the largest diversity was observed, as here *Citrobacter freundii*, an uncultivated *Lachnospiraceae* species and a *Muricomes* population dominated.
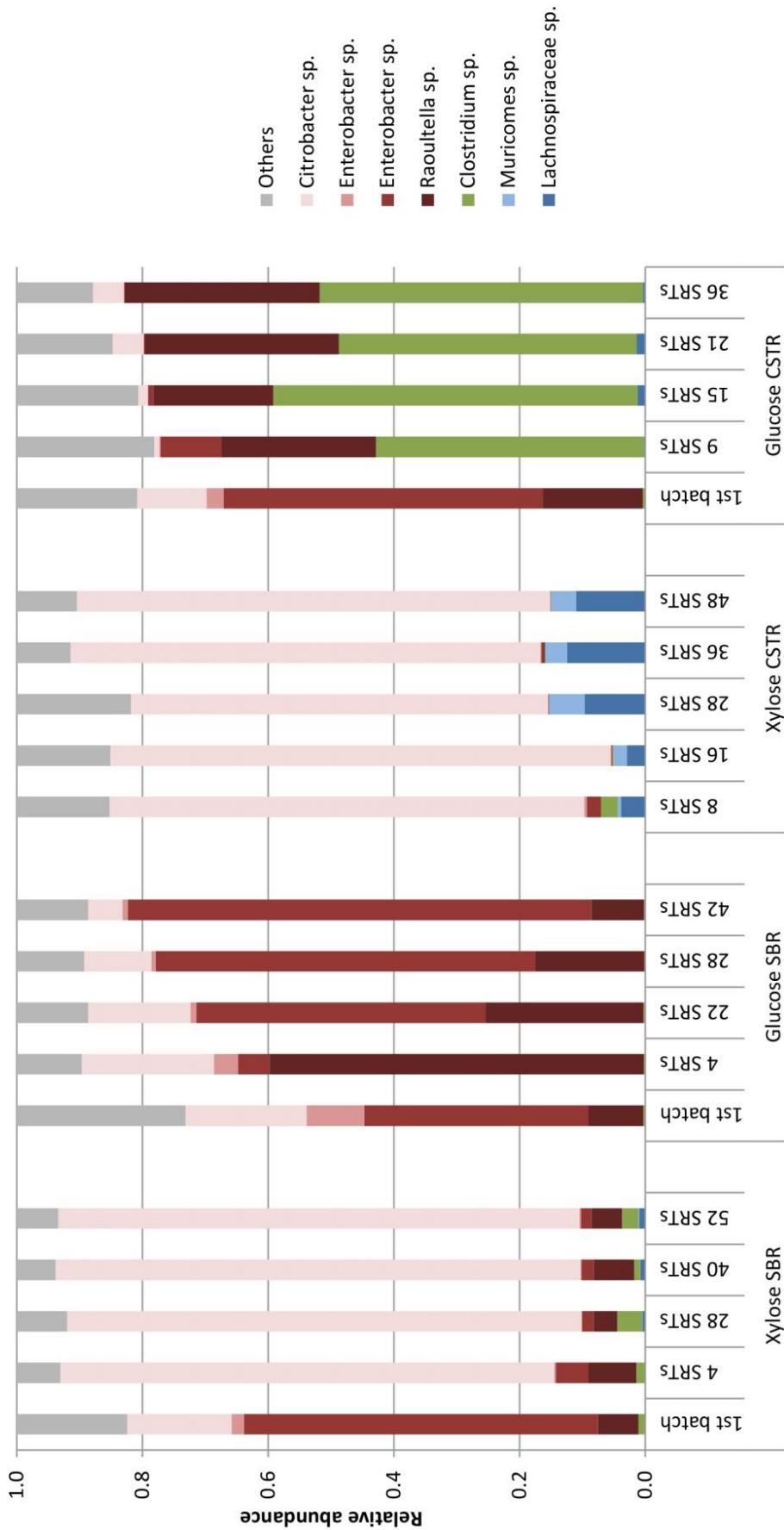
***Figure 2.3***: *Overview of the amplicon results on the V3-V4 region of the 16S rRNA gene on OTU level. All OTUs that contribute to <1% of the reads are grouped into the others fraction (grey). In red OTUs belonging to the Enterobacteriaceae family are denoted, in green OTUs belonging to the Clostridiaceae family and in blue OTUs belonging to the Lachnospiraceae family. Closest related relatives found by BLAST used to characterize the OTU up to genus level (Table 2.S5). OTUs matched at <97% are presented as species from a family.*
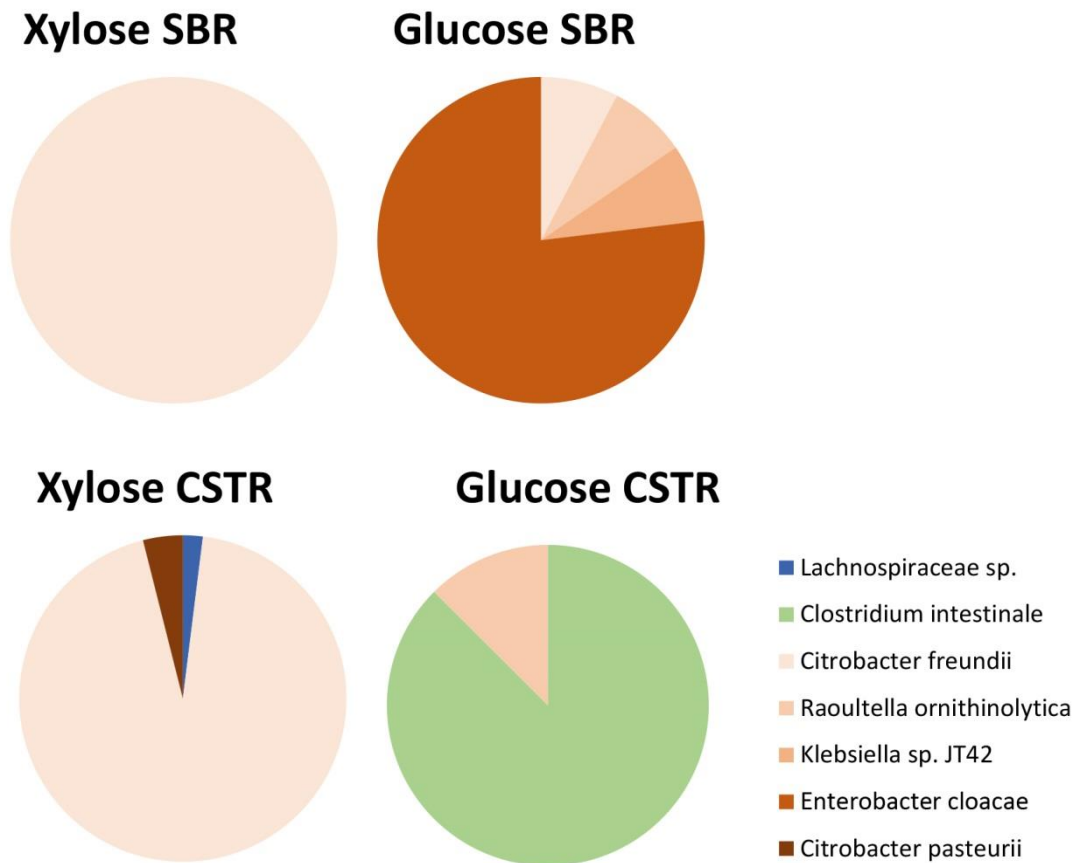
**Figure 2.4**: *Result of the clone library analysis in which strains that were found as closest relative (Table 2.S6) are grouped into species. For the xylose and glucose SBR 12 clones were used, for the xylose CSTR 51 clones were used, for the glucose CSTR 8 clones were used.*

**Table 2.2**: *Result of the FISH quantification (n = 3), with percentages denoting relative abundances calculated from the target-probe surface area compared to EUB338 probe surface. Unidentified populations were calculated as the remaining percentage after summing up the relative abundances of the known populations. The last column shows the amount of surface probed by EUB338 compared to DAPI.*

| | **Chis150** *vs.* EUB338 | **Lac435** *vs.* EUB338 | **Ent183** *vs.* EUB338 | **Unidentified** *vs.* EUB338 | **EUB338** *vs.* DAPI |
|---|---|---|---|---|---|
| Xylose SBR | 2% ± 2% | 5% ± 1% | 90% ± 3% | 2% | 96% ± 2% |
| Glucose SBR | ND | 3% ± 2% | 91% ± 3% | 6% | 100% ± 7% |
| Xylose CSTR | ND | 53% ± 3% | 44% ± 6% | 3% | 104% ± 14% |
| Glucose CSTR | 89% ± 12% | ND | 5% ± 0% | 6% | 89% ± 8% |

## Discussion

### Pathway analysis of the enrichments

Under slightly alkaline and mesophilic conditions acetate and ethanol were the dominant products under SBR conditions, while butyrate formation occurred significantly under CSTR conditions. Compared to the work of Temudo *et al.* [88] we observe a similar product spectrum in the glucose CSTR enrichment, though we observe more ethanol and less butyrate. The xylose CSTR enrichment is dominated by acetate and ethanol, while the enrichment of Temudo *et al.* [88] had produced primarily butyrate and acetate. Acetate and ethanol have been shown as the dominant products at pH 7.9 and 30°C [102], while acetate and butyrate have been dominant products under at pH 7.0 and 36°C [82].

The rate of the supply of inert $N_2$ gas in the reactor broth was the only difference in experimental procedures between the present study and the work of Temudo *et al.* [88]. This could potentially change the hydrogen and carbon dioxide gas partial pressures. The impact of the gas flow rate on the fermentation pattern was investigated, in order to investigate if the gas flow rate could explain the differences in product spectrum observed. Little effect was found on all product yields and hydrogen partial pressure (Figure 2.S1); thus, we expect no major impact of the gas flow rate. Furthermore, the glucose CSTR enrichment was duplicated and the resulting product spectrum of both enrichments was identical (Figure 2.S1) which confirms the reproducibility of the enrichments.

A NADH balance was set up using the generalised metabolic network (Figure 2.1, Table 2.S4), and the derivates from the pyruvate to acetyl-CoA pathway were summed as a yield. The NADH balance of the four enrichments shows that the glucose CSTR has a small net producing NADH balance, whereas the two SBRs and the xylose CSTR have a small net NADH consuming balance. Minor discrepancies from the NADH-balance can possibly be explained by succinate production through an NADH producing pathway, such as through the oxidative branch of the TCA cycle. Assuming no net NADH consumption for succinate production would bring the two SBRs and the xylose CSTR to a closed NADH balance.

*Table 2.3: Net NADH balance calculated using Table 2.S4. Acetyl-CoA derivates were calculated from butyrate, acetate and ethanol production through the pyruvate to acetyl-CoA pathway (Figure 2.1).*

|  | Net NADH balance metabolism ($mol_{NADH}$ $Cmol_S^{-1}$) | Acetyl-CoA derivates (mol $Cmol_S^{-1}$) | Formate + $H_2$ (mol $Cmol_S^{-1}$) |
|---|---|---|---|
| Xylose SBR | -0.03 ± 0.00 | 0.27 ± 0.00 | 0.26 ± 0.00 |
| Glucose SBR | -0.03 ± 0.01 | 0.22 ± 0.00 | 0.23 ± 0.02 |
| Xylose CSTR | -0.06 ± 0.01 | 0.27 ± 0.00 | 0.22 ± 0.01 |
| Glucose CSTR | 0.02 ± 0.01 | 0.24 ± 0.20 | 0.25 ± 0.01 |

Comparable values for the acetyl-CoA derivates and $H_2$/formate production (Table 2.3) indicate that $H_2$/formate production is directly coupled to pyruvate conversion to acetyl-CoA in the metabolic network as in Figure 2.1. Only for the xylose CSTR enrichment there is significantly less formate and $H_2$ found than acetyl-CoA derivates, which suggest that $H_2$ and formate are consumed through homoacetogenesis as proposed by [80].

The stoichiometric data argues for the PPP to be active in the xylose SBR, as acetate and ethanol are present in equimolar amounts and there is no excess of acetyl-CoA derivates compared to formate/$H_2$. If the PKP would have been active, more acetate compared to ethanol would have

been expected and less acetyl-CoA derivates compared to formate/$H_2$. In *Clostridium acetobutylicum* the PKP has been significantly expressed under batch cultivation [103], but here the PPP is estimated to be the only pathway active under SBR conditions.

**Bioenergetics and the role of substrate uptake**

Using the metabolic network (Figure 2.1) the amount of ATP produced was estimated from the different catabolic products ($Y_{ATP,s}$). Combining this yield with the biomass yield, the biomass yield on ATP ($Y_{x,ATP}$) was calculated. The $Y_{x,ATP}$ values for the xylose SBR and CSTR are very similar (Table 2.4), while the $Y_{x,ATP}$ values for the glucose SBR and CSTR enrichments were higher (Table 2.4). $Y_{x,ATP}$ values are confirmed by the dissipation energy, as the xylose SBR and CSTR enrichment showed a similar value, while the value for the glucose SBR enrichment was higher and the highest value was reported for the glucose CSTR enrichment. This means the xylose enrichments had a considerably lower anabolic efficiency than the glucose enrichments. The dissipation values obtained for glucose is in accordance with the average values for glucose (-236 kJ $Cmol_x^{-1}$), while that of xylose is considerably higher than according to the correlation function set up by van der Heijden *et al.* (-246 kJ $Cmol_x^{-1}$) [104].

*Table 2.4: $Y_{x,ATP}$ is calculated by assuming ATP formation per product (Table 2.S4), for the measured data and corrected for substrate uptake. Xylose uptake in the CSTR is assumed by the XylFGH complex and the XylE complex in the SBR. Gibbs energy of dissipation is calculated at 30°C and pH = 8 using the reconciled data.*

| Enrichment | $Y_{x,s}$ (Cmol$_X$ Cmol$_S^{-1}$) | $Y_{ATP,s}$ (mol$_{ATP}$ Cmol$_S^{-1}$) | $Y_{x,ATP}$ observed (g$_X$ mo$_{ATP}$l$^{-1}$) | $Y_{x,ATP}$ corrected (g$_X$ mol$_{ATP}^{-1}$) | Gibbs energy of dissipation (kJ Cmol$_X^{-1}$) |
|---|---|---|---|---|---|
| **Xylose SBR** | 0.12 ± 0.01 | 0.42 ± 0.01 | 7.20 | 8.70 | -378 |
| **Glucose SBR** | 0.13 ± 0.01 | 0.40 ± 0.01 | 8.21 | 8.21 | -285 |
| **Xylose CSTR** | 0.12 ± 0.01 | 0.42 ± 0.01 | 6.80 | 12.8 | -386 |
| **Glucose CSTR** | 0.21 ± 0.01 | 0.49 ± 0.03 | 13.4 | 13.4 | -236 |

[1]Only 90% of glucose conversion is assumed here, as the COD and carbon balance only close for 90%

The higher dissipation in the xylose enrichments can be caused by the cost of transporting xylose over the cell membrane. Xylose can be taken up into the cell by two different mechanisms. XylE is an enzyme which uses the proton motive force to take up xylose from the surrounding medium, through the symport with one proton [105]. When assuming a stoichiometry of 2.67 mol $H^+$ per mol ATP used, this means xylose uptake XylE costs 0.375 mol ATP per mol xylose. A second method for active xylose uptake is via XylFGH, an ATP-binding cassette (ABC) transporter which uses the direct dephosphorylation of ATP to import xylose [106]. XylE is known to be a low affinity transporter, while XylFGH is a high affinity transporter [106]. In *E. coli* it has been demonstrated that in batch conditions XylE plays a minor role in xylose uptake [107].

The genome of the strain with the highest similarity was assessed for the presence of transporters. *Citrobacter freundii* strain P10159, dominant in the xylose SBR enrichment (Table 2.S6), contained the XylE gene and not the analogues XylF, XylG or XylH (accession number CP012554.1) This argues for the nature of XylE as a high-rate xylose transport enzyme. A different *Citrobacter freundii* strain FDAARGOS (accession number CP026056.1) was populating the xylose CSTR, which contained neither XylE nor XylF, XylG or XylH. This suggests novel ABC transporters might be present in the xylose CSTR population.

Glucose uptake can be more energy efficient. The phosphotransferase system (PTS) is an uptake mechanism which couples the transfer of a phosphate group from PEP to glucose to transport glucose over the membrane, thus there is no net ATP cost for importing glucose as glucose-phosphate is directly produced. This complex is assumed to be active in both SBR and CSTR as this is observed to be the main transport system under glucose excess [108] and under substrate limitation [109]. The *Enterobacter cloacae* strain AA4 dominant in the glucose SBR enrichment and the *Clostridium intestinale* strain URNW dominant in the glucose CSTR enrichment both contain all five genes necessary to express the PTS complex in their genomes (accession number CP018785.1 and HM801879.1). When incorporating this biochemical consideration for substrate uptake, the $Y_{x,ATP}$ value for xylose and glucose becomes similar (Table 2.4), while the 50% difference in $Y_{X,ATP}$ between SBR and CSTR enrichments remains.

**Xylose uptake is slower than glucose uptake in SBR**

Xylose and glucose are metabolised by two distinct pathways, the PPP and the EMP pathway respectively. The $q_s^{max}$ of the glucose SBR enrichment is 50% higher than the xylose SBR enrichment. The lower uptake rate for xylose can be explained by a kinetic bottleneck identified in the PPP. Gonzalez *et al.* [110] have shown that in glycolysis *E. coli* metabolises glucose to fructose-6-phosphate at a rate of 90 mmol $g_{DW}^{-1}$ $h^{-1}$, while in the PPP rates to form fructose-6-phosphate did not exceed 37 mmol $g_{DW}^{-1}$ $h^{-1}$. The production of formate, acetate and ethanol exceeded these values for glucose, indicating the lower part of fermentation was not rate limiting. This suggests that the kinetic bottleneck is present in the PPP for xylose metabolism and not in the lower part of the fermentation pathway.

**Acetate and ethanol production as a kinetic advantage**

The $q_s^{max}$ and $\mu^{max}$ for the CSTR grown glucose enrichment producing butyrate is significantly lower than the acetate and ethanol producing enrichment (Table 2.1 and [88]). Furthermore, the xylose CSTR enrichment of Temudo *et al.* [88] and the glucose CSTR enrichment performed here, showed a similar $q_s^{max}$ value (Table 2.1) and both enrichments are producing a significant amount of butyrate. On top of that, both SBRs produce dominantly acetate and ethanol, where $q_s^{max}$ is a more important competitive advantage than in CSTR conditions. The kinetic difference between butyrate forming and acetate and ethanol forming microorganisms is observed in pure cultures. The $\mu^{max}$ of *Clostridium tyrobutyricum*, a butyrate producer, is 0.12 $h^{-1}$ [28] and *Citrobacter* sp. CMC-1, an acetate and ethanol producer, is 0.21 $h^{-1}$ [30] grown under similar conditions. The fact that acetate and ethanol formation is related to higher $\mu^{max}$ is also indirectly shown by the study of Zoetemeyer *et al.* [102], as a $\mu$ of 0.24 $h^{-1}$ was applied here at pH 7.9 and 30°C obtaining a product spectrum of acetate and ethanol. Temudo *et al.* [88] and this study obtain butyrate production at a lower $\mu$ of 0.13 $h^{-1}$. This kinetic advantage seems to hold only for fermentations at pH higher than 6.25, as enrichments performed in CSTR mode at pH 5.5 at $\mu^{max}$ have demonstrated to systemically yield a product spectrum dominated by acetate, butyrate, and lactate [111]. This kinetic effect can be incorporated into model-based evaluation of mixed culture fermentations to improve the prediction of butyrate, acetate and ethanol production at neutral and alkaline pH.

**Butyrate production as an efficient pathway**

If acetate and ethanol production obtains a higher $q_s^{max}$ value than butyrate, and both pathways produce 3 mol ATP, there seems to be no advantage for butyrate production over acetate and ethanol production. Thermodynamically, butyrate formation yields more energy than acetate and ethanol production, (-264 kJ $mol^{-1}$ and -226 kJ $mol^{-1}$ respectively). This energy is available in the step from crotonyl-CoA to butyryl-CoA, which is calculated to be -50 kJ/mol [77]. A direct conversion of this energy into a proton motive force has been rejected [25]. Part of the energy can be conserved by coupling this energy to the transfer of the electrons from NADH to ferredoxin and then oxidizing ferredoxin with $NAD^+$ to generate a sodium motive force using the Rnf enzyme [25].

Two of the six subunits of this complex are found in the genome of the *Clostridium intestinale* strain URNW, indicating the possibility of this mechanism being active in the glucose CSTR enrichment.

## Metabolic strategies in fermentation: r-strategists vs K-strategists

When substrate is only used for growth and no storage products are formed, the competition in a SBR process is based on the $\mu^{max}$ of the competing microorganisms, which can be maximised through $Y_{x,s}$ or $q_s^{max}$. The SBR enrichment cultures described in this chapter maximised $q_s^{max}$ compared to the CSTR enrichment cultures who maximised $Y_{x,ATP}$ (Table 2.1). The CSTR enrichments, when corrected for substrate uptake, show about 50% higher $Y_{x,ATP}$ value than the SBR enrichments. The $q_s^{max}$-value on the other hand is 2-3 times higher for the SBR enrichments compared to the CSTR enrichments.

These observations correspond with the general microbial theory proposed on r- vs K-strategists [112]. A r-strategists is more adapted to a substrate-abundant environment or "uncrowded" environment, where a small population competes for an abundance of food. A r-strategist displays a high $q_s^{max}$ and $\mu^{max}$ value. A K-strategists is more adapted to "crowded" environments where substrate is limited and displays a high $Y_{x,ATP}$ and a low $K_s$ value. The reason r-strategists dissipate more energy than K-strategists in their metabolism may rely on the fact that at increasing growth rate more erroneous proteins are produced due to a higher error rate made during proofreading at higher speed [113]. Thus, more non-functional proteins are produced at higher growth rate. As protein production is estimated to cost >80% of the ATP to synthesise a cell [114], larger error rates will cause increased ATP cost per cell assuming a similar functioning protein content.

The community data shows that *Enterobacteriaceae* dominate the SBR environments, thus the *Citrobacter freundii* and *Enterobacter cloacae* species can be classified as r-strategists. *Enterobacteriaceae* species such as *E. coli* are well known to exhibit high growth rates in anaerobic environments with carbohydrates [115]. *Clostridium* species on the other hand are often dominating in substrate-limited environments such as anaerobic digesters [17], where the rate of hydrolysis of cellulose and hemicellulose is an order of magnitude lower than typical fermentation rates, creating a substrate-limited environment. In the glucose CSTR we observe a dominance of *Clostridium intestinale*, which fits with these observations.

## The microbial community composition and the effect of limiting a single substrate

First of all, it is noteworthy that the FISH imaging and the 16S rRNA gene amplicon sequencing data do not always correspond. In the glucose SBR, the dominance of *Enterobacteriaceae* on OTU-level is confirmed by the FISH analysis, but in the glucose CSTR enrichment the *Enterobacteriaceae* are observed to be a minor fraction on cell-level (FISH image), while 30% of the reads relate to *Enterobacteriaceae*. In the xylose CSTR a similar bias is observed, as 53% of the community is identified as *Lachnospiraceae* using FISH (Table 2.2), while only 15% of the reads relate to *Lachnospiraceae*. As we have corrected the data for copy numbers, the bias is likely caused by DNA extraction and PCR biases, which are known to cause biases in amplicon sequencing data [116]. As proposed by Amann, Ludwig and Schleifer [117], 16S rRNA gene sequencing and FISH analysis are to be used in parallel to obtain an accurate estimation of the microbial community structure, which is confirmed in the study here.

Here, populations of *Enterobacteriaceae*, *Lachnospiraceae* and *Clostridium* dominated the enrichments. *Clostridium* and *Enterobacteriaceae* populations have been reported in enrichments on mineral medium (Table 2.5), though for the first time *Lachnospiraceae* were enriched on xylose. We find that a significant presence of *Clostridium* was linked to butyrate production, as in the glucose CSTR, which is confirmed by other enrichment studies (Table 5). The butyryl-CoA dehydrogenase gene, which is responsible for the reduction of crotonyl-CoA to butyryl-CoA using

NADH, is found in organisms in the *Clostridium* species, while neither in *Enterobacter* nor in *Citrobacter* species according to the NCBI Gene database.

All four enrichments were populated by more than one species, with stabilizing OTUs over time (Figure 2.3). This indicates that species have a reason to coexist in these single substrate limited systems. It is possible that mutualistic relationships between these species were present, *e.g.*, in the form of a B-vitamin exchange between species [118], as these communities are cultivated on mineral medium. It remains an important ecological question why in many cases rather diverse communities remain in very selective conditions with one limiting substrate.

**Table 2.5**: *Reported predominant bacterial species for fermentative microbial communities enriched on xylose or glucose as carbon sources in CSTR mode. Species were detected using PCR and denaturing gradient gel electrophoresis or PCR and single strand conformation polymorphism analysis*

| Substrate | Inoculum | Temperature | pH | Dominant carbon products | Organisms | Source |
|---|---|---|---|---|---|---|
| **Xylose** | Hot spring culture | 45°C | 5.1 | Acetate, butyrate | *Clostridium acetobutylicum* *Citrobacter freundii* | [119] |
| **Xylose** | Hot spring culture | 37°C | 5.1 | Acetate, butyrate, ethanol | *Clostridium acetobutylicum* *Clostridium tyrobutircum* | [119] |
| **Glucose** | Hot spring culture | 37 °C | 5.0 | Acetate, butyrate | 3 species of *Clostridium* 2 uncultured | [120] |
| **Glucose** | Activated sludge, cassava, rabbit droppings | 37 °C | 5.5 | Butyrate, acetate, lactate* | *Clostridium pasteurianum, Clostridium beijerinckii, Lactobacillus paracasei* | [111] |
| **Xylose 4 g/L** | Digestor sludge and acidification tank | 30 °C | 8.0 | Acetate, butyrate | *Clostridium beijerinckii, Clostridium xylanovorans, Clostrdium sp. CCUG* | [121] |
| **Xylose 11 g/L** | Digestor sludge and acidification tank | 30 °C | 8.0 | Acetate, butyrate, ethanol | *Citrobacter farmeri Clostridium intestinale Clostrdium sp. CCUG* | [121] |
| **Glucose** | Digestor sludge and acidification tank | 30 °C | 8.0 | Acetate, butyrate, ethanol | *Clostridium quinii*** | [121] |

* 50% of the COD coming out of the reactor was glucose
** Two other bands are visible which are not mentioned

Overall, this study aimed to show the impact of sequencing batch and continuous culturing on microbial communities fermenting lignocellulosic sugars such as xylose and glucose. Butyrate formation was linked to slow uptake rate, while acetate and ethanol formation was linked to high uptake rates. This kinetic effect can be taken into account in modelling efforts. In SBR, xylose was fermented 33% slower than glucose, likely due to a kinetic bottleneck in the PPP. SBR communities maximised their $q_s^{max}$, while CSTR communities maximised their $Y_{x,ATP}$. SBR communities were dominated by r-strategists like *Citrobacter freundii* and *Enterobacter cloacae*, and the CSTR communities by K-strategists like *Clostridium intestinale* and *Lachnospiraceae* species. No significant storage of either xylose or glucose was observed in the SBR enrichments. The glucose enrichments confirmed the hypothesis that limitation of a single substrate leads to domination of a single species. The xylose enrichments displayed more microbial diversity, with the xylose CSTR up to three dominant populations.

It was expected that, when limiting a single substrate, one specialist will dominate the community after prolonged cultivation, displaying either the highest $\mu^{max}$ or the highest affinity. The glucose enrichments were dominated by a single species (up to 90% of cell surface), which is *Enterobacter cloacae* in the glucose SBR and *Clostridium intestinale* in the glucose CSTR and had one side populating family. For the xylose enrichments, the communities were more diverse. In the xylose SBR, *Citrobacter freundii* dominated the culture, with a side-population of both, *Lachnospiraceae* and *Clostridium*. The xylose CSTR community was even more diverse, populated by two *Lachnospiraceae* genera, one of which was confirmed to be an uncultivated *Lachnospiraceae* species besides to a population of *Citrobacter freundii*. Thus, xylose fermentation resulted in more microbial diversity than glucose fermentation. In all enrichments more microbial diversity was displayed than expected by assuming solely competition. Why this is remains an important ecological question to be answered.

## Supplementary Information

*Table 2.S1*: *Primers used in this study*

| Primer | Primer Sequence (5'- 3') | Reference |
|--------|--------------------------|-----------|
| 341f | CCT AYG GGR BGC ASC AG | [122] [123] |
| 806r | GGA CTAC NNG GGT ATC TAA T | [122] [123] |
| GM3f | AGA GTT TGA TCM TGG CTC AG | [124] |
| GM4r | GGT TAC CTT GTT ACG ACT T | [124] |
| M13f | GTA AAA CGA CGG CCA G | [125] |
| M13r | CAG GAA ACA GCT ATG AC | [125] |

*Table 2.S2*: *FISH probes used in this study with the formamide concentration used during hybridisation*

| FISH Probe | Sequence 5'- 3' | Specificity | Formamide [%] | Reference |
|------------|-----------------|-------------|---------------|-----------|
| EUB338 Cy5 | GCT GCC TCC CGT AGG AGT | Bacteria | 20-25 | [126] |
| ENT183 Cy3 | CTC TTT GGT CTT GCG ACG | *Enterobacteriaceae* family | 20 | [127] |
| Chis150 Cy3 | TCT TCC CTG CTG ATA GA | *Clostridium* genus | 25 | [128] |
| Lac435 Cy3 | TTA TGC GGT ATT AAT CTY CCT TT | *Lachnospiraceae* family | 25 | [129] |

**Figure 2.S1**: *(A) Product spectrum of the glucose CSTR at 215 mL$_n$/min gasflow and 120 mL$_n$/min (gasflow used by Temudo* et al. *[88] and (B) product spectrum of two identically executed glucose CSTRs, both ran at D = 0.13 h$^{-1}$*
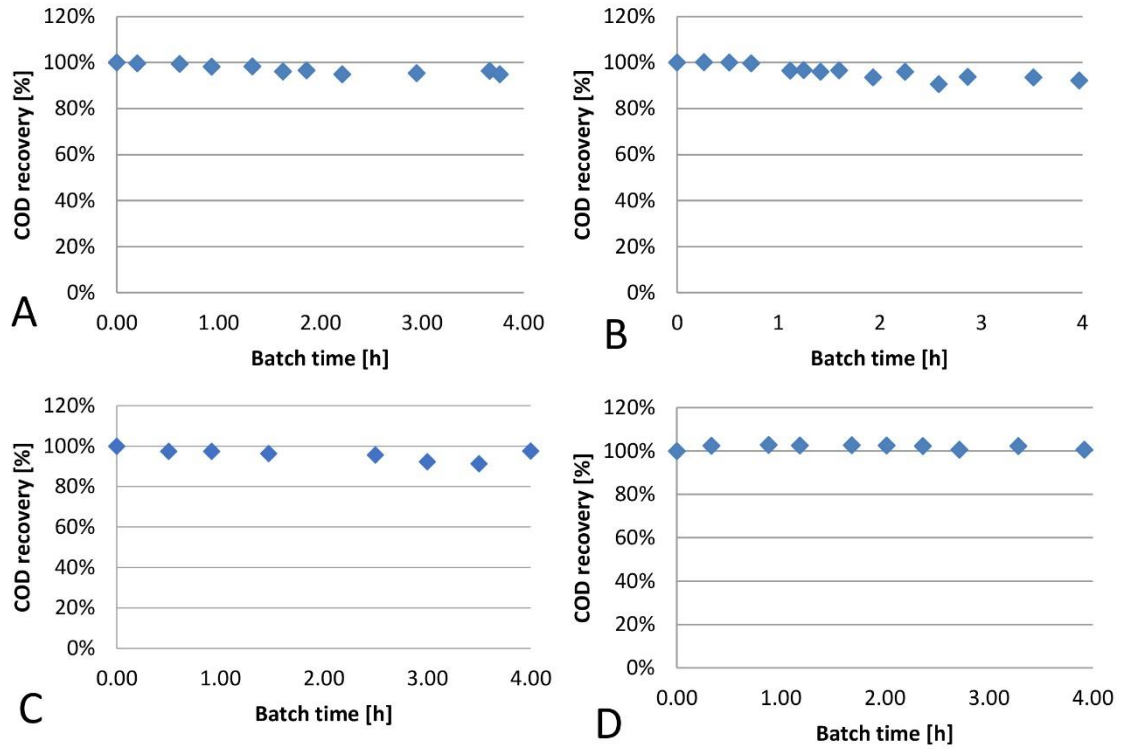
**Figure 2.S2**: *COD recovery during cycle measurement of the Xylose SBR (A), Glucose SBR (B), Xylose CSTR (C), Glucose CSTR (D)*
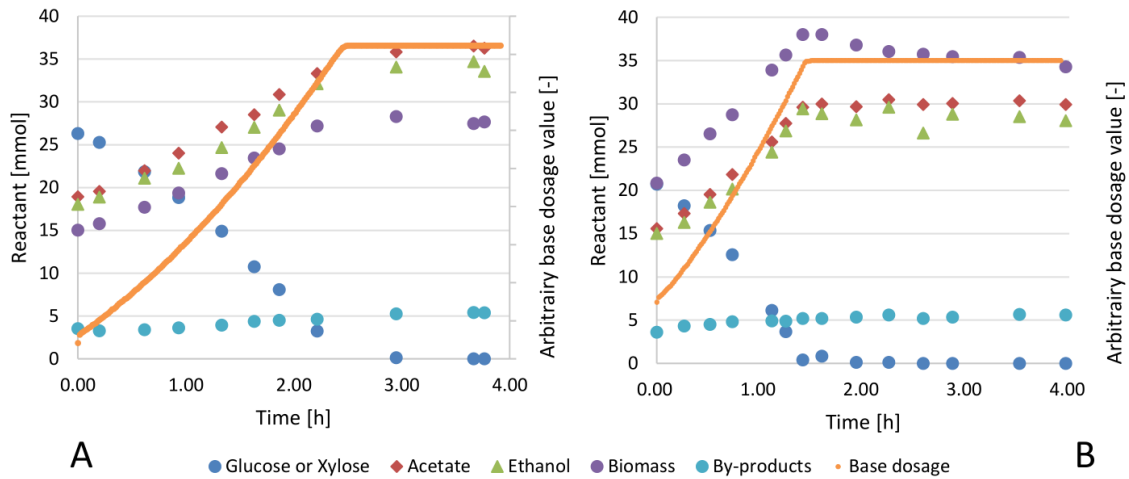


**Figure 2.S3**: *Xylose SBR (A) and glucose SBR (B) cycle measurement in which by-products is the sum of propionate, lactate, succinate and butyrate*
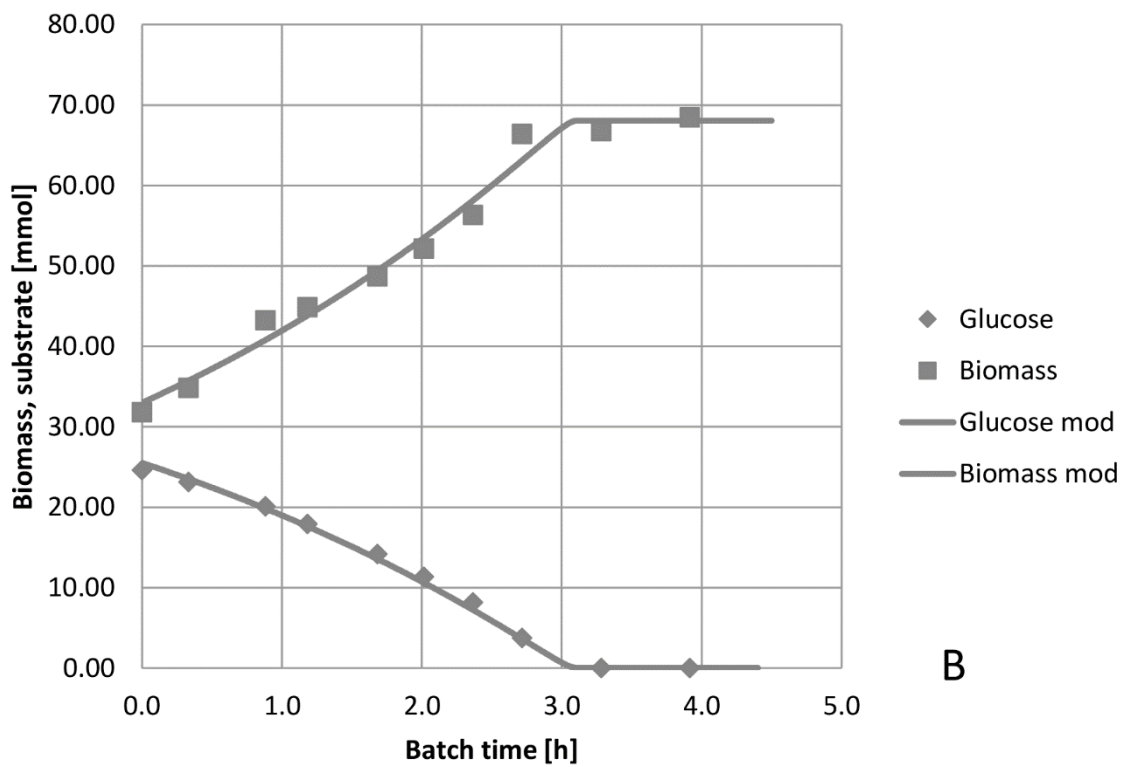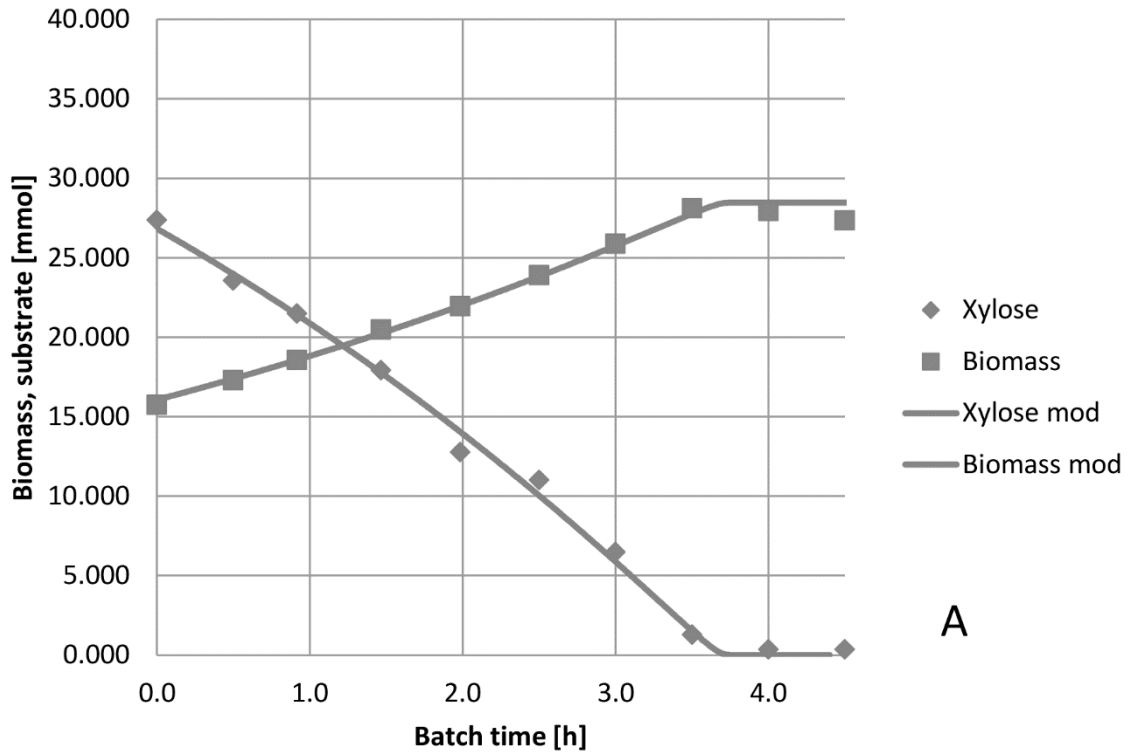
**Figure 2.S4**: Xylose CSTR (A) and Glucose CSTR (B) cycle measurement modelled for $q_s^{max}$

**Table 2.S3**: *the carbon and COD balances expressed as a percentage of outgoing carbon or COD compared to the incoming carbon or COD*

| Experiment | Carbon-recovery [%] | COD-recovery [%] |
|---|---|---|
| Xylose SBR | 99% | 98% |
| Glucose SBR | 89% | 90% |
| Xylose CSTR | 100% | 99% |
| Glucose CSTR 215 $mL_n$/min | 101% | 98% |
| Glucose CSTR 120 $mL_n$/min | 96% | 96% |
| Glucose CSTR duplicate | 103% | 103% |

**Table 2.S4**: *Elemental matrix used to set up NADH, ATP, carbon and COD balances in parallel to estimation of the Gibbs energy of dissipation.*

| | Carbon | COD | Mol. weight | NADH | ATP SLP | Gibbs energy of formation |
|---|---|---|---|---|---|---|
| | No. C | ($g_{COD}$ $mmol^{-1}$) | (g $mol^{-1}$) | (NADH $mol_P^{-1}$) | (ATP $mol_P^{-1}$) | ($\Delta G_f^0{}'$ kj $mol^{-1}$) |
| Glucose | 6 | 1.07 | 180.2 | 0 | 0 | 0 |
| Xylose | 5 | 0.89 | 150.1 | 0 | 0 | 0 |
| Acetate | 2 | 1.07 | 60.1 | 2 | 2 | -369.4 |
| Butyrate | 4 | 1.82 | 88.1 | 0 | 3 | -352.6 |
| Propionate | 3 | 1.30 | 74.1 | -2 | 1 | -361.1 |
| Lactate | 3 | 1.08 | 89.1 | 0 | 1 | -517.1 |
| Succinate | 4 | 0.95 | 118.1 | -2 | 1 | -690.2 |
| Ethanol | 2 | 2.08 | 46.0 | -2 | 1 | -181.8 |
| Formate | 1 | 0.35 | 46.0 | 0 | 0 | -351 |
| $H_2$ | 0 | 7.94 | 2.0 | 0 | 0 | 0 |
| $CO_2$ | 1 | 0.00 | 44.0 | 0 | 0 | -394.4 |
| Biomass | 1 | 1.36 | 24.6 | -0.05 | 0 | -67 |
| $HCO_3^-$ | 1 | 0.00 | 61.0 | 0 | 0 | -586.9 |
| $H_2O$ | 0 | 0.00 | 18.0 | 0 | | -237.2 |
| Ammonium | 0 | 0.00 | 16.0 | 0 | 0 | -79.4 |
| $H^+$ | 0 | 0.00 | 1.0 | 0 | 0 | 0 |

**Estimation of μ^max from base-dosage data**

To identify the timepoint at which the base dosage stopped, by detecting the transition from increasing base value to flat slope using the derivative of the base value in time:

$$dbase = \frac{\Delta base}{\Delta t}$$

(2.4)

At the end of the fermentation, no more base was added, thus the Δbase value became zero. A criterion was set for Δbase to be zero over 30 min of time in order to estimate the fermentation length. From the fermentation length value, μ^max was calculated, using the exponential growth equation for biomass:

$$M_1 = M_0 \cdot e^{\mu \cdot t}$$

(2.5)

Which can be rewritten using the fact that the biomass doubles every cycle, and using the fermentation length as time for growth:

$$\mu^{max} = \frac{\ln(2)}{fermentation\ length}$$

(2.6)

In figure 2.S5 this approach is visualised, where the script targets the plateau region (where the Δbase over time is zero, as no base is dosed). The fermentation length is than saved and converted using formulae 1.3 to obtain the μ^max.
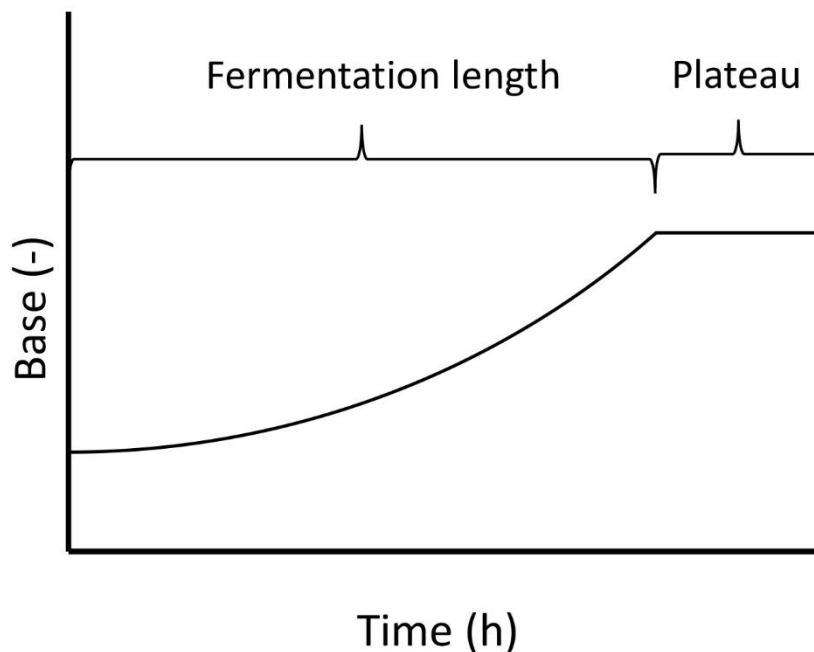


***Figure 2.S5****: characterisation of the fermentation length by the script developed in Matlab used to calculate the μ^max.*

Because not all μ-values are representative for the final μ^max achieved, a certain set of μ-values was chosen where the μ^max-value tends to stabilize. For the glucose SBR the μ-values from 35 SRTs up to the end of the enrichment were chosen (line Figure 2.S6).
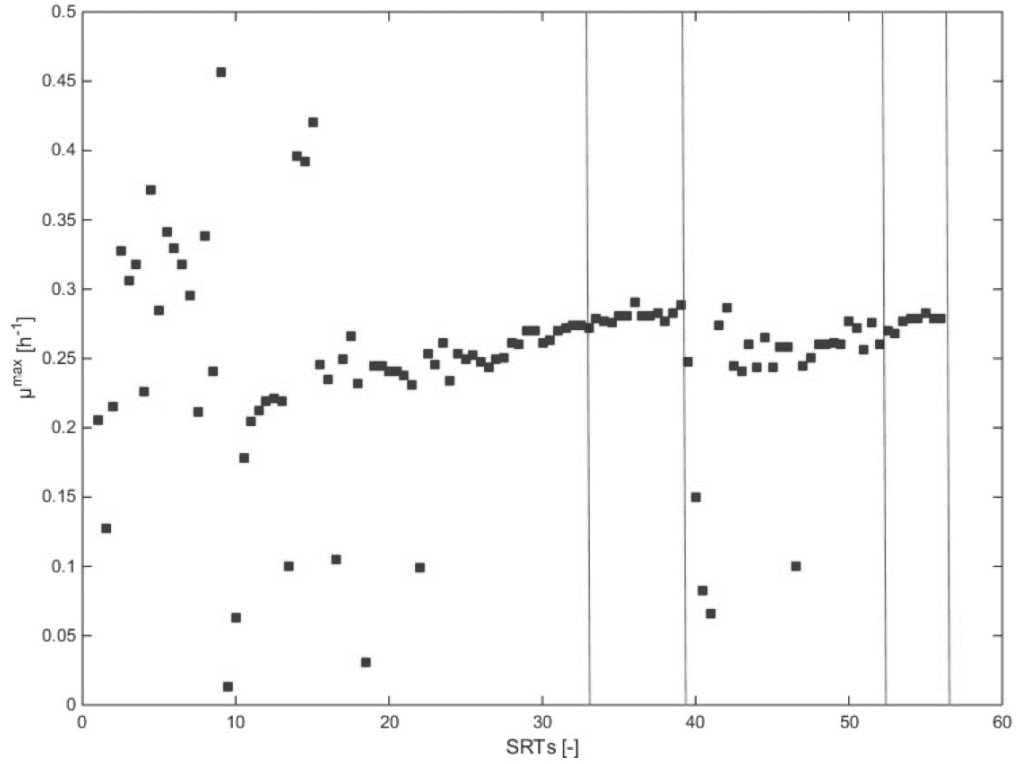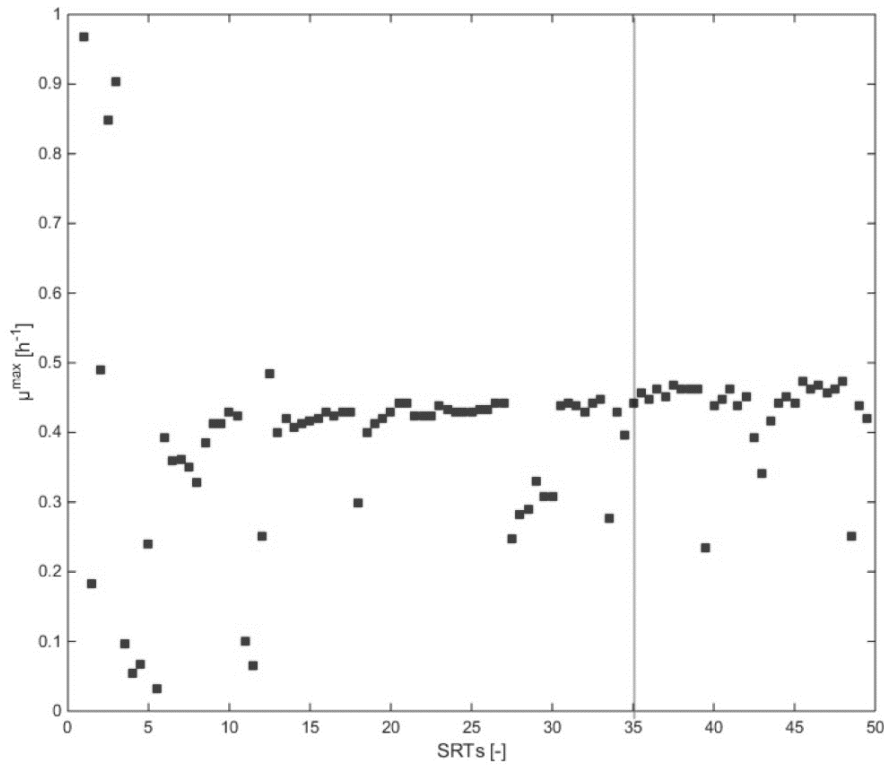
***Figure 2.S6****: Plot of the μ^max-values calculated over the xylose SBR enrichment (A) and glucose SBR enrichment (B) with the cut-off value denoted by the horizontal lines. Xylose (A) has two areas cutted off.*

For the xylose SBR there was an experimental failure, as the base dosage was accidentally stopped at 39 SRTs. Effluent stored in the fridge was reinoculated and the culture recovered as can be seen in the plot. Therefore, the μ-values from 33 SRTs up to 39 SRTs were taken before the failure and μ-values from 53 SRTs until the end of the enrichment were chosen (lines, Figure 2.S6).

Cleaning the reactor influences the μ-value, as the biofilm is removed and 1 cycle there is less than 50% of the biomass at the start as the biofilm was also consuming substrate. Thus, for the glucose SBR a minimum value of μ of 0.4 h$^{-1}$ was assumed. The xylose SBR did not show this behaviour, thus no correction was applied.

*Table 2.S5: Closest related cultivated species as found using BLAST with the 450-bp 16S rRNA gene amplicon sequences*

| Colour Graph | OTU Blast Species | Description | Max score | Total score | Query cover | E value | Identity | Accession |
|---|---|---|---|---|---|---|---|---|
| | *Lachnotalea glycerini* | Lachnotalea glycerini strain DLD10 16S ribosomal RNA gene, partial sequence | 686 | 686 | 100% | 0 | 97% | MF953294.1 |
| | *Muricomes intestini* | Muricomes intestini strain 2PG-424-CC-1 16S ribosomal RNA, partial sequence | 725 | 725 | 100% | 0 | 99% | NR_144617.1 |
| | *Clostridium intestinale* | Clostridium intestinale gene for 16S ribosomal RNA, partial sequence, strain: JCM 7506 | 747 | 747 | 100% | 0 | 100% | LC037210.1 |
| | *Raoultella ornithinolytica* | Raoultella ornithinolytica A25 gene for 16S ribosomal RNA, partial sequence | 793 | 793 | 100% | 0 | 100% | LC331661.1 |
| | *Enterobacter cloacae* | Enterobacter cloacae gene for 16S rRNA, partial sequence, strain: A17T0S Y77 | 793 | 793 | 100% | 0 | 100% | LC373074.1 |
| | *Enterobacter asburiae* | Enterobacter asburiae strain FCC170 16S ribosomal RNA gene, partial sequence | 793 | 793 | 100% | 0 | 100% | JF772103.1 |
| | *Citrobacter freundii* | Citrobacter freundii strain F-CF1 16S ribosomal RNA gene, partial sequence | 793 | 793 | 100% | 0 | 100% | KY968676.1 |
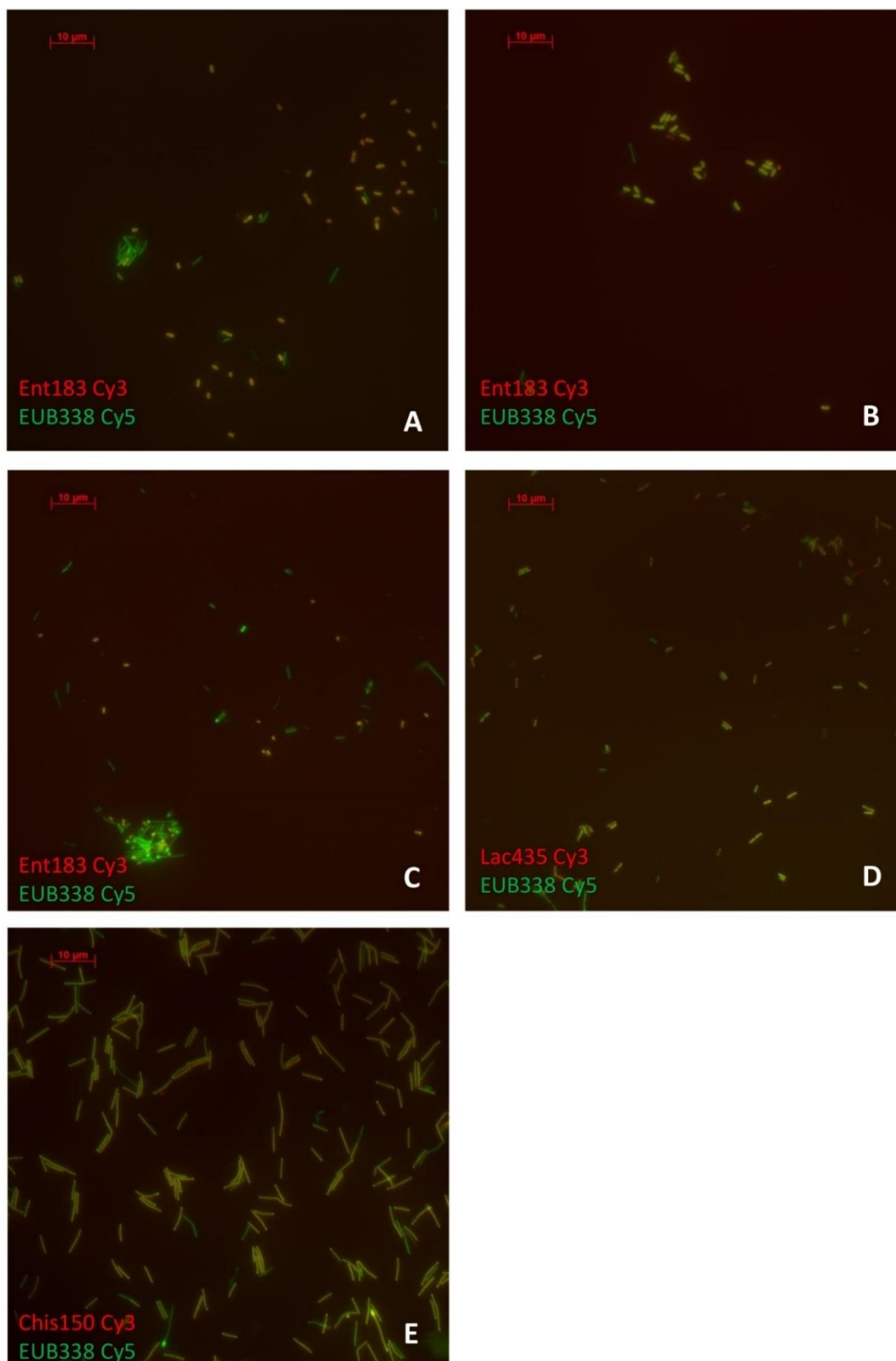
*Figure 2.S7*: *Images acquired at 1000x and probed with a probe of choice and EUB338 of the xylose SBR (A), glucose SBR (B), xylose CSTR (C and D) and glucose CSTR (E) enrichment*

***Table 2.S6****: Heat map of the different 16S sequences and obtained closest related strain by the clone library approach in the four enrichment reactors. Fraction of the sequence compared to all obtained sequences is displayed. In red are all* Enterobacteriaceae *strains, in green all* Clostridium *strains and in blue all* Lachnospiraceae *strains*

| Identity | 96 % | 100 % | 99 % | 99 % | 99 % | 98 % | 99 % | 99 % | 100 % | 99 % | 98 % | 99 % |
|---|---|---|---|---|---|---|---|---|---|---|---|---|
| Accession | MF953294.1 | CP012554.1 | KF358448.1 | AB548827.1 | CP026056.1 | CP026056.1 | CP004142.1 | DQ358738.1 | CP018785.1 | HM801879.1 | KP057683.1 | KP057683.1 |
| Fractions | Lachnospiraceae sp. | Citrobacter freundii strain P10159 | Raoultella ornithinolytica strain FMC41 | Citrobacter freundii strain JCM 24062 | Citrobacter freundii strain FDAARGOS | Citrobacter freundii strain FDAARGOS | Raoultella ornithinolytica B6 | Klebsiella sp. JT42 | Enterobacter cloacae strain AA4 | Clostridium sp. URNW | Citrobacter pasteurii strain CIP 55.13 | Citrobacter pasteurii strain CIP 55.13 |
| **Xylose CSTR** | 0.02 | 0.6 | 0 | 0.02 | 0.2 | 0.02 | 0 | 0 | 0 | 0 | 0.02 | 0.02 |
| **Xylose SBR** | 0 | 1 | 0 | 0 | 0 | 0 | 0 | 0 | 0 | 0 | 0 | 0 |
| **Glucose CSTR** | 0 | 0 | 0.12 | 0 | 0 | 0 | 0 | 0 | 0 | 0.88 | 0 | 0 |
| **Glucose SBR** | 0 | 0 | 0 | 0 | 0 | 0 | 0.083 | 0.083 | 0.83 | 0 | 0 | 0 |

# Chapter 3 - The impact of mixtures of xylose and glucose on the microbial diversity and fermentative metabolism of sequencing-batch or continuous enrichment cultures
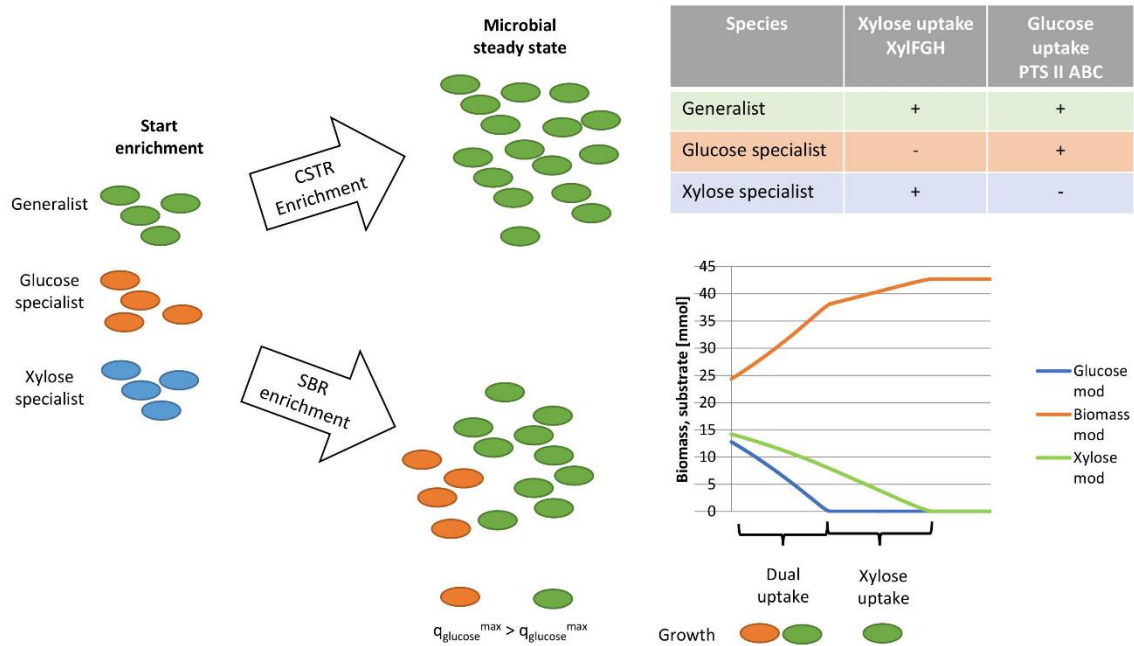
# Abstract

Microbial diversity plays an important role in the functioning of mixed-culture biotechnologies while the drivers behind microbial diversity are still not well understood. Complexity in the carbohydrate source could be one of the governing factors. The effect of feeding equivalent substrates to a microbial community, such a xylose and glucose is not well understood in terms of number of dominant species and how these species compete for substrate. In this work we compare the fermentation patterns achieved and the microbial community structure development in a continuous-flow stirred tank reactor (CSTR) and a sequencing batch reactor (SBR) fed with a mixture of xylose and glucose. We hypothesise that a CSTR will select for generalist species, taking up both substrates. A SBR will select for a diauxic generalist, fermenting first glucose and subsequently xylose, with an additional population of a xylose specialist. We have used 16S rRNA amplicon sequencing and full 16S clone libraries in parallel to fluorescent *in situ* hybridisation (FISH) to accurate determine the microbial community structures. Both enrichment cultures were stoichiometrically and kinetically characterised. The CSTR enrichment culture was dominated by a *Clostridium intestinale* population (91%±2% of the cell surface), which indicated the enrichment of a generalist converting xylose and glucose simultaneous. In the SBR we found a large fraction of *Enterobacteriaceae* (75%±8% of the cell surface), which was dominated by *Citrobacter freundii* and a minor fraction of *Raoultella ornithinolytica*. *Citrobacter freundii* ferments xylose and glucose in a non-diauxic fashion. This indicates that a non-diauxic generalist outcompetes specialists and diauxic generalists in a SBR environment. When designing an industrial batch fermentation using a lignocellulosic feed composed of xylose and glucose, a non-diauxic generalist is expected to be the most preferential type of microorganism to use.

**Keywords**: SBR – chemostat – carbon catabolite repression - microbial selection – mixed substrates

## Introduction

Glucose and xylose are the two most abundant monomers found in lignocellulosic waste streams [78]. Fermentation of these two carbohydrates to valuable compounds such as volatile fatty acids (VFAs), lactic acid, hydrogen or ethanol can enable new biobased processes to be developed [130–132]. Enrichment culturing offers the potential to apply selective conditions to direct a process towards a certain product. Examples of such processes and products are: butyrate in carbohydrate fermentation [133], poly-β-hydroxyalkanoates in an aerobic feast-famine process [65] or medium chain fatty acids from volatile fatty acids and an electron donor like ethanol or lactate [134]. Enrichment cultures select for specific microorganisms based on competition for limiting substrate [81]. Most fermentative enrichment studies have been performed using a continuous-flow stirred tank reactor (CSTR) setup [51, 82, 111]. A CSTR is a system where the fermentable substrate is continuously available at a low concentration. This is similar to anaerobic digestion of lignocellulosic waste. The hydrolysis of a macromolecular substrate, *e.g.* cellulose, is the rate-limiting step in fermentation leading to a hydrolysed monomer substrate, *e.g.* glucose to be continuously available in low residual concentrations [131, 135].

In a CSTR, Monod kinetics describe the relationship between the residual substrate concentration ($C_s$), the maximum biomass specific uptake rate ($\mu^{max}$), and the affinity constant for the substrate ($K_s$):

$$\mu = \mu^{max} \cdot \frac{C_s}{C_s + K_s} \qquad (3.1)$$

Since the growth rates ($\mu$) of microbial populations in a CSTR environment is set by the dilution rate (D) of the reactor, $C_s$ is a function of the dilution rate and the affinity properties ($\mu^{max} K_s^{-1}$) of the microorganisms. The microorganism with the highest affinity for the substrate is expected to dominate the enrichment culture, as is shown for two competing yeast species [136].

In **Chapter 2**, we have demonstrated this effect. In a CSTR enrichment culture limited with glucose we indeed observed one species dominating (>90%) the population. For xylose we however observed a community with at least three dominant species, indicating other mechanisms besides direct substrate competition are complicating the microbial community structure [137].

When mixing two equivalent substrates, like glucose and xylose, the Monod kinetics model is extended. A simple mathematical view on mixed-substrate kinetics is obtained by summing the individual Monod kinetics as proposed by Bell [138]:

$$\mu = \mu_1^{max} \cdot \frac{C_{s,1}}{C_{s,1} + K_{s,1}} + \mu_2^{max} \cdot \frac{C_{s,2}}{C_{s,2} + K_{s,2}} \qquad (3.2)$$

This simple model does not normalise for substrate concentrations or ratios, which can improve the modelling of mixtures of carbon [139], but is sufficient to demonstrate the advantage of a generalist over a specialist microorganism.

Two types of microbial species can compete in a mixed-culture CSTR, a specialist taking up only one substrate and a generalist, taking up both substrates simultaneously. If we assume the generalist and specialist species possessing similar kinetic properties on xylose and glucose ($\mu^{max} K_s^{-1}$), then the generalist, by converting both xylose and glucose simultaneously, can lower the residual concentration of xylose and glucose beyond the capacity of the specialist species, resulting in a wash-out of the specialists [140]. This effect has been demonstrated in pure culture competition experiments with two specialists and one generalist [141]. We thus expect a generalist species to dominate the CSTR environment.

The sequencing batch reactor (SBR) environment offers the opportunity to select for a microbial community based on the maximum biomass-specific growth rate ($\mu^{max}$). When feeding a mixture of xylose and glucose to a microbial community at high concentrations, carbon catabolite repression (CCR) or diauxic behaviour will be the favoured way for substrate uptake, where glucose is first taken up prior to xylose. The preference for glucose is mediated through a cyclic AMP (cAMP) regulated pathway in *E.coli,* therefore glucose is more easy to metabolise [142]. CCR is an abundant mechanism amongst heterotrophic bacteria [143]. It has been demonstrated that in a batch environment, specialist species will outcompete a diauxic generalist species [141]. This theory has been confirmed for an enrichment of microorganisms accumulating PHA on a mixture of acetate and lactate, where *Plasticicumulans acidivorans* was identified as acetate specialist and *Thauera selenatis* as lactate specialist [68]. Thus, we believe a competitive CCR-type species will take up the glucose, leaving a niche for a sole xylose specialist to take up the xylose. In other words, we expect that in an SBR enrichment culture fed with a mixture of glucose and xylose, two specialist species will be enriched in the microbial community.

The fed-batch environment is typically used in industrial fermentations using pure cultures to convert sugars to a desired product [144]. When using a mixture of substrates in a fed-batch, CCR can induce accumulation of the non-preferred substrate, *e.g.* xylose in a dual xylose and glucose fermentation [145]. A way to deal with this problem is to avoid CCR and create a non-diauxic xylose and glucose fermenting generalist [146] or to design xylose- and glucose-specialist species and performing fermentation with this synthetic consortium [147]. The ecological significance of CCR and observed microbial diversity in a mixed-substrate SBR environment fed with xylose and glucose can be used to design novel microbial-based processes using defined mixtures of pure cultures.

Using enrichment culturing with a mixture of xylose and glucose in a CSTR and SBR environment, we aimed to elucidate the impact of mixed-substrate conditions on the microbial diversity and fermentative niche establishment in both environments. This was facilitated by comparing our results to previously published results for similar cultures with a single limiting substrate [137]. Furthermore, we aim to evaluate the ecological significance of CCR using our enrichment culturing approach.

## Material and Methods

All enrichment procedures and analytical methods are described in detail in Rombouts *et al* [137] and **Chapter 2**. The main adaptations for the mixed-substrate experiments are given hereafter.

### Fermentative enrichment culturing

The enrichment procedure was executed as described in Rombouts *et al.* [137] and **Chapter 2**, with the adaptation that 2 g L$^{-1}$ of xylose and 2 g L$^{-1}$ of glucose were fed as a mixture instead of 4 g L$^{-1}$ of one of the individual substrates, resulting in a similar COD influent concentration as in the single-substrate enrichments. The same cow rumen inoculum was used and seeded in the same way in the CSTR and SBR. The reactors were operated at 30°C±0.1, pH of 8.0±0.1 and a hydraulic retention time (HRT) of 8 h, The reactors were continuously stirred at 300 rpm and the solids retention time (SRT) is the same as the HRT applied. Steady state was assumed if during a period of at least 5 days no variation in the concentrations of fermentation products was observed.

### Analytical methods and cycle analysis

The concentrations of the residual glucose and xylose substrates and of the VFAs (formate, $C_1$, to valerate, $C_5$), lactate, succinate, and ethanol substrates were analysed using high performance liquid chromatograph (HPLC) as described in Rombouts *et al.* [137] and **Chapter 2**. For high butyrate concentrations above 1 mmol L$^{-1}$, samples were analysed using gas chromatography (GC) for butyrate and ethanol overlap in the refractive index (RI) spectrum and butyrate can be quantified from the ultraviolet (UV) spectrum, as described in Rombouts *et al.* [137]. The off-gases were monitored on-line for $H_2$ and $CO_2$ using a spectrophotometric method as described in Rombouts *et al.* [137].

Biomass concentration was measured using a standard method which relies on centrifugation to separate the cells from the medium, drying to obtain total suspended solids (TSS) and burning at 550°C to obtain volatile suspended solids (VSS) [94]. This analysis was coupled to absorbance measurement at 660 nm to establish a correlation. Absorbance values were used to calculate the biomass concentration during the batch experiments.

To characterise the kinetics of the cultures in SBR mode, one full cycle was sampled, and metabolite and biomass concentrations were measured in parallel to $H_2$ and $CO_2$ in the off-gas. In the CSTR, batch tests were conducted by removing 1 L of reactor broth and replacing it by 1 L of medium to finally obtain a concentration of 1 g L$^{-1}$ of xylose and 1 g L$^{-1}$ of glucose together with a stoichiometric amount of other nutrients. Sampling and off-gas analysis were carried out as in the SBRs over 5 h.

To characterise the mixed substrate uptake of the single substrate limited SBR enrichments, these enrichments were re-inoculated from with 10 mL effluent that was stored with 10% glycerol at -80°C. These SBRs were operated for one week and then a cycle was characterized using 1 g L$^{-1}$ of xylose and 1 g L$^{-1}$ of glucose.

### Microbial community analysis

Genomic DNA was extracted from 2-mL samples of reactor suspension and the bacterial community compositions analysed as described in Rombouts *et al.* [137] and **Chapter 2**. Analysis of V3-V4 16S rRNA gene-based amplicon sequencing was executed as described in Rombouts *et al.* [137] to get an overview of the predominant populations selected in the enrichments over time. Cloning and sequencing of full-length 16S rRNA genes was conducted following Rombouts *et al.* [137] (**Chapter 2**) to obtain species-level information, picking 38 clones for the CTSR and 24 for the SBR enrichment. Primers used are listed in Table 3.S1. Amplicon sequencing data is available

at NCBI under SRR8718538-SRR8718547 and full 16S clone sequences are available under MK185473-MK185614

Cell fixation and fluorescence *in situ* hybridisation (FISH) were carried out as described by Rombouts *et al.* [137] and **Chapter 2**. Staining with 4′,6-diamidino-2-phenylindole (DAPI) was used to map all microbial cells. Projected cell surface area quantification was carried out using the Quantimet Interactive Programming System (QUIPS) feature of the Leica QWin V3 software (Leica, Germany).

**Mathematical modelling of the batch tests**

Mathematical modelling of the batch tests was carried out as described in Rombouts *et al.* [137] and **Chapter 2**, with following adaptations: (I) separate maximum biomass-specific rates of substrate consumption ($q_s^{max}$) were fitted for xylose and glucose in one batch test; (II) the yields of biomass formation on substrates ($Y_{x,s}$) were fixed on glucose or xylose using the biomass yield obtained for the xylose or glucose SBR or the biomass yield obtained from the cycle measurement performed with the xylose or glucose CSTR from Rombouts *et al.* [137] and **Chapter 2**.

**COD and carbon balances**

At steady state, carbon and chemical oxygen demand (COD) balances were set up using the method described in Rombouts *et al.* [137] and **Chapter 2** and the elemental matrix (Table 2.S4). NADH and acetyl-CoA yields were set up by multiplying the values in supplementary Table 2.S4 with the yield on glucose and xylose.

## Results

### Fermentations in SBR and CSTR enrichment cultures result in different product spectra

The two enrichment cultures operated with a mixture of xylose and glucose in SBR and CSTR mode showed a different fermentation product spectrum (Figure 3.1). The SBR enrichment initially produced predominantly acetate, ethanol and propionate (data not shown). When the steady state was reached, the SBR enrichment shifted to a product spectrum dominated by acetate and ethanol. The CSTR enrichment developed within 20 SRTs to a stable fermentation pattern producing primarily ethanol, acetate and butyrate (Figure 3.1). Mass and electron balances were almost closed with carbon and COD recovered to acceptable amounts (Table 3.1), indicating that all relevant fermentation products were identified.
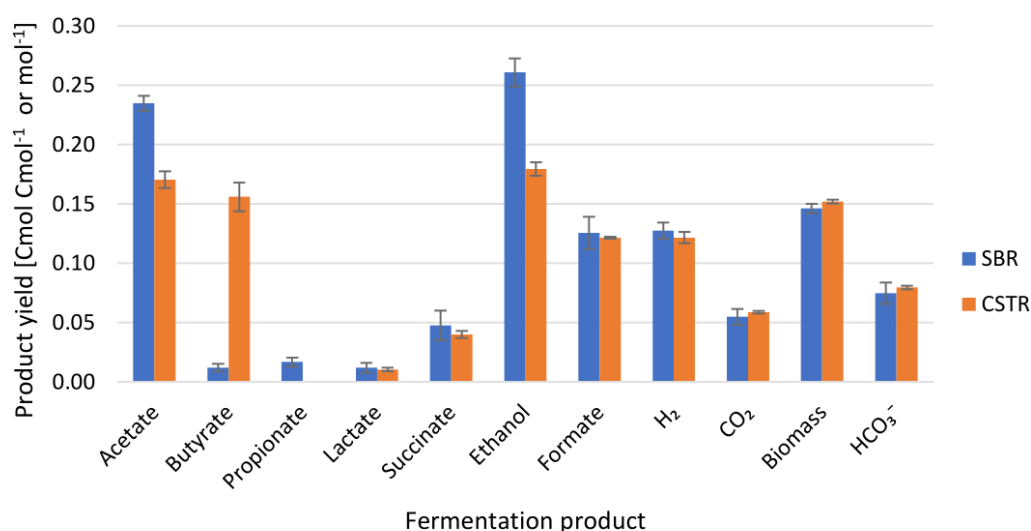


**Figure 3.1**: *Steady state fermentation product spectra of glucose and xylose fed SBR and CSTR in Cmol or mol product per Cmol substrate on the basis of three measurements in time and using a biomass composition of $C_1H_{1.8}O_{0.5}N_{0.2}$ as proposed by Roels et al. [148]. $HCO_3^{-1}$ is estimated using a $k_La$ value of 5.34 $h^{-1}$.*

**Table 3.1**: *Carbon and COD balances, product yields and biomass yields in the glucose and xylose fed SBR and CSTR enrichment cultures. Acetyl-CoA derivates and formate and hydrogen yields and NADH yields were calculated on the basis of our previously published biochemical network [137]. Yields are given per C-mol substrate.*

|  | Carbon (%) | COD (%) | Acetyl-CoA derivates (mol Cmol$^{-1}$) | Formate + H$_2$ (mol Cmol$^{-1}$) | NADH (mol Cmol$^{-1}$) | $Y_{x,s}$ (Cmol Cmol$^{-1}$) |
|---|---|---|---|---|---|---|
| **SBR** | 99 ± 2 | 99 ± 1 | 0.25 ± 0.01 | 0.25 ± 0.02 | -0.07 ± 0.01 | 0.15 ± 0.00 |
| **CSTR** | 97 ± 5 | 96 ± 2 | 0.25 ± 0.01 | 0.24 ± 0.01 | -0.04 ± 0.00 | 0.15 ± 0.00 |

### Xylose and glucose were taken up simultaneously, while xylose uptake was slower than glucose uptake

A cycle analysis or batch experiment was performed to estimate the $q_s^{max}$ and $\mu^{max}$ values of the enrichment cultures. Xylose and glucose were both instantly taken up by the enrichment cultures (Figure 3.2), indicating no carbon catabolite repression of glucose on xylose uptake in either

culture. The xylose uptake rate was 2.7 and 1.7 times slower than glucose uptake rate in the SBR and CSTR enrichment culture, respectively. Both xylose and glucose uptake rates were higher in the SBR than CSTR enrichment culture (Table 3.2), with the summed $q_s^{max}$ values being 2.3 times higher for the SBR than for the CSTR culture. Noteworthy is the fact that the mixed-substrate CSTR enrichment culture displayed a combined $\mu^{max}$ only 31% above the applied dilution rate of 0.11 $h^{-1}$.
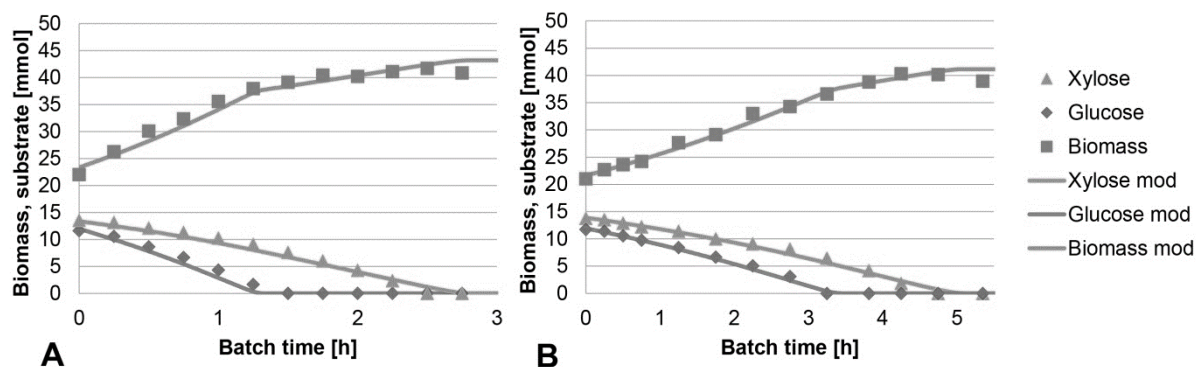


**Figure 3.2**: *Measured and modelled glucose, xylose and biomass concentrations during the cycle analysis in the SBR (A) and CSTR (B) enrichment cultures. Both modelled results showed a $R^2 > 0.99$.*

**Table 3.2**: *Modelled $q_s^{max}$ and $\mu^{max}$ for glucose or xylose and during the cycle analysis with both substrates for the SBR enrichment and the CSTR enrichment (measured data in Figure 3.2). The $\sigma_{qsmax}$ was calculated using error propagation and the covariance of the $C_s$ and $C_{x,0}$ measurement, while $\sigma_{\mu max}$ was calculated using error propagation and the covariance of the $C_x$ and $C_{x,0}$ measurement. Biomass yields used to estimate the growth rate are taken from the enrichments on solely xylose or glucose as growth substrate* [137].

| | | Mixed substrate SBR | Mixed substrate CSTR |
|---|---|---|---|
| **Glucose** | $q_s^{max}$ (Cmol$_s$ Cmol$_x^{-1}$ h$^{-1}$) | 2.01± 0.03 | 0.78 ± 0.01 |
| | $\mu^{max}$ (h$^{-1}$) | 0.26 ± 0.01 | 0.11 ± 0.01 |
| **Xylose** | $q_s^{max}$ (Cmol$_s$ Cmol$_x^{-1}$ h$^{-1}$) | 0.79 ± 0.01 | 0.46 ± 0.01 |
| | $\mu^{max}$ (h$^{-1}$) | 0.09 ± 0.01 | 0.06 ± 0.01 |
| **Summed** | $q_s^{max}$ (Cmol$_s$ Cmol$_x^{-1}$ h$^{-1}$) | 2.80 ± 0.04 | 1.24 ± 0.02 |
| | $\mu^{max}$ (h$^{-1}$) | 0.36 ± 0.04 | 0.17 ± 0.03 |

**Feeding a mixture of xylose and glucose led in both CSTR and SBR enrichments to one dominant microbial species**

According to dynamics of operational taxonomic units (OTUs) revealed by V3-V4 16S rRNA gene amplicon sequencing (Figure 3.4), the sequencing reads from the mixed-substrate CSTR were dominated by four populations affiliating with the genus *Citrobacter*, the family of *Enterobacteriaceae*, the family of *Lachnospiraceae*, and the genus *Clostridium*. All four populations stabilised after 20 SRTs, after an initial predominance of *Raoultella* and *Citrobacter* populations during the initial batch phase after which the reactor was switched into CSTR mode.
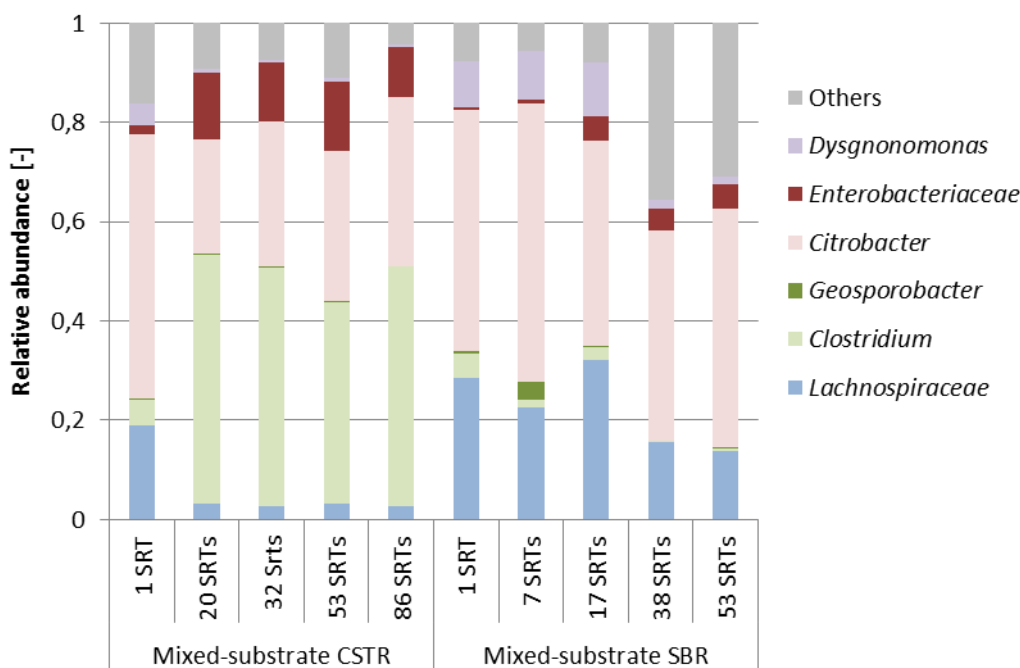
 *Figure 3.4: Relative abundance of genera obtained from V3-V4 16S rRNA gene amplicon sequencing read counts. Genera of the* Enterobacteriaceae *family are shown in red colours and genera of the* Clostridiaceae *are shown in green colours. OTUs accounting for less than 3% of the reads were bundled into others (grey).*
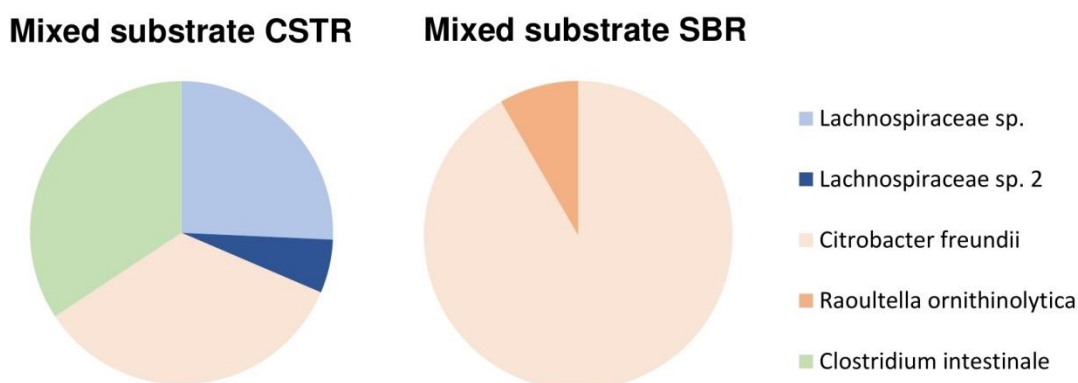


*Figure 3.5: Microbial composition as estimated by cloning and sequencing of full-length 16S rRNA gene sequences of the bacterial populations in the mixed-substrate CSTR and SBR enrichments.* Lachnospiraceae *species are denoted in blue colours,* Enterobacteriaceae *species in red colours and* Clostridiaceae *species in green colours. Samples used are 86 SRTs for CSTR and 53 SRTs for SBR.*

The sequencing reads of the mixed-substrate SBR were dominated by *Citrobacter* and *Enterobacteriaceae*. The same *Lachnospiraceae* genus as detected in the CSTR corresponded initially to 28% of the reads, stabilising at 13-15% later. Initially *Dysgonomonas* were significantly present (11%, respectively, at 16 SRTs), decreasing to less than 2% at 38 SRTs. The fractions of other microbial groups in the SBR remained quite high at the end of the enrichment (31-35%) being composed of mostly of *Proteobacteria*, *Firmicutes*, *Actinobacteria* and *Bacteriodetes*.

The clone library of full-length 16S rRNA gene sequences established at the end of the enrichment was efficient to identify the dominant phylotypes with a species-level resolution (Figure 3.5). The amplicon sequencing results were reflected by the sequenced clone library. The predominance of

*Citrobacter freundii*, *Clostridium intestinale* and two uncultivated *Lachnospiraceae* species gave a similar distribution (Figure 3.5) in the CSTR enrichment. The composition of OTUs of the mixed-substrate SBR was also confirmed, with a predominance of *Citrobacter freundii*, and a 8% fraction of the full 16S rRNA gene sequences corresponding to *Raoultella ornithinolytica*. An amount of 24 clones was picked for this library, which did not result in enough resolution to also identify the *Lachnospiraceae* population or species from the others fraction.

The FISH analysis revealed that the mixed-substrate SBR enrichment was dominated by *Enterobacteriaceae*, with 75% of the cell surface area showing fluorescence of the Ent183 probe (Table 3.3). A side population of *Lachnospiraceae* was also detected (8%). No cells hybridised with the *Clostridium*-targeting Chis150 probe. A significant fraction of 17% of microbial populations of the SBR enrichment remained unresolved by FISH. The CSTR enrichment was dominated by *Clostridium* (91%) with a side population of *Enterobacteriaceae* (11%) and a minor fraction of *Lachnospiraceae* (1%) (Table 3.3). Thus, the SBR enrichment was dominated by *Enterobacteriaceae* species and the CSTR enrichment to an even higher extend by *Clostridium* species. There is a clear discrepancy between the FISH observations and the DNA sequencing-based observations, which will be discussed below.

**Table 3.3**: *Microbial composition analysis based on FISH quantification (average of three different measurements) of dominant populations in the mixed-substrate SBR and CSTR, with percentages denoting relative abundances calculated from the target-probe surface compared to EUB338 surface. Unidentified populations were calculated as the remaining percentage after summing up the relative abundances of the known populations in the first three columns. The last column shows the amount of surface probed by EUB338 compared to DAPI. Samples used were taken at 86 SRTs for CSTR and 37 SRTs for SBR. ND = not detected.*

|  | **Chis150** *vs.* EUB338 [%] | **Lac435** *vs.* EUB338 [%] | **Ent183** *vs.* EUB338 [%] | **Unidentified** *vs.* EUB338 [%] | **EUB338** *vs.* DAPI [%] |
|---|---|---|---|---|---|
| **Mixed substrate SBR** | ND | 8±6 | 75±8 | 17 | 103±24 |
| **Mixed substrate CSTR** | 91±2 | 1±1 | 11±6 | -2 | 102±24 |

## Discussion

### Mixed substrate enrichment led to a similar spectrum of fermentation products as single-substrate enrichments

In this study we observed enrichment cultures on a mixture of glucose and xylose cultivated in the same way as previous enrichment cultures on the individual substrates [137]. A comparison was made between a CSTR regime (always substrate limited uptake rates) and SBR regime (maximal substrate uptake rates). The product spectrum obtained when enriching a microbial community on a mixture of xylose and glucose was similar to the summation of the product spectra obtained on the single substrates (Figure 3.S1) using the same inoculum and enrichment procedure. The formate and $H_2/CO_2$ ratio was different between the mixed-substrate SBR and the single-substrate SBRs summed up. The reason for this difference is not known, but the $k_La$ is likely excluded as we observed previously that different gas flow rates do not affect the formate and hydrogen ratio [137].

The mixed-substrate CSTR was producing more butyrate and less acetate and ethanol than the sum of the individual product spectra would suggest, though the spectrum is similar. Feeding a mixture of xylose and glucose to a CSTR fermentative community enriched on xylose has previously yielded to a similar observation: the product spectrum of a mixed-substrate enrichment has been similar, but not exactly the same to the theoretical summed product spectrum of a single-substrate enrichment [88].

### Pathway analysis of the enrichments reveals pentose phosphate pathway (PPP) for xylose fermentation and no homoacetogenesis and electron bifurcation

When comparing the products derived from acetyl-CoA and the formate and hydrogen yields (Table 3.1), it can be concluded that in both enrichments acetate, ethanol, and butyrate were produced with a direct stoichiometric coupling with hydrogen or formate, through the decarboxylation of pyruvate to acetyl-CoA [51, 137]. The NADH balance showed that slightly more NADH was consumed than produced in both enrichments (Table 3.1). This can be corrected by assuming a net NADH neutral production of succinate through both the reductive and oxidative pathways, equal to -0.04 and -0.02 mol Cmol$^{-1}$ for the SBR and CSTR cultures, respectively.

The PPP was assumed active in both enrichments since acetate and ethanol were produced in equimolar amounts and no excess of acetyl-CoA derivates over formate and hydrogen was detected (Table 3.1). The PKP produces directly one acetate and shuttles three carbon into glycolysis, leading to less production of formate and hydrogen and more acetate than ethanol. Furthermore, the nearly closing NADH balance and the equimolar amounts of acetyl-CoA derivates and formate and hydrogen sustained that homoacetogenesis and electron bifurcation [80] did not play a significant role in these enrichments.

### Microbial community analysis showed a difference in biomass quantification between FISH and 16S-based methodologies

In the mixed-substrate CSTR the 16S rRNA amplicon sequencing and the full 16S clone library suggested that a *Clostridium*, *Citrobacter* and *Lachnospiraceae* population where present in equal amounts in the community (Figure 3.4 and 3.5). The FISH analysis however showed a dominance of *Clostridium* (Table 3.3 and Figure 3.S2B). This difference can arise from a DNA extraction bias or PCR amplification bias [116] or from the fact the *Clostridium* cells contain an equal amount of 16S DNA but are 5-10 times bigger than the *Citrobacter* and *Lachnospiraceae* cells, as visible using light microscopy (Figure 3.S4).The amount of biomass (or biovolume), rather than the cell number, is representative for the share in substrate turn-over in a microbial community. This amount of biomass is assessed by FISH where a quantification is made based on cell-surface area.

Recently in other studies a similar discrepancy between biovolume and cell numbers due to differences in cell size have been reported [149–151] A "full cycle rRNA analysis" of a microbial community structure, as proposed by Amann, Ludwig and Schleifer [117] is needed to get a quantitative view of a microbial community structure. Such as cycle consists of first identifying the dominant taxa in a given sample (*e.g.* 16S rRNA amplicon sequencing), and then using a quantitative tool like FISH to estimate the fractions of these taxa in a sample.

## The CSTR enrichment resulted in a dominance of a generalist species

We originally hypothesised that a CSTR enrichment based on a mixture of equivalent substrates would lead to the dominance of a generalist species over specialist species. The microbial community analysis showed that the mixed-substrate CSTR enrichment was dominated by a *Clostridium* population (Table 3.4, Figure 3.S3) mainly composed of *Clostridium intestinale* (Figure 3.5). This species was also dominating a glucose-limited CSTR enrichment [137] and can be linked to butyrate production, as the CSTR makes a significant amount of butyrate and the SBR does not. Apparently, this species is competitive in both a sole glucose-limited CSTR environment and a dual xylose- and glucose-limited CSTR environment.

To dominate under dual limitations, *C. intestinale* needs to have a high affinity uptake system for glucose and for xylose expressed. For glucose, the phosphotransferase system (PTS) and methyl-galactoside transport system ATP-binding protein (Mgl) have both been described as high-affinity transporters [152]. For xylose, the xylose ABC (ATP-binding cassette) transport operon (XylFGH) is known as high-affinity uptake system [106]. The closest strain of which a genome is available is *C. intestinale* strain JCM 7506 (NCBI:txid1121320), also known as strain DSM 6191 (99% identity). This strain contains all three subunits of the PTS system in its genome and the xylose-binding protein XylF, enabling it to competitively take up glucose and xylose in a continuous substrate limited environment, leading to its dominance in a mixed-substrate environment (Figure 3.6). XylG and XylH are not found in its genome, but other ABC type ATP-binding proteins and membrane spanning proteins, found in the genome could fulfil these roles.



| Species | Xylose uptake XylFGH | Glucose uptake PTS II ABC |
|---|---|---|
| Generalist | + | + |
| Xylose specialist | + | - |
| Glucose specialist | - | + |
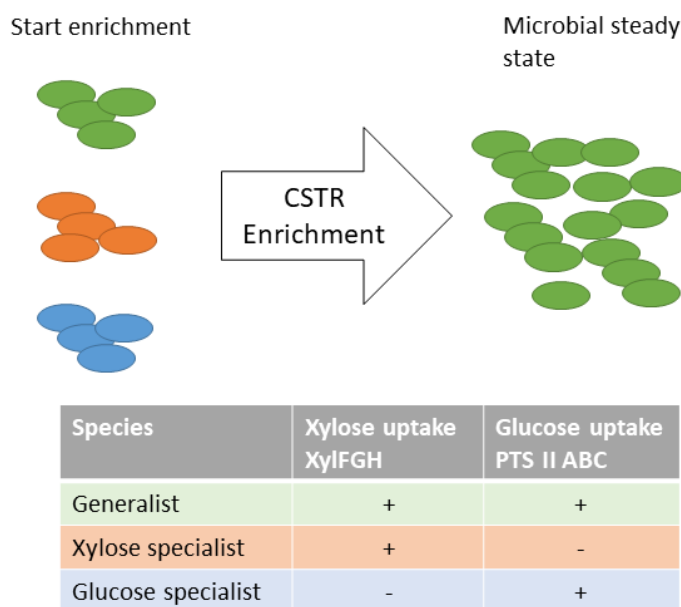
*Figure 3.6*: *A theoretical outcome of a CSTR enrichment with three different types of microbial species present at the start of the enrichment, a generalist, a xylose specialist and a glucose specialist.*

Previously, Temudo *et al.* [121] have characterised the effect of switching from feeding xylose or glycerol to feeding an equal amount of xylose and glucose or glycerol and glucose. They have observed that a similar amount or even less bands were observed in the molecular fingerprint of

the bacterial community obtained by denaturing gradient gel electrophoresis (DGGE). This indicated that adding a mixture of limiting substrates does not necessarily lead to more microbial diversity, as also observed in the mixed-substrate CSTR performed here, where a *C. intestinale* was the dominating the microbial community in terms of biovolume.

## SBR enrichment leads to dominance of a dual xylose- and glucose-fermenting species

In the mixed substrate SBR, a dominance of *Enterobacteriaceae* with a side population of *Lachnospiraceae* affiliates was observed (Table 3.3, Figure 3.S4). Previously we have reported the dominance (>90%) of *Enterobacteriaceae* affiliates on SBRs limited on either glucose or xylose [137]. The significant side population of *Lachnospiraceae* present in the mixed-substrate SBR enrichment might have been caused by rather long cleaning intervals of wall biofilm. In this study the SBR was cleaned every 3-9 SRTs versus 3 SRTs in **Chapter 2** (Table 3.S6). The biofilm formed has presumably added microbial diversity to the community in the form of *Lachnospiraceae*. We expect that a 3 SRT cleaning schedule would have led to an enrichment dominated completely (>90%) by *Enterobacteriaceae*.

Well-studied microorganisms such as *E. coli* display CCR in batch [142]. Therefore, we hypothesised that a diauxic generalist species fermenting first glucose and then xylose would coexist with a specialist for xylose. We find *Citrobacter freundii* as the dominant *Enterobacteriaceae* in the mixed-substrate SBR enrichment, when assuming DNA extraction, copy number and PCR biases to be similar in this family (Figure 3.5) and a non-diauxic uptake of xylose and glucose (Figure 3.2). This species was also dominant in the xylose SBR enrichment (**Chapter 2**), and showed a non-diauxic uptake for xylose when subjected to a cycle with xylose and glucose (Figure 3.S2B).

*Citrobacter freundii* strains are known to ferment both xylose and glucose [153]. The $q_s^{max}$ of the sole xylose enrichment was $2.28\pm0.10$ h$^{-1}$ [137], while the mixed substrate SBR enrichment showed a combined $q_s^{max}$ of $2.80\pm0.04$ Cmol$_s$ Cmol$_x^{-1}$ h$^{-1}$, which is similar to the value of the xylose SBR subject glucose and xylose, $2.68\pm0.04$ Cmol$_s$ Cmol$_x^{-1}$ h$^{-1}$. The dominant *C. freundii* species outcompetes xylose specialists by attaining a higher overall $q_s^{max}$ on xylose and glucose, and therefore a higher $q_s^{max}$ than what is achievable on solely xylose. It has been shown that *E. coli* can achieve a higher catabolic flux when taking glucose compared to xylose [154]. This can underlie why dual xylose glucose uptake in our study led to higher overall flux. Apparently, a xylose specialist or a CCR-type generalist are outcompeted by a non-diauxic dual fermenting generalist.

XylE is a xylose symporter which is associated with high rate and low affinity [106] which makes this transporter likely to be expressed at high growth conditions. Outer membrane protein C (OmpC) and OmpF allow glucose to diffuse into the cell at high substrate concentration (>0.2 mM) while lambda receptor protein B (LamB) is induced under lower glucose concentrations [155]. The dominant strain in the mixed SBR enrichment is *C. freundii* strain P10159 (CP012554.1, 100% identity), which was also the dominant strain in the xylose SBR enrichment [137]. This strain contains the genes to express XylE, OmpC and LamB, which argues for its competitive uptake of both substrates. Xylose uptake is inhibited through a cAMP mediated pathway [155]. Since this species exhibited no CCR in our enrichments, it would be of interest to identify how this species regulated its glucose and xylose uptake.
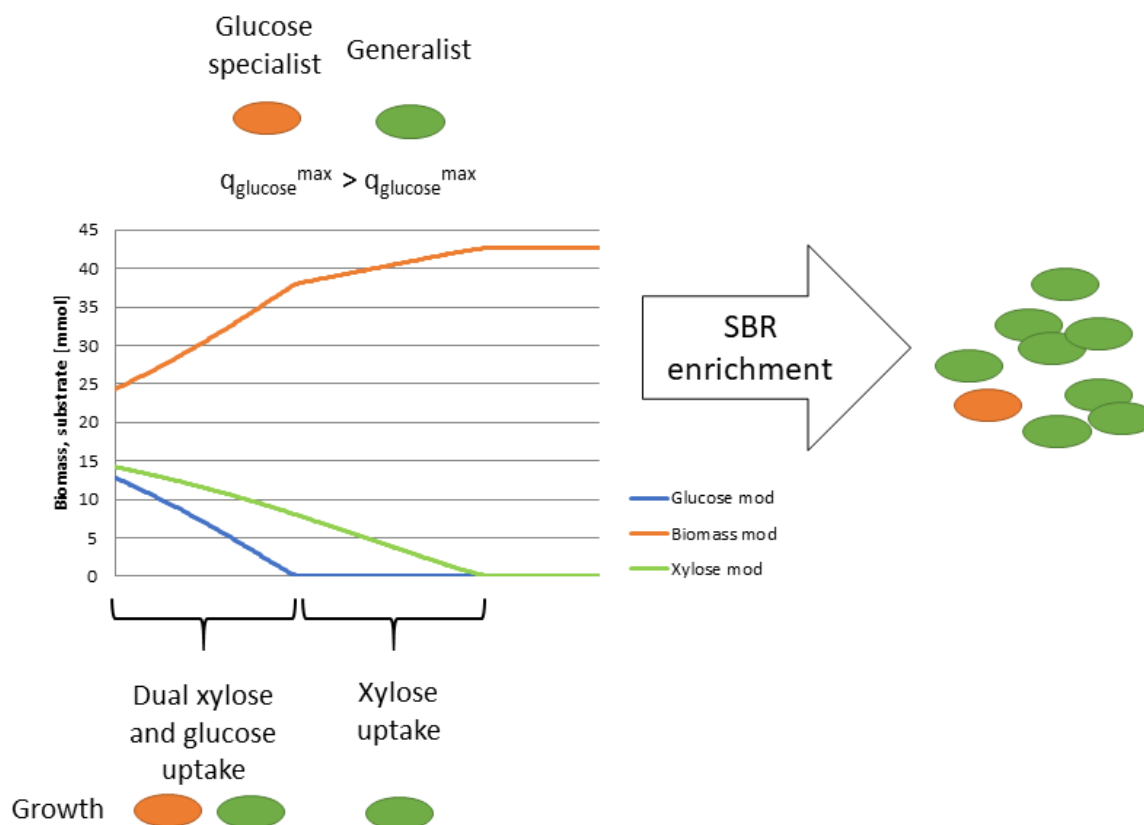
***Figure 3.7***: *Competition between a high-rate glucose specialist (orange) and a dual xylose- and glucose-fermenting generalist. In the first phase, glucose is taken up by both species, while in the second phase xylose is only taken up the generalist.*

A niche is present for a glucose specialist, fermenting glucose at a $\mu^{max}$ and $q_s^{max}$ higher than that of the generalist. A minor fraction of *Raoultella ornithinolytica* was detected (Figure 3.5), which was also detected in a minor amount in the glucose SBR enrichment [137]. Potentially, this species takes up glucose at a higher rate than the generalist, enabling them to coexist (Figure 3.7). Since the generalist grows on both xylose and glucose, this species is assumed to dominate the enrichment, which was reflected by the clone library (Figure 3.5). It has been shown that repeated batch cultivation at 60°C (5 SRTs) led to the presence of three populations for glucose, one for xylose, and four for a mixture of glucose and xylose [156]. Since this study only characterised the microbial community after 5 SRTs, it is well possible that the microbial diversity would have decreased for the all three enrichments. Microbial population dynamics can lead to a relatively long time for communities to stabilize which is visible in the mixed substrate SBR (Figure 3.4). A *Dysgonomonas* population emerged in the reads at 7 SRTs and then became a minor fraction at 38 SRTs, indicating some microbial interaction to take place in this timespan which causes a more diverse community structure.

Here we conclude that enriching in a CSTR using mixed substrates lead to a dominant generalist species, confirming our hypothesis and the chemostat theory that describes the competitive advantage of a generalist in a chemostat. In the SBR, a generalist species was fermenting the xylose and glucose without carbon catabolite repression, which was not expected, postulating that contrary to many pure culture studies xylose and glucose are taken up in the environment by generalists without CCR. In dual substrate uptake, xylose fermentation is slower than glucose fermentation and product spectra of mixture of xylose and glucose are similar to product spectra from solely xylose or glucose. Microbiologists designing an industrial mixed substrate batch fermentation of a lignocellulosic residue containing glucose and xylose should consider that a non-diauxic generalist is competitive in such an environment.

## Supplementary information

*Table 3.S1*: *Primers used in this study*

| Primer | Primer Sequence (5'- 3') | Reference |
|--------|--------------------------|-----------|
| 341f | CCT AYG GGR BGC ASC AG | [122],[123] |
| 806r | GGA CTAC NNG GGT ATC TAA T | [122],[123] |
| GM3f | AGA GTT TGA TCM TGG CTC AG | [124] |
| GM4r | GGT TAC CTT GTT ACG ACT T | [124] |
| M13f | GTA AAA CGA CGG CCA G | [125] |
| M13r | CAG GAA ACA GCT ATG AC | [125] |

*Table 3.S2*: *FISH probes used in this study with the formamide concentration used during hybridisation*

| FISH Probe | Sequence 5'- 3' | Specificity | Formamide [%] | Reference |
|------------|-----------------|-------------|---------------|-----------|
| EUB338 Cy5 | GCT GCC TCC CGT AGG AGT | Bacteria | 20-25 | [126] |
| ENT183 Cy3 | CTC TTT GGT CTT GCG ACG | *Enterobacteriaceae* family | 20 | [127] |
| Chis150 Cy3 | TCT TCC CTG CTG ATA GA | *Clostridium* genus | 25 | [128] |
| Lac435 Cy3 | TTA TGC GGT ATT AAT CTY CCT TT | *Lachnospiraceae* family | 25 | [129] |

*Figure 3.S1*: *The obtained product spectrum for the mixed-substrate SBR (A) and CSTR (B) compared to the theoretical summed SBR (A) and CSTR (B) product spectrum based on the yields obtained for the single substrate enrichments* [137] *and using 50% of the xylose and glucose obtained yields, respectively.*

**Table 3.S3**: *Modelled $q_s^{max}$ and $\mu^{max}$ for glucose or xylose during the cycle analysis with both substrates for the glucose-fed SBR enrichment culture and the xylose-fed SBR enrichment culture enriched previously [137]. Covariance of the biomass and xylose and glucose measurements were used to calculate the covariance of the rates.*

|  |  | **Glucose-fed SBR** | **Xylose-fed SBR** |
|---|---|---|---|
| **Glucose** | $q_s^{max}$ (Cmol$_s$ Cmol$_x^{-1}$ h$^{-1}$) | 2.10 ± 0.03 | 1.56 ± 0.02 |
|  | $\mu^{max}$ (h$^{-1}$) | 0.28 ± 0.00 | 0.21 ± 0.00 |
| **Xylose** | $q_s^{max}$ (Cmol$_s$ Cmol$_x^{-1}$ h$^{-1}$) | 0.00 ± 0.00 | 1.12 ± 0.02 |
|  | $\mu^{max}$ (h$^{-1}$) | 0.00 ± 0.00 | 0.13 ± 0.00 |
| **Summed** | $q_s^{max}$ (Cmol$_s$ Cmol$_x^{-1}$ h$^{-1}$) | 2.10 ± 0.03 | 2.68 ± 0.04 |
|  | $\mu^{max}$ (h$^{-1}$) | 0.28 ± 0.00 | 0.34 ± 0.01 |
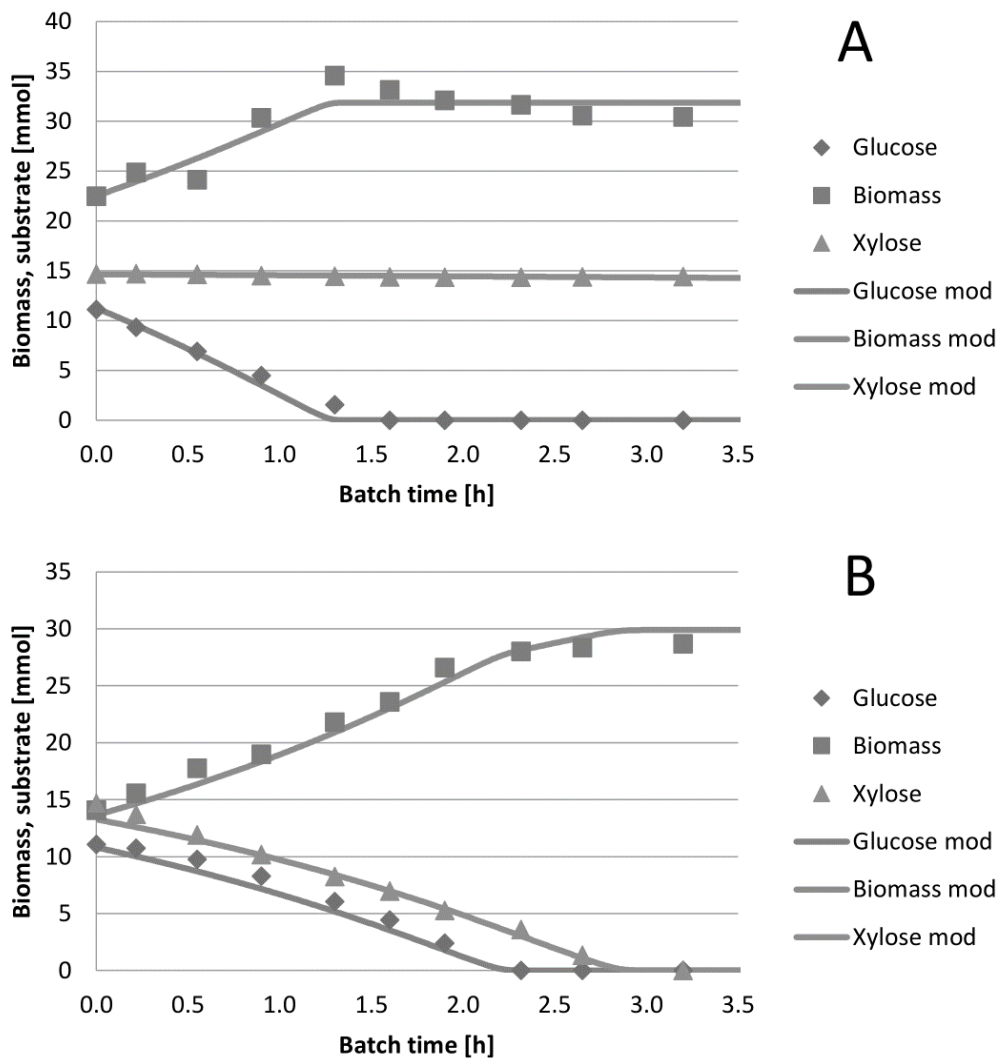


**Figure 3.S2**: *Simultaneous uptake of xylose and glucose during a cycle analysis performed in the glucose-fed SBR enrichment culture (A) and the xylose-fed SBR enrichment culture (B) enriched previously [137]. Biomass yields on xylose and glucose were fixed and obtained from previous reported biomass yields on either xylose or glucose [137]. $R^2$ values are 0.84 and 0.99 for A and B respectively.*

*Table 3.S4: Result using BLASTn of the reference OTU sequences obtained using V3-V4 16S rRNA gene amplicon sequencing*

| Accession number | Identity | E value | Query cover | Total score | Maximum score | Closest cultivated relative | Label figure | Colour |
|---|---|---|---|---|---|---|---|---|
| MG812314.1 | 100% | 0 | 100% | 793 | 793 | Citrobacter freundii strain ER1 16S ribosomal RNA gene, partial sequence | Citrobacter | |
| MH681450.1 | 100% | 0 | 100% | 793 | 793 | Raoultella ornithinolytica strain BE3.4 16S ribosomal RNA gene, partial sequence | Raoultella | |
| MF737172.1 | 100% | 0 | 100% | 793 | 793 | Klebsiella oxytoca strain B2006 16S ribosomal RNA gene, partial sequence | Klebsiella | |
| AJ630276.1 | 99% | 0 | 100% | 767 | 767 | Dysgonomonas gadei partial 16S rRNA gene, clone MFC-EB6 | Dysgonomonas | |
| LT855382.1 | 99% | 0 | 100% | 719 | 719 | Lachnospiraceae bacterium Marseille-P3773 partial 16S rRNA gene, strain Marseille-P3773 | Lachnospiraceae | |
| CP017269.1 | 100% | 0 | 100% | 8196 | 747 | Geosporobacter ferrireducens strain IRF9, complete genome | Geosporobacter | |
| LC037210.1 | 100% | 0 | 100% | 747 | 747 | Clostridium intestinale gene for 16S ribosomal RNA, partial sequence, strain: JCM 7506 | Clostridium | |

*Table 3.S5: Result using BLASTn on the representative sequences per OTU obtained after sequencing of the clone library of full-length 16S rRNA genes. Relative abundance per OTU are given at the bottom of the table.*

| SBR | CSTR | Accession | Ident | E value | Query cover | Total score | Max score | Description - closest related cultivated species | Fractions | Colour |
|---|---|---|---|---|---|---|---|---|---|---|
| 0 | 0.26 | MF953294.1 | 96% | 0.0 | 99% | 2259 | 2259 | *Lachnotalea glycerini* strain DLD10 16S ribosomal RNA gene, partial sequence | *Lachnospiraceae sp.* | |
| 0 | 0.058 | MF574095.1 | 92% | 0.0 | 96% | 1875 | 1875 | *Lachnotalea glycerini* strain CCRI-19302 16S ribosomal RNA gene, partial sequence | *Lachnospiraceae sp. 2* | |
| 0.88 | 0.17 | CP012554.1 | 100% | 0.0 | 100% | 21094 | 2638 | *Citrobacter freundii* strain P10159, complete genome | *Citrobacter freundii* | |
| 0.04 | 0.14 | CP026056.1 | 99% | 0.0 | 100% | 20612 | 2610 | *Citrobacter freundii* strain FDAARGOS_73 chromosome, complete genome | *Citrobacter freundii* | |
| 0 | 0.029 | CP026056.1 | 99% | 0.0 | 100% | 20172 | 2562 | *Citrobacter freundii* strain FDAARGOS_73 chromosome, complete genome | *Citrobacter freundii* | |
| 0.08 | 0 | KF358448.1 | 99% | 0.0 | 100% | 2612 | 2612 | *Raoultella ornithinolytica* strain FMC41 16S ribosomal RNA gene, partial sequence | *Raoultella ornithinolytica* | |
| 0 | 0.34 | AY781385.1 | 99% | 0.0 | 100% | 2588 | 2588 | *Clostridium intestinale* 16S ribosomal RNA gene, complete sequence | *Clostridium intestinale* | |
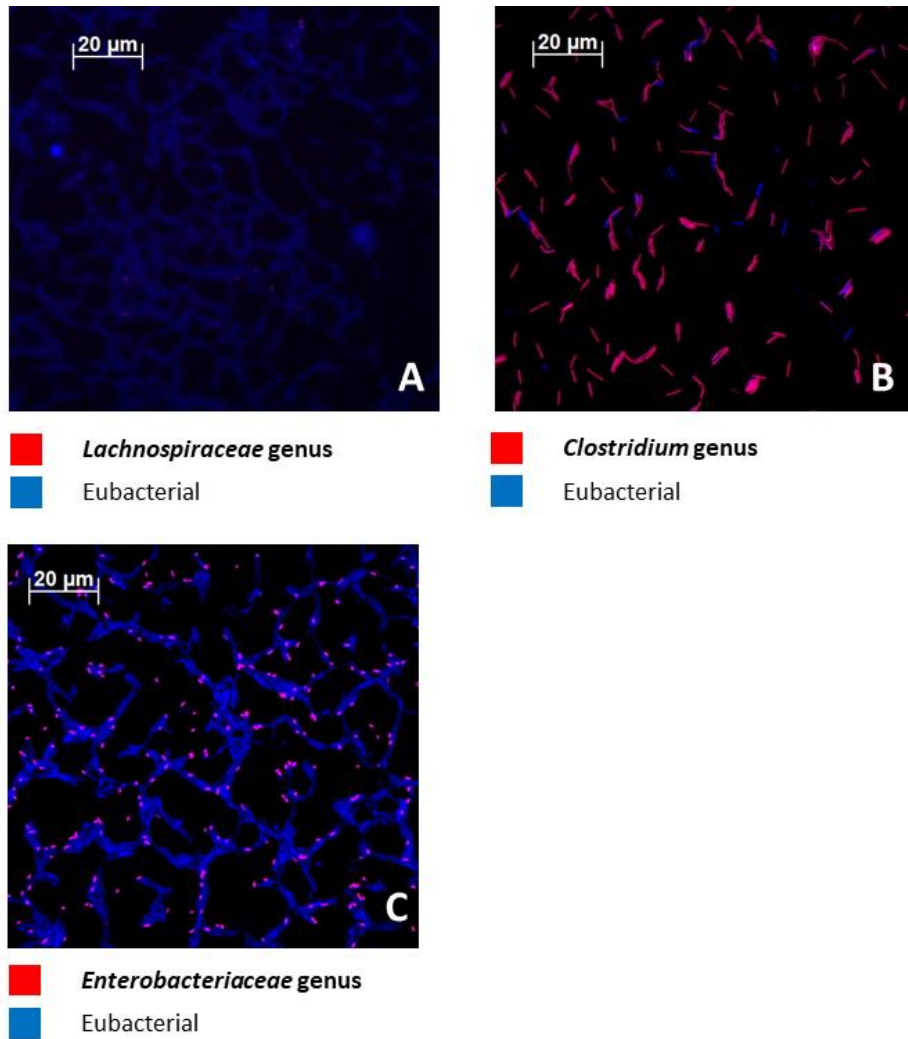
**Figure 3.S3***: Typical result obtained by FISH analysis of the mixed-substrate CSTR enrichment culture after 86 SRTs using the EUB338 mix oligonucleotide probes to target all eubacterial species, Lac435 to target* Lachnospiraceae, *Chis150 to target* Clostridium *and Ent183 to target* Enterobacteriaceae
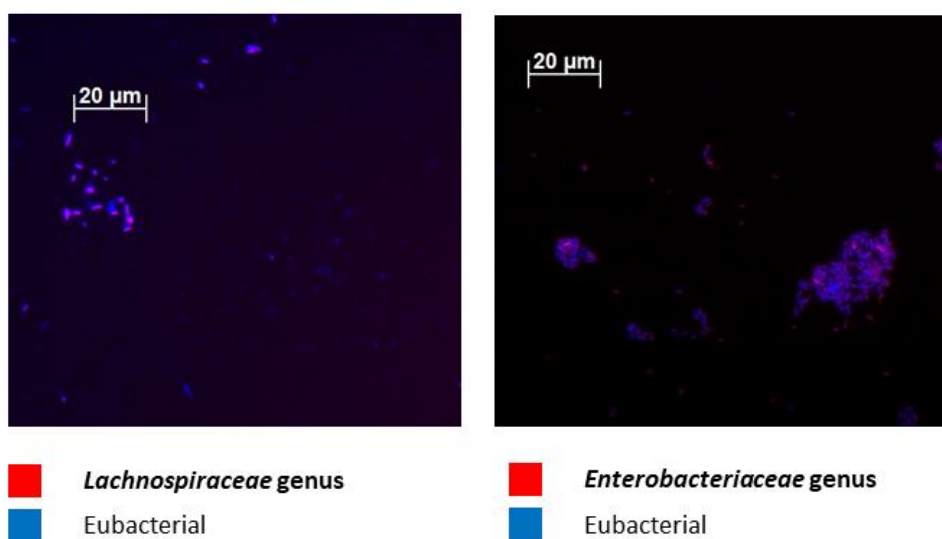


**Figure 3.S4***: Typical result obtained by FISH analysis of the mixed-substrate SBR enrichment culture after 37 SRTs using the EUB338 mix probes to target all eubacterial species, Lac435 probe to target* Lachnospiraceae, *and Ent183 to target* Enterobacteriaceae
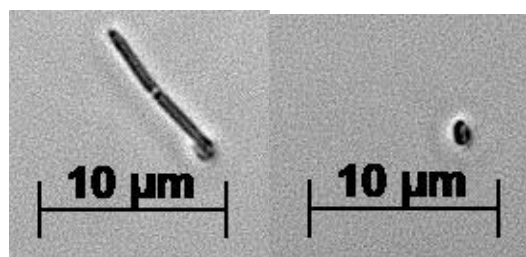
***Figure 3.S5****: Phase contrast image using bright field microscopy of a Clostridium cell (left) and a* Citrobacter *or* Lachnospiraceae *cell (right). The image was digitally sharpened using the Zeiss Axio software*

***Table 3.S6****: Intervals of cleaning of the wall biofilm developing in the mixed-substrate SBR*

| Date | SRTs | SRTs between cleaning |
|---|---|---|
| **23-5-2017** | 1 | 0 |
| **24-5-2017** | 2 | 1 |
| **26-5-2017** | 4 | 2 |
| **29-5-2017** | 7 | 3 |
| **31-5-2017** | 11 | 4 |
| **2-6-2017** | 17 | 6 |
| **4-6-2017** | 23 | 6 |
| **6-6-2017** | 29 | 6 |
| **8-6-2017** | 35 | 6 |
| **9-6-2017** | 38 | 3 |
| **12-6-2017** | 47 | 9 |
| **13-6-2017** | 50 | 3 |
| **14-6-2017** | 53 | 3 |

# Chapter 4 - Selecting for lactic acid producing and utilising bacteria in anaerobic enrichment cultures
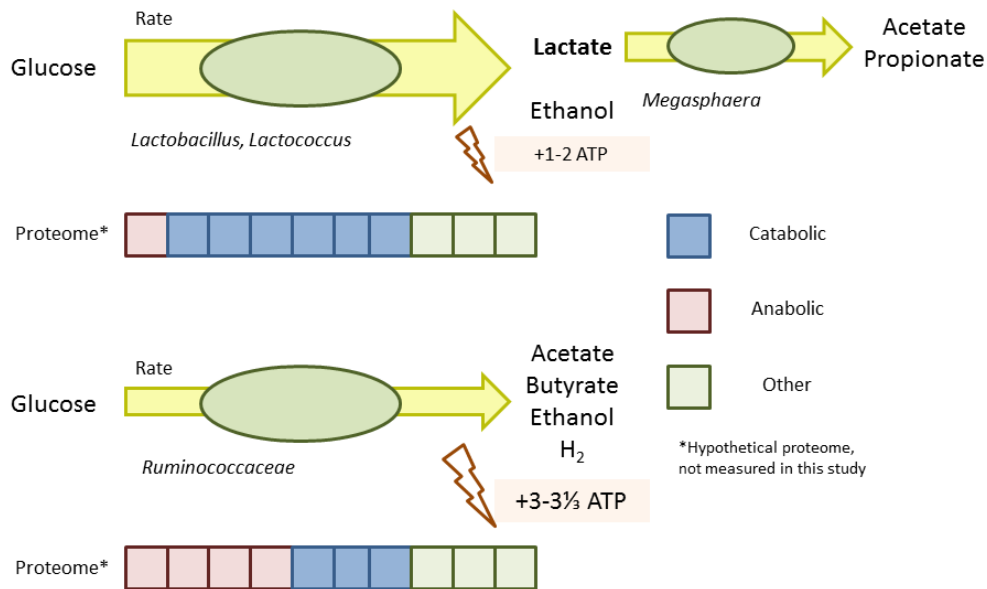
Julius L. Rombouts[1], Elsemiek M. M. Kranendonk[1], Alberte Regueira[2], David G. Weissbrodt[1], Robbert Kleerebezem[1], Mark C. M. van Loosdrecht[1]

[1]Delft University of technology, Department of Biotechnology, Van der Maasweg 9, 2629 HZ Delft, the Netherlands.

[2]Universidade de Santiago Compostela, Institute of Technology, Department of Chemical Engineering, 15782, Santiago de Compostela, Spain

## Abstract

Lactic acid producing bacteria are important in many fermentations, such as the production of biobased plastics. Insight in the competitive advantage of lactic acid bacteria over other fermentative bacteria in a mixed culture enables ecology-based process design and can aid the development of sustainable and energy-efficient bioprocesses. Here we demonstrate the enrichment of lactic acid bacteria in a controlled sequencing batch bioreactor environment using a glucose based medium supplemented with peptides and B vitamins. A mineral medium enrichment operated in parallel was dominated by *Ethanoligenens* species and fermented glucose to acetate, butyrate and hydrogen. The complex medium enrichment was populated by *Lactococcus*, *Lactobacillus* and *Megasphaera* species and showed a product spectrum of acetate, ethanol, propionate, butyrate and valerate. An intermediate peak of lactate was observed, showing the simultaneous production and consumption of lactate. This study underlines that the competitive advantage for lactic acid producing bacteria primarily lies in their ability to attain a high biomass specific uptake rate of glucose, which was two times higher for the complex medium enrichment when compared to the mineral medium enrichment. The competitive advantage of lactic acid production in complex media is discussed based on the resource allocation theory for microbial growth processes.

**Keywords**: Enrichment cultures – Kinetics – Lactic acid bacteria – Microbial ecology – Resource allocation

## Introduction

Lactic acid bacteria are key species in many fermentative processes [157], such as biogas production and food-related fermentations [158]. They also are essential in promoting human health, *e.g.* a healthy human infant microbiome [159]. In an industrial biotechnology setting, these microorganisms are applied in the production of lactic acid, which is used to preserve food and to produce the biobased and biodegradable plastic polylactic acid [160]. The lactic acid market is expected to reach 9.8 billion US dollars by 2025 [161] which shows the economic significance of lactic acid as a product.

Ecology-based design of bioprocesses is a discipline in which ecological principles are used to design biochemical processes. Such designs can aid to the development of more sustainable and energy-efficient bioprocesses. Here, mixed cultures perform the desired conversion, in contrast to a pure culture or synthetic biology approach. Compared to pure culture processes, mixed culture processes offer the advantage of (semi)-continuous bioprocessing and omit the need for sterilisation of the feedstock and equipment [73]. For a stable ecology-based process its design needs to be based on the competitive advantage of the concerned type of conversion, *i.e.* for a lactic acid fermentation the question is which environmental conditions provide lactic acid bacteria with a competitive advantage over other carbohydrate fermenting microorganisms.

Lactic acid bacteria tend to dominate in anaerobic, carbohydrate containing environments characterised by acidic pH and an abundant availability of compounds required for anabolism, such as in fermented milk, meats and vegetables [157]. Most well-studied lactic acid bacteria are part of the *Bacilli* class, such as *Streptococcus*, *Lactococcus*, *Bacillus* and *Lactobacillus* species. Lactic acid bacteria have high maximal biomass specific growth rates ($\mu^{max}$), *e.g. Streptococcus salivarius* shows a $\mu^{max}$ of 2.8 h$^{-1}$ in a complex medium at 37°C at neutral pH [162]. This can be compared to $\mu^{max}$ for *Escherichia coli* strain K12 of around 0.98 h$^{-1}$ at similar conditions [163]. Lactic acid bacteria seem to have a kinetic advantage over other species.

Lactic acid bacteria only display fast growth when sufficient B vitamins and peptides are supplied to their medium environment. For example, *Lactococcus lactis* strains are auxotrophic for 14 of the 20 amino acids [164]. Another study compares the genomes of microbial species to predict auxotrophies for B vitamins and shows that of the 46 *Lactobacillus* species analysed all are potentially auxotrophic for biotin, folate, pantothenate and thiamine [118]. These studies imply that lactic acid bacteria grow poorly or do not grow at all in environments where such growth factors are not available. We therefore suggest that auxotrophy is common among lactic acid bacteria, certainly under conditions of high growth rates.

Prototrophic fermentative microorganisms, which can be found in the genus of *Clostridium* and the family of *Enterobacteriaceae* and *Ruminococcaceae*, in general have lower $\mu^{max}$-values when compared to lactic acid bacteria. *E. coli* is a prototroph, and is reported to have a $\mu^{max}$ of 0.31 h$^{-1}$ at 37 °C and a pH of 7 in a mineral medium with glucose [107], producing acetate, ethanol and formate. We hypothesise that lactic acid bacteria will outcompete prototrophic fermenters by achieving a higher $\mu^{max}$ in complex environments where there is an abundance of peptides and B vitamins.

The switch between lactate production on the one hand, and acetate and ethanol production on the other hand, has been reported for a single species under complex medium conditions. *Lactococcus lactis* (formerly known as *Streptococcus lactis*), switches its catabolism from lactate production to acetate, ethanol and formate or $H_2$ production at lower dilution rates, *i.e.* lower growth rates [165]. Lactate is produced from pyruvate with one enzyme and delivers and acetate and ethanol with five enzymes. Lactate delivers 2 ATP by substrate level phosphorylation, while acetate and ethanol deliver 3 ATP. This switch is thought to be caused by resource allocation, which essentially describes that a cell has a certain amount of functional protein available, and shorter catabolic pathways can evoke a higher biomass specific substrate uptake rate, $q_s^{max}$, [166, 167], often at the expense of less energy harvesting per unit of substrate.

Here, we tested the hypothesis that lactic acid producing enrichment cultures can be obtained by providing a complex medium and selecting on high growth rate. We compared two parallel anaerobic non-axenic or open mixed culture sequencing batch reactors (SBRs) operated under mesophilic and slightly acidic conditions (pH = 5), with either mineral or complex cultivation media at relatively short doubling times (6 hours). The cultures were characterised for their stoichiometric, kinetic and bioenergetic properties and the microbial community structures were analysed.

## Material and Methods

### Bioreactor enrichment

Both enrichments were performed in 3 L jacketed bioreactors with working volumes of 2 L. pH was maintained at 5.0 ± 0.1 using NaOH at 4 mol $L^{-1}$ and HCl at 1 mol $L^{-1}$. Temperature was maintained at 30°C ± 0.1. The cultures were stirred constantly at 300 rpm. Anaerobic conditions were maintained by sparging the reactor with a flow of 576 mmol $N_2$ $h^{-1}$. The off-gas was cooled and dried at 5°C using a gas condenser. A hydraulic retention time (HRT) and solids retention time (SRT) of 12 h was maintained by removing 1 L of culture per cycle under continuous stirring and a cycle time set to 6 h.

The mineral cultivation medium was identical to the one used by Temudo [51] (**Appendix I**), while the complex medium was supplemented by 9 B vitamins and peptides according to Table 4.S1 in the supplementary information. The carbon source, peptides and B vitamins and the ammonium, phosphate and trace elements were fed separately from 12.5× concentrated stock solutions and diluted using $N_2$-sparged demineralized water. Connected to the base pump was a pump supplying 3% (v:v) antifoam C (Sigma Aldrich, St. Louis, Missouri, USA), which ensured a flow of 3-5 mL $h^{-1}$ or 14-17 mL $cycle^{-1}$. The glucose solution was sterilised at 110°C for 20 min. For the complex medium, the peptides were sterilised separately at 110°C for 20 min and the B vitamins were added by filter sterilisation through 0.45 μm and 0.2 μm polyvinylidene fluoride filters.

The inoculum for all enrichments consisted of sludge taken from an anaerobic digester of the wastewater treatment plant (WWTP) Harnaschpolder, The Netherlands. The pH, temperature, and HRT and SRT of the digester in the WWTP were 7-7.2, 36-38°C, and 20 days, respectively. At the beginning of each experiment, the reactor was seeded with approximately 10 mL of 200 μm filtered inoculum (0.5% of the total volume). The reactors were gradually moving from 24-h and 12-h cycles in 3 days to the final desired 6-h cycles to maintain a HRT of 12 h. Steady state was assumed if during a period of at least 5 days little variation was detected in the product concentrations.

### Analytical methods

Samples from the reactors were immediately filtered on 0.45 μm polyvinylidene fluoride membranes (Millipore, USA) and stored at -20°C until analysis. Volatile fatty acids (VFAs; formate to valerate), lactate, succinate and glucose were analysed using high performance liquid chromatograph (HPLC) method described previously [137]. Ethanol was analysed using a gas chromatography (GC) method described previously [137]. A more detailed explanation of the choice for using the refractive index or the ultra violet channel is given in Appendix 4.1. The off-gases were monitored on-line for $H_2$ and $CO_2$ by a connection to a NGA 2000 MLT 1 Multicomponent analyser (Rosemount, Shakopee, Minnesota, USA). Data acquisition (base, $H_2$, $CO_2$) was made using a BBI systems MFCS/win 2.1 (Sartorius, Göttingen, Germany).

Methane was measured manually using GC with a Varian CP 3800 (Varian Medical Systems, Palo Alto, California, USA) equipped with a MolSieve capillary column (1.2 m x 1 mm; 13 x 80/100 mesh, 50 °C) and a thermal conductivity detector (200 °C) with $N_2$ as a carrier gas (2 mL $min^{-1}$).

Biomass concentration was measured using a standard method which relies on centrifugation of 150 mL to separate the cells from the medium, drying these solids to obtain the total suspended solids (TSS) and burning these solids at 550 °C to determine the amount of volatile suspended solids (VSS) [94]. This analysis was coupled to absorbance measurement at 660 nm to establish a correlation. Absorbance values were used to calculate the biomass concentration during the cycle analysis and batch experiments.

**Cycle analysis and batch experiments**

To characterise one cycle, product and biomass concentrations were measured in parallel to $H_2$ and $CO_2$ in the off-gas. Sampling and off-gas analysis were carried out as described above. The biomass concentration was determined spectrophotometrically at 660 nm ($OD_{660}$) and this value was correlated to the three previous measurements of VSS.

A batch test with lactate and a batch test with $H_2$, and $CO_2$ was performed in the complex medium enrichment. This went by adding the peptides and B vitamins and peptides together with the N, P, S, trace elements, and either 11 mmol of lactate or 0.46% of $H_2$ and 1.00% of $CO_2$. Sampling was conducted as in a cycle measurement.

**Microbial community analysis**

Genomic DNA was extracted using the Ultra Clean Soil DNA extraction kit (QIAGEN, Hilden, Germany) following manufacturer's instructions, with the exception of heating the samples for 5 minutes at 65°C prior to bead beating. DNA extracts were checked on a 1% agarose gel. High molecular weight DNA was obtained (>10 kb) with a concentration of 10 ng $\mu L^{-1}$ or higher. Extracted DNA was stored at -20°C until further use.

Analysis of the V3-V4 region of the 16S rRNA gene was conducted using amplicon sequencing. The extracted DNA was sent for amplification and sequencing at a commercial company (Novogene, China). Amplification was achieved using the universal primer set 341f (CCTAYGGGRBGCASCAG) / 806r (GGACTACNNGGGTATCTAA T) [122][123]. All polymerase chain reactions (PCR) were carried out in 30 μL reactions with 15 μL of Phusion® High_fidelity PCR Master Mix (New England Biolabs, USA), 0.2 μmol $L^{-1}$ of forward and reverse primers, and 10 ng template DNA. Thermal cycling started with denaturation at 98°C for 10 s, annealing at 50°C for 30 s, and elongation at 72°C for 60 s for 30 cycles, prior to ending with 72°C for 5 min. These pools of amplicons were sequenced using an Illumina HiSeq2500 platform. The sequencing datasets were cleaned and trimmed according to Jia *et al.* [95] and processed with Qiime [96] using Uparse with a 97% stringency to yield operational taxonomic units (OTUs). OTUs were taxonomically classified using the Mothur classifier [97] with 0.8 confidence interval against the SILVA database 123 release of July 2015. The clean and trimmed sequences can be retrieved at NCBI using accession number SAMN11350619 - SAMN11350630. A technical replicate for the inoculum was made, available in the NCBI database.

Cell fixation and fluorescence *in situ* hybridisation (FISH) were carried out as described by Rombouts *et al.* [137] using the probes listed in Table 4.S2. The samples were analysed using an epifluorescence microscope, Axioplan 2, (Zeiss, Oberkochen, Germany). Digital images were acquired using a Zeiss MRM camera together with Zeiss imaging software AxioVision version 4.7.

## Parameter estimation of kinetics of the enrichment cultures using minimisation of residual error

To estimate the kinetic parameters of the enrichments and to derive the stoichiometry of the process a kinetic model was built. The uptake rate was modelled using Monod equations and no biomass decay or pH inhibition was considered. The saturation constant of the Monod equations for the different microorganisms was assumed to be 0.1 g/L. It is assumed that there is a microbial group degrading glucose and another group degrading lactate (only in the complex medium enrichment). In this last case, the measured biomass was divided between glucose degraders (65%) and lactate degraders (35%), based on the derived stoichiometry and the ATP yield on the substrate corresponding to that stoichiometry. Parameter estimation was performed following the method proposed by González-Gil *et al.* [168] and is further explained in Appendix 4.2.

## ATP yield estimation using the obtained parameters

The model estimates the distribution of substrate to select a set of catabolic pathways to obtain the lowest residual error with respect to the measured metabolic product distribution during a cycle analysis. These fractions are combined with the ATP yield per catabolic reaction to obtain the overall yield of ATP on substrate ($Y_{ATP,S}$). This yield is than combined with the biomass yields on glucose ($Y_{x,s}$) observed in time (n=3) to obtain the biomass yield on ATP harvested ($Y_{X,ATP}$). An argumentation which catabolic routes were selected for both enrichments can be found in Appendix 4.3.

## Estimation of $\mu^{max}$ from on-line data collected from bioreactors

A script was developed in Matlab version 2014 (MathWorks, Natick, Massachusetts, USA) which is based on determining the end of the base dosage in the cycle using a script explained in the supplementary information published previously [137] and explained in **Chapter 2**. Maximum biomass-specific substrate conversion rate ($q_s^{max}$) is calculated using $\mu^{max}$ and $Y_{x,s}$ and the Herbert-Pirt equation [9], neglecting maintenance.

## Carbon and COD balancing

During steady state, carbon and electron (as chemical oxygen demand, COD) balances were defined using the elemental metabolite matrix given in Table 4.S3 multiplied by the in- and outgoing rates in the reactor. COD balances were set up for the cycle analyses by dividing the amount of COD present in the metabolic compounds measured at a time in the cycle by the measured COD at the start of the cycle.

# Results

## A complex medium promotes fermentation to VFAs and ethanol with little hydrogen while a mineral medium promotes acetate-butyrate-hydrogen formation

Two anaerobic SBRs were operated with either a mineral or complex medium. The enrichments displayed distinct fermentation patterns after 20 SRTs. Initially, the mineral-medium enrichment showed a 1:2:1 acetate:propionate:butyrate product spectrum with little ethanol and no lactate (Figure 4.S1). This shifted after 10 SRTs to primarily acetate and butyrate, with a small amount of lactate and ethanol (Figure 4.1). Hydrogen was the major gaseous product in the mineral medium enrichment (13%±1% of incoming COD). Up to 96% ± 3% of the incoming COD could be recovered for this enrichment, which indicates that a minor by-product might have been missed. Succinate, valerate or formate concentrations were below the detection limit of 50 μM.
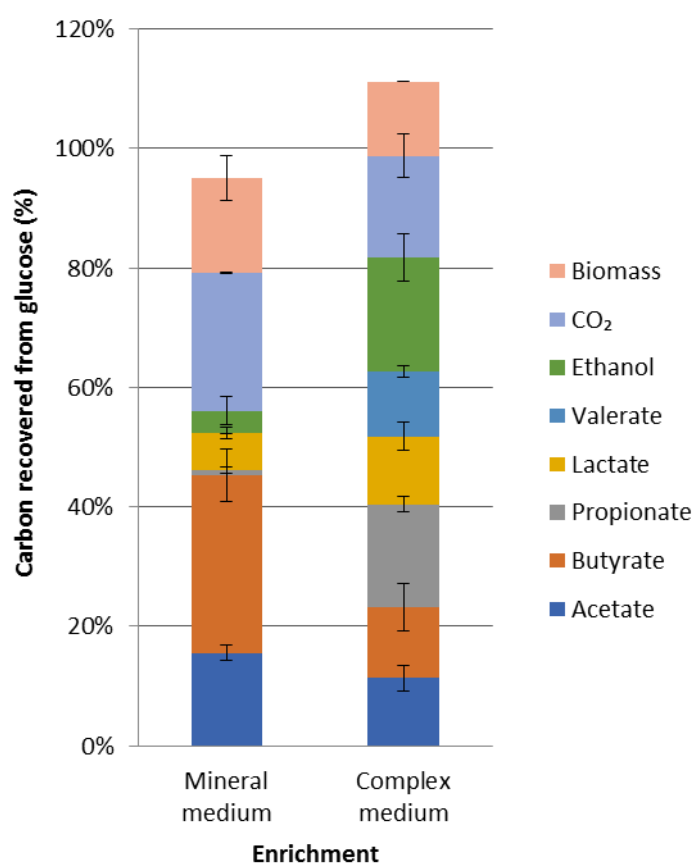


| Enrichment | C-recovery (%) | COD-recovery (%) | $H_2$ yield (mol $Cmol^{-1}$) |
|:---:|:---:|:---:|:---:|
| Mineral | 95% ± 3% | 96% ± 3% | 0.28 ± 0.00 |
| Complex | 113% ± 2% | 118% ± 6% | 0.02 ± 0.00 |

*Figure 4.1: Observed product spectrum on glucose for the mineral and complex medium enrichment and calculated carbon and COD recovery (assuming only glucose is consumed from the medium). Averages and standard deviations are obtained from last three product spectra of the enrichment (Figure 4.S1).*

The complex medium enrichment showed a more dynamic product spectrum development. Initially lactate and acetate were the dominant products (Figure 4.S1). After 3 SRTs, the product spectrum shifted to acetate, propionate, butyrate, valerate, and lactate. After 31 SRTs, 0.19 Cmol ethanol Cmol$^{-1}$ sugar was produced, and only a minor amount of hydrogen was detected in the off-gas (1%±0% of the incoming COD) (Figure 4.1). This product spectrum was more diverse than for the mineral medium enrichment. The carbon balance (based on glucose as the only substrate) displayed a recovery of 113% ± 2%, which most likely is caused by the uptake of tryptone for biomass production. Considering that tryptone uptake is equivalent to the nitrogen requirements for biomass production, the carbon recovery would be 100% ± 2%.

The mineral medium enrichment showed a 25% higher biomass yield on glucose than the complex medium enrichment culture. The $\mu^{max}$ values for the cultures were derived with a cut-off at 20 SRTs (Figure 4.S2). The $\mu^{max}$ in the complex medium enrichment was 58% higher than the mineral medium enrichment, while the maximal biomass specific substrate uptake rate ($q_s^{max}$) was even 94% higher (Table 4.1).

*Table 4.1*: *Key kinetic, stoichiometric and bioenergetic parameters of the glucose fermenting SBR enrichment cultures. Observed $\mu^{max}$ obtained through processing of online base-dosage data after 20 SRTs (1 SRT = 12 h), estimated $q_s^{max}$ and biomass yield on glucose ($Y_{x,s}$). Calculated $Y_{x,ATP}$ using the observed $Y_{x,s}$ and the $Y_{ATP,s}$ obtained from the best fitting catabolic product distribution profile with the 95% confidence interval values given in brackets.*

| Enrichment medium | $\mu^{max}$ (h$^{-1}$) | $q_s^{max}$ (C-mol$_S$ C-mol$_x^{-1}$ h$^{-1}$) | $Y_{x,s}$ (C-mol$_X$ C-mol$_S^{-1}$) | $Y_{ATP,s}$ (mol$_{ATP}$ mol$_S^{-1}$) | $Y_{x,ATP}$ (g$_X$ mol$_{ATP}^{-1}$) |
|---|---|---|---|---|---|
| **Mineral** | 0.17 ± 0.02 | 1.17 ± 0.30 | 0.15 ± 0.04 | 3.04 [3.02, 3.05] | 7.0 [5.4, 8.7] |
| **Complex** | 0.27 ± 0.01 | 2.27 ± 0.11 | 0.12 ± 0.00 | 1.46 [1.43, 1.48] | 7.9 [7.7, 8.0] |

### Cycle analysis reveals potential storage of glucose when using a mineral medium and an intermediate lactate peak when using a complex medium

The product and substrate concentrations during a representative cycle in the SBR are shown in Figure 4.2 for both enrichments. In the enrichment culture on mineral medium, glucose was converted to mainly acetate and butyrate with minor amounts of ethanol and lactate (Figure 4.2A). The formation of fermentation products proceeds after glucose depletion. The COD recovery during the cycle showed that during the glucose consumption phase the COD of consumed glucose is not fully recovered in the measured products (Figure 4.S7A), while in the subsequent period in the cycle the product concentration increased and finally a full recovery of consumed COD is observed. This indicates formation of an intermediate product which is probably a storage product, most likely a polymer of glucose.

In the complex medium enrichment, lactate and ethanol were formed in the glucose consumption phase (Figure 4.2B). When glucose was depleted, ethanol formation stopped, while lactate was consumed. In this secondary fermentation, acetate, propionate, butyrate, valerate and $CO_2$ were formed. This secondary fermentation of lactate was confirmed by a pulse experiment with lactate, peptides, and B vitamins (Figure 4.S5). The COD recovery showed no indications of an intermediate product or storage of glucose, since all COD consumed could be accounted for in the dissolved or gaseous products formed when the glucose was depleted (Figure 4.S7B). No homoacetogenesis was observed when $H_2$ and $CO_2$ where used as substrate in a batch experiment (Figure 4.S6) and no methane was measured during the cycles in the complex medium enrichment (data not shown).
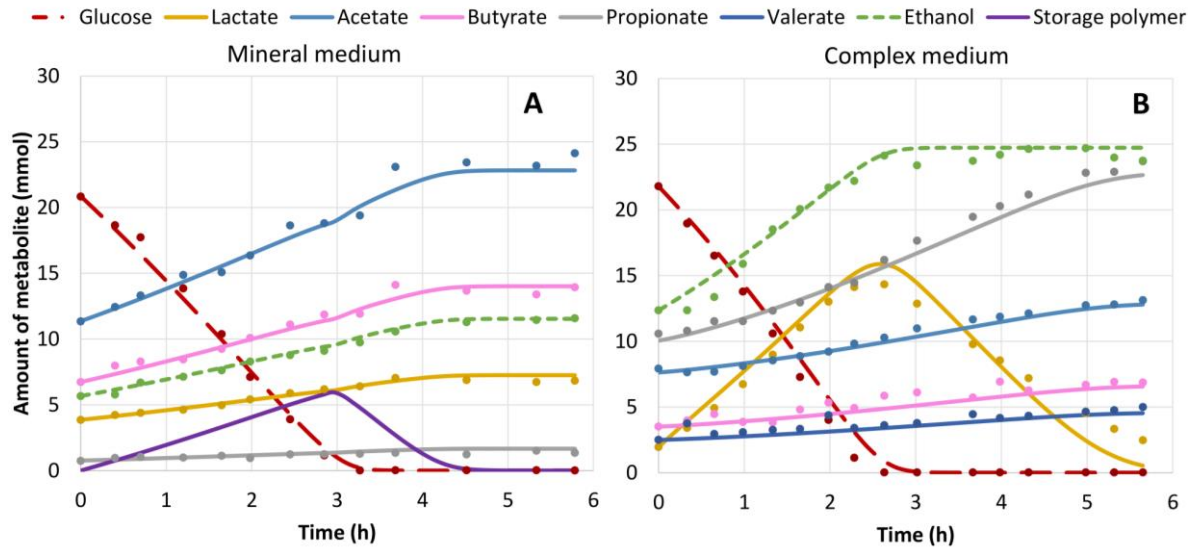
*Figure 4.2*: Observed (points) and modelled (lines) amount of substrate and product in the mineral (A) and complex (B) medium and enrichment at day 33 (40 SRTs) and day 29 (49 SRTs) respectively.

**Supplementing peptides and B vitamins led to significant presence of lactic acid bacteria and more microbial diversity**

*Clostridium* was the dominant OTU (77% at 32 SRTs) with and *Ethanoligenens* second (11% at 32 SRTs) in the mineral medium enrichment culture (Figure 4.3A). FISH analysis showed a different composition and demonstrated dominance in biovolume of *Ruminococcaceae* using the rums279 probe, to which the genus of *Ethanoligenens* belongs (Figure 4.3G). Only a minor biovolume of *Clostridium* was detected using the Chis150 probe (Figure 4.3F). *Lactobacillus* was present as a very minor population (Figure 4.S4) in the mineral medium enrichment. The discrepancy between sequencing results and FISH evaluation shows that complementary observations of the microbial community structure are needed when analysing a microbial community, referred to as the "full cycle rRNA analysis" by Amann *et al.* [169].

*Lactococcus* and *Lactobacillus* were dominant OTUs in the complex medium enrichment (Figure 4.3B and 4.3C). Their dominance was confirmed by FISH analysis using the Lactococcus4 (*Lactococcus*) and Lacto722 (*Lactobacillus*) probes. The presence of *Megasphaera* and minor presence of *Clostridium* was also confirmed using the Mega-X (*Megasphaera*) and the Chis150 (*Clostridium*) probes.

The diversity of the obtained microbial community structures using 16S rRNA amplicon sequencing can be calculated using the Shannon index for the observed genera with a read-abundance >3% of the total OTU's. For the mineral medium the Shannon index was 0.94 (sample at 32 SRTs) and for the complex medium this was 1.34 (sample taken at 41 SRTs). Thus, more microbial diversity was observed in the complex medium enrichment compared to the mineral medium enrichment on the basis of the number of genera found (Figure 4.3A).
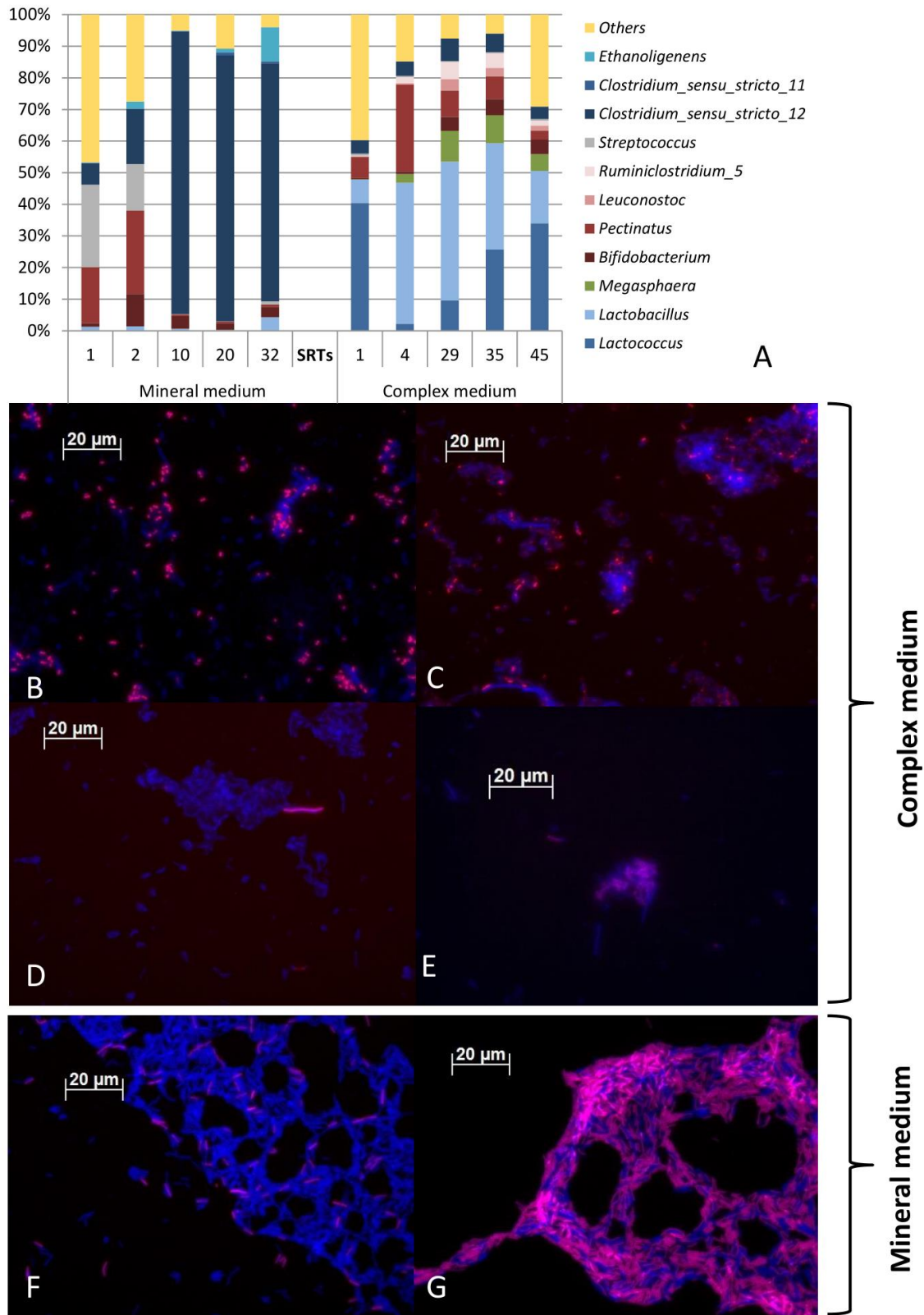
*Figure 4.3: Result of the FISH and V3-V4 16S rRNA gene analysis with OTUs grouped at genus level. 16S rRNA gene identification of the microbial community composition in time for both enrichments (as SRTs) at genus level (A). Less than 3% genera are grouped as others. FISH is shown with target-probe in red using Cy3 as fluorescence marker and EUB338 targeting all eubacterial biomass in blue using Cy5. The pictures show complex medium enrichment probed with Lactococcus4 (B), Lacto722 (C), Chis150 (D) and Mega-X (E) and the mineral medium enrichment probed with Chis150 (F) and rums278 (G).*

## Discussion

**Supplementation of peptides and B vitamins leads to dominance of lactic acid bacteria and high $q_s^{max}$ through resource allocation**

In this work we demonstrate that lactic acid bacteria outcompete prototrophic type fermenters (*e.g.*, *Clostridium* species) when nutritive conditions were favourable, *i.e.*, with sufficient amount of amino acids and B vitamins in an SBR cultivation mode. Kim and colleagues [170] have shown that lactic acid bacteria can be enriched in a continuous-flow stirred tank reactor (CSTR) process. They operated the CSTR anaerobically, at pH 5.0 and thermophilic (50 °C) conditions with a SRT of 12 h, with glucose and yeast extract as fermentable organic substrates. Yeast extract is a well-known source of peptides, amino acids, B vitamins and carbohydrates. In cabbage fermentations lactic acid bacteria are known to be the dominant organism [171], while fermentable substrates with low protein content, such as starch, *Clostridium* species are the dominant organism [172].

Lactic acid bacteria are well known to be auxotrophic for amino acids [173], while their auxotrophy for B vitamins is more ambiguous. Some lactic acid bacteria might actually be producers of B vitamins [174]. Studies with lactic acid bacteria on synthetic medium have demonstrated the specific compounds needed for growth [175], up to individual amino acids [164]. The effect of decreasing medium complexity has been illustrated by Olmos-Dichara *et.al* [176]. When the "richness" of the growth medium was decreased, the $q_s^{max}$ remained stable, while the growth yield decreased. This shows that the medium complexity directly influences the bioenergetics of *L. casei*, resulting in a lower biomass production when peptides and/or B vitamins are insufficiently supplied in the medium.

Lactic acid bacteria have a competitive advantage by attaining high growth rates in complex media. The biomass yield of the complex medium enrichment culture was 20% lower than for the enrichment culture on a mineral medium. The maximal substrate uptake rate was almost double for the community enriched on a complex medium versus mineral medium (Table 4.1). Lactic acid production is clearly a metabolic strategy of high flux but low efficiency. This is supported by the observation that lactic acid bacteria switch to acetate and ethanol production when substrate conversion rates decrease, *i.e.* lower growth rates [93]. Acetate/ethanol production generates 3 instead of 2 moles ATP for lactate fermentation on glucose. This can be placed well in the context of resource allocation theories, given a certain protein budget [177]. Less biosynthetic enzymes needed for amino acids and B vitamin synthesis lead to a smaller anabolic proteome. A smaller anabolic proteome can imply a bigger catabolic proteome, as demonstrated when comparing the proteome from *E.coli* grown in a mineral and complex medium [178]. Lactate catabolism requires one enzyme from pyruvate, while acetate/ethanol production requires at least 5 enzymes. Furthermore, at increasing growth rates, ribosome and RNA polymerase content is higher [179]. Lactic acid bacteria are assumed to have optimally distributed their metabolic enzyme levels [180], enabling a high overall metabolic flux.
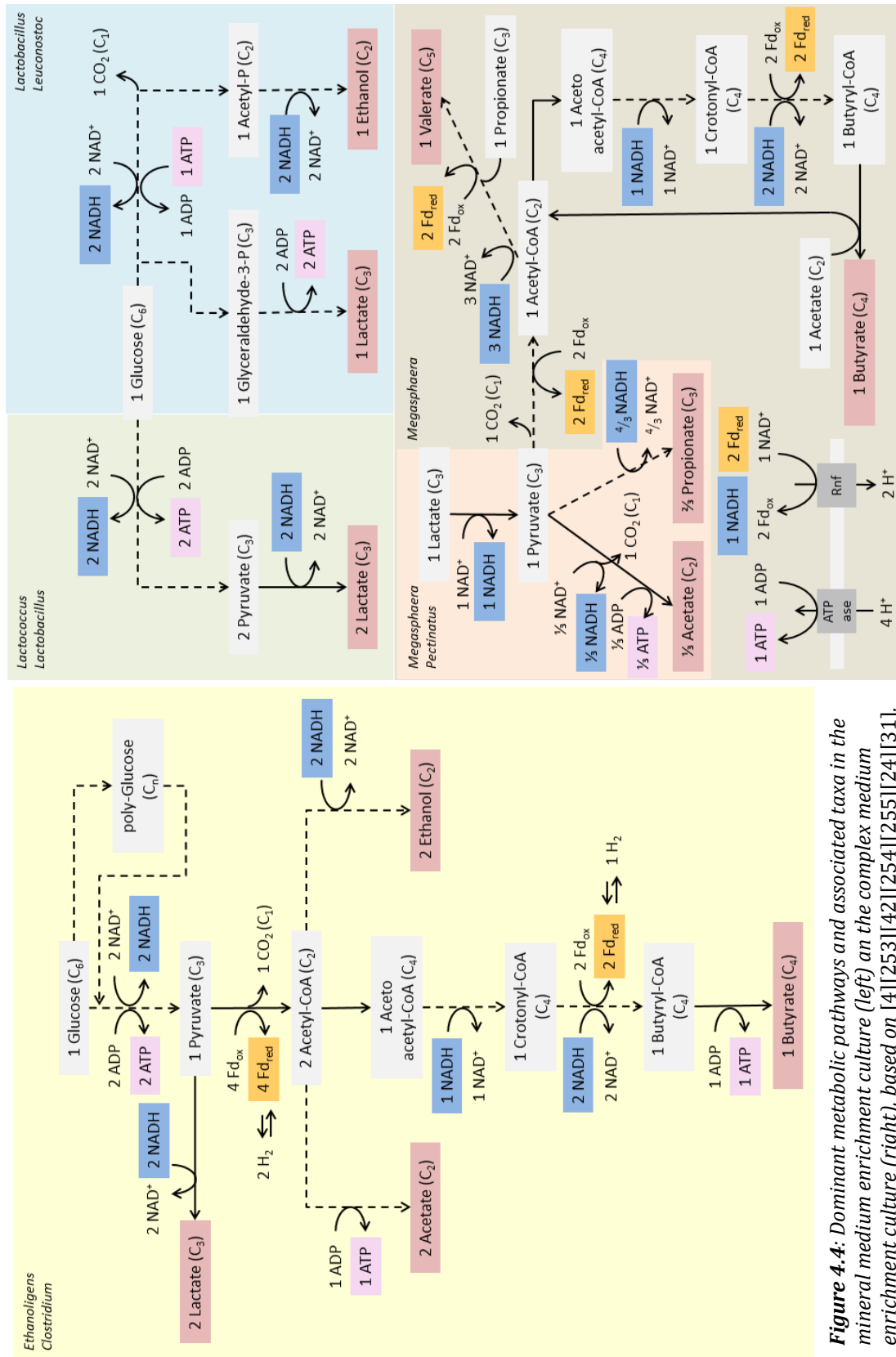
**Figure 4.4**: *Dominant metabolic pathways and associated taxa in the mineral medium enrichment culture (left) an the complex medium enrichment culture (right), based on* [4][253][42][254][255][24][31]. *Dotted lines denote lumped reactions. A detailed explanation on the basis of these metabolic networks is given in Appendix 4.3*

**Mineral medium enriched for an acetate-butyrate type fermentation, potential glucose storage and the class of *Clostridia***

The product formation spectrum from the mineral medium enrichment culture was evaluated to identify the most dominant catabolic route. It was found that our flux-based model fitted best when 44% of the glucose was converted through the acetate-butyrate pathway involving electron bifurcation (Table 4.S4). The microbial community was populated by two genera from the class of *Clostridia*: an *Ethanoligenens* population and *Clostridium* population, with the *Ethanoligenens* population being dominant (Figure 4.3). *Ethanoligenens harbinense* is a species known to produce ethanol, acetate and butyrate [181, 182]. Cluster 12 of *Clostridium* was identified (Figure 4.3A) and *Clostridium pasteurianum* is a well-studied species in this cluster (SILVA release 138). *C. pasteurianum* is known for acetate-butyrate production involving electron bifurcation [24]. This organism has also been found in a fermentative granular enrichment culture which stored poly-glucose [183]. Effectively 20% of the glucose was potentially metabolised via a carbon storage pool (Figure 4.S6A). The storage response in the mineral medium enrichment makes the community maximise its substrate uptake rate (competitive advantage) while growing at a more balanced growth rate over the SBR cycle.

**Complex medium enriched for production of VFAs through lactic acid formation and consumption and is linked with lactic acid bacteria and *Megasphaera***

Evaluating the pathways for the complex medium enrichment showed a best fit when glucose was catabolised through the heterofermentative (69%) and homofermentative (31%) pathway (Table 4.S4). Lactate was subsequently fermented into propionate, butyrate, valerate, $H_2$ and $CO_2$. The secondary lactate fermentation was confirmed in a batch experiment with the enrichment culture and replacing glucose with lactate (Figure 4.S5). The microbial community analysis revealed a dominance of *Lactobacillus*, *Lactococcus* and *Megasphaera* (Figure 4.3).

*Lactococcus* species are known homofermentative lactic acid bacteria, while *Lactobacillus* and *Leuconostoc* species can also be heterofermentative [4]. *Megasphaera elsdenii* is known to produce acetate, propionate, butyrate and valerate from lactate [184]. *Megasphaera* is known to convert lactate in the intestinal tract of cows, pigs and humans [185] and is linked to lactate-mediated medium-chain length carboxylate production microbiomes [42]. *Megasphaera elsdenii* interestingly prefers lactate uptake over glucose uptake, taking up limited amounts of glucose when lactate is present [186], which argues for the *Megasphaera* species having a mainly lactate fermenting role in the community.

**Bioenergetics of complex and mineral-type fermentation: supplementation might lead to a more efficient metabolism**

The lower growth yield in the complex medium (Table 4.1) is counterintuitive since these bacteria grow on a complex medium and do not need to produce amino acids themselves. To compare the impact of the supplementation of peptides and B vitamins on the metabolism, we calculated the $Y_{x,ATP}$ for both enrichments from the catabolic ATP yields estimated (Table 4.1). For the mineral enrichment a 11% lower $Y_{x,ATP}$ value was estimated. This difference is however not statistically significant from the complex medium $Y_{x,ATP}$ (one-tailed t-test gives p=0.45).

Prototrophic fermenters such as *Escherichia coli* and auxotrophic fermenters such as *Lactococcus lactis* have similar protein and RNA content (Table 4.S5). Stouthamer estimated that the supplementation of amino acids only induces a minor decrease in $Y_{x,ATP}$ [187]. The growth yield of *E. coli* fermenting glucose in complex medium is only 13% higher than on mineral medium [188]. The synthesis of amino acids consumes a relatively low amount of ATP, while uptake of amino acids consumes also some ATP. The polymerisation of proteins is the main ATP consuming process, next to RNA synthesis [187]. We expect that the biosynthesis of B vitamins requires a

relatively small ATP-flux, as B vitamins are present in trace amounts in bacterial biomass ($<10^{-5}$ in g g$^{-1}$) [189]. The difference in anabolic efficiency we estimated is much less than the difference observed in $\mu^{max}$, indicating that the complex medium promotes high growth rates rather than high biomass yields. By minimising both the fermentative and the biosynthetic enzyme levels, lactic acid bacteria can allocate more functional protein to increase the growth rate of their cells.

**Directing product formation in open mixed culture fermentation through lactic acid**

The consequence of these different ecological types of fermentations are important for understanding mixed-culture fermentation in bioprocesses aimed to produce economically interesting compounds. The difference in hydrogen production we observed here (Figure 4.1) has been reflected in a meta-study comparing different feedstocks for the production of hydrogen: food and municipal waste streams generate 32-42% less hydrogen than industrial and (pre-treated) agricultural residue waste streams [190]. Food waste typically contains more than 10% (w:w) of protein [191], while agricultural residues contain low amounts of protein, *e.g.*, wheat straw contains 0.6% (w:v) [192]. This leads to food waste fermentations being dominated by lactic acid bacteria and the secondary lactate fermentation producing significantly propionate and no or small amounts of hydrogen gas. In contrast, fermentations of (pre-treated) agricultural residues are dominated by acetate/butyrate producing bacteria, such as *Clostridium* species, resulting in significant amounts of hydrogen produced. Using this ecological understanding, protein-rich feedstocks with readily fermentable carbohydrates are a good target to directly produce lactic acid, while protein-poor feedstocks are a good target to produce VFAs and hydrogen (Figure 4.5).
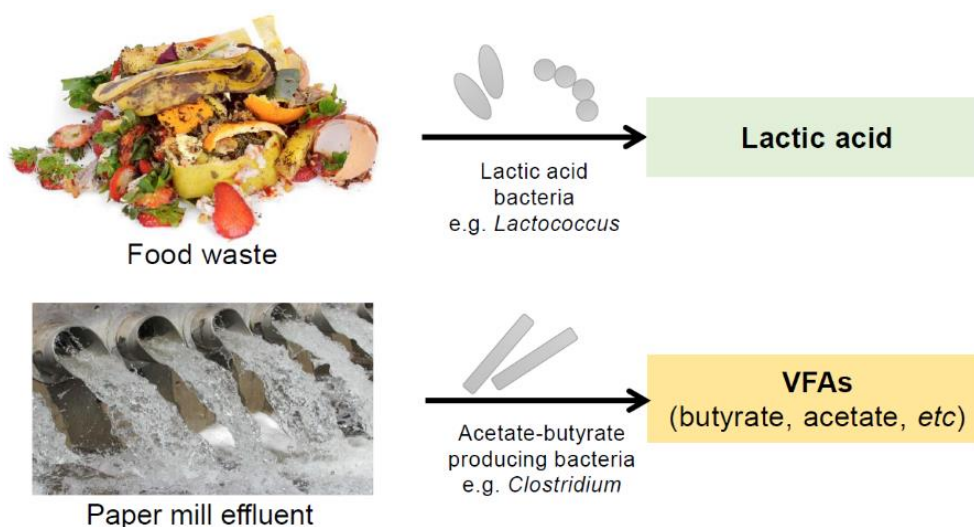


***Figure 4.5***: *Ecology-based design of utilizing abundant waste streams such as protein-rich food waste and protein-poor paper mill effluent for mixed-culture fermentations*

Here we used enrichment culture to better understand the ecological niche of lactic acid bacteria, showing that lactic acid bacteria outcompete prototrophic type fermentative bacteria on high biomass specific substrate uptake rate and growth rate. This behaviour can be explained in line with the resource allocation hypothesis for protein allocation: lactic acid bacteria can dedicate a higher share of their proteome to catabolism, ribosomes and RNA polymerases and therefore are able to attain a significantly higher substrate uptake rate and growth rate. Future research should aim to predict the metabolic performance of fermentative ecosystems using a resource allocation-based strategy, ultimately extending this effort to predict the outcome of competitions between all known microbial metabolisms *a priori*.

## Supplementary Information

*Table 4.S1:* *Medium composition mineral and complex enrichment performed. Trace elements added are in the same concentrations as the enrichments performed previously in our lab* [137]

| Medium A | | Mineral (mg L⁻¹) | Complex (mg L⁻¹) |
|---|---|---|---|
| **Glucose** | | 4000 | 4000 |
| **Tryptone** | | 0 | 800 |
| **B vitamins** | | | |
| **Thiamine** | B1 | - | 0.04 |
| **Riboflavin** | B2 | - | 0.04 |
| **Nicotinic acid** | B3 | - | 0.04 |
| **Ca-pantothenate** | B5 | - | 0.04 |
| **Pyridoxine** | B6 | - | 0.20 |
| **Biotin** | B7 | - | 0.40 |
| **p-Aminobenzoic acid** | Precursor B9 | - | 0.10 |
| **Folic acid** | B9 | - | 0.04 |
| **Cyanocobalamin** | B12 | - | 0.04 |
| | | | |
| **$NH_4Cl$** | | 1340 | 1340 |
| **NaCl** | | 292 | 292 |
| **$KH_2PO_4$** | | 780 | 780 |
| **$MgCl_2 \cdot 6\ H_2O$** | | 120 | 120 |
| **$Na_2SO_4 \cdot 10\ H_2O$** | | 130 | 130 |
| **Trace elements** | | As in **Appendix I** | |

**Table 4.S2:** *FISH probes used in this study. The percentage of formamide during hybridization is given.*

| Probe | Specificity | Formamide (%) | Sequence (5' → 3') | Reference |
|---|---|---|---|---|
| EUB338 | Nearly all eubacteria | 5-25 | GCCTTCCCACATCGTTT | [126] |
| Chis150 | Genus of *Clostridium* - species from sensu stricto I to XII | 25 | TTATGCGGTATTAATCTYCCTTT | [193] |
| Rums278 | Family of *Ruminococcaceae* | 20 | GTCCGGCTACCGATCGCG | [194] |
| Lacto722 | Genus of *Lactobacillus* | 25 | YCACCGCTACACATGRAGTTCCACT | [195] |
| Lactococcus4 | Genus of *Lactococcus* | 5 | CTGTATCCCGTGTCCCGAAG | [196–198] |
| Mega-X | Genus of *Megasphaera* | 25 | GACTCTGTTTTTGGGGTTT | [199] |

**Table 4.S3:** *Elemental metabolite matrix used to set up the carbon and COD balances.*

| Compound | C (Cmol) | COD ($g_{COD}$ $g^{-1}$) |
|---|---|---|
| **Glucose** | 6 | 1.07 |
| **Acetate** | 2 | 1.07 |
| **Butyrate** | 4 | 1.82 |
| **Propionate** | 3 | 1.30 |
| **Lactate** | 3 | 1.08 |
| **Succinate** | 4 | 0.95 |
| **Valerate** | 5 | 2.06 |
| **Ethanol** | 2 | 2.08 |
| **Formate** | 1 | 0.35 |
| **$H_2$** | 0 | 7.94 |
| **$CO_2$** | 1 | 0.00 |
| **Biomass** | 1 | 1.36 |

**Table 4.S4:** *The catabolic distribution of both enrichments with respect to the imposed catabolic reactions obtained from the parameter estimation. The percentages sum up to 100% glucose used in the catabolism and do not include the modelled storage polymer assumed for the mineral medium enrichment.*

| No. | Catabolic reaction | Mineral | Complex |
|-----|--------------------|---------|---------|
| Glucose utilising pathways | | | |
| 1 | 1 glucose → 2 lactate + 2H$^+$ | 9% | 39% |
| 2 | 1 glucose → 1 lactate + 1ethanol + 1H$^+$ + 1 $CO_2$ | | 61% |
| 3 | 1 glucose → 1 acetate + 1 ethanol + 1H$^+$ +2 $H_2$ + $CO_2$ | 33% | |
| 4 | 1 glucose → 0.67 acetate + 0.67 butyrate + 1.33 H$^+$ + 2.67 $H_2$ + 2 $CO_2$ | 44% | |
| 5 | 1 glucose → 1 butyrate + 1H$^+$ + 2 $H_2$ + 2 $CO_2$ | 10% | |
| 6 | 1 glucose → 0.67 acetate + 1.33 propionate + 2H$^+$ + 0.67 $CO_2$ | 4% | |
| Lactate utilising pathways | | | |
| 7 | 3 lactate → 1 acetate + 2 propionate + 2 $CO_2$ | | 78% |
| 8a | 1 lactate + 1 acetate + 1H$^+$ → 1 butyrate + 1 $H_2O$ + 1 $CO_2$ | | 8% |
| 8b | 2 lactate + 1H$^+$ → 1 butyrate + 2$H_2$ + 2 $CO_2$ | | 6% |
| 9 | 1 lactate + 1 propionate + 1H$^+$ → 1 valerate + 1 $CO_2$ | | 7% |

**Table 4.S5**: *Protein and RNA content of two distinct fermentative microorganisms expressed as weight percentage of cell dry weight averaged over a range of dilution rates from chemostat steady states*

| Microorganism | Protein content [%] | RNA content [%] | Reference |
|---------------|---------------------|-----------------|-----------|
| *Escherichia coli* | 55-62 | 10-16 | [200] |
| *Lactococcus lactis* | 45 ± 2 | 6.5-9.5 | [201] |

Figures
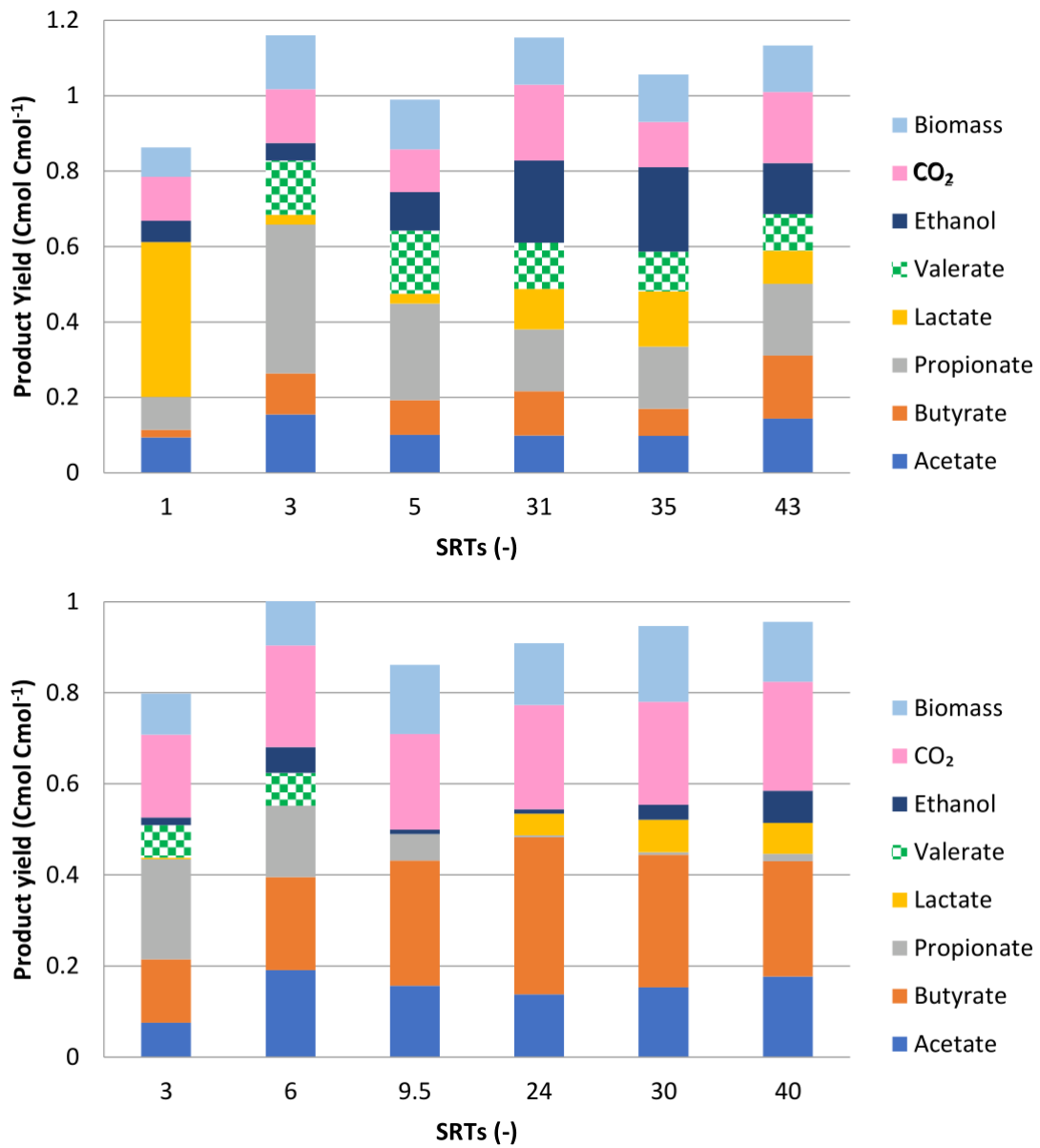


*Figure 4.S1*: *Product yields of the enrichment cultures on mineral (top) and complex (bottom) medium in time.*
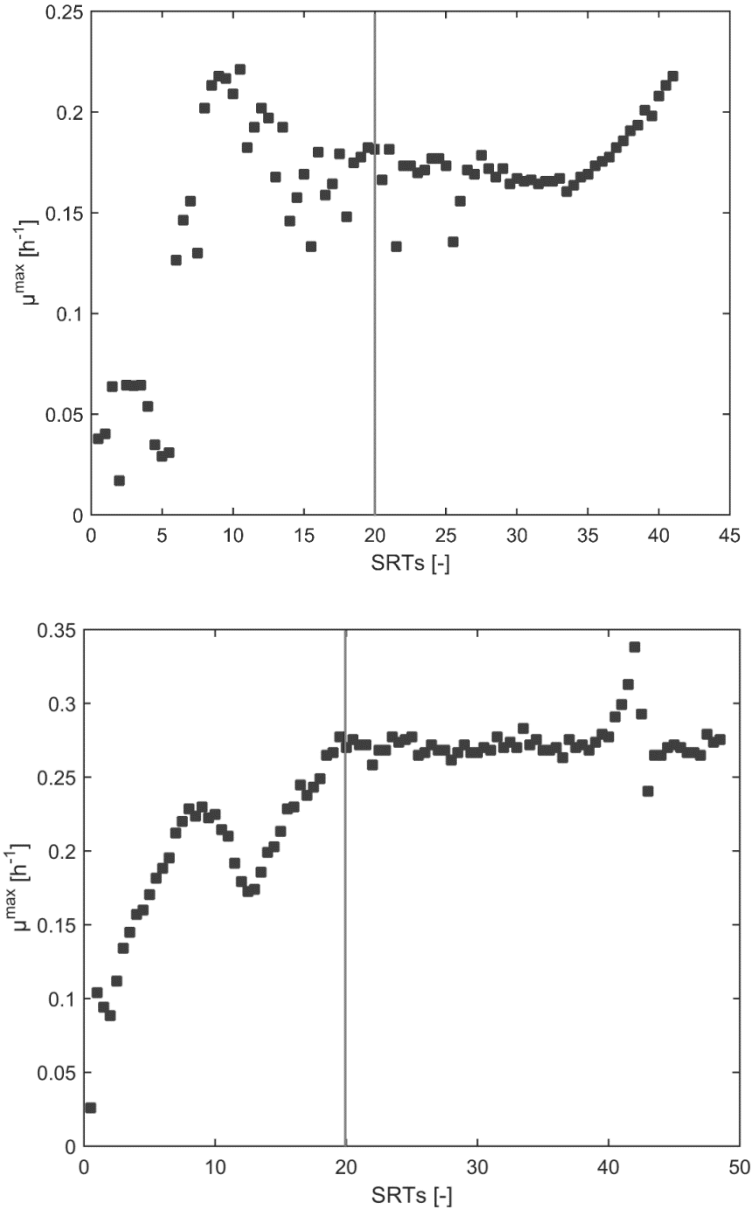
**Figure 4.S2:** *Estimated growth rate for the enrichment cultures on mineral (top) or complex (bottom) media as function of time.* The cut-off chosen to estimate the kinetic parameters of Table 4.1 is given with a line.
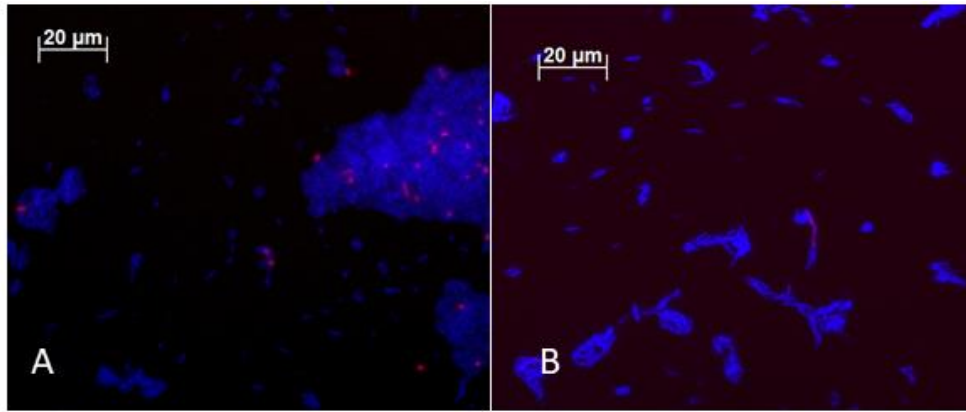
***Figure 4.S3:*** *FISH analysis of the complex medium enrichment using the rums278 probe (A) and the mineral medium enrichment using the Lacto722 probe (B). Target probe is in red using the Cy3 fluorescent label, eubacterial is in blue using the EUB338 and Cy4 as fluorescent label*
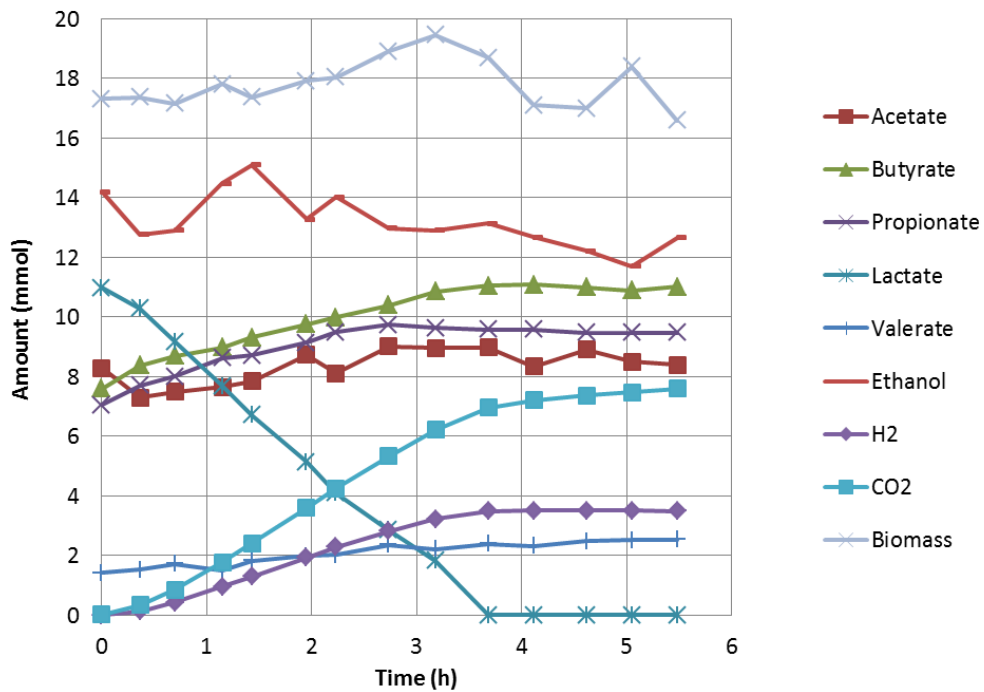


***Figure 4.S4:*** *Batch experiment with lactate as carbon source and the same number of peptides and B vitamins as for glucose in the enrichment culture on the complex medium*
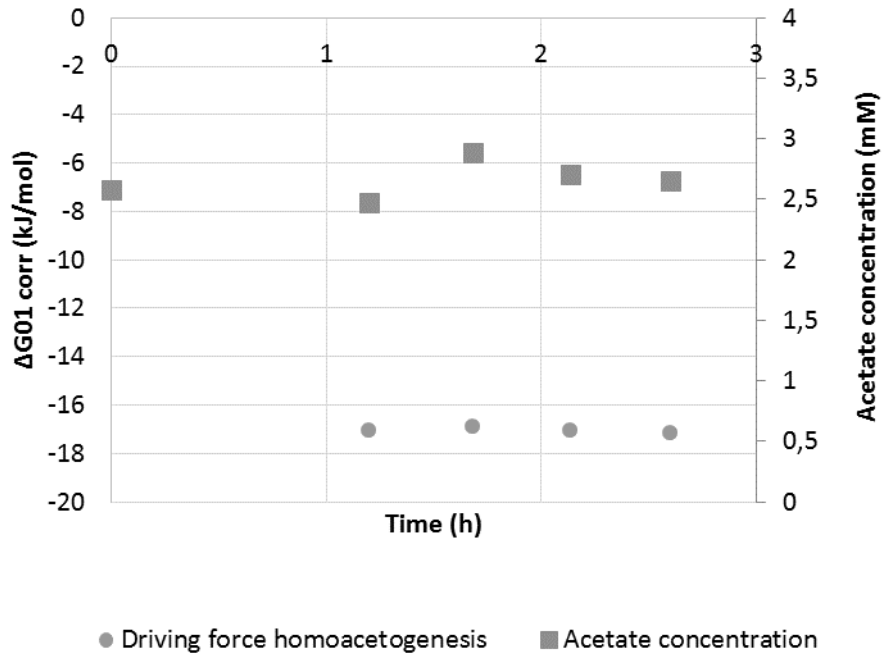
*Figure 4.S5: Thermodynamic analysis (circles) and acetate concentration (squares) during the batch experiment with H₂ and CO₂ in the complex medium enrichment*
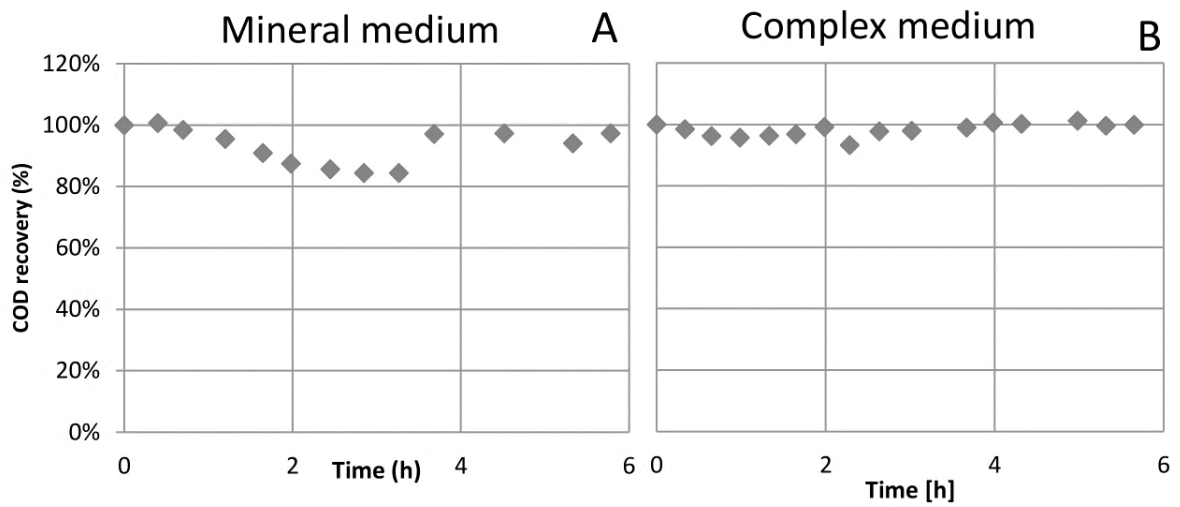


*Figure 4.S6: COD recovery during the SBR cycle displayed in figure 2 for mineral medium (A) and complex medium (B) using the elemental metabolite matrix listed in table S3.*

## Appendix 4.1 – Use of refraction index and UC detectors in the HPLC analysis

In the HPLC analysis, the refraction index (RI) spectrum was always used to check for the presence of peaks in the UV spectrum, as all compounds cause a change in refractive index, while only carboxylic acids absorb in the UV spectrum. In the mineral medium, glucose was quantified from the RI spectrum, and organic acids from the UV spectrum. A significant peak of succinate in the UV was not present in the RI spectrum, thus is not quantified from UV.

In the complex medium, acetate and succinate were quantified from the RI spectrum. At the retention time of these two compounds, a peak was present in the UV spectrum when running a sample of the combined medium A and B, indicating the presence of UV absorbing compounds in the influent.

For the cycle analysis, samples of the complex medium, propionate and butyrate were quantified using RI detection, since absorbance on the UV channel was poor for these peaks. For the cycle analysis, measurements of samples of mineral medium, acetate and butyrate concentrations were obtained from the RI channel.

For the lactate pulse experiment in the complex medium enrichment, acetate and lactate were quantified from the RI spectrum.

## Appendix 4.2 – Bootstrap method

To estimate robust parameters and to avoid being stuck at local minima, the bootstrap methodology was followed [202]. With it the expected parameter values and their confidence intervals were determined.

The model minimises the normalised root squared mean deviation (Eq. 1) between the experimental data and the simulated data of the model.

$$
NRMSD = \sqrt{\frac{1}{m \cdot n} \sum_{i=1}^{m} \sum_{j=1}^{n} \left( \frac{y_{j,i}(\theta) - \hat{y}_{j,i}}{\sigma_j} \right)^2}
\tag{1}
$$

where m is the number of measurement times, n the number of measured compounds (n=9 in the mineral medium enrichment and n=10 in the complex medium enrichment), $y$ is the simulated concentration value, $\hat{y}$ is the experimental concentration value, $\theta$ represent the calibration parameters and $\sigma$ is the experimental standard deviation of the concentration values of a compound. The subscript $i$ refers to the different measurements over time and the subscript $j$ refers to the different compounds.

After the first parameter estimation, the reference residuals (i.e. the difference between the experimental and simulated concentration) are calculated. These residuals are used to generate new synthetic experimental data, which is then used to estimate a new set of parameters. A population of parameters is generated by iterating until convergence and can be used to determine robust estimates and uncertainty quantifications.

A Monte Carlo procedure was used to propagate the uncertainty of the estimated parameters. Samples of the parameter population are chosen using Latin Hypercube Sampling to ensure a maximal coverage of the parameter space [203]. The Monte Carlo procedure can be briefly summarised in three steps: i) select a random sample of the estimated parameter population; ii) run the model and store the solution; iii) iterating 500 times steps i) and ii) until the distribution of model solutions converges.

A reference set of parameters is estimated using the Matlab command *lsqnonlin* (Eq. S1).

$$\theta^* = arg_\theta \min \sum_{i=1}^{m} \sum_{j=1}^{n} \left( \frac{y_{j,i}(\theta) - \hat{y}_{j,i}}{\sigma_j} \right)^2 \tag{S1}$$

where $\theta^*$ is the set of parameters to estimate, $y$ is the simulated concentration value, $\hat{y}$ is the experimental concentration value and $\sigma$ is the experimental standard deviation of the concentration values of a compound. The subscript $i$ refers to the different measurements over time and the subscript $j$ refers to the different compounds.

The vector of reference residuals are determined (Eq. S2)

$$e = y_{j,i}(\theta^*) - \hat{y}_{j,i} \tag{S2}$$

where $e$ is the reference residuals.

Synthetic data is generated by randomly adding the reference residuals to the experimental data (S3).

$$\hat{y}_{j,i}^* = \hat{y}_{j,i} + e_k \tag{S3}$$

where $\hat{y}^*$ are the new synthetic experimental data and $e_k$ are elements randomly sampled from $e$.

A new set of parameters is determined with the new synthetic data (Eq. S4).

$$\theta_j = arg_\theta \min \sum_{i=1}^{m} \sum_{j=1}^{n} \left( \frac{y_{j,i}(\theta) - \hat{y}_{j,i}^*}{\sigma_j} \right)^2 \tag{S4}$$

Where $\theta_j$ is the set of estimated parameters corresponding to iteration $j$.

Iterate through steps 3 and 4 ($n_{It}$=500). The mean and standard variation of the population of estimated parameters are used as convergence indicators.

For a high number of iterations, the expected value of the parameter set can be approximated to the mean value of the distribution of parameters (Eq. S5). The confidence intervals for a α=0.05 significance are determined by the quantile function (Eq. S6)

$$\hat{\theta} = \frac{1}{n_{It}} \cdot \sum_{j=1}^{nIt} \theta_j \tag{S5}$$

where $\hat{\theta}$ is the parameter set expected values.

$$\hat{\theta}_{\frac{\alpha}{2}} = \left\{ \theta : Pr\left( \theta_j \leq \hat{\theta}_{\frac{\alpha}{2}} \right) = \alpha/2 \right\}$$

$$\hat{\theta}_{1-\alpha/2} = \left\{ \theta : Pr(\theta_j \leq \hat{\theta}_{1-\alpha/2}) = 1 - \alpha/2 \right\} \tag{S6}$$

## Appendix 4.3 – Selection of relevant catabolic pathways

An overview of the selected metabolic pathways and associated growth rates shows that all assumed catabolic pathways have sufficient growth rates to occur in the constructed SBR ecosystem (Table 4.S6).

*Table 4.S6: Catabolic stoichiometries derived from metabolic network presented in Figure 4.4. Ferredoxin generated by butyrate (through electron bifurcation) and valerate production can be used to generate extra ATP using a pmf. Propionate is assumed to be produced through the Acrylyl-CoA pathway, as this is a less efficient but faster pathway* [31] *and the SBRs are assumed to select on maximal conversion rates* [137]. *These catabolic stoichiometries are used to fit the product spectrum of both enrichments and the associated possible pathways (Figure 4.S4). Blue coloured conversions are used only for the complex enrichment culture, yellow coloured conversions for the mineral enrichment culture, green coloured conversions are used for both.*

| No. | Catabolic stoichiometry | Reference species | $\mu^{max}$ $(h^{-1})$ | $Y_{ATP,S}$ $(mol\ mol^{-1})$ | Reference |
|---|---|---|---|---|---|
| Glucose utilising pathways | | | | | |
| 1 | 1 glucose $\rightarrow$ 2 lactate + 2H$^+$ | *Lactococcus lactis* | 1.10 | 2 | [175] |
| 2 | 1 glucose $\rightarrow$ 1 lactate +1 ethanol + 1H$^+$ + 1 $CO_2$ | *Lactobacillus reuteri* | 0.43 | 1 | [204] |
| 3 | 1 glucose $\rightarrow$ 1 acetate +1 ethanol + 1H$^+$ +2 $H_2$ +2 $CO_2$ | *Ethanoligenens harbinense* | 0.31 | 3 | [205] |
| 4 | 1 glucose $\rightarrow$ 0.67 acetate + 0.67 butyrate +1.33H$^+$ +2.67 $H_2$ +2 $CO_2$ | *Clostridium pasteurianum* | 0.23 | 3.33 | [206] [207] |
| 5 | 1 glucose $\rightarrow$ 1 butyrate +1H$^+$ +2 $H_2$ +2 $CO_2$ | *Clostridium tyrobutyricum* | 0.21 | 3 | [28] |
| 6 | 1 glucose $\rightarrow$ 0.67 acetate + 1.33 propionate + 2H$^+$ + 0.67 $CO_2$ | *Bacteroides fragilis* | 0.15 | 2.67 | [208] |
| Lactate utilising pathways | | | | | |
| 7 | 3 lactate $\rightarrow$ 1 acetate +2 propionate + 1 $CO_2$ | *Megasphaera elsdenii* | 0.62 | 0.5 | [184] |
| 8 | 2 lactate +2x acetate + 1+xH$^+$ $\rightarrow$ 1+x butyrate + 2-2x $H_2$ + 2 $CO_2$ | | | 0.75+0.25x | |
| 9 | 1 lactate +1 propionate + 1H$^+$ $\rightarrow$ 1 valerate + 1 $CO_2$ | | | 1 | |

## Appendix 4.4 - Argumentation for the selected pathways

<u>Mineral medium</u>

*Ethanoligenens* and *Clostridium* populated the mineral medium enrichment, with *Lactobacillus* confirmed to be absent (Figure 4.3, Figure 4.S3B). *Ethanoligenens* species are known to produce acetate, ethanol and butyrate [181, 182], though electron bifurcation is not investigated in this genus. *Clostridium* species belonging to cluster 12 are known to produce, acetate, ethanol, butyrate and are confirmed to use electron bifurcation [24]. Lactate utilisation was not included, as lactate was not consumed during the cycle (Figure 4.2). Homoacetogenesis and methanogenesis were not considered relevant in this environment. Lactate production from glucose has been measured for *Clostridium pasteurianum* [209]. Propionate production was assumed to be performed through the acrylate pathway [210] , using pyruvate directly from glucose. This is a pathway that generates less ATP but attains higher growth rates [31] and propionate is formed directly from glucose, as no lactate consumption is observed. This catabolism is not matched with the microbial community.

<u>Complex medium</u>

Lactic acid bacteria and *Megasphaera* were observed to be the dominant populations in the complex medium enrichment. Lactic acid bacteria are known to be homo or heterofermentative (reaction 1 and 2, Table 4.S6) [4]. They are also known to produce acetate and ethanol coupled to formate and hydrogen [4]. When including this reaction in the modelling it was not selected, thus it is not used here. *Megasphaera* species are known to utilise all three lactate utilising pathways (reaction 7,8 and 9). Homoacetogenesis and methanogenesis were not considered in the modelling of the carbon fluxes in as both reactions were measured not to be active in this enrichment (Figure 4.S6 and data not shown).

# Chapter 5 - Metabolic interactions driving microbial diversity in a xylose fermenting chemostat enrichment culture
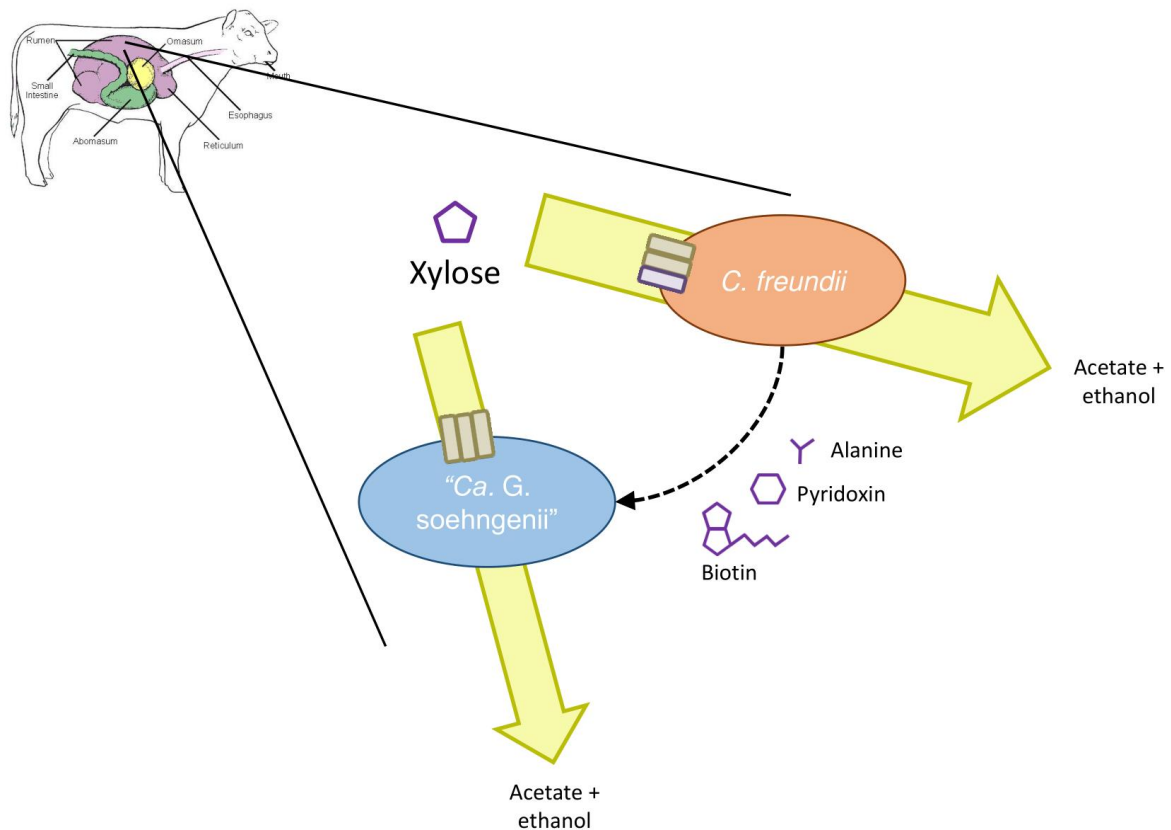


---

*Julius L. Rombouts[1] Kelly Hamers[1], Laura C. Valk[1], Jeroen Frank[2], Sebastian Lücker[2], Dimitri Sorokin[1,3], David G. Weissbrodt[1], Robbert Kleerebezem[1], Mark C.M. van Loosdrecht[1]*

*[1]Section Environmental Biotechnology, Delft University of Technology, Department of Biotechnology, Delft, the Netherlands*

*[2]Department of Microbiology, Institute for Water and Wetland Research, Radboud University, Nijmegen, the Netherlands*

*[3]Winogradsky Institute of Microbiology, Centre for Biotechnology, Russian Academy of Sciences, Moscow, Russia*

## Abstract

Microbial diversity in terms of species is a vast reservoir of complexity which probably outnumbers the stars in our universe. Understanding the mechanisms that drive this diversification is one of the primary goals of microbial ecology. Metabolic interactions, be it competitive or cooperative mechanism, are constantly shaping microbial communities. Here, enrichment culturing is used as a tool reduce the complexity of microbiomes to a case where two dominant species are competing for xylose in a continuous xylose limited environment. A complementary approach of metabolomics, metagenomics and isolation culturing was used to hypothesize how the metabolic interactions in this culture function. *Citrobacter freundii* and "*Ca.* Galacturonibacter soehngenii" were shown to be dominating the created environment as confirmed by metagenomics and quantified using fluorescent *in situ* hybridization (41%±5% and 47%±7% respectively of the bacterial cell surface). We hypothesized that alanine, pyridoxine and biotin are shared by *Citrobacter freundii* toward "*Ca.* Galacturonibacter soehngenii". Initially xylose was the only fermentable carbon source supplied besides a mineral medium. A differential enrichment was performed using a supplemented medium based on the mineral medium with the addition of alanine, pyridoxine and biotin. After 54 solids retention times of culturing, *Citrobacter freundii* and "*Ca.* Galacturonibacter soehngenii" were detected as 21%±9% and 67%±17% of the bacterial cell surface respectively. We propose a model where commensalism and competition drive this coexistence. This model might extend as a general concept in carbohydrate fermentations, where prototrophic r-strategists limit the growth of auxotrophic K-strategists.

**Keywords**: Enrichment culturing – chemostat – xylose – microbial diversity – fermentation – metabolic interactions – metagenomics – metabolomics

## Introduction

The microbial diversity in terms of species that we can observe probably outnumbers the amount of stars in our universe [211]. In line with the theory of evolution proposed by Charles Darwin [212], microbial species have evolved over many generations into their most optimal ecological state due to survival of the fittest. As the microbial world is crowded, metabolic interactions are unavoidable. Microbial diversity is constantly shaped by these metabolic interactions, which trigger evolutionary strategies for the members of a microbial community.

A single microbial member is commonly viewed as a microbial strain or a microbial genotype. Metabolic interactions can be characterized as competitive mechanisms or cooperative mechanisms, us outlined by Hibbing *et al.*[213]*.* Metabolite exchange between bacteria is an example of a cooperative mechanism. Pande and Kost have outlined several hypotheses why and how bacteria are triggered to exchange metabolites [214]. In their scenario that sketches the evolution of metabolite sharing, two community members start by interacting due the secretion of metabolic by-products. This triggers an "auxotrophic loss of function" by the recipient member. This auxotrophic loss of function likely gives the recipient member a fitness benefit, which can be expressed in terms of biomass specific growth rate ($\mu$) and is observed using pure culture approaches using *e.g. E. coli* [215]. Metabolite exchange can occur as exchange of anabolic metabolites, creating anabolic dependencies.

Enrichment culturing can offer the biological complexity of environments while giving the researcher a tool to manipulate the environmental conditions. A chemostat, or continuous-flow stirred tank reactor (CSTR) can be used as a tool to impose a specific dilution rate on a microbial community. Here, the dilution rate equals $\mu$ and Monod kinetics apply to describe the microbial growth on a certain substrate *S*:

$$\mu = \mu^{max} \cdot \frac{C_s}{C_s + K_s} \qquad\qquad (1.1)$$

The maximum biomass specific growth rate ($\mu^{max}$) is commonly estimated using batch cultures. The residual substrate concentration $C_s$ in the bioreactor is determined by the combination of $\mu^{max}$ and the affinity constant for this substrate, $K_s$. In the case of a single substrate limitation, the member of the community with the best "affinity" for the substrate given a certain $\mu$, can lower the residual concentration to such an extent that other members will be washed out. This concept can be illustrated by plotting the $C_s$ against the applied $\mu$ [140]. Competition for substrates is one of the competitive mechanisms driving microbial diversity [213].
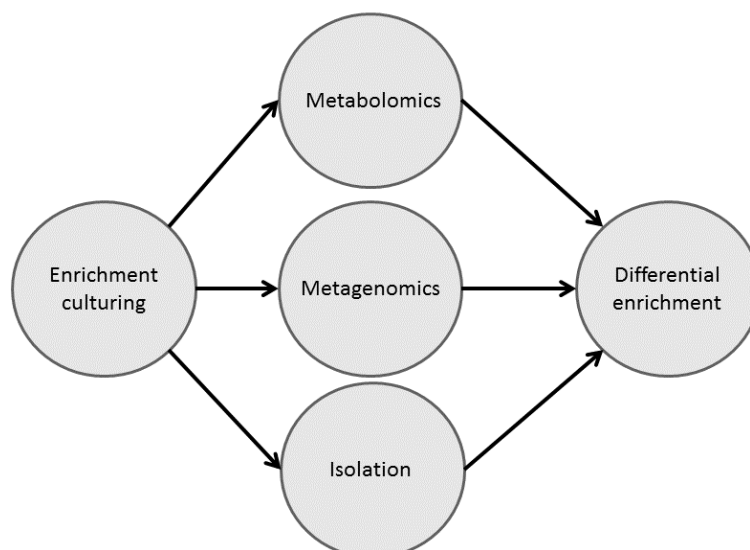
**Figure 5.1**: *The complementary approach used to detect metabolic interactions*

In this chapter, the aim is to understand metabolic exchange between bacterial members using a complementary approach of enrichment culturing, metabolomics, metagenomics and isolation studies (Figure 5.1). A microbial community obtained previously (Chapter 2) was studied which was shown to be dominated primarily by *Citrobacter freundii* and an uncharacterized *Lachnospiraceae* population. This chapter uses enrichment culturing to find its niche in the bridge between pure culture ecosystems and complex microbiomes. The final aim of this work is to contribute to the understanding of how and why microbial populations coexist in natural or man-made ecosystems.

## Material and Methods

### Enrichment culturing

The CSTR was inoculated with enrichment culture remaining from the CSTR as run by Mos *et al.* [137] stored at -20°C with 15% (v:v) glycerol (sample from 07-04-2017). The original inoculum was bovine rumen with 10% glycerol stored at -20°C. The experiment was started with approximately 15 mL of fresh inoculum. The reactor was run in batch mode until the base profile indicated that the exponential growth phase had passed, at which time the operation was switched to continuous mode. This enrichment was performed twice in this study (Figure 5.2).

The initial enrichment was performed using a mineral medium in combination with 4 g $L^{-1}$ of D-xylose as sole carbon source as published previously [137]. Temperature was maintained at 30°C, pH at 8.0 and the solids retention time (SRT) was maintained at 8 hours. The carbon and mineral solutions were prepared and fed separately. The carbon medium was autoclaved at 110 °C for 20 min before use.

A supplemented medium was designed to study the anabolic dependencies of "*Ca.* G. soehngenii". This consisted of the mineral medium used in combination with 4 g $L^{-1}$ of D-xylose and 0.4 mg $L^{-1}$ of biotin, 0.2 mg $L^{-1}$ of pyridoxine and 55.2 mg $L^{-1}$ of L-alanine (Merck, Darmstadt, Germany).

## Isolation of *Citrobacter freundii* XYL1

Isolation of *C. freundii* was carried out using the same medium as for the enrichment culturing on mineral medium and xylose. Volumes of 100 µL of $10^{-4}$ and $10^{-6}$ diluted samples from the CSTR were plated on 2% (w/v) agar plates with this medium. After ~48 h of incubation, colonies were picked and streaked on fresh agar plates, which was repeated four times to ensure that pure cultures were obtained. This was validated through 16S rRNA gene sequencing of the full 16S rRNA gene region directly.

Following this, colonies were picked from the last plate and used to inoculate 50 mL round-bottom shake flasks containing 30 mL of the cultivation medium at pH 8. The flasks were incubated at room temperature for approximately a week on a shaking incubator at 200 rpm. All incubation steps were carried out in an anaerobic chamber (Bactron III, Sheldon Manufacturing Inc., Cornelius, OR, United States) with a gas composition of 89 % $N_2$, 6 % $CO_2$ and 5 % $H_2$.
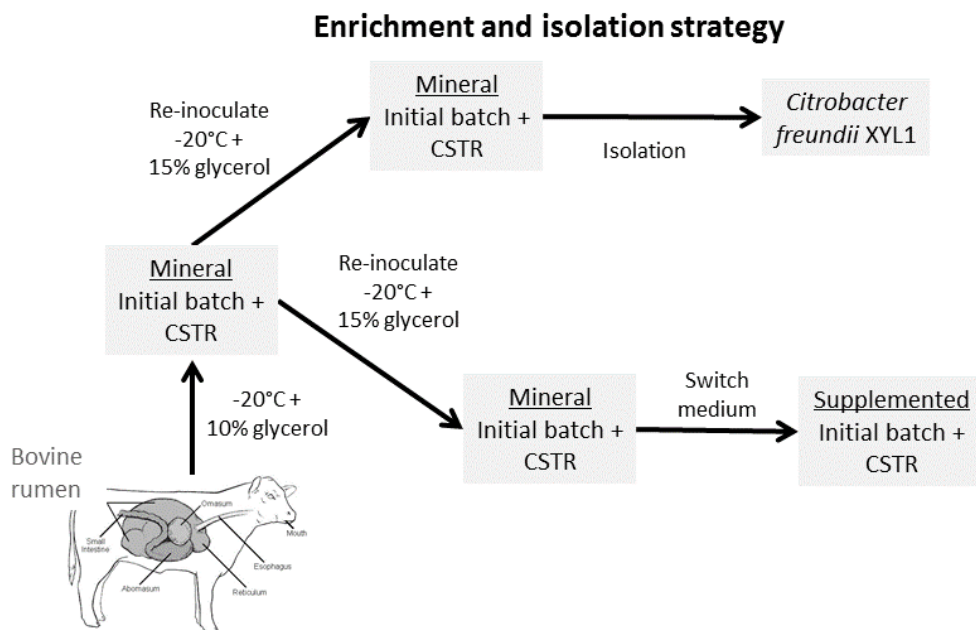


*Figure 5.2*: *Enrichment strategy employed to study metabolic interactions in a xylose limited CSTR environment. Grey boxes indicate the type of ecosystem obtained, with the type of medium underlined (mineral or supplemented medium). Arrows indicate the method used to bring one system to the next. In all three enrichment studies an initial batch phase (monitored by the online base addition) was used, after which the reactor was switched to continuous mode*

## Metagenomics

### Sampling

A volume of 50 mL of reactor effluent was collected on ice and subsequently centrifuged for 15 min at 4,200 rpm (Sorvall Legend X1R centrifuge, Thermo Fisher Scientific, Pittsburgh, PA, United States). Supernatant was discarded and the pellet was stored at -20 °C. Using the Genomic DNA kit with Genomic-tips 100/G (Qiagen Inc, CA, USA), DNA for library construction was extracted. The protocol was deviated from in the addition of 2.6 mg/mL zymolyase (20T, Amsbio, UK) and 4 mg/mL lysozyme to lyse cells. The amount and quality of the purified DNA was determined using the Qubit dsDNA HS assay kit (ThermoFisher Scientific) and a NanoDrop™ 2000 spectrophotometer (ThermoFisher Scientific), respectively.

### Sequencing

The gDNA extracts were sent to the Department of Microbiology of the University of Nijmegen (Nijmegen, the Netherlands) to perform the sequencing using an Illumina MiSeq Sequencer (Illumina, San Diego, CA, USA), with MiSeq® Reagent Kit v3 (2 x 300 bp read length). The Illumina Nextera XT DNA sample preparation kit was used for the DNA libraries and BBDuk (BBTOOLS version 37.17, DOE Joint Genome Institute) was employed for quality-trimming, adapter removal and contaminant-filtering of paired-end sequencing reads.

### Trimming and binning

Trimmed reads were co-assembled with metaSPAdes v3.10.1 [216]. The program also assembled the metagenome (iterative with kmer size 21, 33, 55, 77, 99 and 127) of the mixed culture. The Burrows-Wheeler Aligner 0.7.15 employing the "mem" algorithm mapped the reads of each sample back to the metagenome and the mapping files were converted using SAMtools 2.1 [217, 218].The algorithms BinSanity v0.2.5.9, COCACOLA, CONCOCT, MaxBin 2.0 2.2.3 and MetaBAT 2 2.10.2 binned the metagenome [219–223] to extract genomes of single lineages out of the metagenome. Subsequently, DAS Tool 1.0 used the five bin sets as input for consensus binning, resulting in the final optimized bins of single-lineage genomes [224]. Their quality was assessed with CheckM 1.0.7 [225].

### Gene annotation and interpretation of auxotrophies

Bins were manually scanned on relevance (coverage, redundancy and completeness) and the relevant bins (coverage > 100) were uploaded to RAST version 2.0 for functional gene annotation [226–228], in combination with the SEED database [226].  The KEGG database was used to study biosynthetic pathways [1]. BLASTn [229] was used to compare 16S rRNA gene sequences obtained in this study to sequences provided by L.C. Valk [230].

In the event that all genes were identified in the genome of "*Ca*. Galacturonibacter soehngenii" strain XYL1, it was assumed the organism was prototrophic for an amino acid. In the event that >50% of the genes were identified in the genome of *ca*. Galacturonibacter soehngenii strain XYL1, it was assumed the organism was prototrophic for a vitamin.

**Fluorescent *in situ* hybridisation**

In this work we have used the protocol described previously [137]. A specific probe set was designed and tested to target "*Ca.* G. soehngenii", with the aim to have it species-specific (see supplementary information). The ARB software, version 5.2 was ran using RedHat 5.6 64bit and Xconfig version 14.0.0.350 and the SILVA database version 132 (released 13th of December 2017) was loaded. The full 16S rRNA gene obtained from the metagenome bin of "*Ca.* G. soehngenii" was used to construct a set of three 18 base pair probes to target this species (Table 5.S1), of which Lac87 was chosen. Overnight hybridization was used as this method significantly improves the signal observed when detecting gram positive microorganisms, such as "*Ca.* G. soehngenii", in combination with a paraformaldehyde fixation (data not shown).

**Full 16S rRNA gene sequencing of *C. freundii* isolates**

Samples for 16S rRNA gene amplicon sequencing were obtained by centrifuging 1-2 mL of cell culture for 3 min at 13,000 rpm (Heraeus Pico 17, Thermo Fisher Scientific). The supernatant was discarded and DNA was extracted from the pellet using a protocol based on bead-beating (DNeasy UltraClean Microbial Kit, Qiagen, Hilden, Germany). DNA extraction was assessed by loading 5 μL of the extracted sample on a 1% (v/w) agarose gel (SYBR Green stained) and DNA concentrations were determined using the Qubit dsDNA HS assay (Thermo Fisher Scientific). volume of 25 μL of samples that had been pure cultures was at this point sent to BaseClear (Leiden, The Netherlands) for Sanger sequencing.

**Metabolomics**

High performance liquid chromatography (HPLC) was performed as described previously, with the aim to detect major metabolic compounds [137]. For analysis of the amino acids, rapid sampling using a specific volume of cold steel balls was employed. The balls were -80°C at the moment of sampling, resulting in 2°C of filtered supernatant. This supernatant was stored at -80°C, thawed and analysed for amino acids using a method described elsewhere in the supplementary information.

## Results

**Microbial community analysis using FISH showed a community dominated by *Enterobacteriaceae* and "*Ca.* Galacturonibacter soehngenii"**

A previously described enrichment [137] was reproduced, enriching on a mineral medium containing 4 g L$^{-1}$ of xylose as fermentable carbon source. The enrichment culture showed a stable catabolic production of dominantly acetate, ethanol and coupled formate and hydrogen and $CO_2$ after 9 SRTs (data not shown). The enrichment culture showed after 60 SRTs a distribution of roughly equal amounts of *Enterobacteriaceae* and "*Ca.* G. soehngenii" (Figure 5.3). "*Ca.* G. soehngenii" is a member of the *Lachnospiraceae* family. The microbial community composition obtained here was similar to the distribution of *Enterobacteriaceae* and *Lachnospiraceae* of our previous enrichment under the same conditions, which was 53%±3% *Lachnospiraceae* and 44%±6% *Enterobacteriaceae* ([137] and **Chapter 2**).
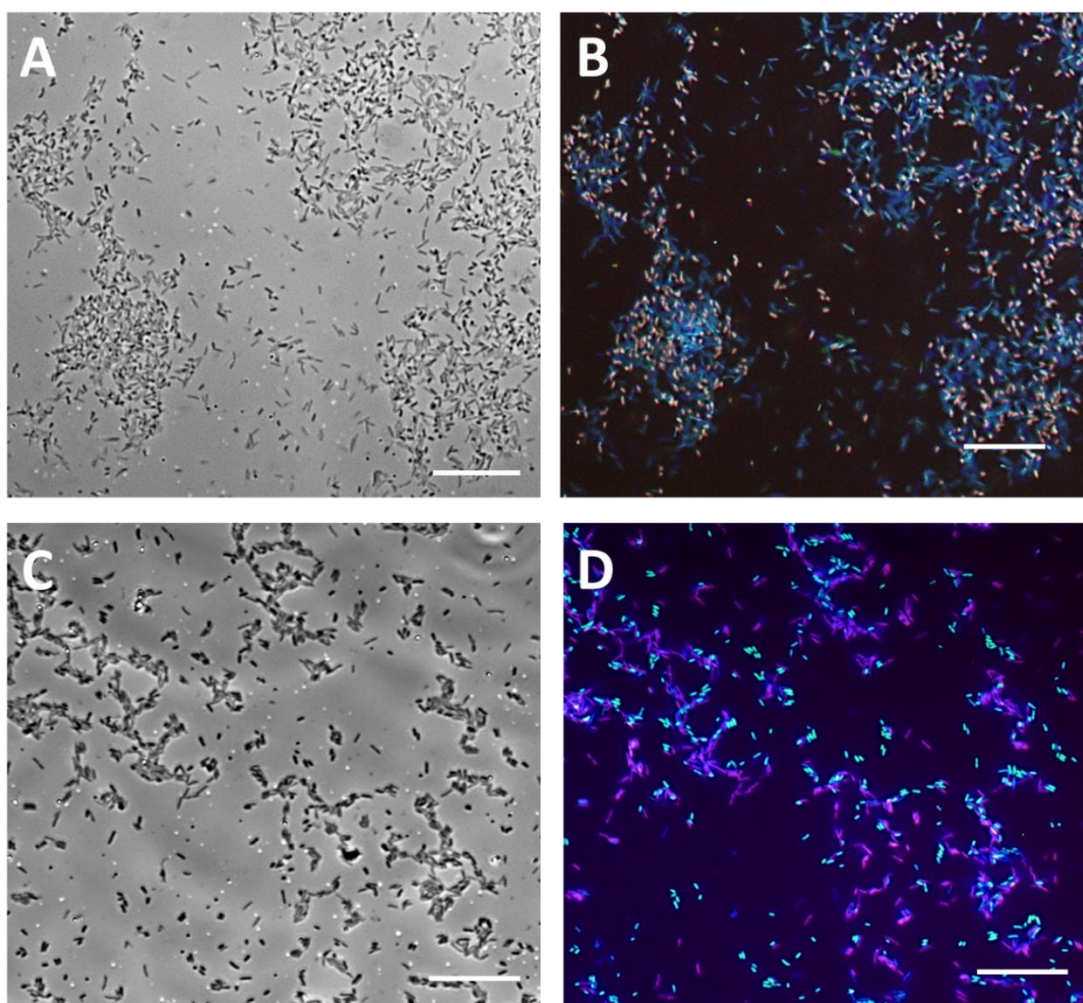


***Figure 5.3***: *Fluorescence in situ hybridization (FISH) of the anaerobic chemostat xylose enrichment culture at day 60 SRTs. The culture was stained with DAPI (blue), a general probe for bacteria (EUB338, green) and a probe for members of the Enterobacteriaceae family (ENT183, red, panel B) or a probe for "Ca. G. soehngenii" (Lac87, red, panel D). Panels A and C show unstained cells obtained using phase contrast microscopy. Scale bars in all panels represent 20 µm.*

After 103 SRTs, a cell pellet was used to extract DNA to construct a metagenome from the enrichment culture. The metagenome showed three dominant bins (Table 5.1). One bin was classified as a species in the family of *Lachnospiraceae*, another bin was classified as *Citrobacter*

*freundii*. The metagenome data supported the FISH analysis, as 51% of the metagenome was linked to *Lachnospiraceae* and 35% to *Citrobacter freundii*, an *Enterobacteriaceae*. The obtained 16S rRNA gene sequence of the *Lachnospiraceae* bin was compared to the 16S rRNA gene of a bin obtained from a galacturonate-limited enrichment culture study performed previously by Valk *et al.* [230]. This resulted in 100% similarity (using BLASTn). This confirmed that the recently discovered "*Candidatus* Galacturonibacter soehngenii" was present in our enrichment system.

*Table 5.1: The phylogeny of the three obtained binned genomes using the metagenomic approach. The closest matching taxa of the binned genomes is given as population, the completeness and coverage of the bin is given and the fraction of the population compared to the rest of the community is estimated.*

| Population | f. *Lachnospiraceae* | s. *Citrobacter freundii* | g. *Ruminococcus* |
|---|---|---|---|
| Completeness | 98.42% | 97.17% | 97.08% |
| Coverage | 1063.72 | 710.19 | 135.4 |
| Est. community % | 50.7% | 35.1% | 6.6% |

**Xylose transport and biosynthetic pathways of "Ca. G. soehngenii"**

The xylose symporter XylE and the ABC transporter XylFGH were both found to be present in *C. freundii* (Table 5.2). Only XylG and XylG were found to be present in "*Ca.* G. soehngenii". XylF was also found in the bin of "*Ca.* G. soehngenii", but its E value was quite high ($4e^{-11}$). This gene was identified through RAST and SEED as a ribose ABC transport system (RbsB). It is likely that this gene represents the gene for RbsB and not that of XylF.

**Table 5.2**: *An overview of the xylose transport systems derived from the genomic bins of C. freundii and "Ca. G. soehngenii". The name, TC number, genetic nomenclature of the genes with the highest annotation and their corresponding expected value (E value) are shown*

| Protein | Gene | TC number | E value (-) *C. freundii* | "Ca. *G. soehngenii*" |
|---|---|---|---|---|
| D-xylose-proton symporter | *xylE* | 2.A.1.3.3. | $1e^{-104}$ | No hits |
| D-xylose-binding periplasmic protein | *xylF* | 3.A.1.2.4 | $4e^{-11}$ | $4e^{-79}$ |
| Xylose import ATP-binding protein | *xylG* | 3.A.1.2.4 | $1e^{-151}$ | $1e^{-156}$ |
| Xylose transport system permease | *xylH* | 3.A.1.2.4 | $7e^{-52}$ | $6e^{-75}$ |

The biosynthetic pathways of "*Ca.* G. soehngenii" were evaluated using a specific substrate. Of the 20 amino acids evaluated, all 20 amino acids showed complete pathways (Table 5.3). L-aspartate showed all genes present for two distinct pathways (Table 5.3). The analysis of the biosynthetic pathways for 8 B-vitamins and Coenzyme A were also evaluated (Table 5.4), which indicated a potential auxotrophy for pyridoxine and biotin.

The incompleteness of a B vitamin pathway was set at 50% of absent genes. This percentage was chosen to provide space for the chance of a gene being present but not being detected (false negative). The completeness of the "*Ca.* G. soehngenii" bin is relatively high (98%). The chance of 1 or more genes being missed due to the method used for a 5 gene pathway is 10% ($p=1-0.98^n$, n=5), while being 13% for 7 genes. Thus 50% was chosen as a safe border for short biosynthetic pathways (<10 genes). The complex pathway of cobalamin does show a significant number of missing genes (35%), but the probability for 1 or more genes not detected is also high here (41%). Therefore, it was considered as a pathway that is likely to cause an auxotrophy in "*Ca.* G. soehngenii".

**Table 5.3**: *The amino acid biosynthesis pathways identified in the genome of "Ca. Galacturonibacter soehngenii", with the substrate, genes present and missing (gene names derived from RAST version 2.0) and if prototrophy was assumed, based on the number of identified genes in the pathway.*

| Amino acid | Substrate | Genes present | Genes missing | Assumption prototrophic* |
|---|---|---|---|---|
| L-serine | pyruvate | *sdaAA, tdcB* | | Yes (2/2) |
| Glycine | L-serine | *glyA* | | Yes (1/1) |
| L-cysteine | L-serine | *cysE, cysK* | | Yes (2/2) |
| L-methionine | L-cysteine | *mccB, metCH* | | Yes (3/3) |
| L-tryptophan | chorismate | *trpAbBCDE* | | Yes (5/5) |
| L-aspartate | Oxaloacetate | *aspB, nadB* | | Yes (2/2) |
| L-glutamine | Glutamate | *glnA* | | Yes (1/1) |
| L-asparagine | L-aspartate | *asnB* | | Yes (1/1) |
| Arginine | Glutamate | *argABCDFGHJ* | | Yes (8/8) |
| Glutamate | A-ketoglutarate | *gltBD* | | Yes (2/2) |
| L-aspartate | Fumarate | *purAB* | | Yes (2/2) |
| Histidine | 5P-α-D-ribose-1DP | *hisABCDEGHIN* | | Yes (9/9) |
| Threonine | Oxaloacetate | *aspC, thrABC, asd, hom,* | | Yes (6/6) |
| L-lysine | L-aspartate | *lysAC, asd, dapABFL,* | | Yes (7/7) |
| L-alanine | Pyruvate | *GGAT or alaR, iscR, ilvE* | | Yes (4/4) |
| tyrosine | chorismate | *tyrABC* | | Yes (3/3) |
| phenylalanine | chorismate | *tyrABC, pheA* | | Yes (4/4) |
| L-proline | glutamate | *proABC* | | Yes (3/3) |
| L-valine | pyruvate | *ivlCDM, avtA* | | Yes (4/4) |
| leucine | 2-oxoisovalerate | *leuABCD,avtA* | | Yes (5/5) |
| L-isoleucine | Threonine | *ivlACDM, avtA* | | Yes (5/5) |

**Table 5.4**: *The B-vitamin biosynthesis pathways identified in the genome of "Ca. Galacturonibacter soehngenii", with the substrate, genes present and missing (gene names derived from RAST version 2.0) and if prototrophy was assumed, based on the number of identified genes in the pathway.*

| B vitamin | Chemical name | Genes present | Genes missing | Uptake | Assumption prototrophic+ |
|---|---|---|---|---|---|
| 1 | Thiamine | *ThiCDEFLMNS, dxs* | *thiGHO45* | *thiT* | Yes (9/16) |
| 2 | Riboflavin | *ribBEH* | | *ribU* | Yes (3/3) |
| 3 | Nicotinate/nicotinamide | *nadABCD, pynN, pupG, pncB, nudC* | *nadERM, pncAC* | | Yes (8/12) |
| 5 | Pantothenate | *ilvCDM, panBCD* | | | Yes (6/6) |
| 6 | Pyridoxine | *Dxs, pfxF* | *pdxABJP, edp* | | **No** (2/7) |
| 7 | Biotin | *bioA* | *bioBCFW* | *bioY* | **No** (1/5) |
| 9 | Folate | *pbaAB, folC12, folM, thyA* | *pbaC, folP* | | Yes (5/7) |
| 12 | Cobalamin | *EPRS, hemABDL, cobACUS, cbiBPHFDCAJ,* | *HemC, cobPO, cbiETJGL* | *btuBCF* | Yes (17/26) |
| | Coenzyme A | *coaABCDE* | | | Yes (5/5) |

## Isolation and metabolic characterization of *Citrobacter freundii*

*Citrobacter freundii* was successfully isolated from the reactor using a consecutive agar-plate approach. The identity was confirmed through comparing the obtained full 16S rRNA gene sequences from the isolated culture to the NCBI database (99% identity with multiple *C. freundii* strains). The isolated strain was able to grow anaerobically and aerobically on mineral medium with xylose as sole carbon source using shake flasks.
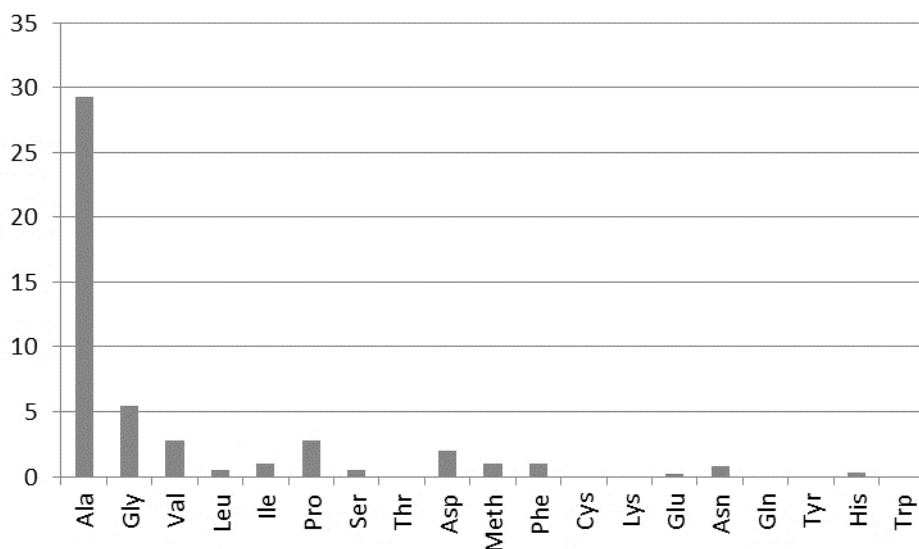


***Figure 5.4**: Ratio of the averaged measured amino acids concentration (n=2) in supernatant of the C. freundii pure culture and that of the xylose mineral medium enrichment.*

The supernatant of the isolated *C. freundii* strain grown anaerobically was sampled to analyse the amino acid composition. Alanine had the highest relative and absolute concentration in the supernatant of the *C. freundii* pure culture compared to the enrichment culture (Figure 5.4). The absolute alanine concentration in the pure culture was measured to be between 0.11 and 0.16 mM (Table S3).

## FISH analysis revealed an increase in relative abundance of "*Ca.* G. soehngenii" after supplementation of the medium

The enrichment was inoculated with frozen effluent obtained from the enrichment using xylose as sole carbon source with a mineral medium in CSTR mode [137] and enriched in an equivalent way as reported. The FISH imaging showed that after the 1st batch was performed, nearly all bacterial cells were detected as *Enterobacteriaceae* and "*Ca.* G. soehngenii" was not detected (Figure 5.5 and 5.6). After 4 SRTs, the *Enterobacteriaceae* fraction decreased and remained at about 20-50% of the cells as observed manually. At 51 SRTs, the fraction of *Enterobacteriaceae* was quantified as 41%±5%, while the fraction of "*Ca.* G. soehngenii" was quantified as 21%±9% (Figure 5.7) as compared to all probed eubacterial cells.

After 51 SRTs, the medium was switched to a medium containing L-alanine, biotin and pyridoxine as supplementation. The *Enterobacteriaceae* fraction decreased to 10-20% of the cell surface, while the fraction of "*Ca.* G. soehngenii" increased to 50-80% as observed manually. After 54 SRTs of enrichment with supplemented medium, the fraction of *Enterobacteriaceae* was estimated to be 21%±9% and "*Ca.* G. soehngenii" was 67%±17% (Figure 5.7). We thus observe that when supplementing L-alanine, biotin and pyridoxine to the mineral medium, the fraction of *Enterobacteriaceae* decreases, while the fraction of "*Ca.* G. soehngenii" increases.
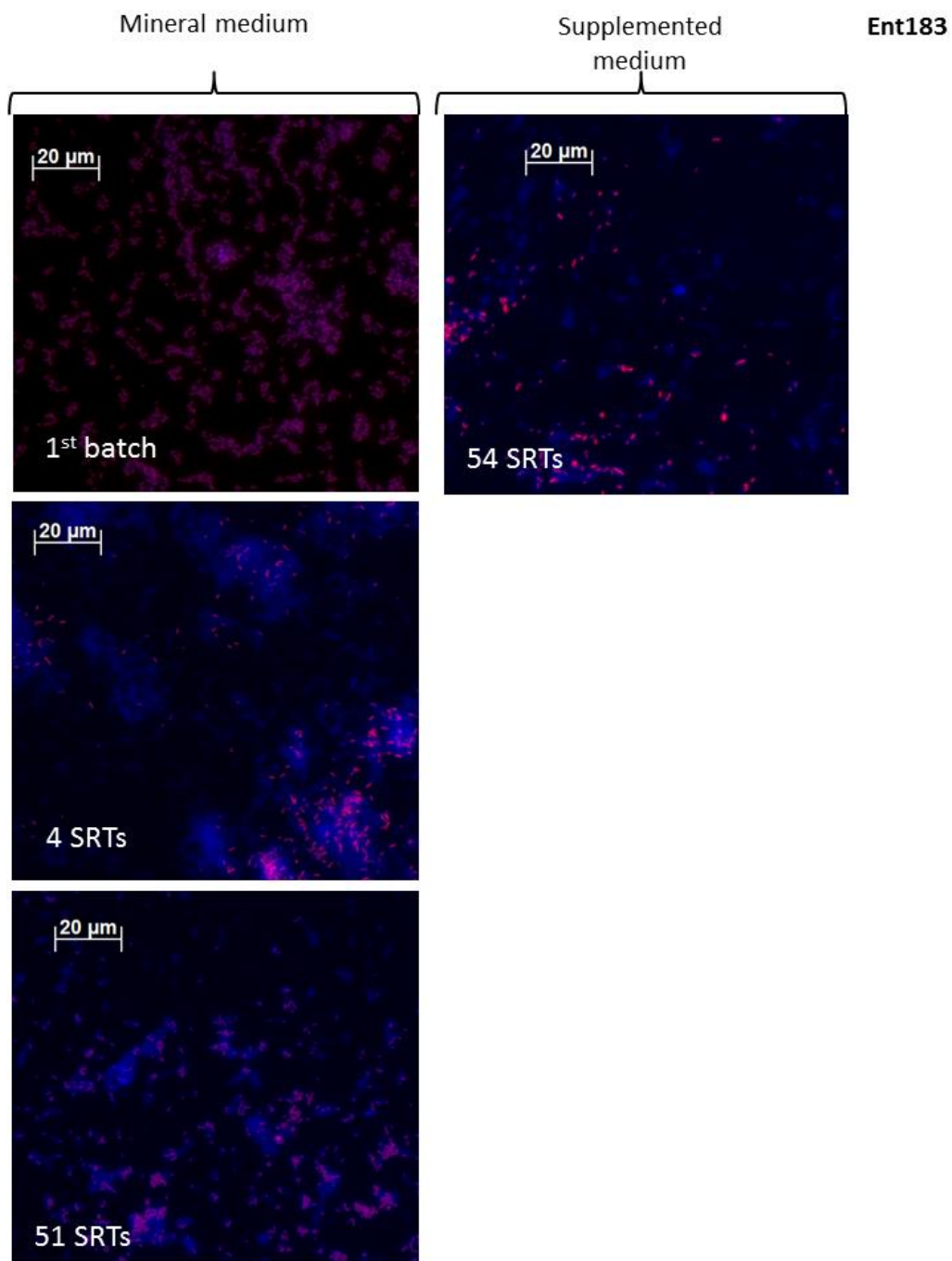
***Figure 5.5***: *FISH imaging obtained for the differential enrichment culture experiment performed probing for Enterobacteriaceae at 400x magnification. Red is Ent183 probe, blue is EUB338 probe. SRTs for either mineral or supplemented medium are given per picture.*
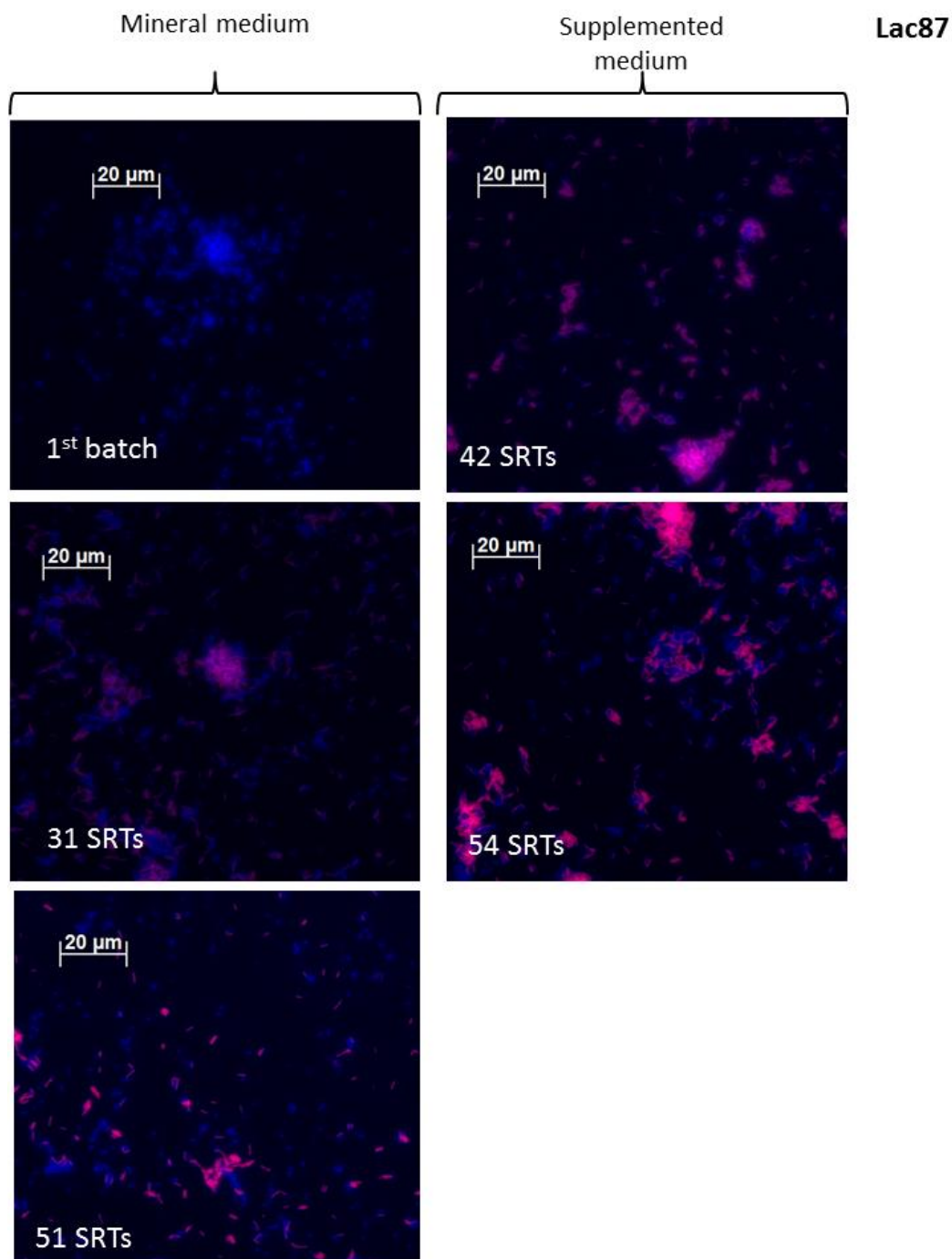
**Figure 5.6**: *FISH imaging obtained for the differential enrichment culture experiment performed probing for "Ca. G. soehngenii" at 400x magnification. Red is Lac87 probe, blue is EUB338 probe. SRTs for either mineral or supplemented medium are given per picture.*
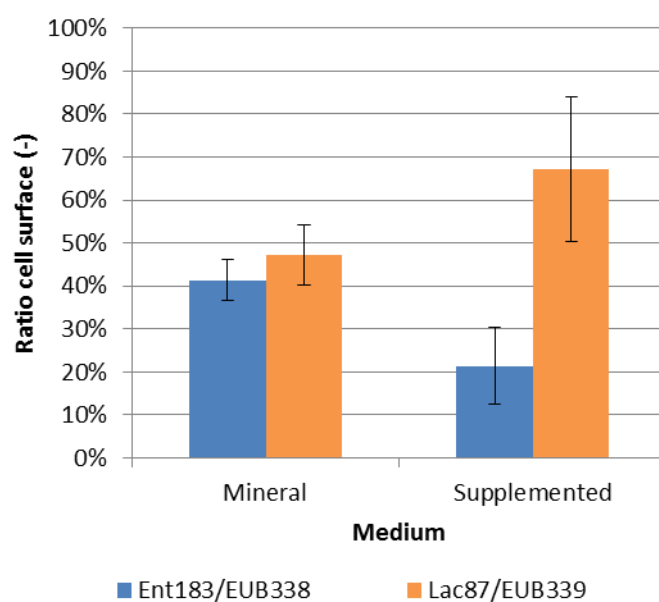
***Figure 5.7****: Ratios of quantified cell surface of the Enterobacteriaceae probe (Ent183) or "Ca. G. soehngenii" probe (Lac87) compared to the Eubacteria probe (EUB338) for either the mineral medium or supplemented medium enrichment, with two images used for mineral and three used for supplemented. Images are taken at 51 SRTs for mineral and 54 SRTs for supplemented medium. The averages of both time points sum to 89% cell surface.*

**Maximum growth rate decreased moving from a batch enrichment to mineral chemostat enrichment to supplemented chemostat enrichment**

The maximum biomass-specific growth rate ($\mu^{max}$) of the enrichment culture was determined during the initial batch phase after inoculation with the thawed enrichment culture to be 0.23 $h^{-1}$. After 51 SRTs of enrichment using the mineral medium, the $\mu^{max}$ was determined to be 0.18 $h^{-1}$. The medium was switched to the supplemented medium and after 54 SRTs of enrichment the $\mu^{max}$ was determined to be 0.15 $h^{-1}$.

***Table 5.5****: The $\mu^{max}$ values determined for the xylose limited enrichment culture. Growth rates were measured using OD measurements taken during a batch experiment performed after 51 and 54 SRTs of enrichment using mineral or supplemented medium respectively.*

| Enrichment phase | $\mu^{max}$ (h$^{-1}$) |
|---|---|
| **Initial batch**[1] | **0.23** ($R^2$ = 0.995) |
| **Mineral** | **0.18** ($R^2$ = 0.999) |
| **Supplemented** | **0.15** ($R^2$ = 0.997) |

[1]Estimated from the base dosage during the batch phase at the start of the enrichment

## Discussion

### Competition for xylose: "*Ca.* G. soehngenii" is likely more competitive in a fermentative xylose limited environment

*Enterobacteriaceae* attained a high presence after the initial batch phase prior to the CSTR enrichment (Figure 5.5). The $\mu^{max}$ of the highly *Enterobacteriaceae* enriched community during the initial batch phase (Table 5.5) was 28% higher than that of the roughly equally divided *Enterobacteriaceae* and *"Ca.* G. soehngenii*"* mineral medium CSTR enrichment (Table 5.5). When enriching using the supplemented medium, the fraction *Enterobacteriaceae* and *"Ca.* G. soehngenii*"* shifted to 21%±9% vs 67%±17% (Figure 5.7) and the $\mu^{max}$ was 20% lower than measured in the mineral medium enrichment (Table 5.5). Thus, a higher fraction of *"Ca.* G. soehngenii*"* is linked to a lower $\mu^{max}$.

The $K_s$ for xylose uptake is likely lower for *"Ca.* G. soehngenii". This difference is caused by the observed different xylose uptake systems detected (Table 5.2). The two studied import mechanisms are XylE, a proton symporter and XylFGH, an ATP-binding cassette (ABC) transporter which uses direct phosphorylation to uptake one molecule of xylose [106]. All three genes of the XylFGH complex are found in bin of "*Ca* G. soehngenii", while xylF is likely missing in the *C. freundii* bin. RbsB is found, which is reported to bind ribose [231]. XylF is the xylose-binding domain of the complex and is structurally related to RbsB [106]. It is therefore possible that *C. freundii* has a high $K_s$ value for xylose than "*Ca* G. soehngenii", as it employs RbsB.

Microorganisms in a chemostat environment are competing on the lowest $C_s$ [232], which can be realized through attaining a high $\mu^{max}$ or a low $K_s$ value (equation 1.1). Andrews and Harris proposed a way to classify microbial selection through a continuum of r-vs K-strategists [112]. K-strategists are better adapted to a "crowded" environment, where substrate is limited and high $Y_{X,ATP}$ and low $K_s$ values are displayed, while r-strategists are better adapted to "uncrowded" environments, where substrate is abundant and a high $\mu^{max}$ is displayed. *C. freundii* can be classified as more a r-strategist, while "*Ca.* G. soehngenii" can be classified as more a K-strategist.

### Commensalism: biotin, pyridoxine and alanine likely supplied by *C. freundii* and taken up by "*Ca.* G. soehngenii"

Based on the metagenomic and metabolomic data, a supplemented medium was designed to evaluate if "*Ca.* G. soehngenii" showed indeed auxotrophies. Biotin and pyridoxine were chosen as B-vitamins, as the metagenomic data showed 71% and 80% of the genes absent in the "*Ca.* G. soehngenii" bin (Table 5.4). "*Ca.* G. soehngenii" was therefore assumed to be auxotrophic for biotin and pyridoxine.

The isolated *C. freundii* strain was shown to be a prototrophic microorganism, growing significantly batch wise in an anaerobic xylose mineral medium. The high relative and absolute presence of alanine in the supernatant of the *C. freundii* culture (Figure 5.4) shows that alanine is likely produced by *C. freundii* and then alanine is consumed in the enrichment culture. Alanine can be produced in a redox balanced way from xylose, if the pentose phosphate pathway is assumed:

0.6 xylose + 1 $NH_4^+$ → 1 L-alanine + 1 $H^+$ + 1 $H_2O$
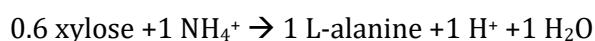
Per alanine, 1 ATP can be produced in glycolysis. Alanine can be an alternative fermentative pathway as opposed to succinate production, which is produced at about 0.1 Cmol Cmol$^{-1}$ in the enrichment culture and yields a similar ATP yield. Microbial species have been reported to produce alanine naturally, such as *Thermococcus kodakaraensis* [233]. It is likely that alanine production is part of the metabolic strategy of *C. freundii,* as part of an inefficient r-strategist metabolic response.

Biotin and pyridoxine both fulfil essential metabolic roles (Table 5.6). Biotin is a costly commodity for a cell to produce. In *E. coli* its production is estimated to be 20 ATP per molecule from glucose [234]. Its octanol water coefficient is quite high (0.5) compared to pyridoxine (-0.77). This shows biotin dissolves more in octanol, while pyridoxine dissolves more in water. Biotin is a more hydrophobic B vitamin than pyridoxine. This means it can diffusive passively over cell membranes, while this is unlikely for pyridoxine. Biotin is suspected to leak away from *C. freundii* toward "*Ca.* G. soehngenii". One of the three import proteins of active biotin uptake was found in the metagenome (Table 5.4) and this complex is an ATP-binding cassette system. It is therefore possible that "*Ca.* G. soehngenii" actively imports biotin, "pulling" the gradient of biotin into its cell.

*Table 5.6: Biological roles of pyridoxine and biotin*

| No. | Name | Function | Reference |
|---|---|---|---|
| **B6** | Pyridoxine | The active form pyridoxal 5'-phosphate, which catalyses reactions in amino acid synthesis, plays a role in fatty acid metabolism and storage carbohydrate degradation and protects against reactive oxygen species | [235] |
| **B7** | Biotin | Involved in (de)carboxylation reactions. Biotin-dependent enzymes play key roles in fatty acid and amino acid biosynthesis and gluconeogenesis. | [236] |

The reason for pyridoxine overproduction of *C. freundii* is unclear. Pyridoxine production from xylose costs 1 ATP intracellularly, when assuming it to be formed from D-Erythrose-4-phosphate, and $C_4$ intermediate of the pentose phosphate pathway. It needs to be exported as it diffusion over the membrane is very limited. Its degree of reduction is 4.63 electrons per Cmol, xylose has 4 electrons per Cmol. This means pyridoxine formation can be coupled to acetate formation. This combined pathway will cost *C. freundii* net energy. From a bioenergetics point of view, sharing pyridoxine is costly for *C. freundii*. The cost of this sharing is potentially repaid by limiting the growth of "*Ca.* G. soehngenii". Summarizing, *C. freundii* shows a growth strategy of commensalism and can potentially limit the growth of "*Ca.* G. soehngenii" through sharing alanine, biotin and/or pyridoxine.

## Oxygen scavenging as an additional way to explain the enrichment of C. freundii

*Enterobacteriaceae* are known to be facultative fermenters, allowing them to metabolise carbohydrates aerobically and anaerobically [237]. The isolated *C. freundii* XYL1 strain was shown to grow aerobically in this work. "*Ca.* G. soehngenii" is expected to be an obligate anaerobe. Its closest cultivated relative, *Lachnotalea glycerini*, is found to be highly sensitive towards oxygen [238]. We therefore hypothesize that *C. freundii* can scavenge oxygen in the reactor after the periodical cleaning during which the bioreactor is opened (once per 6-9 SRTs). "*Ca.* G. soehngenii" would benefit from the anaerobiosis provided potentially by *C. freundii*.

***Figure 5.6****: Putative interactions and metabolic features driving the coexistence of* C. freundii *and "*Ca. *G. soehngenii" in the xylose-limited enrichment culture.* C. freundii *displays a commensalism strategy (dotted arrow), while "*Ca. *G. soehngenii" shows a competitive strategy (dotted inhibition).*

## Metabolite sharing of *Proteobacteria* as a strategy to avoid being outcompeted by *Firmicutes*

The coexistence of these two species is thus assumed to be driven by the oxygen scavenging and metabolite sharing features of *C. freundii*, allowing both species to coexist (Figure 5.6). Actual concentrations of B vitamins or amino acids from *C. freundii* can influence the biomass yield of "*Ca.* G. soehngenii" by creating a second growth limitation next to xylose. The exhibited kinetic properties of "*Ca.* G. soehngenii" on the other hand can cause the *C. freundii* population to slowly wash out. "*Ca.* G. soehngenii" is expected create a lower residual xylose concentration, through which it can outcompete *C. freundii*.

The lack of biosynthetic genes for biotin and pyridoxine in "*Ca.* G. soehngenii" fits in the multi-genome assessment of gut microbes performed by Magnusdottir *et al.* [118]. They report that the genes of the biosynthetic pathway for biotin are rarely found in *Firmicutes*, while they are very common in *Proteobacteria*. They also report that the gene to synthesize pyridoxal-5-phosphate is found in many *Proteobacteria* and only in a few *Firmicutes*. *C. freundii* is a *Proteobacteria*, "*Ca.* G. soehngenii" is a *Firmicutes*. We have also observed a coexistence of *Clostridium intestinale* (a *Firmicutes*) and *Enterobacteria* (*Proteobacteria)* in a glucose limited enrichment culture (Chapter 2). Such an coexistence is also reported by Valk *et al.* [230], where *Klebsiella* (*Proteobacteria*) and *Lachnospiraceae* (*Firmicutes*) coexist. Horn *et al.* show that glucose is co-metabolized by both *Clostridiaceae* and *Enterobacteriaceae* in the earthworm gut [239]. The co-occurrence of *Firmicutes* and *Proteobacteria* in a substrate limited fermentative ecosystem can be argued to be a more general ecological concept, driven by the commensalism of more prototrophic *Proteobacteria* toward more auxotrophic *Firmicutes*.

This work shows that a combination of hypothesis-driven research, using bioreactor enrichment culturing and targeted "omics"-approaches leads to novel insights in the functioning of microbial communities. Microbial diversity is shaped by both competition and cooperation. Future work to characterize *in situ* metabolic interactions will aid from meta-proteomics to validate functional enzymes and the detection of B vitamins using chromatography and MS. The proposed model for metabolic interactions might extend as a general concept in carbohydrate fermentations, where a prototrophic r-strategists limit the growth through metabolite sharing of auxotrophic K-strategists.

## Supplementary material

### Design, specificity and testing of Lac87 probe

***Table 5.S1***: *Overview of the three probes designed to target specifically "*Ca. *G. soehngenii" using the SSU r132 database released by SILA and the ARB software*

|  | Sequence | BLAST position number | Region | GC | Formamide (%) |
|---|---|---|---|---|---|
| **Lac189** | CGGCCUCGUUGGCUUAUG | 172-189 | V2 | 61% | 39 |
| **Lac203** | CCAACUAGGCCAUGCGGC | 186-203 | V2 | 61% | 39 |
| **Lac87** | UCAGACUUGCAUCGCCAC | 70-87 | V1 | 56% | 36 |

Three probes were designed to target "*Ca*. G. soehngenii" specifically. No matches were found with the SILVA database using the TestProbe function available at the SILVA website ([https://www.arb-silva.de](https://www.arb-silva.de) ). Zero mismatches were allowed and SSU r132 was used. The formamide concentration was calculated from the 0.9M Na$^+$ concentration used during hybridization and the GC content. All three probes were tested *in vivo* with a sample obtained from the xylose limited enrichment culture as a positive control and a glucose limited enrichment culture ran in SBR mode as a negative control The latter culture was shown to be >90% dominated by *Enterobacter cloacae*, an *Enterobacteriaceae* species and 16S amplicon sequencing showed <0.001% relative abundance using 16S rRNA gene amplicon sequencing with the *Lachnotalea* genus, which is the closest matching genus with *Galacturonibacter* [137]. All three probes showed little hybridization with the negative control sample (<0.1% of the cell surface of DAPI and EUB338). Both Lac189 and Lac87 showed good hybridization and Lac87 was used at 35% formamide concentration onwards.

***Table 5.S2***: *Oligonucleotide probes used for FISH analysis in this study*

| Probe | Sequence 5'-3' | Formamide % (v/v) | Specificity | Reference |
|---|---|---|---|---|
| **EUB338** | GCWGCCWCCCGTAGGWGT | - | Most bacteria | [126] |
| **Ent183** | CTCTTTGGTCTTGCGACG | 20 | *Enterobacteriaceae* except *Proteus spp.* | [127] |
| **Lac435** | TCTTCCCTGCTGATAGA | 25 | *Lachnospiraceae* | [129] |
| **Lac87** | GTGGCGATGCAAGTCTGA | 35 | "*Ca.* Galacturonibacter soehngenii" | This study |

### GC-MS/RP-ESI-Q-TOF-MS/MS result to detect amino acids in the supernatant

Gas chromatography (GC) was coupled to reverse phase (RP) liquid chromatography. An electrospray ionisation (ESI) was used to inject the liquid phase into the mass spectrometer (MS), which consisted of a Q time of flight (TOF) unit to detect charged fragments. This method was designed according to previously published work which describes the use of a GC coupled to isotope dilution mass spectrometry detecting pentose phosphate pathway intermediates [240].

*Table S3*: *The raw data of the GC-MS analysis for the amino acids. An "x" indicates that the measurement was compromised due to the background (which is likely due to salts). An "<" indicates that the detected value was below the detection limit. R_7 indicates three technical replicate supernatant samples from the enrichment chemostat cultures while C_1 and C_2 indicate C. freundii pure culture supernatant samples, taken at 26th and 27th of June 2018. Concentrations are measured in µM.*

| Sample | Trp | His | Tyr | Gln | Asn | Glu | Lys | Cys | Phe | Meth | Asp | Thr | Ser | Pro | Ile | Leu | Val | Gly | Ala |
|---|---|---|---|---|---|---|---|---|---|---|---|---|---|---|---|---|---|---|---|
| R_7_1 | 0.03 | 0.11 | 624.78 | 0.04 | 0.17 | 4.92 | 0.32 | 0.11 | 0.07 | 0.11 | 0.86 | 0.13 | 0.77 | 0.18 | 0.09 | 0.11 | 0.39 | 1.3 | 3.62 |
| R_7_2 | 0.03 | 0.11 | 624.78 | 0.2 | 0.17 | 6.97 | 0.32 | 0.11 | 0.07 | 0.11 | 1.11 | 0.19 | 0.79 | 0.18 | 0.09 | 0.11 | 0.39 | 1.3 | 3.92 |
| R_7_3 | 0.02 | 0.13 | 483.82 | 0.3 | 0.17 | 9.3 | 0.32 | 0.11 | 0.05 | 0.09 | 1.09 | 0.14 | 0.57 | 0.15 | 0.05 | 0.07 | 0.35 | 1.14 | 4.28 |
| 2606_C_1 | < | 0.03 | x | < | 0.11 | 1.54 | < | x | 0.07 | 0.1 | 2.27 | < | 0.39 | 0.5 | 0.04 | 0.05 | 0.81 | 7.05 | 109.65 |
| 2606_C_2 | < | 0.05 | x | < | 0.17 | 1.63 | < | x | 0.06 | 0.1 | 1.77 | < | 0.3 | 0.46 | 0.12 | 0.05 | 1.29 | 6.53 | 121.42 |
| 2706_C_1 | 0.07 | 0.09 | x | < | 0.09 | 9.02 | < | 0 | 0.83 | 0.13 | 0.95 | x | x | 1.27 | 0.41 | 0.24 | 1.26 | 8.56 | 139.84 |
| 2706_C_2 | 0.08 | 0.11 | x | < | 0.16 | 8.59 | < | x | 0.68 | 0.13 | 1.12 | x | x | 1.27 | 0.4 | 0.2 | 1.39 | 9.79 | 155.7 |

# Chapter 6 - General conclusions and an outlook for future research

*This chapter was written and/or revised by:*

*Julius L. Rombouts, David G. Weissbrodt and Mark C.M. van Loosdrecht*

## General conclusions

The aim of this thesis was to explore and understand microbial strategies for interaction in fermentative environments. To achieve this goal, a specific set of experiments was designed according to pre-defined research questions. The overarching method was to evaluate enrichment cultures using a combined approach characterising the stoichiometry, kinetics, and microbial community structure, where glucose and xylose were used as model substrates.

In **Chapter 1**, the ecology of carbohydrate fermenting systems is introduced, with a focus on bioenergetics and kinetics. The industrial applications of mixed culture fermentation experiments are also introduced here. In **Chapter 2 and 3,** xylose and glucose were used in combination with the mineral medium used by Temudo *et al.* [51] (**Appendix I**). The environmental parameters were chosen to compare the results of these chapters to the work on xylose and glucose fermentations presented by Temudo [6]. The addition of SBRs to CSTRs was used to explore the ecological response of microbial communities to these opposite environments. Single or dual substrate limitation was performed for more than 30 SRTs, to accurately observe the impact of this setting. In **Chapter 4,** amino acids and B vitamins were used to test the influence of these nutrients compared to the mineral medium with the aim to study the ecology of lactic acid bacteria. In **Chapter 5**, pyridoxine, biotin, and alanine were supplemented to identify a potential commensalism mechanism shaping the microbial diversity in a xylose limited continuous culture. Open, non-sterile (*i.e.*, non-axenic) two-litre bioreactors were used to perform a specific set of enrichment cultures that are all carried out under mesophilic conditions (30°C±0.1) and at relatively high dilution rates (final SRTs ranging from 8 to 12 h). Bovine rumen and mesophilic anaerobic digestor sludge were the two different inocula used.

A relatively concise amount of conditions was tested (Table 6.1), as the aim was to thoroughly analyse the enrichment cultures in terms of kinetics, bioenergetics and microbial community structure. There is a significant number of 303 peer-reviewed articles available up to 2018 that have explored fermentative enrichment cultures, as reviewed by Moscoviz *et al.* [190], were these experiments are termed "dark fermentation". Most enrichment culture studies do not exceed the level of resolution of a stoichiometric analysis of a predefined ecosystem in a bioreactor with 16S rRNA gene sequencing, where most studies are performed in continuous or CSTR mode. SBR enrichments are not often characterised. SBRs, in combination with online data harvesting, offer the option to analyse the kinetics of the enrichment over every microbial generation. As explained in the supplementary information of **Chapter 2**, the growth rate can be calculated for every cycle, but also hydrogen and $CO_2$ yields can be calculated per cycle. This additional benefit should be considered next to choosing a selection on $\mu^{max}$ or $q_s^{max}$ (SBR, **Chapter 2**) or on "affinity" (**Chapter 2 and 3**).

**Table 6.1:** An overview of the performed enrichments described in this thesis with the compared environmental conditions

| Enrichment | Chapter | Operation conditions | | | | Observed response | |
|---|---|---|---|---|---|---|---|
| | | Inoculum | Substrate(s) | Reactor regime | pH | Dominant carbon products[1] | Dominant[2] population(s) |
| 1 | 2 | Bovine rumen | Xylose | SBR | 8 | Acetate, ethanol | *Citrobacter freundii* |
| 2 | 2 | Bovine rumen | Xylose | CSTR | 8 | Acetate, ethanol | *Citrobacter freundii* *Lachnospiraceae* |
| 3 | 2 | Bovine rumen | Glucose | SBR | 8 | Acetate, ethanol | *Enterobacter cloacae* |
| 4 | 2 | Bovine rumen | Glucose | CSTR | 8 | Acetate, ethanol, butyrate | *Clostridium intestinale* |
| 5 | 3 | Bovine rumen | Xylose + Glucose | SBR | 8 | Acetate, ethanol | *Citrobacter freundii* |
| 6 | 3 | Bovine rumen | Xylose + Glucose | CSTR | 8 | Acetate, ethanol, butyrate | *Clostridium intestinale* |
| 7 | 4 | Anaerobic digester sludge | Glucose | SBR | 5 | Acetate, butyrate | *Ethanoligenens* |
| 8 | 4 | Anaerobic digester sludge | Glucose + peptides + 9 B vitamins | SBR | 5 | Acetate, propionate, lactate, butyrate, valerate | *Lactococcus* *Lactobacillus* |
| 9 | 5 | Xylose CSTR Ch 2 | Xylose | CSTR | 8 | Acetate, ethanol | *Citrobacter freundii* *Ca.* Galacturonibacter soehngenii" |
| 10 | 5 | Xylose CSTR Ch. 2 | Xylose + pyridoxin + biotin + L-alanine | CSTR | 8 | Acetate, ethanol | *Citrobacter freundii* "*Ca.* Galacturonibacter soehngenii" |

[1]Acetate, ethanol, propionate, lactate, succinate, butyrate, valerate are considered here, which form the main dominant catabolic products in this thesis besides formate, hydrogen and $CO_2$. >10% of Cmol $Cmol^{-1}$ was chosen as a border for dominant product here

[2]>20% cell surface using fluorescent in situ hybridisation and complemented with 16S rRNA gene sequencing or metagenomics

Solely performing 16S rRNA gene amplicon sequencing, or a comparable method, such as denaturing gradient gel electrophoresis (DGGE) or terminal restriction fragment length polymorphism (TRFLP) is common practice in literature, when aiming to characterise a microbial community. Solely extracting DNA and using such methods when characterising a microbial community structure offers information on the identity of taxa, not on the quantity of taxa, due to systematic biases [241]. Fluorescent *in situ* hybridisation coupled to epifluorescence microscopy offers (semi) biovolume quantification at family, genus or species level. As discussed in **Chapter 2, 3 and 4**, a "full-cycle rRNA analysis" is required to complete the microbial community analysis [169]. Other methods such as flow cytometry or modern day metaproteomics can offer a similar (semi) biovolume quantification. Besides, complementary methods are useful to check the accuracy of a given method. Ambiguous terms such as "predominant" were avoided in this thesis, due to attempting "complete" microbial community analyses.

The main conclusions following out of these experiments are detailed in this section. Metabolic strategies that microorganisms employ to compete for substrate(s) were evaluated using the proposed approach of analysing the stoichiometries, kinetics, and microbial community structures.

**At pH 8.0** this resulted in the observations that:

1. Xylose and glucose were fermented to similar products at pH 8.0 (**Chapter 2 and 3**):
   a. The dominant observed catabolic products were acetate, ethanol, butyrate and formate, hydrogen, and $CO_2$;
   b. CSTR environments favoured more butyrate production and SBR environments favoured more acetate and ethanol production;

2. Butyrate formation was linked to slow uptake rates, while acetate and ethanol formation was linked to high uptake rates (**Chapter 2**)

3. *Enterobacteriaceae* dominated SBR environments, while *Clostridiales* dominated CSTR environments at pH 8.0 (**Chapter 2 and 3**).

Building upon known catabolic networks, catabolic ATP yields of the observed product spectra were calculated. Using this approach, **anabolic efficiencies ($Y_{x,ATP}$) and substrate fluxes ($q_s^{max}$)** values could be compared, which resulted in the conclusion that:

4. SBR communities maximised their $q_s^{max}$, while CSTR communities maximised their $Y_{x,ATP}$ (**Chapter 2**).

5. SBR communities enriched on either mineral or complex medium show a similar $Y_{x,ATP}$ value while the $q_s^{max}$ was almost double on complex medium (**Chapter 4**)

These conclusions are in line with the microbial ecology model proposed for r- and K-selection by Andrews and Harris [112]. Their opinion paper proposes the continuum of r- and K-selection, where organisms maximise their fitness for survival in either "crowded" (r-selection) or "uncrowded" (K-selection) environments. SBR and CSTR enriched communities are cultivated in opposite environments of "crowded" or "uncrowded". Or in terms of actual reactor conditions: with high (>10 mM) or low (<0.05 mM) substrate concentrations. Cycles in SBR enrichments have high substrate concentrations (>10 mM of carbohydrate in **Chapter 2, 3 and 4**), continuous enrichment in CSTRs have low substrate concentrations (<0.05 mM in **Chapter 2, 3 and 5**).

Supplementation of additional nutrients used in anabolism, in the form of amino acids and B vitamins, led to a significant substrate flux increase ($q_s^{max}$ was 94% higher, **Chapter 4**). This difference in flux was explained through the hypothesis of resource allocation [242]. This hypothesis states that functional proteins are "expensive" to biosynthesise (in terms of ATP). Therefore, cells attempt to allocate resources (ATP) in an optimal way to dominate a given environment. When enriching for communities in SBRs, $q_s^{max}$ is apparently optimised, as this increased the observed $\mu^{max}$ the most (**Chapter 4**). This resulted in the selection of the microbial community which optimised its resource allocation: a heterofermentative community producing lactic acid and ethanol in complex medium and an acetate-butyrate-$H_2$ type producing community in mineral medium.

Here, it should be noted again that storage of substrate uncouples growth from substrate uptake. In other words, if a community stores glucose as *e.g.* trehalose [243] $q_s^{max}$ and $\mu^{max}$ are not linearly correlated anymore. Storage was estimated to take place significantly (about 20% of incoming COD) in the mineral medium glucose fed enrichment at pH 5.0 using a SBR (**Chapter 4**).

Microbial diversity was analysed using a combination of 16S rRNA gene sequencing and FISH coupled to epifluorescence microscopy, with or without cell surface quantification. In this way **community structures** were estimated accurately, following the proposed "full-cycle rRNA analysis" approach of Amman, Ludwig and Schleifer as discussed earlier[169]. In **Chapter 2 and 3**, a full 16S rRNA analysis was employed to increase the taxonomic resolution. This led to the following conclusions:

6.  Single substrate limited enrichments can lead to communities highly enriched for one species (**Chapter 2 and 3**), though multiple species can also coexist limiting a single substrate (**Chapter 2 and 3**);

7.  Dual substrate enrichment in a CSTR system led to a very similar microbial diversity as the CSTR enrichment on glucose, with both systems being highly enriched for *Clostridium intestinale* (>85% of projected cell surface, **Chapter 2 and 3**);

8.  *Ethanoligenens* was the dominant genus in the mineral medium SBR enrichment at pH 5.0, while *Lactococcus, Lactobacillus*, and *Megasphaera* populations coexisted on complex medium (**Chapter 4**).

**Carbon catabolite repression** is an ecological phenomenon that is reported often during the uptake of xylose and glucose simultaneously in pure cultures of fermentative microorganisms [142].

9.  Carbon catabolite repression was not observed for dual substrate fermentation on mixtures of xylose and glucose in either SBR or CSTR enrichments (**Chapter 3**).

Glucose can be intracellularly stored in microorganisms as trehalose, glycogen or other $C_6$ based polymers [243]. The potential **storage of carbohydrates** occurring in the enrichment cultures was evaluated by performing a batch experiment or cycle analysis. The measured concentrations of metabolites were used to construct a COD recovery over the cycle, thereby estimating the amount of potential storage polymer formed during the substrate uptake phase.

10. No significant storage of either xylose or glucose was estimated in the SBR enrichments performed at pH 8.0 using a mineral medium (**Chapter 2 and 3**);

**11.** Significant storage of glucose (20% of incoming COD) was estimated in the mineral medium SBR enrichment at pH 5.0, while no storage was estimated using a complex medium in the same conditions (**Chapter 4**).

In **Chapter 5**, metagenomics and metabolomics were used to study the phylogeny and potential metabolism and generate a hypothesis on possible metabolic interactions occurring *in situ*.

**12.** In the bin of "*Ca.* Galacturonibacter soehngenii" the biosynthetic pathway for biotin and pyridoxine formation were considered incomplete, suggesting an auxotrophy for these two B vitamins

**13.** Metabolomics of the enrichment culture and *Citrobacter freundii* XYL1 revealed that alanine is likely used by "*Ca.* Galacturonibacter soehngenii"

A differential enrichment culture by an initial mineral medium enrichment, and subsequently supplementing biotin, pyridoxine and L-alanine showed that the fraction of "*Ca.* Galacturonibacter soehngenii" in the enrichment culture increased. This suggests that "*Ca.* Galacturonibacter soehngenii" was indeed growth limited by one, two or all three supplied nutrients.

# Directions for further research

## 1 The technological challenge in mixed culture fermentation: how to direct product formation?

Microbial community engineering attempts to direct product formation through a mechanistic understanding of the ecology of the relevant microbial functionalities. In mixed culture fermentation, the industrial challenge is to direct the electrons to only hydrogen, lactate, ethanol, or to even ($C_2$ and $C_4$) or uneven ($C_3$ or $C_5$) fatty acids. In full scale systems, these conversions are performed using "real" feedstocks (*e.g.*, wastewater effluent) as opposed to "synthetic" feedstocks used in this thesis (*e.g.*, glucose and yeast extract). Then, how to study ecological concepts? Complex microbiomes offer the ecological relevance and can still be used to answer a certain ecological question when different operational parameters are compared in reproducible experiments (Figure 6.1). There is however a difficulty in understanding how such complex microbiomes function, which can be formulated in the question "Who is doing what and why?". More specifically this question asks: why does a certain metabolism prevail over another metabolism under different conditions? Mechanistic understanding of which environmental conditions cause which effect to the resulting microbial community and product spectrum is difficult to achieve in complex microbiomes: the feedstock composition and SRT (*i.e.*, applied growth rate) are difficult to manipulate. Feedstocks vary widely in content and can change over the course of the experiment as they are often not suited for sterilisation. Enrichment cultures can aid here, as feedstock composition and SRT can be carefully controlled (Figure 6.1). Thus, complex microbiomes offer relevant ecological knowledge to be generated, but suffer from careful controlling of essential parameters that determine the ecological niche studied preventing the researcher from mechanistically understanding the system.
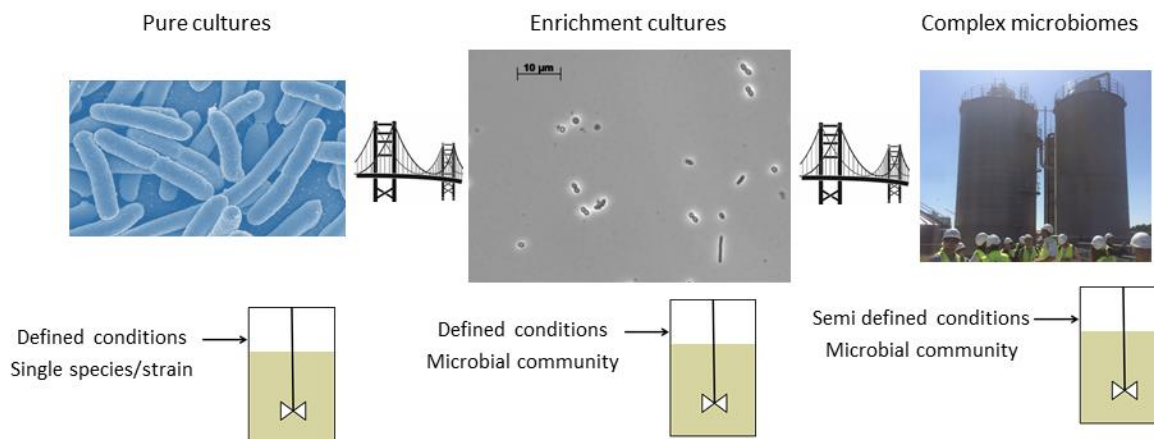


**Figure 6.1**: *Bridging the gap between pure culture studies and complex microbiomes observed in full scale systems using enrichment cultures.* E. coli *electron microscope image (Public Health Matters, UK government), microscope image using 400x magnification and anaerobic digestor at Royal Cosun B.V. site in Dinteloord, the Netherlands.*

Enrichment cultures bridge the gap from complex microbiomes to pure cultures (Figure 6.1). Pure cultures are useful to simplify genomic and proteomic potential of a given culture and offer the advantage of knocking genes out or introducing new genes to verify how genotypes affect phenotypes. Pure cultures however offer limited ecological relevance, as virtually no microbial niche is inhabited by only one microbial species, let alone one strain. Interspecies interactions might be crucial to the functioning of microbiomes and are missed out in pure culture research.

Therefore, enrichment cultures offer a useful tool to the microbiologist, essentially bridging the gap from pure cultures to complex microbiomes.

Temperature, pH, HRT (and coupled SRT) are relatively well studied for mixed culture fermentation or fermentative enrichment cultures as concisely outlined in **Chapter 2** and reviewed by Dionisi *et al.* [244]. The feedstock composition is part of the molecular composition of the fermentative environment, which includes (i) the presence of certain types of salts (cations and anions), the type of fermentable carbohydrate (*e.g.* glucose), the presence of other metabolic nutrients (such as alanine), but also the metabolic products produced during fermentation. The exact mechanism of how different concentrations of certain molecules influence or do not influence the fermentative functionalities, *e.g.*, the product spectrum, remains to be largely solved.

Efforts have been taken to study the effect of the hydrogen partial pressure on the product spectrum [87] (**Chapter 2**). A first research opportunity (I) will lie in studying the effect of other gaseous compounds that can be crucial in controlling the product spectrum, such as the partial pressure of $CO_2$ (more "oxidative" environment) or of $H_2S$ (potential toxicity at higher pH due to futile cycling). Secondly, the impact of cations on a fermentative ecosystem can also be a direction for further research (II), as fermentative mixed cultures have not been compared well on the impact of concentrations $Na^+$, $K^+$, $Ca^{2+}$, $Mg^{2+}$ or other relevant cations in terms of product spectrum, kinetics and microbial community structure yet. Halophilic and alkaliphilic (high salt, high pH) environments are present in natural and manmade habitats, such as soda salt lakes [245] and in residual cellular fractions of NaOH treated carbohydrates. Such cellular fractions are available through processing aerobic granular sludge [246]. The residual fraction after extracellular polymeric substance (EPS) extraction, contains carbohydrates and proteins and can be used for mixed culture fermentation to produce economically interesting products, such as introduced in **Chapter 1**. The question if it is economically more feasible to produce an exopolymer, like *Kaumera* [247] or a bulk chemical, such as lactate (**Chapter 4**), remains to be solved by the biochemical industry and ultimately, the consumer.

A third research opportunity lies in understanding the ecology of fermentations in food using enrichment cultures (III). Specifically, the influence of the composition of nutrients available at the start of the fermentation (*e.g.*, types and amounts of amino acids) is of interest to research, to be able to better understand the fermentative mechanisms at work in food ecology, such as during kimchi or "natural wine" fermentations. Fourthly, in the light of the ecology of food fermentations, very low pH enrichment cultures (pH<3.5) are also interesting (IV), as grape juice has an average pH of 3.3. The SRT of the enrichment will have de be adapted to low growth rates, so a membrane bioreactor or a granular sludge reactor as used by Tamis *et al.* [248] are expected to be suitable for this type of work.

Fifthly, studying the impact of the composition of the feedstock used to produce spectra of VFAs for either chain elongation or PHA production is a promising research opportunity (V). Feedstocks containing only slowly hydrolysable polymers such as cellulose and hemicellulose in combination with a relatively large content of salts (*e.g.*, paper mill effluent) could induce a very different ecological effect in the fermentation/hydrolysis than the organic fraction of municipal waste (*e.g.*, fruit and vegetable waste), as discussed with Dr. L. Welles at the Orgaworld waste processing site, Lelystad, the Netherlands (internal communication). Enrichment cultures can aid this research field, by exact control and evaluation of the stoichiometry, kinetics, and microbial community structure to understand the ecology of these fermentations, and ultimately to direct product formation as proposed by Temudo in 2008 [6] and further developed in this thesis.

## 2 What drives product formation: kinetics or ATP maximisation?

Competing for substrate, microorganisms basically have two options to optimise their growth rate ($\mu$), either optimising their maximum rate of substrate uptake ($q_s^{max}$) or optimising their yield of biomass formation on substrate ($Y_{x,s}$).

$$\mu = Y_{xs} \cdot q_s + m_s \qquad\qquad (6.1)$$

Optimising for flux or rate ($q_s^{max}$) means optimising the internal enzymatic network. When assuming Michaelis-Menten type enzyme kinetics for a single substrate enzymatic reaction, then:

$$r_e = \frac{k_{cat} \cdot c_e \cdot S}{S + K} \qquad\qquad (6.2)$$

In which $r_e$ is the enzymatic rate, $k_{cat}$ is the "turnover" rate specific for this enzymatic reaction, $c_e$ is the enzyme concentration, $S$ is the substrate concentration and $K$ is the Michaelis-Menten constant of this specific reaction. If kinetics are optimised, than cells have to optimise their metabolic reactions as such that the "best" enzyme concentration levels are found. The best "fit" of the cellular enzyme concentrations levels with the applied conditions enables the highest $q_s^{max}$, which in turn enables the highest $\mu$, or $\mu^{max}$ if no substrate is limiting growth and no inhibition takes place. This reasoning forms the basis behind the resource allocation hypothesis used in **Chapter 4**.

The biomass yield on substrate ($Y_{x,s}$) on the other hand can also be optimised to favour a high $\mu$. As outlined in the introduction, biomass formation (anabolism) is coupled to catabolism. Thus, if a higher amount of energy (ATP) can be harvested in catabolism and if anabolism is equally "costly", than with this higher $Y_{ATP,s}$ a higher $Y_{x,s}$ can be realised by this metabolism.

A higher ATP harvested in catabolism can be realised by a longer enzymatic pathway. For example, 2 ATP is harvested using substrate phosphorylation when fermenting glucose to lactate, while 3 ATP is harvested when fermenting glucose to acetate and ethanol. Electrons available at the start of the metabolism are cascaded to a lower energy state, than what would have been possible with a shorter enzymatic pathway. This is illustrated by the case of ethanol and coupled acetate production versus butyrate production (**Chapter 2**), and the case of heterofermentation versus acetate-butyrate-ethanol-$H_2$ production (**Chapter 4**). To produce acetate and ethanol from acetyl-CoA, 4 enzymes are needed, while 6 enzymes and potentially an ATPase and a motive force generating complex are used for butyrate production. Thus it seems that longer catabolic pathways relate to more potential for energy harvesting, but they also burden the proteome available in a cell. The question is than, how do microbiomes "choose" their pathways, and why is that so?

## 3 Can we predict product formation?

Resource allocation based models, such as proposed by Molenaar *et al.* [242] can be extended to microbial communities to attempt to predict the product formation in fermentative ecosystems. This prediction can be realised through simulating the optimisation enzyme levels to obtain the highest $\mu$ (equation 6.1), given a certain set ecological niche (see **Chapter 1**). In numerical terms, a vector $c_{e,i}$ for a number of enzymatic reactions *i* will have to be optimised to obtain the maximum growth rate $\mu$ given a certain environment. Layers of biochemical complexity can be added stepwise, such as futile cycles and more detailed biochemistry for anabolism. Predicting the switch between acetate, butyrate, ethanol, and hydrogen production on the one hand, and lactate and ethanol formation (by heterofermentation [4]) on the other hand under acidic pH conditions (**Chapter 4**) could be realised using a resource allocation based approach (as discussed in the previous section). Such species-independent models can realise the prediction of the metabolic properties dominating given a certain environment *a priori*.

To add to the complexity of constructing a predictive model, equation 6.2 shows that the rate of an enzymatic reaction is dependent on the substrate concentration S. In catabolic reactions, redox reactions can occur which are dependent on conserved moieties, such as NADH, Fd, CoA, ATP etc. If a certain metabolite, such as NADH, is present in a relatively low concentration, the enzymatic rate of this reaction will decrease, affecting the overall substrate uptake and product formation kinetics. In a dynamic environment, such as the SBR environment, intracellular metabolites are assumed to change concentrations, which also affects the enzymatic rates that form the metabolism. Enzymatic reactions form the basis of metabolic fluxes, and thus the regulation of enzymatic reactions through the levels of conserved moieties can help to understand the directing carbon is flowing in mixed culture fermentation. An attempt has been made in the context of this thesis to predict lactate over actete-butyrate-ethanol-$H_2$ formation (**Chapter 4**) using a species-independent model for a continuous glucose limited enrichment culture, which showed that lactic acid production is favourable when little anabolic enzymes are expressed for biosynthetic pathways (data not shown). Future modelling work should aim to evaluate the resource allocation and the metabolite concept to obtain an accurate prediction of product formation in open fermentative ecosystems.

## 4 Biochemistry is driving functionality not taxonomy

The evaluation of the metabolism displayed by enriched microbial communities in this thesis is based on genomic information available for microbial strains, species and genera which is available in public databases and peer-reviewed articles (**Chapter 2, 3 and 4**). Metagenomics offered the possibility to evaluate the potential metabolism of one enrichment culture (**Chapter 5**). There is a scientific opportunity for proteomic verification of assumed metabolic networks, in which meta-proteomics offers the advantage of the measurement of potentially functional proteins, supporting metabolic assumptions. Attempts have been made to measure XylF, XylG and XylH as compared to XylE in the xylose limited CSTR enrichment (**Chapter 5**), but this stranded in attempting to obtain soluble membrane proteins for targeted mass spectrometry experiments (data not shown). Comparing the presence of these two xylose uptake systems can prove the hypothesis that ATP-binding proteins are used for xylose transport under substrate limitation (CSTR), while proton mediated xylose uptake is used under substrate excess (SBR). Other suitable targets for proteome analysis are the verification of the Rnf complex with butyrate production at pH 8.0, and its absence when acetate and ethanol are produced. This measurement can support the concept of alternative ATP harvesting using an electrochemical potential, which likely led to a competitive advantage under growth limitation. The Mgl and PTS system can also be attempted to be measured in the glucose limited CSTR and SBR enrichment at pH 8.0, which can prove the assumption of ATP-binding proteins to be present under substrate limitation and not under substrate excess. The proteins involved in the metabolic network proposed in **Chapter 4** can be verified using a similar approach.

Proteomics is not straightforward. Soluble proteins (intracellular proteins) are easier to use for mass spectrometry than insoluble proteins (membrane proteins). Protein extraction, solubilisation and protein separation prior to injection in the mass spectrometer will have to be evaluated to obtain accurate and reproducible results. A direct stable isotope fingerprint method, as published by Kleiner *et al.* [249], could be used to obtain such metaproteomic data. In their work, the feeding of labelled carbon is combined with metaproteomics to determine active catabolic proteomes in a microbial community. Ultimately, metaproteomics can characterise the metabolic network, whilst also characterising the microbial community structure by comparing the proteome of a sample to proteomes of microbial taxa in databases, thereby analysing a microbiome on the two phylogenetic and functional levels simultaneously (Figure 6.2).

Enzymatic assays can complement proteomic data, to validate the presence and (potential) rate of a certain assumed enzymatic reaction of the studied metabolism. The stoichiometry-based balancing in **Chapter 2**, resulted in the conclusion that the pentose phosphate pathway (PPP) was

active, whilst the phosphoketolase pathway (PKP) was not active. The verification of this conclusion can be achieved using specifically designed enzymatic assays for to target these pathways. An attempt was made in this thesis, which indicated that the PKP was not measurable in a cell free extract of the xylose limited SBR enrichment culture, be it due to analytical or biological reasons (**Chapter 2**, data not shown).

Metabolomics can offer the evaluation of the intracellular and extracellular metabolite concentrations in time, which can help to solve questions on limited enzymatic rates. Intracellular NADH, NAD+, Fd, CoA, ADP and ATP levels could be measured to understand the product formation from a metabolite point of view, as has been attempted for NADH/NAD+ to understand the impact of the hydrogen partial pressure on the product spectrum in mixed culture fermentation [87]. Extracellular metabolomics, as performed in **Chapter 5**, offers the investigation of extracellular composition of mixed or pure cultures. This is useful to generate ecological hypotheses of how microorganisms might be cooperating.
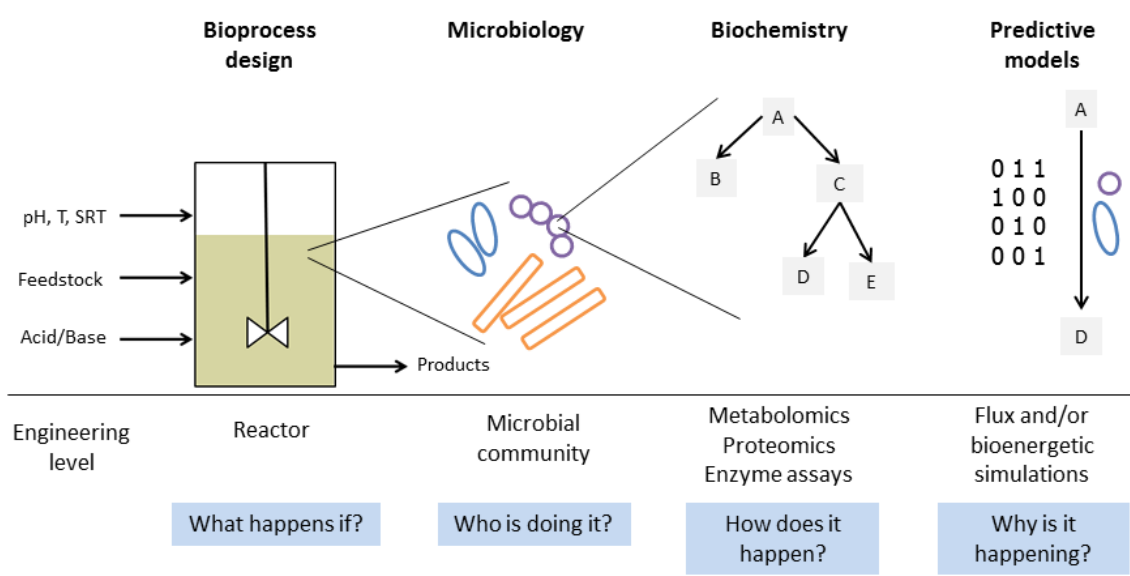


*Figure 6.2*: *Levels of complexity involved in mechanistically understanding mixed culture fermentation. The blue boxes indicate the type of research question that can be typically answered through using a certain approach.*

Depending on the type of research question asked, a certain type of methodology can generate results to support a hypothesis (**Figure 6.2**). Bioprocess design relies on differential experiments, varying environmental conditions and observing the impact of a certain variable. Many of such studies have been published. Meta-studies have also been performed to understand these experiments. Moscoviz *et al*. have analysed four hundred scientific documents to analyse the COD spectrum in different fermentative systems, including the combination with microbial electrolysis and photofermentation [190]. Their effort resulted in the observation that in dark fermentation experiments the hydrogen yield on incoming COD is 47% higher when using agricultural and green residues as feedstock compared to food waste. They also observed that the lactate yield was highest in a batch experiment using food waste (0.63 $g_{COD}$ $g_{COD}^{-1}$). These observations are likely a direct consequence of the ecology offered by these different fermentable feedstocks, as discussed in **Chapter 4**.

Microbial community analysis can show which microbial populations are the dominant fraction of a community. Linking this presence to a certain metabolism is more challenging. Databases such as NCBI and SILVA can be used to correlate microbial populations to functionalities. Recently

different types of software have been developed to perform such analyses, such as tax4fun [250]. Such pattern recognition-based tools can predict functionalities, if the dataset of functionalities is abundant and accurate enough. They cannot, however, explain the mechanism behind the prevalence of a functionality over another competing functionality. Data generated by 16S rRNA gene amplicon sequencing is useful to correlate microbial communities and functionalities, not to explain causal effects. The question of how microbial communities are shaped is not solved by linking microbial community structures to functionalities. The tools used in **Chapter 2, 3 and 4** are useful to perform the ecological experiment of "who is doing what", which is the essence of taxonomy (Figure 6.2).

Biochemistry methods such as proteomics and metabolomics can solve the issue which metabolic pathways are active under certain conditions and can thereby validate metabolic networks. Hassa *et al.* discuss the bundling metagenomics, metatranscriptomics and metabolomics when analysing anaerobic digestion plants [251]. They show that cellulose and hemicellulose decomposing enzymes in these plants are indeed verified by metaproteomics, which shows the power of metaproteomics to verify assumed metabolic networks. Predictive models are useful to understand why a certain functionality dominates over another functionality, given a certain theoretical set of axioms to the model as shown  for the catabolic shift of *Lactococcus lactis* by Molenaar *et al.* [167]. Most likely, a continuous iteration between all these layers of complexity (Figure 6.2) will result in an accurate understanding of how and why fermentative microbiomes behave the way they do.

## 5 Strategies for growth: to cooperate or to compete?

Microbial interactions likely driving microbial diversity, which is the inspiration for the work performed in **Chapter 5**. Hibbing *et al.* outline in their review paper different experimental studies which reveal metabolic interactions [213]. They discuss only one example of interactions occurring in mixed cultures or enrichment cultures, which shows the ample opportunity for scientists to use enrichment cultures as a tool to investigate metabolic interactions (Figure 6.1).

Commensalism in parallel to competition as the mechanisms driving microbial diversity is not very widely noted in literature. A paper from Christensen proposes that these two mechanisms drive the interaction of *Pseudomonas putida* and *Acinetobacter* in synthetic co-culture which was grown on a single carbon source, benzyl alcohol [252]. They use this hypothesis to explain the biofilm formation occurring between the two used strains. If commensalism is more prevalent in fermentative ecosystems than mutualism remains to be settled by future work.

# Appendices

## Appendix I – Medium and trace element solution used throughout this thesis

The medium solution used in this thesis is replicated from the medium solution used by Temudo [6]. The solution used in this thesis has the same elemental composition, while some salts were added in a different water crystal form (*e.g.* $CaCl_2$).

***Table A1:*** *Concentration of compounds in the influent entering the bioreactor setup. The trace element solution was designed to be 1250x concentrated compared to the influent concentration. EDTA was used to keep especially iron in solution.*

| Compound | Influent concentration (g L$^{-1}$) | Concentration trace solution (g L$^{-1}$) |
|---|---|---|
| Carbohydrate | 4.00 | |
| $NH_4Cl$ | 1.34 | |
| $KH2PO_4$ | 0.78 | |
| NaCl | 0.292 | |
| $Na2SO_4*10H_2O$ | 0.130 | |
| $MgCl_2*6H_2O$ | 0.120 | |
| **Trace elements** | | |
| $FeSO_4*7H_2O$ | 0.0031 | 3.875 |
| $CaCl_2$ | 0.0006 | 0.750 |
| $H_3BO_3$ | 0.0001 | 0.125 |
| $Na_2MoO_4*2H_2O$ | 0.0001 | 0.125 |
| $ZnSO_4*7H_2O$ | 0.0032 | 4.000 |
| $CoCl_2*H_2O$ | 0.0006 | 0.750 |
| $CuCl_2*2H_2O$ | 0.0022 | 2.750 |
| $MnCl_2*4H_2O$ | 0.0025 | 3.125 |
| $NiCl_2*6H_2O$ | 0.0005 | 0.625 |
| $Na_3$ EDTA (titriplex III) | 0.05 | 62.50 |

## Appendix II – Relevant fermentative and non-fermentative stoichiometries

Potentially, many different metabolisms can occur when enriching for fermentative metabolisms. A kinetic, thermodynamic and bioenergetics evaluation of relevant metabolisms was performed as introduced in **Chapter 1** (Table 1.2), which was used as a tool to determine the effectiveness of "washing out" non-desired metabolisms (such as sulphate reduction or methanogenesis). The stoichiometries presented in Table A2 form the basis of the thermodynamic evaluation.

*Table A2:* *The following catabolic stoichiometries are used to evaluate the Gibbs energy change of a catabolism presented in Table 1.2 in the introduction (**Chapter 1**)*

| Substrate(s) | Product(s) | Catabolic stoichiometry |
|---|---|---|
| Glucose | Ethanol, $CO_2$ | $-1\ C_6H_{12}O_6 +2\ C_2H_6O +2\ CO_2$ |
| | Lactic acid | $-1\ C_6H_{12}O_6 +2\ C_3H_6O_3$ |
| | Butyrate, $CO_2$, $H_2$ | $-1\ C_6H_{12}O_6 +1\ C_4H_7O_2^{1-} +2\ CO_2 +2\ H_2$ |
| | Propionate, acetate | $-1\ C_6H_{12}O_6 +1\ C_3H_5O_2^{1-} +1\ C_2H_3O_2^{1-} +1\ CO_2 +1\ H_2 +2\ H^{1+}$ |
| | Ethanol, acetate | $-1\ C_6H_{12}O_6 -1\ H_2O +1\ C_2H_6O_1 +1\ C_2H_3O_2^{1-} +2\ CO_2 +2\ H_2 +1\ H^{1+}$ |
| Lactate | Propionate, acetate, $CO_2$ | $-1\ C_3H_5O_3^{1-} +0.33\ C_2H_3O_2^{1-} +0.67\ C_3H_5O_2^{1-} +0.33\ CO_2 +0.33\ H_2O$ |
| Lactate, acetate | Butyrate, hydrogen, $CO_2$ | $-1\ C_3H_5O_3^{1-} -0.5\ C_2H_3O_2^{1-} +0.75\ C_4H_7O_2^{1-} +1CO_2 +0.5\ H_2 +1\ H_2O -0.75\ H^+$ |
| Ethanol | Propionate, acetate, $CO_2$ | $-1\ C_2H_6O -0.67\ CO_2 +0.67\ C_3H_5O_2^{1-} +0.33\ C_2H_3O_2^{1-} +0.33\ H_2O +1\ H^+$ |
| Lactate, $SO_4^{2-}$ | Acetate, $CO_2$, $H_2S$ | $-1\ C_3H_5O_3^{1-} -0.5\ SO_4^{2-} -1\ H^{1+} +1\ C_2H_3O_2^{1-} +0.5\ H_2S +1\ CO_2 +1\ H_2O$ |
| $H_2$, $CO_2$ | Acetate | $-5\ H_2 -2\ CO_2 +1\ C_2H_3O_2^{1-} +2\ H_2O +1\ H^+$ |
| | Methane | $-4\ H_2 -1\ CO_2 +1\ CH_4 +2\ H_2O$ |
| Ethanol, acetate | Butyrate, $H_2$ | $-1\ C_2H_6O -0.67\ C_3H_5O_3^{1-} -0.67\ H^{1+} +0.67\ H_2O +0.75\ H_2 +1\ C_4H_7O_2^{1-}$ |

# References

1. Kanehisa M, Goto S. KEGG: Kyoto Encyclopedia of Genes and Genomes. *Nucleic Acids Res* 2000; **28**: 27–30.

2. Stewart EJ. Growing unculturable bacteria. *J Bacteriol* 2012; **194**: 4151–4160.

3. Bakalar N. Earth May Be Home to a Trillion Species of Microbes. *New York Times* . 2016.

4. Madigan MT, Martinko JM. Brock Biology Of Microorganisms 11th edition. 2006. Pearson Prentice Hall.

5. Gujer W, Zehnder AJB. Conversion Processes in Anaerobic Digestion. *Water Sci Technol* 1983; **15**: 127–167.

6. Temudo M. Directing Product Formation by Mixed Culture Fermentation. 2008.

7. Großkopf T, Soyer OS. Synthetic microbial communities. *Curr Opin Microbiol* 2014; **18**: 72–77.

8. Morris BEL, Henneberger R, Huber H, Moissl-Eichinger C. Microbial syntrophy: Interaction for the common good. *FEMS Microbiol Rev* 2013; **37**: 384–406.

9. Pirt SJ. The maintenance energy of bacteria in growing cultures. *Proc R Soc London Ser B Biol Sci* 1965; **163**: 224 LP – 231.

10. Lavefve L, Marasini D, Carbonero F. Chapter Three - Microbial Ecology of Fermented Vegetables and Non-Alcoholic Drinks and Current Knowledge on Their Impact on Human Health. In: Toldrá FBT-A in F and NR (ed).2019. Academic Press, pp 147–185.

11. Menz G, Aldred P, Vrieskoop F. Growth and Survival of Foodborne Pathogens in Beer. *J Food Prot* 2011; **74**: 1670–1675.

12. Castro H, Ogram A, Reddy KR. Phylogenetic Characterization of Methanogenic Assemblages in Eutrophic and Oligotrophic Areas of the Florida Everglades. *Appl Environ Microbiol* 2004; **70**: 6559 LP – 6568.

13. Sweeney TE, Morton JM. The human gut microbiome: a review of the effect of obesity and surgically induced weight loss. *JAMA Surg* 2013; **148**: 563–569.

14. Nelson MC, Morrison M, Yu Z. A meta-analysis of the microbial diversity observed in anaerobic digesters. *Bioresour Technol* 2011; **102**: 3730–3739.

15. Sundberg C, Al-Soud WA, Larsson M, Alm E, Yekta SS, Svensson BH, et al. 454 pyrosequencing analyses of bacterial and archaeal richness in 21 full-scale biogas digesters. *FEMS Microbiol Ecol* 2013; **85**: 612–626.

16. Ren Z, Ward TE, Logan BE, Regan JM. Characterization of the cellulolytic and hydrogen-producing activities of six mesophilic Clostridium species. *J Appl Microbiol* 2007; **103**: 2258–2266.

17. Burrell PC, O'Sullivan C, Song H, Clarke WP, Blackall LL. Identification, Detection, and Spatial Resolution of Clostridium Populations Responsible for Cellulose Degradation in a Methanogenic Landfill Leachate Bioreactor. *Appl Environ Microbiol* 2004; **70**: 2414–2419.

18. Castelle CJ, Banfield JF. Major New Microbial Groups Expand Diversity and Alter our Understanding of the Tree of Life. *Cell* 2018; **172**: 1181–1197.

19. Monier V, Mudgal S, Escalon V, O'Connor C, Gibon T, Anderson G, et al. Preparatory Study on Food Waste Across EU 27. *BIO Intelligence Service* . 2010.

20. Goldberg RN, Tewari YB. Thermodynamic and Transport Properties of Carbohydrates and their Monophosphates: The Pentoses and Hexoses. *J Phys Chem Ref Data* 1989; **18**: 809–880.

21. Körner C. Carbon limitation in trees. *J Ecol* 2003; **91**: 4–17.

22. Kleerebezem R, Van Loosdrecht MCM. A Generalized Method for Thermodynamic State Analysis of Environmental Systems. *Crit Rev Environ Sci Technol* 2010; **40**: 1–54.

23. Atkinson D. Cellular Energy Metabolism and its Regulation. 1977. Academic Press, Waltham.

24. Buckel W, Thauer RK. Energy conservation via electron bifurcating ferredoxin reduction and proton/Na+ translocating ferredoxin oxidation. *Biochim Biophys Acta - Bioenerg* 2013; **1827**: 94–113.

25. Herrmann G, Jayamani E, Mai G, Buckel W. Energy Conservation via Electron-Transferring Flavoprotein in Anaerobic Bacteria. *J Bacteriol* 2008; **190**: 784–791.

26. Hermans M a, Neuss B, Sahm H. Content and composition of hopanoids in Zymomonas mobilis under various growth conditions. *J Bacteriol* 1991; **173**: 5592–5.

27. Jensen PR, Hammer K. Minimal Requirements for Exponential-Growth of Lactococcus lactis. *Appl Environ Microbiol* 1993; **59**: 4363–4366.

28. Liu X, Yang S-T. Kinetics of butyric acid fermentation of glucose and xylose by Clostridium tyrobutyricum wild type and mutant. *Process Biochem* 2006; **41**: 801–808.

29. Cove JH, Holland KT, Cunliffe WJ. Effects of oxygen concentration on biomass production, maximum specific growth rate and extracellular enzyme production by three species of cutaneous propionibacteria grown in continuous culture. *J Gen Microbiol* 1983; **129**: 3327–3334.

30. Mangayil R, Santala V, Karp M. Fermentative hydrogen production from different sugars by Citrobacter sp. CMC-1 in batch culture. *Int J Hydrogen Energy* 2011; **36**: 15187–15194.

31. Seeliger S, Janssen PH, Schink B. Energetics and kinetics of lactate fermentation to acetate and propionate via methylmalonyl-CoA or acrylyl-CoA. *FEMS Microbiol Lett* 2002; **211**: 65–70.

32. Muñoz-Tamayo R, Laroche B, Walter É, Doré J, Duncan SH, Flint HJ, et al. Kinetic modelling of lactate utilization and butyrate production by key human colonic bacterial species. *FEMS Microbiol Ecol* 2011; **76**: 615–624.

33. Reis M a, Almeida JS, Lemos PC, Carrondo MJ. Effect of hydrogen sulfide on growth of sulfate reducing bacteria. *Biotechnol Bioeng* 1992; **40**: 593–600.

34. Koster IW, Koomen E. Ammonia inhibition of the maximum growth rate (??m) of hydrogenotrophic methanogens at various pH-levels and temperatures. *Appl Microbiol Biotechnol* 1988; **28**: 500–505.

35. Straub M, Demler M, Weuster-Botz D, Dürre P. Selective enhancement of autotrophic acetate production with genetically modified Acetobacterium woodii. *J Biotechnol* 2014; **178**: 67–72.

36. Weimer PJ, Stevenson DM. Isolation, characterization, and quantification of Clostridium kluyveri from the bovine rumen. *Appl Microbiol Biotechnol* 2012; **94**: 461–466.

37. Thauer RK, Jungermann K, Henniger H, Wenning J, Decker K. The Energy Metabolism of Clostridium kluyveri. *Eur J Biochem* 1968; **4**: 173–180.

38. Wang S, Huang H, Moll J, Thauer RK. NADP+ reduction with reduced ferredoxin and NADP+ reduction with NADH are coupled via an electron-bifurcating enzyme complex in Clostridium kluyveri. *J Bacteriol* 2010; **192**: 5115–5123.

39. Holtzapple MT, Granda CB. Carboxylate platform: The MixAlco process part 1: Comparison of three biomass conversion platforms. *Appl Biochem Biotechnol* 2009; **156**: 95–106.

40. Mishra P, Krishnan S, Rana S, Singh L, Sakinah M, Ab Wahid Z. Outlook of fermentative hydrogen production techniques: An overview of dark, photo and integrated dark-photo fermentative approach to biomass. *Energy Strateg Rev* 2019; **24**: 27–37.

41. Kim DH, Lim WT, Lee MK, Kim MS. Effect of temperature on continuous fermentative lactic acid (LA) production and bacterial community, and development of LA-producing UASB reactor. *Bioresour Technol* 2012; **119**: 355–361.

42. Spirito CM, Richter H, Stams AJ, Angenent LT. Chain elongation in anaerobic reactor microbiomes to recover resources from waste. *Curr Opin Biotechnol* 2014; **27**: 115–122.

43. Achinas S, Achinas V, Euverink GJW. A Technological Overview of Biogas Production from Biowaste. *Engineering* 2017; **3**: 299–307.

44. Fuchs W, Wang X, Gabauer W, Ortner M, Li Z. Tackling ammonia inhibition for efficient biogas production from chicken manure: Status and technical trends in Europe and China. *Renew Sustain Energy Rev* 2018; **97**: 186–199.

45. Weiland P. Biogas production: Current state and perspectives. *Appl Microbiol Biotechnol* 2010; **85**: 849–860.

46. Zafeiris T. Feasibility study Substituting natural gas with biogas in industries. 2013. Arnhem.

47. Andrews E. Why Hydrogen Could Improve the Value of Renewable Energy. *Grad Sch Stanford Bus* . 2019. Stanford.

48. Global Market Study on Hydrogen: Robust Growth in the Adoption of Hydrogen Across Various Applications to be Observed in North America in the Coming Years. 2018. New York City.

49. Ghimire A, Frunzo L, Pirozzi F, Trably E, Escudie R, Lens PNL, et al. A review on dark fermentative biohydrogen production from organic biomass: Process parameters and use of by-products. *Appl Energy* 2015; **144**: 73–95.

50. Levin DB, Pitt L, Love M. Biohydrogen production: Prospects and limitations to practical application. *Int J Hydrogen Energy* 2004; **29**: 173–185.

51. Temudo MF, Kleerebezem R, van Loosdrecht M. Influence of the pH on (open) mixed culture fermentation of glucose: a chemostat study. *Biotechnol Bioeng* 2007; **98**: 69–79.

52. Sauer M, Russmayer H, Grabherr R, Peterbauer CK, Marx H. The Efficient Clade: Lactic Acid Bacteria for Industrial Chemical Production. *Trends Biotechnol* 2017; **35**: 756–769.

53. Tokiwa Y, Calabia BP, Ugwu CU, Aiba S. Biodegradability of plastics. *Int J Mol Sci* 2009; **10**: 3722–3742.

54. Lactic Acid Market Size, Share & Trends Analysis Report By Raw Material (Sugarcane, Corn, Cassava), By Application (Industrial, F&B, Pharmaceuticals, Personal Care, PLA), And Segment Forecasts, 2018 - 2025. 2018.

55. Powered with renewed energy. 2018. Washington D.C.

56. Darwin, Cord-Ruwisch R, Charles W. Ethanol and lactic acid production from sugar and starch wastes by anaerobic acidification. *Eng Life Sci* 2018; **18**: 635–642.

57. Della-Bianca BE, Basso TO, Stambuk BU, Basso LC, Gombert AK. What do we know about the yeast strains from the Brazilian fuel ethanol industry? *Appl Microbiol Biotechnol* 2013; **97**: 979–991.

58. Zhu X, Tao Y, Liang C, Li X, Wei N, Zhang W, et al. The synthesis of n-caproate from lactate: A new efficient process for medium-chain carboxylates production. *Sci Rep* 2015; **5**: 1–9.

59. Grootscholten TIM, Steinbusch KJJ, Hamelers HVM, Buisman CJN. Chain elongation of acetate and ethanol in an upflow anaerobic filter for high rate MCFA production. *Bioresour Technol* 2013; **135**: 440–445.

60. Van Zoelen B. Fabriek in haven produceert alternatief voor antibiotica. *Het Parool* . 2017. Amsterdam.

61. Marang L. Scale-Up Aspects of PHA Production by Microbial Enrichment Cultures. 2017. Delft University of Technology.

62. Global Polyhydroxyalkanoate (PHA) Market Analysis & Trends - Industry Forecast to 2025. 2017.

63. Tokiwa Y, Calabia BP, Ugwu CU, Aiba S. Biodegradability of plastics. *Int J Mol Sci* 2009; **10**: 3722–3742.

64. Tamis J. Resource recovery from organic waste streams by microbial enrichment cultures. 2015. Delft University of Technology.

65. Johnson K, Jiang Y, Kleerebezem R, Muyzer G, Loosdrecht MCM Van. Enrichment of a Mixed Bacterial Culture with a High Polyhydroxyalkanoate Storage Capacity. *Biomacromolecules* 2009; **10**: 670–676.

66. Marang L, Jiang Y, van Loosdrecht MCM, Kleerebezem R. Butyrate as preferred substrate for polyhydroxybutyrate production. *Bioresour Technol* 2013; **142**: 232–239.

67. Jiang Y, Hebly M, Kleerebezem R, Muyzer G, van Loosdrecht MCM. Metabolic modeling of mixed substrate uptake for polyhydroxyalkanoate (PHA) production. *Water Res* 2011; **45**: 1309–1321.

68. Jiang Y, Marang L, Kleerebezem R, Muyzer G, van Loosdrecht MCM. Polyhydroxybutyrate production from lactate using a mixed microbial culture. *Biotechnol Bioeng* 2011; **108**: 2022–2035.

69. Yamane T, Chen X-F, Ueda S. Polyhydroxyalkanoate synthesis from alcohols during the growth of Paracoccus denitrificans. *FEMS Microbiol Lett* 1996; **135**: 207–211.

70. Tamis J, Lužkov K, Jiang Y, Loosdrecht MCM van, Kleerebezem R. Enrichment of Plasticicumulans acidivorans at pilot-scale for PHA production on industrial wastewater. *J*

*Biotechnol* 2014; **192**: 161–169.

71.  Deutscher J. The mechanisms of carbon catabolite repression in bacteria. *Curr Opin Microbiol* 2008.

72.  Ghisellini P, Cialani C, Ulgiati S. A review on circular economy: the expected transition to a balanced interplay of environmental and economic systems. *J Clean Prod* 2016; **114**: 11–32.

73.  Kleerebezem R, van Loosdrecht MC. Mixed culture biotechnology for bioenergy production. *Curr Opin Biotechnol* 2007; **18**: 207–212.

74.  Lin Y, de Kreuk M, van Loosdrecht MCM, Adin A. Characterization of alginate-like exopolysaccharides isolated from aerobic granular sludge in pilot-plant. *Water Res* 2010; **44**: 3355–64.

75.  Marshall CW, LaBelle E V, May HD. Production of fuels and chemicals from waste by microbiomes. *Curr Opin Biotechnol* 2013; **24**: 391–397.

76.  Rodriguez J, Kleerebezem R, Lema JM, Van Loosdrecht MCM. Modeling product formation in anaerobic mixed culture fermentations. *Biotechnol Bioeng* 2006; **93**: 592–606.

77.  González-Cabaleiro R, Lema JM, Rodríguez J. Metabolic Energy-Based Modelling Explains Product Yielding in Anaerobic Mixed Culture Fermentations. *PLoS One* 2015; **10**: 1–17.

78.  Anwar Z, Gulfraz M, Irshad M. Agro-industrial lignocellulosic biomass a key to unlock the future bio-energy: A brief review. *J Radiat Res Appl Sci* 2014; **7**: 163–173.

79.  Li F, Hinderberger J, Seedorf H, Zhang J, Buckel W, Thauer RK. Coupled Ferredoxin and Crotonyl Coenzyme A (CoA) Reduction with NADH Catalyzed by the Butyryl-CoA Dehydrogenase/Etf Complex from Clostridium kluyveri . *J Bacteriol* 2008; **190**: 843–850.

80.  Regueira A, González-Cabaleiro R, Ofiţeru ID, Rodríguez J, Lema JM. Electron bifurcation mechanism and homoacetogenesis explain products yields in mixed culture anaerobic fermentations. *Water Res* 2018; 5–13.

81.  Beijerinck M. Anhaufungsversuche mit Ureumbakterien. *Cent f Bakteriol* 1901; **7**: 33–61.

82.  Fang HHP, Liu H. Effect of pH on hydrogen production from glucose by a mixed culture. *Bioresour Technol* 2002; **82**: 87–93.

83.  Zoetemeyer RJ, Arnoldy P, Cohen A, Boelhouwer C. Influence of temperature on the anaerobic acidification of glucose in a mixed culture forming part of a two-stage digestion process. *Water Res* 1982; **16**: 313–321.

84.  Chunfeng C, Yoshitaka E, Yuhei I, Hainan K. Effect of hydraulic retention time on the hydrogen yield and population of Clostridium in hydrogen fermentation of glucose. *J Environ Sci* 2009; **21**: 424–428.

85.  Ren NQ, Chua H, Chan SY, Tsang YF, Wang YJ, Sin N. Assessing optimal fermentation type for bio-hydrogen production in continuous-flow acidogenic reactors. *Bioresour Technol* 2007; **98**: 1774–1780.

86.  Rafrafi Y, Trably E, Hamelin J, Latrille E, Meynial-Salles I, Benomar S, et al. Sub-dominant bacteria as keystone species in microbial communities producing bio-hydrogen. *Int J Hydrogen Energy* 2013; **38**: 4975–4985.

87.  de Kok S, Meijer J, van Loosdrecht MCM, Kleerebezem R. Impact of dissolved hydrogen

partial pressure on mixed culture fermentations. *Appl Microbiol Biotechnol* 2013; **97**: 2617–2625.

88. Temudo MF, Mato T, Kleerebezem R, Van Loosdrecht MCM. Xylose anaerobic conversion by open-mixed cultures. *Appl Microbiol Biotechnol* 2009; **82**: 231–239.

89. Kuenen JG. Continuous Cultures (Chemostats). *Reference Module in Biomedical Research* . 2014. Elsevier Inc.

90. Monod J. The Growth of Bacterial Cultures. *Annu Rev Microbiol* 1949.

91. Prakash O, Shouche Y, Jangid K, Kostka JE. Microbial cultivation and the role of microbial resource centers in the omics era. *Appl Microbiol Biotechnol* 2013; **97**: 51–62.

92. Flamholz A, Noor E, Bar-Even A, Liebermeister W, Milo R. Glycolytic strategy as a tradeoff between energy yield and protein cost. *Proc Natl Acad Sci U S A* 2013; **110**: 10039–44.

93. De Vries W, Kapteijn WMC, Van Der Beek EG, Stouthamer AH. Molar Growth Yields and Fermentation Balances of Lactobacillus casei L3 in Batch Cultures and in Continuous Cultures. *Microbiology* 1970; **63**: 333–345.

94. APHA. Standard Methods for the Examination of Water and Wastewater, 20th ed. 1998. American Public Health Association, Washington D.C.

95. Jia H-R, Geng L-L, Li Y-H, Wang Q, Diao Q-Y, Zhou T, et al. The effects of Bt Cry1Ie toxin on bacterial diversity in the midgut of Apis mellifera ligustica (Hymenoptera: Apidae). *Sci Rep* 2016; **6**: 24664.

96. Caporaso JG, Kuczynski J, Stombaugh J, Bittinger K, Bushman FD, Costello EK, et al. QIIME allows analysis of high-throughput community sequencing data. *Nat Methods* 2010; **7**: 335.

97. Wang Q, Garrity GM, Tiedje JM, Cole JR. Naive Bayesian classifier for rapid assignment of rRNA sequences into the new bacterial taxonomy. *Appl Environ Microbiol* 2007; **73**: 5261–7.

98. DeSantis TZ, Hugenholtz P, Larsen N, Rojas M, Brodie EL, Keller K, et al. Greengenes, a Chimera-Checked 16S rRNA Gene Database and Workbench Compatible with ARB. *Appl Environ Microbiol* 2006; **72**: 5069–5072.

99. Johnson M, Zaretskaya I, Raytselis Y, Merezhuk Y, McGinnis S, Madden TL. NCBI BLAST: a better web interface. *Nucleic Acids Res* 2008; **36**: W5–W9.

100. Janda JM, Abbott SL. 16S rRNA Gene Sequencing for Bacterial Identification in the Diagnostic Laboratory: Pluses, Perils, and Pitfalls. *J Clin Microbiol* 2007; **45**: 2761–2764.

101. van der Heijden RTJM, Heijnen JJ, Hellinga C, Romein B, Luyben KCAM. Linear constraint relations in biochemical reaction systems: I. Classification of the calculability and the balanceability of conversion rates. *Biotechnol Bioeng* 1994; **43**: 3–10.

102. Zoetemeyer RJ, van den Heuvel JC, Cohen A. pH influence on Acidogenic Dissimilation of Glucose in an Anaerobic Digestor. *Water Res* 1982; **16**: 303–311.

103. Liu L, Zhang L, Tang W, Gu Y, Hua Q, Yang S, et al. Phosphoketolase Pathway for Xylose Catabolism in Clostridium acetobutylicum Revealed by 13C Metabolic Flux Analysis. *J Bacteriol* 2012; **194**: 5413–5422.

104. Heijnen JJ, van Loosdrecht MCM, Tijhuis L. A black box mathematical model to calculate

auto- and heterotrophic biomass yields based on Gibbs energy dissipation. *Biotechnol Bioeng* 1992; **40**: 1139–1154.

105. Davis EO, Henderson PJ. The cloning and DNA sequence of the gene xylE for xylose-proton symport in Escherichia coli K12. *J Biol Chem* 1987; **262**: 13928–13932.

106. Sumiya M, O Davis E, C Packman L, P McDonald T, Henderson P. Molecular genetics of a receptor protein for D-xylose, encoded by the gene xylF in Escherichia coli. *Receptors Channels* 1995; **3**: 117–128.

107. Hasona A, Kim Y, Healy FG, Ingram LO, Shanmugam KT. Pyruvate Formate Lyase and Acetate Kinase Are Essential for Anaerobic Growth of Escherichia coli on Xylose. *J Bacteriol* 2004; **186**: 7593–7600.

108. Steinsiek S, Bettenbrock K. Glucose Transport in Escherichia coli Mutant Strains with Defects in Sugar Transport Systems. *J Bacteriol* 2012; **194**: 5897–5908.

109. Babu R, M.P. N, Vignesh M, R. MM. Proteome analysis to assess physiological changes in Escherichia coli grown under glucose-limited fed-batch conditions. *Biotechnol Bioeng* 2005; **92**: 384–392.

110. Gonzalez JE, Long CP, Antoniewicz MR. Comprehensive analysis of glucose and xylose metabolism in Escherichia coli under aerobic and anaerobic conditions by 13C metabolic flux analysis. *Metab Eng* 2017; **39**: 9–18.

111. Rafrafi Y, Trably E, Hamelin J, Latrille E, Meynial-Salles I, Benomar S, et al. Sub-dominant bacteria as keystone species in microbial communities producing bio-hydrogen. *Int J Hydrogen Energy* 2013; **38**: 4975–4985.

112. Andrews JH, Harris RF. r- and K-Selection and Microbial Ecology. In: Marshall KC (ed). *Advances in Microbial Ecology*. 1986. Springer US, Boston, MA, pp 99–147.

113. Yamane T, Hopfield JJ, Yue V, Coutts S. Experimental evidence for kinetic proofreading in the aminoacylation of tRNA by synthetase. *Proc Natl Acad Sci* 1977; **74**: 2246–2250.

114. Hespell RB, Bryant MP. Efficiency of Rumen Microbial Growth: Influence of some Theoretical and Experimental Factors on YATP. *J Anim Sci* 1979; **49**: 1640–1659.

115. De Vrije T, Claassen PAM. Dark hydrogen fermentations. *Bio-methane & Bio-hydrogen* 2003; 103–123.

116. Brooks JP, Edwards DJ, Harwich MD, Rivera MC, Fettweis JM, Serrano MG, et al. The truth about metagenomics: Quantifying and counteracting bias in 16S rRNA studies Ecological and evolutionary microbiology. *BMC Microbiol* 2015; **15**: 1–14.

117. Amann RI, Ludwig W, Schleifer KH. Phylogenetic identification and in situ detection of individual microbial cells without cultivation. *Microbiol Rev* 1995; **59**: 143–169.

118. Magnúsdóttir S, Ravcheev D, de Crécy-Lagard V, Thiele I. Systematic genome assessment of B-vitamin biosynthesis suggests co-operation among gut microbes. *Front Genet* . 2015. , **6**: 148

119. Mäkinen AE, Nissilä ME, Puhakka JA. Dark fermentative hydrogen production from xylose by a hot spring enrichment culture. *Int J Hydrogen Energy* 2012; **37**: 12234–12240.

120. Karadag D, Puhakka JA. Effect of changing temperature on anaerobic hydrogen production and microbial community composition in an open-mixed culture bioreactor.

*Int J Hydrogen Energy* 2010; **35**: 10954–10959.

121. Temudo MF, Muyzer G, Kleerebezem R, Van Loosdrecht MCM. Diversity of microbial communities in open mixed culture fermentations: Impact of the pH and carbon source. *Appl Microbiol Biotechnol* 2008; **80**: 1121–1130.

122. Muyzer G, de Waal EC, Uitterlinden AG. Profiling of complex microbial populations by denaturing gradient gel electrophoresis analysis of polymerase chain reaction-amplified genes coding for 16S rRNA. *Appl Environ Microbiol* 1993; **59**: 695–700.

123. Caporaso JG, Lauber CL, Walters WA, Berg-Lyons D, Lozupone CA, Turnbaugh PJ, et al. Global patterns of 16S rRNA diversity at a depth of millions of sequences per sample. *Proc Natl Acad Sci U S A* 2011; **108 Suppl**: 4516–22.

124. Weisburg WG, Barns SM, Pelletier DA, Lane DJ. 16S ribosomal DNA amplification for phylogenetic study. *J Bacteriol* 1991; **173**: 697–703.

125. Invitrogen. TOPO TA Cloning Kit for Sequencing. 2014. Carlsbad.

126. Amann RI, Binder BJ, Olson RJ, Chisholm SW, Devereux R, Stahl DA. Combination of 16S rRNA-targeted oligonucleotide probes with flow cytometry for analyzing mixed microbial populations. *Appl Environ Microbiol* 1990; **56**: 1919–1925.

127. Friedrich U, Van Langenhove H, Altendorf K, Lipski A. Microbial community and physicochemical analysis of an industrial waste gas biofilter and design of 16S rRNA-targeting oligonucleotide probes. *Environ Microbiol* 2003; **5**: 183–201.

128. Franks AH, Harmsen HJM, Raangs GC, Jansen GJ, Schut F, Welling GW. Variations of bacterial populations in human feces measured by fluorescent in situ hybridization with group-specific 16S rRNA-targeted oligonucleotide probes. *Appl Environ Microbiol* 1998; **64**: 3336–3345.

129. Kong Y, He M, McAlister T, Seviour R, Forster R. Quantitative Fluorescence In Situ Hybridization of Microbial Communities in the Rumens of Cattle Fed Different Diets. *Appl Environ Microbiol* 2010; **76**: 6933–6938.

130. Dionisi D, Anderson J a., Aulenta F, McCue A, Paton G. The potential of microbial processes for lignocellulosic biomass conversion to ethanol: a review. *J Chem Technol Biotechnol* 2015; **90**: 366–383.

131. Kleerebezem R, Joosse B, Rozendal R, Van Loosdrecht MCM. Anaerobic digestion without biogas? *Rev Environ Sci Biotechnol* 2015; **14**: 787–801.

132. Guo XM, Trably E, Latrille E, Carrère H, Steyer J-P. Hydrogen production from agricultural waste by dark fermentation: A review. *Int J Hydrogen Energy* 2010; **35**: 10660–10673.

133. Kleerebezem R, van Loosdrecht MC. Mixed culture biotechnology for bioenergy production. *Curr Opin Biotechnol* 2007; **18**: 207–212.

134. Steinbusch KJJ, Hamelers HVM, Plugge CM, Buisman CJN. Biological formation of caproate and caprylate from acetate: Fuel and chemical production from low grade biomass. *Energy Environ Sci* 2011; **4**: 216–224.

135. Noike T, Endo G, Chang J-E, Yaguchi J-I, Matsumoto J-I. Characteristics of carbohydrate degradation and the rate-limiting step in anaerobic digestion. *Biotechnol Bioeng* 1985; **27**: 1482–1489.

136. Postma E, Kuiper A, Tomasouw WF, Scheffers WA, Van Dijken JP. Competition for glucose between the yeasts Saccharomyces cerevisiae and Candida utilis. *Appl Environ Microbiol* 1989; **55**: 3214–3220.

137. Rombouts JL, Mos G, Weissbrodt DG, Kleerebezem R, van Loosdrecht MCM. Diversity and metabolism of xylose and glucose fermenting microbial communities in sequencing batch or continuous culturing. *FEMS Microbiol Ecol* 2019; **95**.

138. Bell WH. Bacterial utilization of algal extracellular products. 1. The kinetic approach. *Limnol Oceanogr* 1980; **25**: 1007–1020.

139. Lendenmann U, Egli T. Kinetic models for the growth of Escherichia coli with mixtures of sugars under carbon-limited conditions. *Biotechnol Bioeng* 1998; **59**: 99–107.

140. Kuenen JG. Continuous Cultures (Chemostats)☆. *Reference Module in Biomedical Sciences* . 2015. Elsevier Inc.

141. Gottschal JC, de Vries S, Kuenen JG. Competition between the facultatively chemolithotrophic Thiobacillus A2, an obligately chemolithotrophic Thiobacillus and a heterotrophic spirillum for inorganic and organic substrates. *Arch Microbiol* 1979; **121**: 241–249.

142. Deutscher J. The mechanisms of carbon catabolite repression in bacteria. *Curr Opin Microbiol* 2008; **11**: 87–93.

143. Görke B, Stülke J. Carbon catabolite repression in bacteria: many ways to make the most out of nutrients. *Nat Rev Microbiol* 2008; **6**: 613.

144. Meyer H-P, Minas W, Schmidhalter D. Industrial-scale fermentation. *Ind Biotechnol Prod Process* 2017; 1–53.

145. Kim JH, Block DE, Mills DA. Simultaneous consumption of pentose and hexose sugars: An optimal microbial phenotype for efficient fermentation of lignocellulosic biomass. *Appl Microbiol Biotechnol* 2010; **88**: 1077–1085.

146. Kim SM, Choi BY, Ryu YS, Jung SH, Park JM, Kim G-H, et al. Simultaneous utilization of glucose and xylose via novel mechanisms in engineered Escherichia coli. *Metab Eng* 2015; **30**: 141–8.

147. Verhoeven MD, de Valk SC, Daran J-MG, van Maris AJA, Pronk JT. Fermentation of glucose-xylose-arabinose mixtures by a synthetic consortium of single-sugar-fermenting Saccharomyces cerevisiae strains. *FEMS Yeast Res* 2018; **18**: 1–12.

148. Roels JA. Energetics and kinetics in biotechnology. 1983. Elsevier B.V., Amsterdam.

149. Domaizon I, Rimet F, Jacquet S, Trobajo R, Tapolczai K, Corniquel M, et al. Avoiding quantification bias in metabarcoding: Application of a cell biovolume correction factor in diatom molecular biomonitoring. *Methods Ecol Evol* 2017; **9**: 1060–1069.

150. Saccà A. A simple yet accurate method for the estimation of the biovolume of planktonic microorganisms. *PLoS One* 2016; **11**: 1–17.

151. Rubio-Rincón FJ, Welles L, Lopez-Vazquez CM, Abbas B, van Loosdrecht MCM, Brdjanovic D. Effect of Lactate on the Microbial Community and Process Performance of an EBPR System. *Front Microbiol* 2019; **10**: 1–11.

152. Jahreis K, Pimentel-Schmitt EF, Brückner R, Titgemeyer F. Ins and outs of glucose

transport systems in eubacteria. *FEMS Microbiol Rev* 2008; **32**: 891–907.

153. Farmer JJ, Davis BR, Hickman-Brenner FW, McWhorter A, Huntley-Carter GP, Asbury MA, et al. Biochemical identification of new species and biogroups of Enterobacteriaceae isolated from clinical specimens. *J Clin Microbiol* 1985; **21**: 46–76.

154. Gonzalez JE, Long CP, Antoniewicz MR. Comprehensive analysis of glucose and xylose metabolism in Escherichia coli under aerobic and anaerobic conditions by13C metabolic flux analysis. *Metab Eng* 2017; **39**: 9–18.

155. Luo Y, Zhang T, Wu H. The transport and mediation mechanisms of the common sugars in Escherichia coli. *Biotechnol Adv* 2014; **32**: 905–919.

156. Hniman A, O-Thong S, Prasertsan P. Developing a thermophilic hydrogen-producing microbial consortia from geothermal spring for efficient utilization of xylose and glucose mixed substrates and oil palm trunk hydrolysate. *Int J Hydrogen Energy* 2011; **36**: 8785–8793.

157. Axelsson L, Ahrné S. Lactic acid bacteria. *Applied microbial systematics*. 2000. Springer, pp 367–388.

158. Leroy F, De Vuyst L. Lactic acid bacteria as functional starter cultures for the food fermentation industry. *Trends Food Sci Technol* 2004; **15**: 67–78.

159. Solís G, de los Reyes-Gavilan CG, Fernández N, Margolles A, Gueimonde M. Establishment and development of lactic acid bacteria and bifidobacteria microbiota in breast-milk and the infant gut. *Anaerobe* 2010; **16**: 307–310.

160. Straathof AJJ. Transformation of Biomass into Commodity Chemicals Using Enzymes or Cells. *Chem Rev* 2014; **114**: 1871–1908.

161. Lactic Acid Market Analysis By Application (Industrial, F&B, Pharmaceuticals, Personal Care) & Polylactic Acid (PLA) Market Analysis By Application (Packaging, Agriculture, Transport, Electronics, Textiles), And Segment Forecasts, 2018-2025. 2017.

162. Roger P, Delettre J, Bouix M, Béal C. Characterization of Streptococcus salivarius growth and maintenance in artificial saliva. *J Appl Microbiol* 2011; **111**: 631–641.

163. Kim Y, Ingram LO, Shanmugam KT. Construction of an Escherichia coli K-12 mutant for homoethanologenic fermentation of glucose or xylose without foreign genes. *Appl Environ Microbiol* 2007; **73**: 1766–1771.

164. Cocaign-Bousquet M, Garrigues C, Novak L, Lindley ND, Loublere P. Rational development of a simple synthetic medium for the sustained growth of Lactococcus lactis. *J Appl Microbiol* 1995; **79**: 108–116.

165. Thomas TD, Ellwood DC, Longyear VMC. Change from homo- to heterolactic fermentation by Streptococcus lactis resulting from glucose limitation in anaerobic chemostat cultures. *J Bacteriol* 1979; **138**: 109–117.

166. de Groot DH, van Boxtel C, Planqué R, Bruggeman FJ, Teusink B. The number of active metabolic pathways is bounded by the number of cellular constraints at maximal metabolic rates. *bioRxiv* 2018; 167171.

167. Molenaar D, van Berlo R, de Ridder D, Teusink B. Shifts in growth strategies reflect tradeoffs in cellular economics. *Mol Syst Biol* 2009; **5**.

168. Gonzalez-Gil L, Mauricio-iglesias M, Carballa M, Lema JM. Why are organic micropollutants not fully biotransformed? A mechanistic modelling approach to anaerobic systems. *Water Res* 2018; **142**: 115–128.

169. Schleifer KH, Amann RI, Ludwig W. Phylogenetic identification and in situ detection of individual microbial cells without cultivation . Phylogenetic Identification and In Situ Detection of Individual Microbial Cells without Cultivation. 1995; **59**: 143–169.

170. Kim D-H, Lee M-K, Hwang Y, Im W-T, Yun Y-M, Park C, et al. Microbial granulation for lactic acid production. *Biotechnol Bioeng* 2016; **113**: 101–11.

171. Plengvidhya V, Breidt Jr F, Lu Z, Fleming HP. DNA fingerprinting of lactic acid bacteria in sauerkraut fermentations. *Appl Environ Microbiol* 2007; **73**: 7697–7702.

172. Lin C, Chang C, Hung C. Fermentative hydrogen production from starch using natural mixed cultures. *Int J Hydrogen Energy* 2008; **33**: 2445–2453.

173. Kitay E, Snell EE. Some additional nutritional requirements of certain lactic acid bacteria. *J Bacteriol* 1950; **60**: 49.

174. LeBlanc JG, Laiño JE, del Valle MJ, Vannini V, van Sinderen D, Taranto MP, et al. B-Group vitamin production by lactic acid bacteria – current knowledge and potential applications. *J Appl Microbiol* 2011; **111**: 1297–1309.

175. Novak L, Cocaign-Bousquet M, Lindley ND, Loubiere P. Metabolism and energetics of Lactococcus lactis during growth in complex or synthetic media. *Appl Environ Microbiol* 1997; **63**: 2665–2670.

176. Olmos-Dichara A, Ampe F, Uribelarrea J-L, Pareilleux A, Goma G. Growth and lactic acid production by Lactobacillus casei ssp. rhamnosus in batch and membrane bioreactor: influence of yeast extract and Tryptone enrichment. *Biotechnol Lett* 1997; **19**: 709–714.

177. Bachmann H, Molenaar D, Branco dos Santos F, Teusink B. Experimental evolution and the adjustment of metabolic strategies in lactic acid bacteria. *FEMS Microbiol Rev* 2017; **41**: S201–S219.

178. Li Z, Nimtz M, Rinas U. The metabolic potential of Escherichia coli BL21 in defined and rich medium. *Microb Cell Fact* 2014; **13**: 45.

179. Bosdriesz E, Molenaar D, Teusink B, Bruggeman FJ. How fast-growing bacteria robustly tune their ribosome concentration to approximate growth-rate maximization. *FEBS J* 2015; **282**: 2029–2044.

180. Teusink B, Bachmann H, Molenaar D. Systems biology of lactic acid bacteria: a critical review. *Microb Cell Fact* 2011; **10**: S11.

181. Tang J, Yuan Y, Guo WQ, Ren NQ. Inhibitory effects of acetate and ethanol on biohydrogen production of Ethanoligenens harbinese B49. *Int J Hydrogen Energy* 2012; **37**: 741–747.

182. Xing D, Ren N, Li Q, Lin M, Wang A, Zhao L. Ethanoligenens harbinense gen. nov., sp. nov., isolated from molasses wastewater. *Int J Syst Evol Microbiol* 2006; **56**: 755–760.

183. Tamis J, Joosse BM, Loosdrecht MCM va., Kleerebezem R. High-rate volatile fatty acid (VFA) production by a granular sludge process at low pH. *Biotechnol Bioeng* 2015; **112**: 2248–2255.

184. Prabhu R, Altman E, Eiteman MA. Lactate and acrylate metabolism by Megasphaera

elsdenii under batch and steady-state conditions. *Appl Environ Microbiol* 2012; **78**: 8564–8570.

185.   Duncan SH, Louis P, Flint HJ. Lactate-utilizing bacteria, isolated from human feces, that produce butyrate as a major fermentation product. *Appl Environ Microbiol* 2004; **70**: 5810–5817.

186.   Marounek M, Fliegrova K, Bartos S. Metabolism and some characteristics of ruminal strains of Megasphaera elsdenii. *Appl Environ Microbiol* 1989; **55**: 1570–1573.

187.   Stouthamer a H. A theoretical study on the amount of ATP required for synthesis of microbial cell material. *Antonie Van Leeuwenhoek* 1973; **39**: 545–565.

188.   Lawford HG, Rousseau JD. Comparative Energetics of Glucose and Xylose Metabolism in Ethanologenic Recombinant Escherichia coil B. *Appl Biochem Biotechnol* 1995; **51**: 179–195.

189.   Waller JR, Lichstein HC. Biotin transport and accumulation by cells of Lactobacillus plantarum. II. Kinetics of the system. *J Bacteriol* 1965; **90**: 853–856.

190.   Moscoviz R, Trably E, Bernet N, Carrère H. The environmental biorefinery: State-of-the-art on the production of hydrogen and value-added biomolecules in mixed-culture fermentation. *Green Chem* 2018; **20**: 3159–3179.

191.   Paritosh K, Kushwaha SK, Yadav M, Pareek N, Chawade A, Vivekanand V. Food Waste to Energy: An Overview of Sustainable Approaches for Food Waste Management and Nutrient Recycling. *Biomed Res Int* 2017; **2017**: 2370927.

192.   Kaparaju P, Serrano M, Thomsen AB, Kongjan P, Angelidaki I. Bioethanol, biohydrogen and biogas production from wheat straw in a biorefinery concept. *Bioresour Technol* 2009; **100**: 2562–2568.

193.   Franks AH, Harmsen HJM, Raangs GC, Jansen GJ, Schut F, Welling GW. Variations of Bacterial Populations in Human Feces Measured by Fluorescent In Situ Hybridization with Group-Specific 16S rRNA-Targeted Oligonucleotide Probes. *Appl Environ Microbiol* 1998; **64**: 3336–3345.

194.   Xia Y, Massé DI, McAllister TA, Beaulieu C, Talbot G, Kong Y, et al. In situ identification of keratin-hydrolyzing organisms in swine manure inoculated anaerobic digesters. *FEMS Microbiol Ecol* 2011; **78**: 451–462.

195.   Sghir A, Antonopoulos D, Mackie RI. Design and Evaluation of a Lactobacillus Group-specific Ribosomal RNA-targeted Hybridization Probe and its Application to the Study of Intestinal Microecology in Pigs. *Syst Appl Microbiol* 1998; **21**: 291–296.

196.   Sanguin H, Remenant B, Dechesne A, Thioulouse J, Vogel TM, Nesme X, et al. Potential of a 16S rRNA-based taxonomic microarray for analyzing the rhizosphere effects of maize on Agrobacterium spp. and bacterial communities. *Appl Environ Microbiol* 2006; **72**: 4302–4312.

197.   Sanguin H, Herrera A, Oger-Desfeux C, Dechesne A, Simonet P, Navarro E, et al. Development and validation of a prototype 16S rRNA-based taxonomic microarray for Alphaproteobacteria. *Environ Microbiol* 2006; **8**: 289–307.

198.   Demaneche S, Sanguin H, Pote J, Navarro E, Bernillon D, Mavingui P, et al. Antibiotic-resistant soil bacteria in transgenic plant fields. *Proc Natl Acad Sci* 2008; **105**: 3957–3962.

199. Ohnishi A. Megasphaera as lactate-utilizing hydrogen-producing bacteria. In: Kalia VC (ed). *Microbial Factories: Biofuels, Waste treatment: Volume 1*. 2015. Tokyo, pp 47–71.

200. Ataai MM, Shuler ML. Simulation of the growth pattern of a single cell of Escherichia coli under anaerobic conditions. *Biotechnol Bioeng* 1985; **27**: 1027–1035.

201. Lahtvee P-J, Adamberg K, Arike L, Nahku R, Aller K, Vilu R. Multi-omics approach to study the growth efficiency and amino acid metabolism in Lactococcus lactis at various specific growth rates. *Microb Cell Fact* 2011; **10**: 12.

202. Frutiger J, Marcarie C, Abildskov J, Sin G. A Comprehensive Methodology for Development, Parameter Estimation, and Uncertainty Analysis of Group Contribution Based Property Models-An Application to the Heat of Combustion. *J Chem Eng Data* 2016; **61**: 602–613.

203. Helton JC, Davis FJ. Latin hypercube sampling and the propagation of uncertainty in analyses of complex systems. *Reliab Eng Syst Saf* 2003; **81**: 23–69.

204. El-Ziney MG, Arneborg N, Uyttendaele M, Debevere J, Jakobsen M. Characterization of growth and metabolite production of Lactobacillus reuteri during glucose/glycerol cofermentation in batch and continuous cultures. *Biotechnol Lett* 1998; **20**: 913–916.

205. Liu B-F, Xie G-J, Wang R-Q, Xing D-F, Ding J, Zhou X, et al. Simultaneous hydrogen and ethanol production from cascade utilization of mono-substrate in integrated dark and photo-fermentative reactor. *Biotechnol Biofuels* 2015; **8**: 8.

206. Heyndrickx M, Vos P De, Ley J De. Fermentation characteristics of Clostridium pasteurianum LMG 3285 grown on glucose and mannitol. *J Appl Bacteriol* 1991; **70**: 52–58.

207. Brosseau JD, Zajic JE. Hydrogen-gas Production with Citrobacter intermedius and Clostridium pasteurianum. *J Chem Technol Biotechnol* 1982; **32**: 496–502.

208. Chen M, Wolin MJ. Influence of heme and vitamin B12 on growth and fermentations of Bacteroides species. *J Bacteriol* 1981; **145**: 466 LP – 471.

209. Dabrock B, Bahl H, Gottschalk G. Parameters Affecting Solvent Production by Clostridium pasteurianum. *Appl Environ Microbiol* 1992; **58**: 1233–1239.

210. Gonzalez-Garcia R, McCubbin T, Navone L, Stowers C, Nielsen L, Marcellin E. Microbial Propionic Acid Production. *Fermentation* 2017; **3**: 21.

211. Curtis T. Crystal ball - 2007 Theory and the microbial world. *Environ Microbiol* 2007; **9**: 1.

212. Darwin C. On the Origin of Species. 1859. London.

213. Hibbing ME, Fuqua C, Parsek MR, Peterson SB. Bacterial competition: surviving and thriving in the microbial jungle. *Nat Rev Microbiol* 2010; **8**: 15–25.

214. Pande S, Kost C. Bacterial Unculturability and the Formation of Intercellular Metabolic Networks. *Trends Microbiol* 2017; **25**: 349–361.

215. Pande S, Merker H, Bohl K, Reichelt M, Schuster S, De Figueiredo LF, et al. Fitness and stability of obligate cross-feeding interactions that emerge upon gene loss in bacteria. *ISME J* 2014; **8**: 953–962.

216. Nurk S, Meleshko D, Korobeynikov A, Pevzner PA. MetaSPAdes: A new versatile metagenomic assembler. *Genome Res* 2017; **27**: 824–834.

217. Li H, Durbin R. Fast and accurate long-read alignment with Burrows-Wheeler transform. *Bioinformatics* 2010; **26**: 589–595.

218. Li H, Handsaker B, Wysoker A, Fennell T, Ruan J, Homer N, et al. The Sequence Alignment/Map format and SAMtools. *Bioinformatics* 2009; **25**: 2078–2079.

219. Alneberg J, Bjarnason BS, De Bruijn I, Schirmer M, Quick J, Ijaz UZ, et al. Binning metagenomic contigs by coverage and composition. *Nat Methods* 2014; **11**: 1144–1146.

220. Wu Y-W, Simmons BA, Singer SW. MaxBin 2.0: an automated binning algorithm to recover genomes from multiple metagenomic datasets. *Bioinformatics* 2016; **32**: 605–607.

221. Lu YY, Chen T, Fuhrman JA, Sun F, Sahinalp C. COCACOLA: Binning metagenomic contigs using sequence COmposition, read CoverAge, CO-alignment and paired-end read LinkAge. *Bioinformatics* 2017; **33**: 791–798.

222. Graham ED, Heidelberg JF, Tully BJ. BinSanity: unsupervised clustering of environmental microbial assemblies using coverage and affinity propagation. *PeerJ* 2017; **5**: e3035.

223. Kang DD, Froula J, Egan R, Wang Z. MetaBAT, an efficient tool for accurately reconstructing single genomes from complex microbial communities. *PeerJ* 2015; **3**: e1165.

224. Sieber CMK, Probst AJ, Sharrar A, Thomas BC, Hess M, Tringe SG, et al. Recovery of genomes from metagenomes via a dereplication, aggregation and scoring strategy. *Nat Microbiol* 2018; 1–8.

225. Parks DH, Imelfort M, Skennerton CT, Hugenholtz P, Tyson GW. CheckM: assessing the quality of microbial genomes recovered from isolates, single cells, and metagenomes. *Genome Res* 2015; **25**: 1043–55.

226. Overbeek R, Olson R, Pusch GD, Olsen GJ, Davis JJ, Disz T, et al. The SEED and the Rapid Annotation of microbial genomes using Subsystems Technology (RAST). *Nucleic Acids Res* 2014; **42**: D206-14.

227. Brettin T, Davis JJ, Disz T, Edwards RA, Gerdes S, Olsen GJ, et al. RASTtk: A modular and extensible implementation of the RAST algorithm for building custom annotation pipelines and annotating batches of genomes. *Sci Rep* 2015; **5**: 8365.

228. Aziz RK, Bartels D, Best AA, DeJongh M, Disz T, Edwards RA, et al. The RAST Server: Rapid Annotations using Subsystems Technology. *BMC Genomics* 2008; **9**: 75.

229. McEntyre J, Ostell J, Madden T. The BLAST Sequence Analysis Tool. *The NCBI Handbook*. 2003.

230. Valk LC, Frank J, de la Torre-Cortés P, van 't Hof M, van Maris AJA, Pronk JT, et al. Galacturonate metabolism in anaerobic chemostat enrichment cultures: Combined fermentation and acetogenesis by the dominant sp. nov. 'Candidatus Galacturonibacter soehngenii.' *Appl Environ Microbiol* 2018; **84**.

231. Clifton MC, Simon MJ, Erramilli SK, Zhang H, Zaitseva J, Hermodson MA, et al. In vitro reassembly of the ribose ATP-binding cassette transporter reveals a distinct set of transport complexes. *J Biol Chem* 2015; **290**: 5555–5565.

232. Kuenen J., Johnson OJ. Encyclopedia of Microbiology. 2009.

233. Kanai T, Imanaka H, Nakajima A, Uwamori K, Omori Y, Fukui T, et al. Continuous hydrogen

production by the hyperthermophilic archaeon, Thermococcus kodakaraensis KOD1. *J Biotechnol* 2005; **116**: 271–282.

234. Feng Y, Zhang H, Cronan JE. Profligate biotin synthesis in α-proteobacteria - a developing or degenerating regulatory system? *Mol Microbiol* 2013; **88**: 77–92.

235. Mooney S, Leuendorf JE, Hendrickson C, Hellmann H. Vitamin B6: A long known compound of surprising complexity. *Molecules* 2009; **14**: 329–351.

236. Satiaputra J, Eijkelkamp BA, McDevitt CA, Shearwin KE, Booker GW, Polyak SW. Biotin-mediated growth and gene expression in Staphylococcus aureus is highly responsive to environmental biotin. *Appl Microbiol Biotechnol* 2018; **102**: 3793–3803.

237. Octavia S, Lan R. The Family Enterobacteriaceae. *The Prokaryotes*. 2014. Springer, Berlin, Heidelberg.

238. Jarzembowska M, Sousa DZ, Beyer F, Zwijnenburg A, Plugge CM, Stams AJM. Lachnotalea glycerini gen. nov., sp. nov., an anaerobe isolated from a nanofiltration unit treating anoxic groundwater. *Int J Syst Evol Microbiol* 2016; **66**: 774–779.

239. Wüst PK, Horn MA, Drake HL. Clostridiaceae and Enterobacteriaceae as active fermenters in earthworm gut content. *ISME J* 2011; **5**: 92–106.

240. Cipollina C, ten Pierick A, Canelas AB, Seifar RM, van Maris AJA, van Dam JC, et al. A comprehensive method for the quantification of the non-oxidative pentose phosphate pathway intermediates in Saccharomyces cerevisiae by GC-IDMS. *J Chromatogr B Anal Technol Biomed Life Sci* 2009; **877**: 3231–3236.

241. Amend AS, Seifert K a, Bruns TD. Quantifying microbial communities with 454 pyrosequencing: does read abundance count? *Mol Ecol* 2010; **19**: 5555–65.

242. Molenaar D, van Berlo R, de Ridder D, Teusink B. Shifts in growth strategies reflect tradeoffs in cellular economics. *Mol Syst Biol* 2009; **5**: 323.

243. Shimada T, Zilles J, Raskin L, Morgenroth E. Carbohydrate storage in anaerobic sequencing batch reactors. *Water Res* 2007; **41**: 4721–9.

244. Dionisi D, Silva IMO. Production of ethanol , organic acids and hydrogen : an opportunity for mixed culture biotechnology? *Rev Environ Sci Bio/Technology* 2016; **15**: 213–242.

245. Sorokin DY, Banciu HL, Muyzer G. Functional microbiology of soda lakes. *Curr Opin Microbiol* 2015; **25**: 88–96.

246. Felz S, Al-Zuhairy S, Aarstad OA, van Loosdrecht MCM, Lin YM. Extraction of structural extracellular polymeric substances from aerobic granular sludge. *J Vis Exp* 2016; **2016**: 1–8.

247. Didde R. Kameleon-gel uit afvalwater goed voor potjes en stropdassen. *De Volkskrant* . 2019.

248. Tamis J, Joosse BM, van Loosdrecht MCM, Kleerebezem R. High-rate volatile fatty acid (VFA) production by a granular sludge process at low pH. *Biotechnol Bioeng* 2015; **112**: 2248–2255.

249. Kleiner M, Dong X, Hinzke T, Wippler J, Thorson E, Mayer B, et al. Metaproteomics method to determine carbon sources and assimilation pathways of species in microbial communities. *Proc Natl Acad Sci U S A* 2018; **115**: E5576–E5584.

250. Aßhauer KP, Wemheuer B, Daniel R, Meinicke P. Tax4Fun: Predicting functional profiles from metagenomic 16S rRNA data. *Bioinformatics* 2015; **31**: 2882–2884.

251. Hassa J, Maus I, Off S, Pühler A, Scherer P, Klocke M, et al. Metagenome, metatranscriptome, and metaproteome approaches unraveled compositions and functional relationships of microbial communities residing in biogas plants. *Appl Microbiol Biotechnol* 2018; **102**: 5045–5063.

252. Christensen BB, Haagensen JAJ, Heydorn A, Molin S. Metabolic commensalism and competition in a two-species microbial consortium. *Appl Environ Microbiol* 2002; **68**: 2495–2502.

253. Piveteau P. Metabolism of lactate and sugars by dairy propionibacteria: A review. *Lait* 1999; **79**: 23–41.

254. Louis P, Flint HJ. Diversity, metabolism and microbial ecology of butyrate-producing bacteria from the human large intestine. *FEMS Microbiol Lett* 2009; **294**: 1–8.

255. Tholozan J, Membr J, Kubaczka M. Effects of culture conditions on Pectinatus frisingensis metabolism: a physiological and statistical approach. *J Appl Bacteriol* 1996; **80**: 418–424.

# Acknowledgements

Acknowledgements go beyond just a list and actions. I would like to express my thankfulness toward all those that have helped me along this journey. Here we go…

**Mark**, for believing in my ability to achieve a PhD degree, helping me to get it done, trying to steer me into becoming a successful scientist and away from the dark crevasses of science, and always, challenging me. Discussions between us were at times fierce but were always accompanied by a healthy amount of respect and trust. Dank Mark, je bent een vrij briljant en uitzonderlijk gedreven wetenschapper. Ook dank voor je vertrouwen, om samen dit avontuur aan te gaan, mogen we er nog velen beleven.

**Robbert**, thank you for laying aside our differences and managing to keep inspiring me and other young scientists to wonder at the mysteries offered to us by the microbial world. Dank je ook voor je inzet en voor je charismatische toevoeging aan deze reis! Je nieuwsgierigheid is awesome en je bent een zeer begaafde docent.

**David**, tu es un homme très, très sympathique ! *Merci beaucoup* for all the times you stood by my side, listened, helped, reviewed and spent effort to improve the work that we have been doing together. Your team spirit and passion for details are remarkable, *merci*.

**Eef**, dank voor je oprechte begeleiding van mijn Master thesis, voor het uiteindelijk samen publiceren van mijn 1ᵉ paper en onze 1ᵉ paper samen, en voor al je vrolijkheid, empathie en doorzettingsvermogen. De *office life* was ook top met je, vooral het herhaaldelijk vloeken en tieren op je PC vond ik vrij *epic*.

**Jure**, my man with the smoking gun from Croatia, your observations are razor sharp and your philosophies go beyond my comprehension. To my belief, I have never met someone like you. You have been a great friend, colleague and officemate, in times of joy and misery, but above all, we could have a lot of fun, joking for hours, listening to the hip hop I threw at you and pondering on the big questions of life.

Then, to the true knights of enrichment studies, **Jelmer**, you were a bit like a big brother to me. Your actions inspired me, though I also disagreed quite frequently with your opinions on life (especially the racial ones). The surfing we did was nice and I would like to continue surfing in the future. You charge waves like no other. Talking about surfing, **Welles**, we have had nice surf, but the best thing about you, I could always crack a joke with you. Your fight with the PhD showed me the relentlessness of human nature, I admire that still. **Gerben**, you were a great companion throughout this adventure, your intellect is stunning and your brainwaves can come fast and hard. But you have some soft waves also, you supported me in difficult times, I truly appreciate that. Bedankt mannen, voor al deze mooie tijden.

**Michele** and **Marta**, my Italian office *amici*. You have shown me affection and brought good and passionate spirits to the office. Your energy and bravery encourage me to pursue my next steps, *grazie mille* for that.

My SIAM ladies, **Laura**, **Marissa**, **Leonor**, thank you for your positive attitudes and kindness. It has been a pleasure working alongside you. Laura, it was nice to collaborate on the work in chapter five, you will make a great academic! **Yuemei**, also thank you for your kindness and easy-going attitude, bringing a friendly Asian spirit to our lab. It was nice to chat with you about difficult situations.

Then, a small hommage to my students. **Hessel**, je was de eerste en misschien de meest toegewijde student, ik zie je nog staan in 37°C + oven die de van Iterson hal kon zijn, de SBRs aan het managen of moet ik zeggen aan het Hesselen/husslen/hosselen? Respect. **Galvin**(o) en **Els**, jullie waren een superteam, meer dan ik kon wensen. **Lars**, we hebben *FISH* naar level 2 gebracht samen, je toewijding was fenomenaal. **Sara**, *muchas gracias* for your dedicated analytical effort, you rock Matlab like no other. **Kelly**, je doorzettingsvermogen en vriendelijkheid waren een geschenk, het was een plezier je te begeleiden. **Maxim**, ik weet nog goed dat ik het project aan je voorstelde in die bar naast station Den Haag HS, je wilde er vol voor gaan! Je motivatie, humor en ondernemende geest hebben mijn laatste PhD jaar veel toffer gemaakt, dank. **Philip**, dank voor je *commitment* en energie tijdens mijn laatste zomer als promovendus, we hebben het *mixed culture* melkzuur concept naar een serieuze fase geloodst.

To my officemates, **Maria** Paula, **Rhody**, **Michel**, **Leonie**, **Maaike**, **Simon**, **Rubén**, **Morez**(zi), **Viktor**, many thanks for receiving my awkward remarks and bad jokes in kind spirit. **Monica**, I admire your struggle for life, your honesty and joyfulness, you have been a great companion, your feminism is unmatched and our conversations have helped me to kind of balance out the rational and emotional side inside of me, thank you.

Life comes in waves, as do colleagues. EBTeans of the new wave, **Danny**, **Ingrid**, **Sergio**, **David**(e), **Roel**, **Shengle**, **Aina**, **Sueellen**, **Chris**, **Hugo**, **Edward**, **Janis**, **Felipe**, you were awesome colleagues. EBTeans of the old wave, **Emma**, **Emmanuelle**, **Bart**, **Steef**, **Mario**, **Peter,** fellow BTeans, **Eleni**, **Florence**, **Yaya**, **Pilar**, **Jasmine**, **Koen**, **Robin** Schumax, **Arthur**, **Anna**, **Nick**, **Maarten**, **Marijke**, **Aurin**, **Wijb**, **Jonna**, **Ana Maria**, **Mariana**, **Victor**, **Phillip**, I appreciated your company and help much throughout the years. **Dimitri**, thank you for sharing your stark, honest and brave Russian guidance throughout my studies. **Duncan** and **Albert**, thank you for working on the biochemistry of this story. **Karel**, your Cuban spirit and effort to unravel enzyme activities were a great addition, thank you. **Martin**, **Patricia**, thank you for the help in our mission to measure B vitamins and amino acids. **Julio** (Perez), *gracias* for your advice both on professional and family level. **Helena**, thank you for taking me on my first mission to a Master's thesis, which unfortunately did not yield the desired result, but has thought me a few important aspects about myself and how I function well.

**Jack**, thank you for your guidance. **Sef**, thank you for your honesty and all the engineering you have taught me. **Gijs**, thank you for your friendly and honest approach to how we can understand the microbial world and for stepping up to Mark that one time during my Go/No-Go. **Geert-Jan**, dank voor je hulp en vertrouwen, en je bereidheid zo nu en dan tijd voor mij vrij te maken. **Ton**, thank you for your help now and then.

Where would I have been without technicians? **Ben**, **Zita**, **Udo**, **Dirk**, **Rob**, **Song**, **Mitchell**, **Cor**, **Stef**, **Johan,** thank you for all help and troubleshooting and being great company. Also the MSD dames, **Astrid**, **Jannie**, **Apilena**, zonder jullie was het niet zo *smooth* gegaan. **Nayyar**, thanks. **Miranda** en **Kawieta**, dank voor de *backoffice* support.

My mentors, **Aljoscha**, **Walter**, on several occasions you have turned my energy into productivity and growth instead of anger and frustration, dankjewel daarvoor.

And to the SIAM, which comprises of many people. Thank you, **Mike**, **Fons**, **Jaap** Sinninghe Damsté and **Willem** for leading the effort to land the SIAM funding. **Francisca**, dank voor al je inzet. **Sebastian** Lücker, **Jeroen** Frank, dank voor de samenwerking, your metagenomic tricks are unparalleled. Other SIAMers, thank you, **Daan**, **Martijn**, **Suda**, **Peer**, **Sigrid**, **Stefanie**, **Melvin**, **Cornelia**, **Clara**. **Chris**(topher Lawson), thanks for cooperating on the attempt to measure amino acids and B vitamins in the supernatant of my chemostat enrichment cultures. To my Canadian connection, **Joe** Ho, **Steven** Hallam, your part of the adventure has been a great experience, you showed me a whole new perspective on microbial ecology and Joe, your discipline is admirable.

René, dank je voor je steun en advies vanuit Paques. To the Santiago connection, *gracias* Alberte, it was very nice working with you. Rebeca, thank you for the nice discussions. At DSM, Margarida, thank you for your input. Also thank you Carolina for helping us in giving the nature's principles adventure a higher success rate.

I wish to express my gratitude towards the Graduate School, for encouraging to study myself and my environment, to learn and to be the better part of myself. Regards also to the Faculty of Applied Sciences and Department of Biotechnology for hosting my project.

And then, closer and more private to me...

My diverse and contagious group of friends, Team Flip, Joris, Harman, Jos, Fishermen Friends, Cees, Jaap, Rogier, Jorik, Patrick, Yorian, Hengelen met de mannen, Louw, Rob SJ, Frits/Floris, Sjos, Jurrit, Rits, Paul, Martijn, Bob, Rogier. En verder, Jord, Silvan, Steffen, Haiko, Bas, Teun, Bart, en vele andere Plankenkoorts legends. Videha en Yannick. Dank voor de gelegenheden stoom af te blazen, 's nachts op pad te gaan, te surfen, te reizen en te genieten van het leven.

Mijn LST-bachelor maatjes, Rik, Charlotte, Robbert. Dank voor jullie steun en de mooie momenten die we hebben meegemaakt. En verder, Daniel, Sietske, Elise, Loes, Xavier, Luis, Lot, Floor, Ron, dank voor het vergezellen van mijn reis door de wetenschap en studies (*gracias*).

To my family, mijn ouders Wob ben Trix, dank voor, boven alles, het schenken van mijn leven (toch vrij essentieel) en voor de steun gedurende al die jaren van studie. Titus, broer, je bent de beste broer die ik kan wensen en bedankt dat je een rondje redactie op de introductie hebt gedaan. Floris, dank voor je humor en vertrouwen, en dank aan alle Lutterveltjes. Hanneke, ondanks je eigen twijfels, dank voor je inspiratie en liefde. Peter, al ben je er niet meer, dank voor je energie en de *disruptive* houding om de wereld een betere plek proberen te maken, je was een inspirerende oom.

Oma Titia, u liet mij zien wat *female power* is en u was immer in voor een verhelderende conversatie, dank voor uw liefde. Thomas en Lisa, jullie energie vibreert door tot deze tak van de familie, dank. En dan, overgrootvader Faddy, ik ken u helaas niet persoonlijk maar uw heroïsche daden en ondernemende geest zullen mij blijven inspireren, de zeepfabriek in Wageningen prikkelt mijn geest. Dank ook aan de andere Romboutsen en van Schaiks voor alle affectie. De Janssens en Farjons, Marian, Rob, Joe, dank voor jullie liefde en steun.

En, als laatste, Annie, dank om aan mijn zijde te staan, wat er ook gebeurt, hoe diep de dalen ook zijn, je liefde voelt onvoorwaardelijk, je vrolijkt me altijd weer op, dankjewel voor alles tot nu toe...

## Curriculum Vitae

Julius (Jules) L. Rombouts was born on the 18th of December 1987 in Rotterdam, the Netherlands. He finished his primary school at the public Montessori school in Schiebroek. He graduated from the Wolfert van Borselen (Rotterdam), receiving his bilingual pre-university diploma (TVWO) in the direction of sciences, with an optional degree in philosophy.

After graduating in 2006, he pursued a nine-month working holiday in Oceania and Asia, working in hospitality services and agriculture. Returning to the Netherlands in 2007, he started the Bachelor of Science in Life Science and Technology. He successfully obtained this degree in 2012 from Delft University of Technology and Leiden University, defending a thesis on microbial community structures of desert soil samples from Utah, USA.

He carried out a five-month industrial internship at Hortimare B.V. and the Royal Netherlands Institute for Sea Research (NIOZ), studying the physiology of macroalgae (seaweeds) under different light regimes for industrial purposes. In 2015, he successfully defended his Master of Science with a thesis on the competition between denitrification and ammonification using chemostat enrichment cultures.

His initial ambition to work as a scientist in industry led him to return to Delft, to start a PhD thesis under the supervision of prof. Mark van Loosdrecht. From 2019 onwards, he is engaged in starting the company Nature's Principles B.V. and aims to launch a new concept of lactic acid production to the global market. He dreams of providing a more sustainable future for Planet Earth and for many human generations yet to come.

## List of peer-reviewed publications

1. <u>Julius L Rombouts</u>, Galvin Mos, David G Weissbrodt, Robbert Kleerebezem, Mark C M Van Loosdrecht,

   *"Diversity and metabolism of xylose and glucose fermenting microbial communities in sequencing batch or continuous culturing"*,

   **FEMS Microbiology Ecology**, Volume 95, Issue 2, February 2019

   https://doi.org/10.1093/femsec/fiy233

2. <u>Julius L Rombouts</u>, Galvin Mos, David G Weissbrodt, Robbert Kleerebezem, Mark C M Van Loosdrecht,

   *"The impact of mixtures of xylose and glucose on the microbial diversity and fermentative metabolism of sequencing-batch or continuous enrichment cultures"*,

   **FEMS Microbiology Ecology**, Volume 95, Issue 8, August 2019

   https://doi.org/10.1093/femsec/fiz112

3. Eveline M van den Berg, <u>Julius L Rombouts</u>, J Gijs Kuenen, Robbert Kleerebezem, Mark CM van Loosdrecht,

   *"Role of nitrite in the competition between denitrification and DNRA in a chemostat enrichment culture"*.

   **AMB Express**, Volume 7, Issue 1, 2017

   https://doi.org/10.1186/s13568-017-0398-x

# List of conference contributions

This list of conference contributions includes both oral and poster presentations.

*"Mixed culture fermentation of lignocellulosic sugars: linking microbial communities to fermentative behaviour"*, Koninklijke Nederlandse Vereniging voor Microbiologie, Spring Meeting 2016, Papendal, the Netherlands, March **2016**

*"Microbial selection in sequencing batch reactors for anaerobic fermentation of glucose and xylose"*, 1st Symposium on Microbiological Methods for Waste and Water Resource Recovery **2017**, Delft, the Netherlands

*"Microbial selection in sequencing batch reactors for anaerobic fermentation of glucose or xylose"*, 3rd International Conference on Biogas Microbiology, Wageningen, the Netherlands, July **2017**

*"Microbial selection, stoichiometry and kinetics of glucose and xylose in an anaerobic sequencing batch reactor"*, Soehngen Institute for Anaerobic Microbiology symposium, Utrecht, the Netherlands, September **2017**

*"Microbial selection and stoichiometry of glucose and xylose fermentations in mixed-culture ecosystems of anaerobic sequencing batch reactors"*, Federation of European Microbiological Societies – Microbiology Congress 2017, Valencia, Spain, July **2017**

*"Microbial diversity in xylose or glucose fermenting enrichments: the impact of continuous growth limitation"*, Microbiology Centennial Symposium 2017, Wageningen, the Netherlands, October **2017**

*"Toward a circular economy: biopolymers recovered from waste streams"*, World of Technology and Science – Koninklijke Nederlandse Chemie Vereniging seminar, Utrecht, the Netherlands, October **2018**

*"The impact of mixtures of xylose and glucose on the microbial diversity of a sequencing batch enrichment culture"*, Netherlands Biotechnology Congress 2019 – the Sound of Biotech, Wageningen, the Netherlands, May **2019**

*"Stimulating lactic acid production in enrichment cultures by B vitamin and peptides"*, 16th International Water Association World Conference on Anaerobic Digestion, Delft, the Netherlands, June **2019**

*"Diversity and metabolism of xylose and glucose enrichment cultures"*, Federation of European Microbiological Societies – Microbiology Congress 2019, Glasgow, United Kingdom, July **2019**

*"Competing for carbon: how lactic acid bacteria are able to dominate anaerobic ecosystems"*, Koninklijke Nederlandse Vereniging voor Microbiologie – section Microbial Ecology, fall meeting, Wageningen, the Netherlands, December **2019**

## Awards

Audience vote prize, YES!Delft and DSM Pitchevent for start-ups in the Biotechnology sector, 19th July **2019**

## List of patents

"High yield lactic acid production using mixed cultures"

J.L. Rombouts, M.C.M. van Loosdrecht, R. Kleerebezem, D.G. Weissbrodt, G. Stouten, M.T. Allaart, filed 10th May **2019**

**Notes**